Effects of LXRα phosphorylation on the regulation of lipid metabolism and hepatic fibrosis

Natalia Becares Salles

University College London

Division of Medicine
Centre for Clinical Pharmacology
Rayne Institute
London

This thesis is submitted for the degree of Doctor of Philosophy

2017

I, Natalia Becares Salles, confirm that the work presented in this thesis is my own. Where information has been derived from other sources, I confirm that this has been indicated in the thesis.

London, June 2017.

Abstract

Liver X Receptors (LXRα and β) are members of the nuclear receptor superfamily of ligand-activated transcription factors. LXRs are activated by oxidised metabolites of cholesterol and several synthetic ligands, play a crucial role in the regulation of cholesterol and fatty acid homeostasis, and act as strong modulators of inflammation and immunity. This has positioned them as targets for the treatment of several pathologies, including atherosclerosis and obesity. Besides ligand binding, LXR activity can be modulated by post-translational modifications, and previous work has shown that phosphorylation of LXRα alters its transcriptional activity in a gene-specific manner in a macrophage cell line.

This thesis has focused on better understanding the regulation of LXRα phosphorylation and investigating how changes in the receptor's phosphorylation status modulate its activity *in vivo*; more specifically, in relation to its effects on hepatic lipid metabolism, and the development of inflammation and fibrosis. To do so, I have used a novel mouse model that expresses a whole-body non-phosphorylatable mutant version of LXRα (S196A) and have assessed its responses to a High Fat and High Cholesterol diet, as a dietary model of Non-Alcoholic Fatty Liver Disease (NAFLD). Furthermore, I have studied how the transcriptional capacity of the mutant receptor is modulated, assessing its differential binding to DNA and to other proteins. In order to evaluate the relevance of my findings in the context of human disease, I have also examined LXR activity on the activation of human hepatic stellate cells, key players in the development of liver fibrosis. Lastly, I have sought to examine new stimulants capable of inducing LXRα phosphorylation *in vitro*, and how this phenomenon can be pharmacologically impaired by using already-available kinase inhibitors.

Overall, the work described in this thesis shows that LXRα phosphorylation critically acts as a novel nutritional sensor that promotes a unique diet-induced transcriptome and modulates metabolic, inflammatory and fibrotic responses that are key in NAFLD progression This novel work significantly contributes to our understanding of LXRα activity in liver disease in a pre-clinical setup, and places the modulation of LXRα phosphorylation as a potential anti-inflammatory/anti-fibrotic therapeutic target.

Impact statement

Benefits inside academia

To date, the physiological roles of modifications such as phosphorylation, sumoylation and acetylation of LXRα have only been studied *in vitro* or non-specifically in animal models, by pharmacologically or genetically altering the enzymes enhancing or inhibiting these modifications. My PhD thesis is the first study to address the pathophysiological impact of LXRα phosphorylation by directly impeding this modification genetically, and has positioned the S196A mice as an optimal *in vivo* model for the study of this modification. This could benefit the academic community by establishing this animal model as an important tool to investigate regulation of LXRα phosphorylation as a potential therapeutic target. This impact will be brought about by dissemination of results in conferences and scientific journals, as well as future collaborations with other academic experts in the field of nuclear receptor biology.

Benefits outside academia

The WHO estimates over 650m people worldwide have a chronic liver condition. Alarming increases in obesity rates and parallel increases in rates of non-alcoholic fatty liver disease (NAFLD), plus an ageing population predicts it to become the most frequent indication for liver transplantation by 2030. In the UK, NAFLD affects about 33% of the UK population, and 2-5% progress to non-alcoholic steatohepatitis (NASH).

Despite its vast clinical relevance, current treatment options such as lifestyle changes (diet change and weight loss) are inadequate for a large number of patients. Pharmacological therapies such as insulin sensitizers, antioxidants, and lipid-lowering agents are aimed at treating its associated conditions and therefore display only limited efficacy. Thus, there is a clear unmet medical need for development of novel direct pharmacological therapies targeting NAFLD. My PhD findings could be the basis for further research into the discovery of new pharmaceutical therapies for Non Alcoholic Liver Disease (NAFLD). This impact could be brought about by dissemination of results in conferences and scientific journals, as well as future collaborations with partners in industry.

Acknowledgements

I want to thank my supervisor, Dr. Inés Pineda-Torra, who has supported me and given me guidance throughout my PhD studies. I would also like to thank her for giving me the opportunity to present my work at national and international conferences, and for her mentorship and input. I have truly benefited from her experience and knowledge in the field of nuclear receptors. I would also like to express my gratitude to my secondary supervisor, Professor Rachel Chambers, who has provided excellent feedback and discussions as well as offered very useful advice.

Special thanks to all the members of the Pineda-Torra group, present and past, in particular to Matt and Kirsty. You have been a very important source of help and scientific discussions, but also of laughter and great moments both inside and outside the lab.

Moreover, I would like to express my gratitude to several other members of the UCL community, whose assistance and guidance have pushed this project forwards. A special mention to Dr. Krista Rombouts at the ILDH, and members of CVB, the Gilroy lab and UCL Respiratory.

I would also like to acknowledge all the help and support given by the groups of Dr. Eckardt Treuter at Karolinska Institutet and Prof. Michael Garabedian at New York University.

I want to say how deeply grateful I am to my mother, brother and friends who have always supported and encouraged me to keep going whenever I needed a boost in morale. Thank you for having my back and helping me keep things into perspective.

Lastly, I would like to specially thank my sister Laia, who has offered me endless support and patience; and has always stood by my side, providing me with immense care and unconditional love. This thesis is dedicated to her.

This research was made possible thanks to the funding provided by the Medical Research Council, UCL SLMS Grand Challenge Studentships and UCL's Division of Medicine.

Table of contents

List of figures

List of tables

List of abbreviations

ºC – Degree Celsius

ABCA1 – ATP-binding cassette, sub-family A member 1

ABCG1 – ATP binding cassette subfamily G member 1

ABCG5 – ABC transporters, sub-family G member 5

ABCG8 – ABC transporters, sub-family G member 8

CK2 – Casein Kinase 2

ChIP – Chromatin Immunoprecipitation

DBD – DNA-binding domain

ER – Endoplasmic reticulum

EC – Epoxycholesterol

HDAC – Histone deacetylases

HDL – High Density Lipoprotein

HFHC – High Fat-High Cholesterol

HSC – Hepatic Stellate Cell

IL – Interleukin

LBD – Ligand-binding domain

LXR – Liver X Receptor

LDL – Low Density Lipoprotein

mRNA – Messenger ribonucleic acid

NAFLD – Non-Alcoholic Fatty Liver Disease

NASH – Non-Alcoholic steatohepatitis

NEFA – Non-Esterified Fatty Acid

NCoR – Nuclear receptor corepressor

PBS – Phosphate buffer saline

PTMs – Post-translational modifications

qPCR – Quantitative polymerase chain reaction

RXR – Retionoid X Receptor

RCT – Reverse Cholesterol Transport

rpm – Revolutions per minute

RNA – Ribonucleic acid

RNA-seq – RNA-sequencing

TBLR1 – Transducin beta like 1 X-linked receptor 1

S6K1 – p70 ribosomal S6 kinase-1

SCD1 – Stearoyl-CoA desaturase 1

SREBP1c – Sterol regulatory element binding transcription protein 1c

TSS – Transcription start site

UPR – Unfolded protein response

WAT – White adipose tissue

Publications and conferences arising from thesis

Publications

Becares N**,** Gage MC, Martin-Gutierrez L, Pourcet B, Pello OM, Luong TV, Goñi S, Liang N, Pichardo C, Røberg-Larsen H, Diaz V, Steffensen KR, Garabedian MJ, Rombouts K, Treuter E, Pineda-Torra. Changes in LXRα phosphorylation promote a novel diet-induced transcriptome that alters the transition from fatty liver to steatohepatitis. In preparation. Pre-print at bioRxiv 127779; doi: https://doi.org/10.1101/127779

Becares N, Gage MC, Pineda-Torra I. Post-translational modifications of lipid-activated nuclear receptors: Focus on metabolism. Endocrinology. 2017 Feb 1;158(2):213-225.

Conferences, abstracts and presentations

Becares N, Gage M, Rombouts K, Luong TV, Chambers R & Pineda-Torra I. (2016, October). *Changes in LXRα phosphorylation attenuate diet-induced liver inflammation and fibrosis.* Paper presented at the D17 European Club Liver Cell Biology 7th Edition. Ascot, United Kingdom.

Becares N, Gage M, Rombouts K, Luong TV, Chambers R & Pineda-Torra I. (2016, May). *Changes in LXRα phosphorylation attenuate diet-induced liver inflammation and fibrosis.* Poster presentation at the London Inflammation Network by QMUL Barts and the London School of Medicine and Dentistry. London, United Kingdom.

Becares N, Gage M, Luong TV, Chambers R & Pineda-Torra I. (2016, April). *Changes in LXRα phosphorylation attenuate diet-induced liver inflammation and fibrosis.* Poster presentation at The International Liver Congress by the European Association for the Study of the Liver. Barcelona, Spain

Becares N, Gage M, León T, Chambers R & Pineda-Torra I (2014, December). *Changes in LXRα phosphorylation selectively modulate macrophage lipid metabolism and inflammatory gene expression*. Poster presentation at 45th London Vascular Biology Forum. London, United Kingdom.

Chapter 1. Introduction

1.1. Liver X Receptors

1.1.1. LXR structure and activity

LXRs are members of the nuclear receptor superfamily, a set of structurally conserved, ligand-dependent transcription factors that act as integrators of several diverse signals (inflammatory, nutritional and hormonal) and regulate diverse aspects of development and homeostasis through changes in gene expression. Most proteins in the nuclear receptor family share a similar structure, consisting of a variable amino-terminal activation domain (AF-1), a central DNA-binding domain (DBD) which recognizes specific DNA sequences known as response elements, a hinge region that permits structural flexibility, and a ligand-binding domain (LBD) located on the carboxy-terminal part (Figure 1.1. A). Nuclear receptors can be grouped into four categories according to their ligand, DNA binding and dimerization properties (1). The LXR family consists of two different subtypes, LXRα and LXRβ (NR1H3 and NR1H2, respectively) and its name comes from the initial isolation of the LXRα receptor from a human liver cDNA library, where it is highly expressed (2,3). The two receptors share approximately 75% sequence homology in both their DBD and LBD, and differ mainly on their N-terminal sequence and their expression pattern; while LXRα is most highly found in liver and other metabolically active tissues and cell types, such as intestine and macrophages, LXRβ is ubiquitously expressed (2–4). The mechanisms controlling expression of the LXR genes are not fully understood. In the case of LXRα, its promoter has been shown to be under the regulation of the peroxisome proliferator-activated receptors alpha (PPARα) and gamma (PPARδ) in liver, adipocytes and macrophages (5–7). For example, expression of the LXRα receptor has been shown to be induced in the presence of fatty acids, which are classic PPARα ligands, through an increase in its transcriptional rates but also stabilization of the LXRα transcript (8). In addition, expression of the LXRα gene has

been demonstrated to be autoregulated by LXR activation in mouse adipose tissue (9) and human macrophages (10).

Both LXRs regulate transcription by forming permissive heterodimers with the Retinoid X Receptor (RXR), where ligands for either partner can activate the complex (3,11). Upon dimerization with RXR, LXRs bind to the DNA through their DBD, which contains a double zinc structure. The LXR/RXR heterodimer binds with high affinity to specific motifs known as LXR-responsive elements (LXREs), which consist of direct repeats (DRs) of several derivatives of the consensus half-site AGGTCA separated by 4 nucleotides (DR4), located in the regulatory regions (promoter and/or enhancers) of their target genes (2,3,12) (Figure 1.1. B,C).

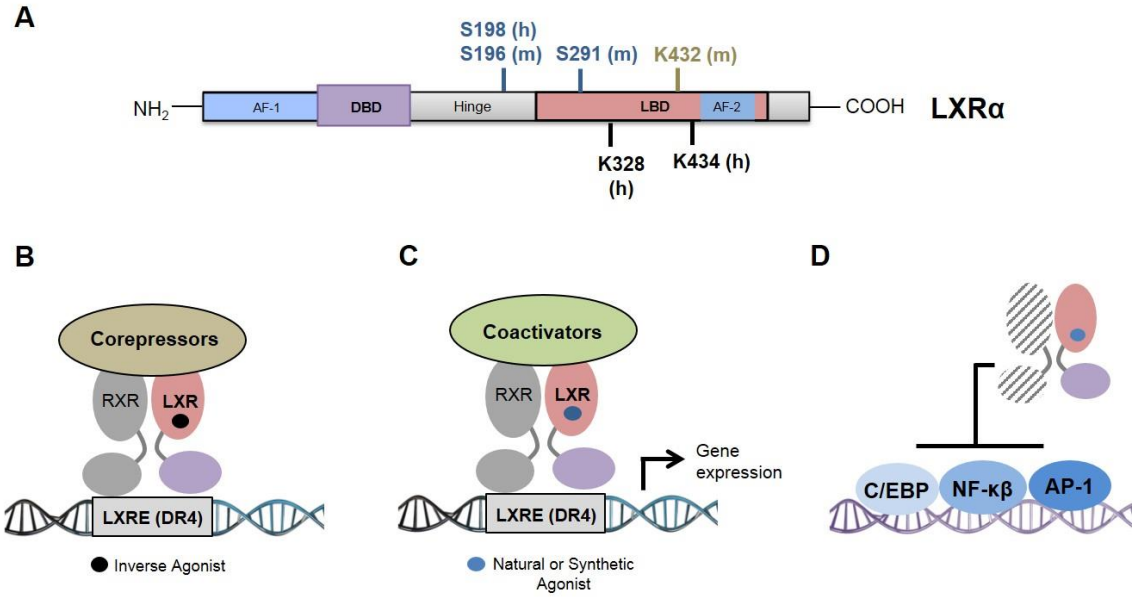

Figure 1.1. Primary structure and general action mechanisms of Liver X Receptors
A) Scheme of the primary structure of LXRα receptor with location of residues modified by acetylation (brown), phosphorylation (blue) and SUMOylation (black). Residues are depicted based on the species of the receptor sequence: human (h) or murine (m).
B-C) *Ligand-dependent transactivation*. In the absence of ligand, gene transcription is silenced. Binding of agonist leads to the exchange from corepressor to coactivator complexes, and induction of gene transcription. D) *Ligand-dependent transrepression.* LXRs can antagonize the activity of other transcription factors upon ligand activation without binding directly to DNA.

Early work by Willy and colleagues showed that the RXR receptor sits on the 5' end of the LXRE and is responsible for the ligand activation of the complex, whereas LXRs contribute to the DNA specificity and bind to the 3' region (13).

Gene activation and repression is mediated by changes in chromatin structure, mediated by a wide variety of proteins that will affect mainly DNA methylation (14), chromatin remodelling and histone modifications (15). In the absence of ligand, the LXR/RXR heterodimer is sitting on the LXREs and interacting with corepressors such as the nuclear receptor corepressor (NCoR) (16) and silencing mediator of retinoic acid and thyroid hormone receptor (SMRT) (17), thereby silencing gene expression, also known as ligand-independent active repression (18) (Figure 1.1. B). The repressive activity of cofactors such as NCoR or SMRT is believed to be caused, in part, by their capacity to recruit histone deacetylases (HDACs), which in turn deacetylase histones and thus compact chromatin and reinforce its repressive effect (19). For example, HDAC1 and 2 are present in the Sin3 complex, where they interact with the NCoR (20) and SMRT (21) corepressors. HDAC3 also binds these corepressors albeit within distinct complexes (22,23).

Once nuclear receptors bind to the ligand, their LBD suffers a structural shift onto a more stable position, inhibiting co-repressor interaction and creating a high-affinity site for co-activator proteins, which interact mainly through the specific sequence motif LXXLL (where L is for Leucine and X for any aminoacid) (24), also known as NR box. These co-activator complexes are responsible for the modification of chromatin structure, thus facilitating the assembly of the general transcriptional machinery to the gene promoter and inducing ligand-dependent transactivation of gene expression (25) (Figure 1.1. C). Nonetheless, this model of transactivation doesn't seem to be exclusive, as other studies have shown that this exchange between corepressor-coactivator complexes and subsequent de-repression of genes requires at times the active removal of the former complex by a proteasome-dependent mechanism (26–28). This process has been proven to be mediated, in part, by transducin beta like 1 X-linked receptor 1 (TBLR1X1 or TBLR1) and its partner TBL1, originally discovered as members of the NCoR/SMRT

complex (27,29–31). Therefore, those signals that induce activation of gene expression must do so in a parallel and coordinated fashion, on one hand activating the transcriptional machinery, as well as relieving the corepressor complex from the promoter.

LXRs can also regulate gene-expression through a mechanism known as ligand-dependent transrepression (Figure 1.1. D). Unlike transcriptional activation, they exert their function not by directly binding to DNA sequences, but rather by antagonizing the activity of other signal-dependent transcription factors, such as the nuclear factor-κβ (NF-κβ) and activator protein 1 (AP-1). It appears this is, in part, the mechanism through which LXRs exert their anti-inflammatory functions (32–34). Interestingly, the same corepressor complexes involved in LXR ligand-independent repression can also be recruited to the promoters of inflammatory genes in the presence of LXR ligands and induce active transrepression by LXRs (35).

LXRs must be present in the nucleus in order to regulate the transcription of their target genes, and the α subtype has been shown to maintain a nuclear localization both in the absence and presence of its ligands (36,37). Nonetheless, several studies have demonstrated that, at least a small fraction of LXRβ, can be found in the cytoplasm, suggesting that this receptor may have other non-nuclear functions involving interaction with other cytoplasmic proteins (38–41). This is likely to occur in a tissue- cell-specific manner; however, detailed enough studies are currently unavailable to conclude this.

1.1.2. LXR ligands

1.1.2.1. Endogenous agonists

LXRs were originally classified as “orphan” receptors, meaning they had no known physiological ligands (2,42); however, it is now well established that oxysterols, oxidised metabolites of cholesterol, are the most important group of LXR natural ligands, capable of activating both isotypes at physiological concentrations (11,43). Oxysterols were first

identified as LXR ligands through the observation that gonad extracts, which contain high levels of sterols, were capable of strongly activating LXRs *in vitro* (11), which raised the possibility that LXRs could be sensitive to cholesterol metabolites. Subsequent screening of over 70 different compounds proved that only those sterols with a position-specific monooxidation on the side chain can bind LXRs with high-affinity and induce the expression of its target genes (11). The establishment of this particular subset of naturally-occurring oxysterols as *bona fide* LXR ligands was later confirmed through proximity-binding studies (43) and reporter assays (44,45). Examples of this group of sterols shown to be important regulators of LXR activity in mouse liver are the 24(S)-Hydroxycholesterol (24(S)-OHC), 25-Hydroxycholesterol (25-OHC), and 27-hydroxycholesterol (27-OHC) (46) (Table 1.1).

Nonetheless, one of the most potent LXR-activating oxysterols found to date is 24(S),25-Epoxycholesterol (24(S),25-EC) (44,47) (Table 1.1). First discovered in the human liver (48), it has a different origin from the rest of oxysterols, since instead of being a metabolite of cholesterol, it is actually formed *de novo* from a parallel cholesterol synthesis pathway (49) (Figure 1.2).

Later, Yang *et al*. found that stigmasterol, a plant sterol that shares a great similarity with cholesterol, increased the transcriptional activity of LXR (50). This led to the discovery of 24-Dehydroxycholesterol (or Desmosterol), an intermediate of the cholesterol biosynthetic pathway, as a molecule that binds directly to LXR and activates its transcriptional activity (51) (Table 1.1). Subsequent studies have shown desmosterol to be the main endogenous ligand found on mouse macrophage foam cells and human atherosclerotic lesions; where it induces LXR target genes and supresses pro-inflammatory responses (52). Nonetheless, the effect of this ligand on LXR activity in other cell types and tissues is still to be determined.

Albeit sometimes controversial, several studies have emerged recently claiming that other compounds not structurally-related to cholesterol are also capable of activating LXRs and act as their ligand at physiological concentrations. For example, Mitro and colleagues suggested that glucose can bind to and consequently activate LXRs *in vitro* (53). However, it was later proposed that the aforementioned effects of glucose, a hydrophilic compound, were in fact caused by its downstream signalling, presumably through post-translational modifications, rather than the direct binding to the LXR highly hydrophobic ligand-binding pocket (54).

	Compound	Effects	References
Endogenous Agonists	**22RHC** (22(R)-Hydroxycholesterol)	• EC_{50} = 1.5 μM • Intermediate in hepatic synthesis of bile acids and steroid hormones	Janowski *et al*., 1996 (11)
	24,25EC (24(S),25-Epoxycholesterol)	• EC_{50} = 460 ± 80 nM • Product in cholesterol biosynthetic shunt pathway	Lehmann *et al*., 1997 (44)
	25-OHC (25-Hydroxycholesterol)	• EC_{50} = 1.16 ± 0.02 μM • Suppressor of SREBP activity	Spencer *et al*., 2001 (45) Adams *et al*., 2004 (55)
	24-OHC (24(S)-Hydroxycholesterol)	• EC_{50} = 7 μM (LXRα) and 1.5 μM (LXRβ) • Most abundant oxysterol in the brain	Lehmann *et al*., 1997 (44)
	27-HC (27-Hydroxycholesterol)	• EC_{50} = 85 nM (LXRα) and 71 nM (LXRβ) • Produced in response to cholesterol loading	Fu *et al.,* 2001 (56)
	Desmosterol (24-Dehydroxycholesterol)	• EC_{50} **n/a** • Present in high concentrations in atherosclerotic foam cells	Yang *et al*., 2006 (51)
	Stigmasterol	• EC_{50} **n/a** • Plant sterol, source of dietary cholesterol	Yang *et al.,* 2004 (50)
Endogenous Antagonists	**Unsaturated Fatty Acids**	• pIC_{50} **n/a** • Inhibits LXR's binding to coactivators and DNA	Ou *et al.,* 2001 (57) Yoshikawa *et al.,* 2002 (58)
	GGPP (Geranylgeranyl Pyrophosphate)	• pIC_{50} **n/a** • Inhibits LXR/RXR heterodimerization and binding to DNA	Forman *et al*., 1997 (59) Yeh *et al*., 2016 (60)

Table 1.1. LXR endogenous ligands

1.1.2.2. Synthetic agonists

Nowadays, there are several synthetic compounds that act as potent LXR activators, the most commonly used in pre-clinical research being the non-steroidal full agonists T0901317 (61) and GW3965 (62) (Table 1.2). T0901317 was the first and most extensively studied synthetic LXR activator; however, later studies showed that this molecule can also activate the nuclear receptors FXR (63) and PXR (64), prompting the need for more selective ligands. On the other hand, GW3965 was initially identified by screening a library of tertiary amines, standing as a full and selective agonist for both human LXRα and LXRβ (62). These two synthetic compounds have been shown to inhibit atherosclerosis development in several animal studies (65,66). Unfortunately, side-effects such as observed increase in hepatic and plasma triglycerides (61,65) haven't allowed for these molecules to progress into human therapeutics. Although these first-generation agonists haven't been proved suitable as pharmaceutical drugs, they still stand as one of the main tools for conducting clinical research on LXR activity. Concurrently, subsequent efforts on LXR therapeutics have focused on bypassing the afore-mentioned undesirable effects. Examples of these new compounds are the small intestine-specific agonist GW6340 (67) and the synthetic oxysterol DMHCA, a compound that has been shown to reduce atherosclerosis is mouse models in a gene-selective manner, avoiding induction of hepatic steatosis and hypertriglyceridemia (68) (Table 1.2). More recently, the pharmaceutical company GlaxoSmithKline has created new synthetic compounds with specific actions, i.e. GSK9772 is capable of inducing the transrepressive effects of LXR on inflammatory genes without promoting the expression of lipogenic genes (69) (Table 1.2).

	Compound	Effects	References
Synthetic agonists	**T0901317** *N*-(2,2,2-trifluoroethyl)-*N*-[4–(2,2,2-trifluoro-1-hydroxy-1-trifluoromethylethyl)-phenyl]-benzenesulfonamide	• EC_{50} = 20 nM • First described LXR synthetic compound, can also activate FXR and PXR • Used in research only	Schultz et al., 2000 (61) Houck et al., 2004 (63) Mitro et al., 2007 (64)
	GW3965 3-[3-[N-(2-Chloro-3-trifluoromethylbenzyl)-(2,2-diphenylethyl)amino]propyloxy]phenylacetic acid	• EC_{50} = 125 nM • Proven to reduce atherosclerosis in two *in vivo* models	Collins et al., 2002 (62) Joseph et al., 2002 (65)
	GSK9772 4-[(Butyl{4-[2,2,2-trifluoro-1-hydroxy-1 (trifluoromethyl)ethyl]phenyl} amino)methyl]-2,6-dichlorophenol	• LXRβ EC_{50} = 30 nM • Induces great LXR transrepressive activity via a SUMOylation-dependent mechanism	Chao et al., 2008 (69)
	DMHCA N,N-dimethyl-3β-hydroxycholenamide	• LXRα EC_{50} = 0.41 µM	Kaneko et al., 2003 (70)
	GW6340	• Intestinal-specific LXR agonist, it is the ester form of GW3965 • EC_{50} **n/a**	Yasuda et al., 2010 (67)
Synthetic antagonist	**GSK2033** (2,4,6-Trimethyl-N-{[30-(methylsulfonyl)-4-biphenylyl]methyl}-N-{[5-(trifluoromethyl)-2-furanyl]methyl}benzenesulfonamide)	• LXRβ pIC_{50} = 7.5 nM • First potent synthetic LXR antagonist • Rapid hepatic metabolism impedes its *in vivo* use	Zuercher et al., 2010 (71)
Synthetic inverse agonist	**SR9238** Ethyl 5-[[[[3'-(Methylsulfonyl)[1,1'-biphenyl]-4-yl]methyl][(2,4,6-trimethylphenyl)sulfonyl]amino]methyl]-2-furancarboxylat	• LXRα pIC_{50} = 214 nM • LXRβ pIC_{50} = 43 nM • Acts by increasing LXR's interaction with corepressor	Griffett et al., 2013 (72)

Table 1.2. LXR synthetic ligands

1.1.2.3. Antagonists and inverse agonists

Few compounds have been shown to directly antagonise LXR activity endogenously. Unsaturated fatty acids, such as arachidonic acid, can inhibit the LXR-mediated transcription of Srebp-1c *in vitro* by acting as a competitive agonist of LXR endogenous ligands thus decreasing binding of the receptor to coactivators (57) and/or to DNA (58) (Table 1.1). Furthermore, geranylgeranylpyrophosphate (GGPP), a metabolite of mevalonic acid which is a precursor in the cholesterol biosynthetic pathway, also inhibits LXR activity by two different mechanisms: interfering with LXR/RXR heterodimer formation, and/or binding of the receptor(s) to DNA (59,60) (Table 1.1). Lastly, LXR antagonism through the reduction of cofactor recruitment has also been shown for several cholesterol sulfates found in human plasma (73).

Regarding synthetic compounds, GlaxoSmithKline has recently identified GSK2033 as an LXR antagonist that displays high binding affinity for LXR and antagonises its target gene expression *in vitro* (71) (Table 1.2). However, this drug failed to repress the expression of LXR target genes and inflammatory genes in the liver of mice on a diet-induced NAFLD model (74). Intriguingly, SR9238, a novel liver selective LXR inverse agonist, has been recently shown to suppress hepatic fatty acid synthesis and lipid accumulation while also inhibiting hepatic inflammation in a diet-induced obesity rodent model (72,75) (Table 1.2).

1.1.3. LXR effects and their therapeutic opportunities

1.1.3.1. Cholesterol homeostasis

Cholesterol and its metabolites serve essential functions in eukaryotic cells, such as cell proliferation (76,77). However, abnormally high cholesterol levels in the system can have serious consequences leading to cellular toxicity and the development of several pathologies, including cardiovascular disease (78) and diabetes (79). For this reason,

vertebrate cells have evolved to tightly regulate cholesterol homeostasis, which involves the control of cholesterol uptake, biosynthesis, catabolism to bile acids and excretion. Numerous studies for over the past 20 years have established LXRs to play a key role as modulators of lipid metabolism. LXRs act as whole-body cholesterol sensors, by responding to high intracellular sterol levels and driving, in consequence, the expression of several genes involved in the transport, catabolism and elimination of cholesterol.

Mammalian cells acquire their cholesterol from dietary sources, as well as from endogenous biosynthesis. Despite interpersonal differences, including genetic variations and dietary styles, the biggest source of cholesterol is from *de novo* synthesis, as dietary availability and intestinal absorption of cholesterol can be limited. It must be noted, though, that humans and mice have significant differences in their synthetic rates; whereas mice can synthesise an average of ~160 mg/day/kg of cholesterol, the daily rate in humans is approximately ~10 mg/day/kg (80). Moreover, cholesterol synthesis in the liver compared to other extrahepatic tissues has been proven to have a bigger contribution in mice than in humans (81). These and other differences need to be considered when translating findings in mice and other rodents onto humans. Indeed, these differences are behind the need to genetically modify mice and alter their cholesterol metabolism in order to use them as *in vivo* experimental models of disease that are more comparable to the human pathology.

1.1.3.2. Cholesterol biosynthesis

The cholesterol molecule is obtained from Acetyl CoA in a serial three-stage process consisting on a total of 30 different enzymatic reactions (82). A diagram depicting the cholesterol biosynthesis pathways as well as the main enzymes involved can be found in Figure 1.2.

.

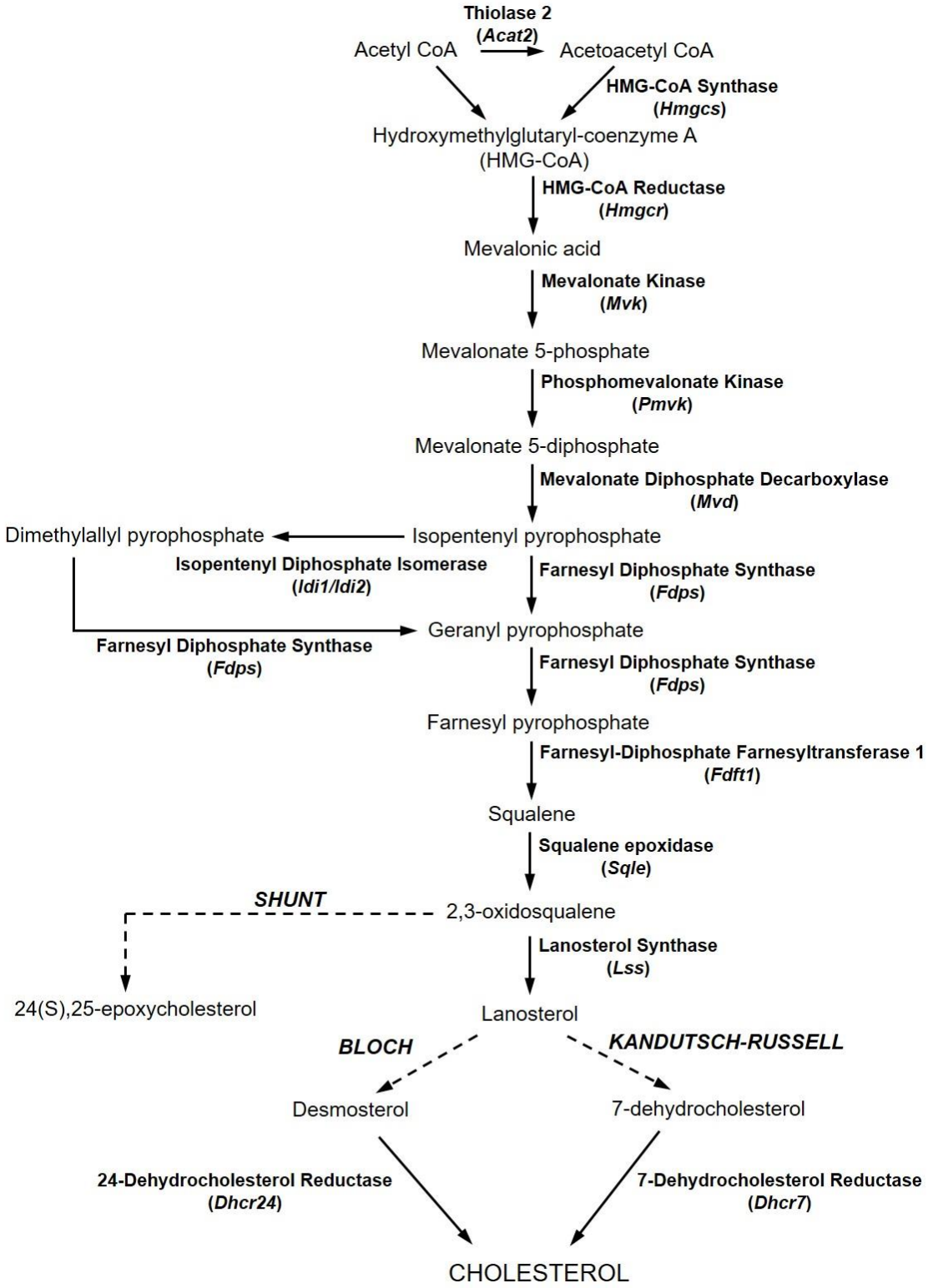

Figure 1.2. Cholesterol biosynthetic pathway

Scheme showing the main steps and enzymes involved

The first part of this process is known as the Mevalonate Pathway, and it takes place in the cytosol. The Acetyl CoA utilised in this process is obtained as a product of mitochondrial (i.e. fatty acid oxidation) and cytosolic (glycolysis) metabolic processes. The rate-limiting enzyme of this section is hydroxymethylglutaryl CoA reductase (HMG-CoAR), which converts HMG-CoA into mevalonic acid and is a target for the extensively used lipid-lowering drug statins (83). This step ends with the production of isopentenyl pyrophosphate (IPP), a key building block for the production of cholesterol and many other molecules such as steroid hormones. The second step consists of the condensation (chemical reaction where two or more molecules fuse to form a new one) of six IPP molecules into squalene. The third and last stage starts with the conversion of squalene into lanosterol, this being the first committed step in the synthesis of cholesterol. The last 19 downstream steps can occur through two different parallel pathways, that differ mainly on the step in which the carbon 24 double bond is reduced. That is, in the Kandutsch-Russell pathway, cholesterol is obtained from the reduction of 7-dehydrocholesterol by 7-Dehydrocholesterol Reductase (DHCR7) (84); whereas in the Bloch pathway, desmosterol serves as the immediate cholesterol precursor and is catalysed by the 24-dehydrocholesterol reductase (DHCR24).

1.1.3.3. Cholesterol absorption

To relieve the energetic burden of constant cholesterol *de novo* synthesis, organisms have evolved to increase their rate of cholesterol take up, performed through its absorption in the gastrointestinal tract. Dietary intake provides about a quarter of the cholesterol entering the intestinal lumen, while the remaining three-quarters are derived from biliary cholesterol excretion from the liver. Due to the lipophilic nature of the cholesterol molecule, its absorption by intestinal enterocytes first requires its emulsification, solubilisation, and transportation into micelles (85).

Several proteins have been identified for their role on intestinal cholesterol uptake. Absorption of free cholesterol contained in the micelles is mediated by Niemann–Pick

C1 Like 1 (NPC1L1), a receptor located in the brush (intestinal) border of the enterocytes found in the jejenum, the middle segment of the small intestine (86). Ezetimibe, a widely-used drug for the treatment of hypercholesterolemia, effects its action by selectively blocking NPC1L1 (87), and thus causing a reduction in Low Density Lipoprotein (LDL)-cholesterol in plasma of around 17% (88). NPC1L1 colocalizes with the ATP-binding cassette (ABC) transporters ABCG5 and ABCG8 in the proximal part of the small intestine (89,90). These proteins are responsible for the efflux of the intracellular cholesterol back into the lumen (91) and therefore antagonise the actions of NP1CL1, creating a fine balance between cholesterol uptake and excretion that will shift depending on the need for cholesterol. The remaining cholesterol in the enterocytes that has not been effluxed will then be esterified by the Acyl-CoA:cholesterol acyltransferase 2 (ACAT2) and packaged into chylomicrons alongside triglycerides and phospholipids for its transport to the lymph. Intracellular cholesterol can also be transferred into apoAI-High Density Lipoprotein (HDL) particles via ATP-binding cassette transporter A1 (ABCA1). Nonetheless, *in vivo* studies with animals lacking the intestinal Abca1 gene have proven that this transporter has no effect in the regulation of cholesterol intestinal absorption (92).

1.1.3.4. Cholesterol catabolism and excretion

Cholesterol can be removed from the body in two different forms: either as a neutral sterol, or after it has been catabolised into bile acids (93). Both compounds are excreted mainly through the faeces, although there is also a minimal part that can be excreted through the skin (94).

Cholesterol excretion is performed in great part through Reverse Cholesterol Transport (RCT), a multi-step process by which peripheral cholesterol is returned to the liver where it gets sent to the intestinal lumen through the bile for its faecal removal. In the first part of this process, cholesterol accumulated in peripheral cells and tissues (i.e. macrophages) is sent to the liver mainly through HDL particles (95). This step is

facilitated by the ATP-binding cassette transporters ABCA1 (96,97) and ABCG1 (98), which efflux intracellular cholesterol onto lipid-free apolipoproteins (such as apoAI, apoCII and ApoE) and mature HDL particles, respectively. Consequently, Tangier Disease (OMIM entry #205400), a recessive homozygous disorder that impairs the function of the *ABCA1* gene, is characterised by low levels of circulating HDL and subsequent cholesterol deposition in several organs (99).

In the second step of RCT, circulating lipoproteins are taken up by the liver primarily by the LDL-Receptor (LDLR) for LDL and Very Low Density Lipoproteins (VLDL) (100) uptake, and the scavenger receptor B1 for HDL uptake (101). Once in the liver, cholesterol is secreted apically from the hepatocytes to the bile duct directly as free cholesterol or as bile acids. Again, due to the hydrophobic nature of cholesterol and of phospholipids, their biliary excretion needs to be coupled with salts that will solubilize these compounds due to their "detergent" characteristics. Therefore, secretion rate of bile acids regulate cholesterol and phospholipid excretion (102). Cholesterol and plant sterols are secreted to the bile by the ABCG5 and ABCG8 transporters (91), whereas bile acid excretion is elicited mainly by ABCB11, also referred to as the bile salt export pump (BSEP) (103). It must be noted though, that animals deficient for the *Abcb11* gene show no drastic phenotype as they still have considerably residual bile acid excretion (104), suggestive of a compensatory mechanism, found to be through an increase in the MDR1 (Mdr1a and Mdr1b in mice) transporter (105). Then, biliary cholesterol enters the lumen, where a small fraction of it will be reabsorbed and the rest will leave the body via faecal excretion.

LXRs are substantially involved in hepatic lipid metabolism, and its importance was first shown *in vivo* in a mouse strain lacking the LXRα isoform ($Lxra^{-/-}$) (106). These animals were unable to catabolise dietary cholesterol, which led to rapid accumulation of cholesteryl esters in the liver, in part due to their incapacity to induce the expression of the Cholesterol 7 alpha-hydroxylase (CYP7A1) gene, which encodes the rate-limiting enzyme in the classical pathway of cholesterol conversion to bile acids. It must be noted

that although LXRβ is also found in the liver (4), and both isoforms share the same ligand-binding specificity, $Lxrb^{-/-}$ (LXRβ knock-out) mice show resistance to dietary cholesterol (107), indicating that LXRα is the predominant isoform involved in hepatic cholesterol metabolism and that the α and β subtypes don't necessarily have redundant roles. This is mainly based on their different expression patterns, since they both share a high level of structure homology (see section 1.1.1) and bind to the same ligands (see section 1.1.2).

Interestingly, mice deficient for both LXR subtypes develop several degenerative processes in the brain, such as enlarged brain blood vessels, in part caused by alterations in the cholesterol metabolism in these animals as well as an increased presence of lipid droplets in the brain (108).

Nonetheless, a big part of the faecal cholesterol excretion is not done through the classical hepatobiliary pathway, but through an alternative mechanism known as Transintestinal cholesterol excretion (TICE). The finding of this mechanism arose from the observation that people and animals that had very low levels of biliary excretion were still able to maintain, or even increase, their net cholesterol excretion levels (109–111). Briefly, in TICE cholesterol in the blood can be excreted directly into the faeces *via* intestinal enterocytes. Even though the specific molecular mechanisms through which TICE occurs remain unknown, several recent studies have demonstrated that LXR and PPARδ agonists induce this process (110,112,113). Regardless, the contribution that TICE has on healthy humans is still unclear at present.

One of the best studied effects of LXRs is the promotion of RCT (114,115), a multi-step process by which peripheral cholesterol is returned to the liver for excretion, hence making these receptors attractive drug targets to combat cardiovascular diseases. LXRs control the expression of members of the ATP-Binding cassette (ABC) family of transporters, including the members from the sub-family A1 (ABCA1) (116) and G1 (ABCG1) (117), whose function is the efflux of cholesterol from inside the cell, i.e.

macrophages, to lipoproteins found in the plasma for its transport (see section 1.1.3.1; or the ABC transporters, sub-family G members 5 and 8 (ABCG5 and ABCG8, respectively), responsible for limiting sterol absorption in the gut, and mediating its excretion from the liver (118) (see section 1.1.3.1). In two different animal models of atherosclerosis, it was reported that administration of GW3965 was able to decrease the development of atherosclerotic lesions, as a direct result of the increased expression of *Abca1* in macrophage foam-cells (65). However, recent studies are suggesting that it is indeed the activation of LXR on other tissues, like the liver (119) and intestine (115), that are key in the promotion of RCT and consequent reduction of atherosclerotic lesions, highlighting the importance of LXR activity in specific organs for whole-body effects.

1.1.3.5. Fatty acid and triglyceride metabolism

Alongside the adipose tissue, the liver is the main responsible for fatty acid and triglyceride synthesis from glucose and citrate, a process known as *de novo* lipogenesis (DNL). This is a highly regulated mechanism that starts with the conversion of acetyl-CoA to malonyl-CoA by the acetyl-CoA carboxylase (ACC) enzyme, which creates the essential substrate for fatty acid formation (120). Then, a sequential addition of two-carbons by fatty acid synthetase (FAS) will lead to the production of palmitate (C16:0) (121), which can be further elongated and/or desaturated through the introduction of double bonds in their structure by several enzymes located in the endoplasmic reticulum membrane. Fatty acid elongation is catalysed by elongation of very long-chain fatty acid (ELOVL) proteins; out of which Elovl6, which catalyses elongation of fatty acids consisting of 12, 14 or 16 carbons, is of particular importance since mice deficient for this protein are more susceptible to developing hepatic steatosis and obesity, but are somehow protected against insulin resistance (122).

Fatty acid length and desaturation status have important consequences on the fate and impact that these lipid species have on hepatic homeostasis and play an important role in the development of diseases with a metabolic component, as is the case of Non

Alcoholic Fatty Liver Disease (NAFLD) (123,124). A key enzyme involved in fatty acid desaturation is stearoyl-CoA desaturase (SCD), a rate-limiting enzyme in the synthesis of monounsaturated fatty acids from saturated fatty acids (125). In rodents, this enzyme family contains two members, SCD-1 and SCD-2, whose expression has been shown to be differently regulated (126). Lastly, these newly synthesized fatty acids will be used to esterify glycerol-3-phosphate in order to generate lysophosphatidic acids, which along the line, will be processed into diacylglycerols, followed by the formation of triglycerides through acyl-CoA:diacylglycerol acyltransferase (DGAT) (127).

LXRs control the expression of several genes involved in fatty acid and triglyceride metabolism, mainly through the modulation of the transcription factor sterol regulatory element binding protein-1c (SREBP-1c) (128,129), as well as the transactivation of some of its direct target genes, such as *Fas* (130) and *Scd-1* (131).

Moreover, fatty acids can reach the liver through their uptake from the circulation (132). This process has proven to be more complex than initially thought, and basically depends on the physical properties of fatty acids (133). Initially, it was presupposed that fatty acids would just diffuse through the cell membrane (134), although there is now strong evidence for protein-mediated transfer. Some of these proteins are part of the family of fatty acid transport proteins (FATPs) (135) and the scavenger receptor B3 (SCARB3 or CD36) (136). A recent study has established *Cd36* as an LXR target gene (137), and proposed that, besides increased *de novo* lipogenesis, LXR activity was promoting increased fat levels in the liver through the upregulation of this receptor and its consequential rise in fatty acid uptake.

Once in the cytosol, and due to their intrinsic hydrophobic nature, fatty acids will need to be transported between organelles by a set of proteins known as fatty acid binding protein (FABP). Out of this family, the most highly expressed isoform in the liver is L-FABP (138). The relevance of this protein in the regulation of hepatic fat metabolism was

demonstrated in mice deficient for the *L-Fabp* gene, which showed to be protected from diet-induced obesity and hepatic steatosis (139,140).

1.1.3.6. Glucose metabolism

More recently, a line of research has arisen involving LXRs with glucose homeostasis. Activation of LXRs by their synthetic agonists induces a significant decrease in blood glucose in a rat model of Type 2 Diabetes, through the suppression of gluconeogenic genes in the liver (141), and improves glucose tolerance in a diet-induced obesity and insulin resistance model (142). Moreover, deletion of both isoforms of LXR (Lxrαβ$^{-/-}$ or double knock-out) shows resistance to diet-induced obesity and its consequent insulin-resistance (143). Tissue-specific improvement of insulin resistance was further confirmed on a model of mouse obesity (ob/ob background) as well as a protective effect against fatty liver and hepatic steatosis (144).

1.1.3.7. Inflammation and fibrosis

A large amount of evidence has emerged showing that besides its role in lipid homeostasis, LXRs also function as transcriptional repressors of a specific cluster of inflammatory genes, antagonizing several pro-inflammatory stimuli in conjunction with other nuclear receptors (33). LXR function in immunity regulation has been demonstrated through many pathological contexts; as they are expressed in several immune cells, such as neutrophils and T-lymphocytes (77), although their role in macrophage biology has received a particularly large interest, due to their contribution to the development of atherosclerosis (145). Indeed, *Lxra*$^{-/-}$*Lxrb*$^{-/-}$ mice, exhibit increased susceptibility to infection by *Mycobacterium tuberculosis,* an effect caused in part by dysregulation of Th1 and Th17 responses in the lungs of these animals (146).

Joseph *et al*. showed that LXR activation inhibits the expression of several inflammatory-mediators, such as *Cox-2* and *Il-6*, both in an *in vitro* and *in vivo* model of contact dermatitis (32). This same group later showed that certain types of inflammatory stimuli

are capable of repressing LXR target genes, such as *Abca1* and *Srebp-1c* (147), establishing a crosstalk between inflammation and lipid metabolism in macrophages, mediated through LXR.

Beyer and colleagues were the first ones to demonstrate LXR's anti-fibrotic properties, through the use of T0901317, the potent synthetic LXR agonist, on several animal models of skin fibrosis (148). Intriguingly, the authors argued that the observed effect upon LXR activation was mediated by a reduced expression of interleukin (IL)-6 by macrophages, and not through a direct effect on fibroblasts. Indeed, a recent study looking at the regulation of LXRα by the microRNA (miR)-155, showed that increased lung fibroblast LXRα expression and activity in miR-155 knock-out mice correlated with exacerbated bleomycin-induced lung fibrosis (149). Moreover, they also demonstrated that human lung fibroblasts from patients with Idiopathic Pulmonary Fibrosis (IPF) have constitutively higher LXRα protein levels. Therefore, these contradicting studies suggest that LXR activity is probably tissue and context specific.

With regard to liver disease, LXRs have demonstrated strong anti-inflammatory and anti-fibrotic activities in several *in vivo* models. Certainly, treatment of hyperlipidemic mice with T0901317 reduced hepatic inflammation and caused reduction of diet-induced NASH in these animals (150). This was due to the receptor's ability to repress the expression of several pro-inflammatory mediators. Moreover, mice lacking both Liver X Receptors display a higher fibrotic response in a model of chemical acute liver injury (151). Consequently, LXRs are emerging as important therapeutic targets for the management of liver inflammation and fibrosis. Intriguingly, a novel liver selective LXR inverse agonist (SR9238) was recently shown to suppress hepatic fatty acid synthesis and lipid accumulation while also inhibiting hepatic inflammation in a diet-induced obesity rodent model (152,153). Thus, the dichotomy in LXR function as a lipogenic agent on one hand, and a strong inhibitor of inflammation and fibrosis on the other must be further elucidated in order to establish how its modulation can be translated into a therapeutic target.

1.1.4. Post-translational modifications of LXR

1.1.4.1. Acetylation

Acetylation of lysine residues was initially identified in histones for their critical role in the control of gene expression (154). Enzymes that add or remove acetyl groups from proteins are named histone acetyltransferases (HATs) and HDACs, respectively. Approximately 85% of all eukaryotic non-histone proteins are acetylated (155). In mammals, there are 2 different families of HDACs. The classical HDAC family (comprising HDAC 1-10) and the sirtuin family of NAD+-dependent deacetylases, also known as Type III HDACs (155). HDACs can act as part of large multiprotein complexes.

Removal of acetyl groups from lysines in LXRs by the SIRT1 deacetylase (at K432 in LXRα and K433 in LXRβ), promotes the receptor's ubiquitination and subsequent degradation by the proteasome, while being a positive regulator of its transcriptional activation (156) (Table 1.3). Li *et al*. suggested that ligand-dependent deacetylation of LXR and consequent degradation leads to its clearance from gene promoters, which facilitates the next round of transcription and thus increases the expression of its target genes. Interestingly, this study also demonstrated that animals deficient in *Sirt1* showed higher levels of LXRA protein and displayed impaired lipid metabolism and defective Reverse Cholesterol Transport. This was in part due to reduced *Abca1* expression and subsequent decrease in HDL levels, as well as increased hepatic and testicular cholesterol levels (Table 1.3). This mechanism was further supported by a study in human skeletal muscle, where SIRT1 was shown to regulate the expression of the lipogenic LXR target gene *Srebp1c* (157).

Modification	Residue	Mechanism	Effect on activity	*In vivo* effects	References
Deacetylation	Lys432 (m) (LXRα) Lys433 (m) (LXRβ)	Ubiquitination of receptor	↑	Deficiency causes impaired lipid metabolism and decrease in plasma HDL levels in mice	Li *et al*.,2012 (142) Defour *et al*.,2012 (143)
Phosphorylation	Ser198 (h) Ser196 (m) (LXRα)	NCoR recruitment	↓ (gene specific)	Decrease leads to reduction in hepatic fat in mice on a HFD Induction caused reduction of circulating cortisol and glucose in rats	Chen *et al*.,2006 (150) Cho *et al*., 2015 (156) Hwahng *et al*.,2009 (155) Torra *et al*.,2008 (149) Yamamoto *et al*., 2007 (152) Wu *et al*., 2015 (151)
	Thr290 (m)	Decreased DNA binding Reduced coactivator and increased corepressor recruitment	↓		
	Ser291(m)				
SUMOylation	Lys328,434 (h) (LXRα) Lys410,448 (h) (LXRβ)	Increased correpressor interaction	↑ Transrepression		Ghisletti *et al*., 2007 (29) Huang *et al*.,2011 (160) Pascual-García *et al*., 2015 (161)

Table 1.3. Summary of LXR post-translational modifications with known residues
Residues are described based on whether they refer to the human (h) or murine (m) sequence of the receptor.
Adapted from Becares *et al*., 2016 (158)

1.1.4.2. O-GlcNacylation

GlcNAcylation is the addition and removal of a single sugar modification, O-linked-β-N-acetylglucosamine (O-GlcNAc), to the hydroxyl groups of serine and/or threonine residues of target proteins. The majority of this modification is found on intracellular proteins and around one-quarter of all identified O-GlcNAcylated proteins are involved in transcription or translation (159). GlcNAcylation is catalysed by uridine diphospho-N-acetylglucosamine:polypeptide β-N-acetylglucosaminyltransferase (OGT) and removed by O-GlcNAcase in response to several energetic and nutritional stimuli, including glucose (160) and phosphatidylinositol (3,4,5)-trisphosphate (161), a mediator in the insulin signalling pathway. The activity of these enzymes is strictly regulated and several pathologies have been linked to aberrant GlcNAcylation including Alzheimer's disease and insulin resistance (159).

Albeit controversial, a study claiming that glucose is capable of activating LXRs and act as their ligand at physiological concentrations raised new insights into how LXR activity may be directly regulated by other mechanisms besides ligand binding (53). This was followed by a study on human hepatic cells and an animal model of streptozotocin-induced insulitis and diabetes in which it was reported that LXRs undergo O-GlcNacylation in response to glucose *in vitro* or by refeeding *in vivo* (54). The authors propose that previously reported effects by glucose (53), a hydrophilic compound, were caused by its downstream signalling presumably through post-translational modifications, rather than the direct binding to the LXR highly hydrophobic ligand-binding domain. This study also argues that this modification affects the expression of the lipogenic transcription factor *Srebp1c* although the exact mechanisms through which O-GlcNacylation regulates LXR activity need to be further elucidated.

1.1.4.3. Phosphorylation

Phosphorylation is defined as the covalent modification of phosphate groups to specific amino acids; the most common in eukaryotic cells being serine, threonine and tyrosine. Phosphorylation is catalysed by kinases, and removal of phosphate groups is performed by phosphatases. These processes regulate of almost every single basic cellular process (162).

LXRα is phosphorylated at Serine198 (Ser198 or Ser196 in the human and murine sequence, respectively) both *in vitro*, and *in vivo* in atherosclerotic plaques of ApolipoproteinE-deficient mice (163–165). This modulates LXRα transcriptional activity in a gene-selective manner (see Table 1.3), and is enhanced by both endogenous (24S, 25-epoxycholesterol) and synthetic (T0901317 and GW3965) LXR ligands (163,165). In a murine macrophage cell line stably expressing LXRα ligands for the RXR receptor, such as the 9-cis-retinoic acid (9cRA) and bexarotene inhibited Ser198 phosphorylation, leading to changes in LXR/RXR-regulated gene expression, particularly on genes sensitive to changes in LXRα phosphorylation at this residue, such as *Ccl24* (163). The

Ser198 residue is located in the hinge region of LXRα, and was shown to be targeted by Casein Kinase 2 (CK2) (163). Peptide molecular modelling studies suggest Ser198 phosphorylation affects LXRα conformation, possibly influencing the recruitment of cofactors such as NCoR (163,165). In their article, Pineda and colleagues have mentioned they didn't observe changes in DNA binding by the non-phosphorylatable S198A mutant version of the receptor (163). Nonetheless, how changes in phosphorylation specifically at the S198 residue affects the receptor's binding to DNA or nuclear localisation remains to be shown. Further evidence also supports these gene-selective changes by LXRα phosphorylation. For instance, macrophage expression of CCR7 is markedly induced by LXRα when the receptor is not phosphorylated at Ser198 (165). This is associated with decreased levels of chromatin repression marks (H3K9me3 and H3K27me3) at the *Ccr7* locus in cells expressing the non-phosphorylated version of the receptor.

Phosphorylation of LXRα by other kinases, including Protein Kinase A (PKA), has been reported at several residues (Ser195, Ser196, Thr290, Ser291) in rat primary hepatocytes and mouse liver, although detailed mutagenesis studies were not performed (166). PKA-mediated phosphorylation of LXRα leads to the repression of Srebp1c expression, a well-established LXR target gene, caused by decreased binding of the RXR/LXRα heterodimer to DNA, as well as reduced coactivator (steroid receptor coactivator-1 or SRC-1) and increased corepressor (NCoR) occupancy (Table 1.3). The regulation of LXRα phosphorylation by cholesterol and oxysterols (163) prompted other studies investigating the effect of nutrient-regulated kinases. Oltipraz [4-methyl-5-(2-pyrazynyl)-1,2-dithiole-3-thione] is a member of the dithiolethione family, a series of compounds naturally found in cruciferous vegetables with a broad range of therapeutic uses including chemoprevention (167) and liver fibrosis (168). Interestingly, oltipraz attenuates LXRα phosphorylation at an unspecified serine residue(s) in mouse liver through the inhibition of p70 ribosomal S6 kinase-1 (S6K1) (169), a major downstream effector of the mammalian target of rapamycin (mTOR) signalling pathway. This

decrease in LXRα serine phosphorylation leads to a reduction in Srebp1c target gene expression in culture. In addition, oltipraz administration to mice fed a high fat diet caused a decrease in hepatic fat content, pointing to oltipraz and the modulation of LXR phosphorylation as potential therapeutic targets for the treatment of fatty liver. Furthermore, a recent report examining the metabolic effects of metformin showed this compound induces LXRα phosphorylation (at a threonine residue) in rat pituitary cells. This in turn causes a reduction in the expression of its target gene *Pomc*, a precursor of the adrenocorticotropic hormone, leading to an overall reduction of systemic cortisol and glucose (170). In this context, LXRα threonine phosphorylation is shown to be induced by activated AMPK, which had been previously associated with the pleiotropic actions of metformin.

1.1.4.4. Sumoylation

SUMOylation is the covalent binding or conjugation of members of the small-ubiquitin modifier (SUMO) family to proteins. In mammals, the SUMO family consists of three members: SUMO-1, SUMO-2 and SUMO-3 (171). SUMOylation is reversible, and uses a specific set of enzymes for processing and attachment - such as the E1 SUMO-activating enzyme subunits 1/2 or members of the E3 ligases Protein Inhibitor of Activated STAT (PIAS) family (172) - and removal, known as SUMO peptidases.

As the mechanistic basis for the transcriptional repression of pro-inflammatory genes, Ghisletti *et al*. initially demonstrated that ligand-induced SUMOylation of LXR is required for its interaction with the NCoR corepressor in mouse primary macrophages and RAW264.7 macrophage-like cells (see Table 1.3) (173). In addition to synthetic ligands, these authors demonstrated sumoylation was promoted by the LXR endogenous ligands 22(R)-hydroxycholesterol, 24(S),25-epoxycholesterol, and 24S-hydroxycholesterol. In contrast to PPARγ, whose sumoylation is dependent on PIAS1 and SUMO 1 (174), LXR-mediated transrepression involves SUMOylation by SUMO2 and SUMO3, with HDAC4 acting as the SUMO E3 ubiquitin ligase. It was later shown that the interaction between

SUMOylated-LXR and NCoR was facilitated by Coronin 2A, a member of the actin-binding protein family that acts both as a docking site for LXR and an exchange factor for NCoR, proving necessary for the derepression of several Nuclear Factor- kappa B (NF-κB) induced pro-inflammatory gene promoters (175). Moreover, a later study showed that mutant forms of both LXRs lacking SUMO acceptor sites (LXRα K328R/K434R and LXRβ K410R/K448R) have a decreased capacity to prevent the binding of the pro-inflammatory Signal Transducer and Activator of Transcription 1 (STAT1) transcription factor to the Nos2 promoter (176) (Table 1.3), further establishing the importance of LXR SUMOylation on its transrepressive capacity. However, this transrepression model has now been challenged. Ito and colleagues recently postulated that repression of inflammatory genes by LXRs is dependent on changes in cellular lipid metabolism rather than SUMOylation of the receptor (177). In their report, the authors propose a mechanism whereby LXR-dependent expression of the ATP-Binding Cassette transporter A1 (ABCA1), which mediates intracellular cholesterol efflux to Apolipoprotein A1, is critical for the repression of pro-inflammatory genes by LXR. Increased ABCA1 expression leads to a decrease in membrane cholesterol levels as a result of a higher rate of cholesterol efflux by ABCA1, thus increasing membrane permeability and disrupting Toll-like Receptor (TLR) signalling due to the inability of TLRs to recruit its signal transducers. This study demonstrates that LXRs are capable of strong repressive actions even in the absence of SUMOylation in immortalised mouse embryonic fibroblasts in vitro, suggesting that nuclear receptor activity is regulated by different independent pathways. It would be interesting to assess if this SUMOylation-independent transrepression mechanism also occurs in other cell types and under physiological conditions. Thus, depending on the cell type and disease context, these two models may not be mutually exclusive. In any case, it still remains unclear what the consequences are of altering LXR SUMOylation on inflammatory diseases or other patho-physiological contexts.

1.2. Non-Alcoholic Fatty Liver Disease

1.2.1. Definition and epidemiology

Non Alcoholic Fatty Liver Disease (NAFLD) is a condition that represents a wide spectrum of liver diseases, ranging from simple fatty liver (steatosis), through steatosis accompanied by inflammation with or without fibrosis (steatohepatitis or NASH) that can progress to necrosis, cirrhosis and hepatocellular carcinoma (178,179). NAFLD is currently defined as the accumulation of fat in hepatocytes that surpasses 5% of total liver weight (180); with an alcohol consumption well below the threshold of other alcohol-related diseases and no presence of any chronic viral hepatitis (181,182) or other competing hepatic aetiologies such as steatosis-inducing drugs (183). Even though fatty liver was initially considered to be relatively benign and NASH was seen as the pathogenic extreme of the spectrum, recent studies have established steatosis not only as the consequence but also as a risk factor for metabolic diseases such as insulin resistance and cardiovascular disease (184,185). These results have thus prompted the medical and scientific communities to regard the early stages of NAFLD as less benign than previously thought.

NAFLD risk factors include obesity (186,187), dyslipidaemia (188) and Type 2 Diabetes (189,190), which has placed NAFLD to be considered as the hepatic manifestation of the metabolic syndrome (191,192). For this reason, the prevalence of NAFLD worldwide, but especially in Western countries, has suffered a rapid and dramatic increase. In a recent article, Younossi *et al.* performed a meta-analysis of over 100 different individual studies reaching all continents, and established that NAFLD has a prevalence of around 25% of adults, when diagnosed by imaging (193). This prevalence varies within the different regions in the world, with a higher presence in the Middle East and South America (193). Moreover, out of all the patients diagnosed with NAFLD by biopsy, NASH was present in 59.10% of them, with a progression rate to fibrosis of 9% (193). NAFLD

is also more prevalent in males, and its occurrence has been shown to increase with age (193,194).

Although liver disease is only the third cause of death amongst NAFLD patients (195), it is still in the trajectory of becoming the most common cause for liver transplantation by 2030 (196,197). In addition, the contribution of NAFLD to its associated conditions, i.e. cardiovascular disease and Type 2 Diabetes, provokes NAFLD patients to have an overall higher mortality than the general population (198). Furthermore, individuals with established NASH are at great risk of progressing into liver cancer, increasing their risk of liver-related death (199).

1.2.2. Diagnosis

The gold-standard for NAFLD diagnosis is still the liver biopsy (200), even though one of the main disadvantages of this procedure is its high sampling variability. Hence, in order to maintain some consistency and reproducibility, especially during clinical trials, a standardised score was created by a group of experts known as the NALFD activity score (NAS) (201). This grading ranges from 0 to 8, where a NAS ≥ 5 is considered a definitive NASH diagnosis; and is based on a sum of different scores regarding steatosis (0-3), lobular inflammation (0-3) and hepatocyte ballooning (0-2) (201). Even though fibrosis was initially included in the NAS score, it was later removed from the overall grading as it is less reversible than the other parameters, and thus may not truly reflect changes upon a therapeutic intervention. For this reason, other grading systems such as the "Brunt's fibrosis score" (202), are more commonly used in clinical practice, since they are considered to be better predictors of disease progression (185).

Nonetheless, the highly invasive and costly nature of liver biopsies has urged in the recent years for the use of new methodologies, such as radiologic imaging techniques like ultrasound and magnetic resonance imaging (MRI) (203). Furthermore, whenever diagnosis by image is not possible, serum biomarkers such as Tumour necrosis factor

alpha (TNF-α) and Adiponectin (204,205) can also be used as diagnostic tools. Although these less-invasive techniques have proven to be highly successful at diagnosing steatosis, the presence and location of several key NASH features such as inflammation, hepatocyte ballooning and fibrosis still requires histological assessment of a liver biopsy (200).

1.2.3. Pathogenesis

The pathogenesis behind NAFLD is not yet fully understood, although we know that the mechanisms behind its onset and progression are multifactorial. Initially, the progression from steatosis to NASH had been explained by the "two-hit hypothesis" (206). This considered steatosis or hepatic fat accumulation to act as a "first hit", increasing the susceptibility to liver damage caused by a "second hit", eventually leading to inflammation and/or fibrosis. This second stressor-category comprised of a variety of factors such as oxidative stress (207) or adipose-tissue secreted adipokines (208). However, more recent studies have relegated this hypothesis as oversimplifying and it is now believed that, in fact, it is the presence of a myriad of different factors acting synergistically that is behind NAFLD pathogenesis; including but not restricted to, insulin resistance, oxidative stress and an inflammatory cascade (209).

1.2.3.1. Steatosis and lipotoxicity

Several mechanisms can lead to accumulation of fat in the liver (210) (Figure 1.3). Firstly, this fat can come from external sources as a consequence of excessive dietary energy intake, particularly from diets high in saturated fats and carbohydrates (211), like the so-called "Western diet" (212). Second, expansion and inflammation of the adipose tissue leads to increased lipolysis and higher levels of circulating fatty acids, which will then be taken up by the liver. Under normal physiological conditions, the role of the white adipose

tissue (WAT) is to provide lipid energy to other tissues in the form of Non-Esterified Fatty Acids (NEFAs), which are released as a result of triglyceride hydrolysis by lipases (213).

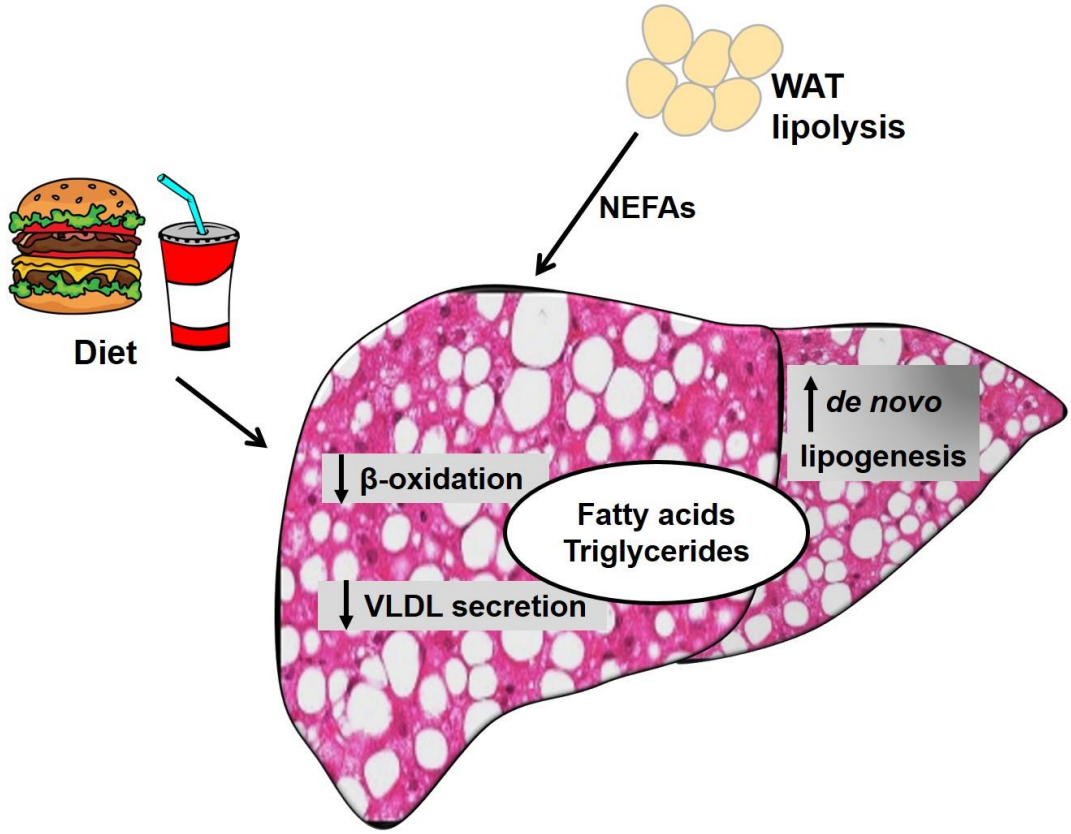

Figure 1.3. Possible sources of hepatic fatty acids and triglycerides contributing to NAFLD pathogenesis

Then, when this high-energy demand is over, WAT lipolysis is suppressed by numerous hormones, such as catecholamine and insulin (213). However, in obese individuals with type 2 diabetes, the adipose tissue undergoes an increase in mass and is subjected to a pro-inflammatory environment, leading to insulin resistance and a consequential rise in the flux of NEFAs to the liver (210,214).

As causes with a hepatic origin, deficiency in fatty acid oxidation and/or increased DNL programmes can also lead to a heightened hepatic fat content (see section 1.1.3.1). Hepatic fat originating from DNL plays a very important role in the pathogenesis of

NAFLD (215), and it can account for a quarter of all triglyceride levels (210). This increase in the lipogenic programme usually arises from hepatic insulin resistance (189,216), even though it remains unknown if insulin resistance is either a cause or a consequence of hepatic steatosis.

The balance in triglyceride levels under steady-state is controlled, in part, by a mechanism known as fatty acid oxidation. This process is needed for the generation of adenosine triphosphate (ATP) and ketone bodies, which will be used for extrahepatic organs for energy whenever glucose levels are low (217). Under normal nutritional states, the preferred source of energy in the body is glucose. However, during prolonged starvation, glycogen gets quickly depleted and metabolic energy needs to be derived from fats (217). Fatty acid β-oxidation occurs in the mitochondria and peroxisomes, where mitochondrial β-oxidation is the dominant oxidative pathway for the disposal of fatty acids under normal physiologic conditions (217). Mitochondrial abnormalities are highly common in patients with both fatty liver and NASH (218–220), which demonstrates that defective fatty acid β-oxidation plays an important role in the pathogenesis of NAFLD.

Lastly, impaired VLDL secretion can also exacerbate hepatic fat accumulation. VLDL is a triglyceride-rich lipoprotein, covered by hydrophilic phospholipids and apolipoprotein B (apoB) 100, and is secreted by the liver in order to transport this fat to peripheral tissues. The rate of VLDL secretion depends not only on the levels of intrahepatic triglycerides, but also on VLDL assembly (221). Thus, deficiencies in VLDL assembly and/or secretion will lead to increased intrahepatic triglycerides (222,223).

As mentioned above, it is now recognised that the progression from fatty liver to NASH is probably due to a combination of several factors, in conjunction with the overall cellular injury caused by high levels of hepatic lipids, also known as lipotoxicity. Besides triglycerides, many other lipid metabolites like NEFAs, phospholipids and cholesterol may also build up; and it is now actually considered that triglyceride accumulation may be in fact acting as an adaptive protective mechanism by mitigating the excess of NEFAs (224).

High levels of neutral lipids will assemble in cytosolic lipid droplets (LDs), a heterogeneous set of structures formed by a lipidic core surrounded by a monolayer of phospholipids (225). Thus, the presence of very large LDs is considered the histological landmark of steatosis. These droplets contain a variable mixture of proteins, including peripilins, whose presence and function has been shown to be also involved in the pathogenesis of NAFLD (226).

1.2.3.2. Apoptosis

Apoptosis, or programmed cell death, can develop in response to fat accumulation (lipoapoptosis), and is now considered to be one of the key pathogenic mechanism behind liver disease (227,228). Hepatocyte apoptosis can occur *via* a variety of mechanisms: both extrinsic, known as receptor-mediated apoptosis, which is facilitated, for example, by the FAS and TNF-related apoptosis-inducing ligand (TRAIL) receptors (227,229,230); as well as intrinsic, activated by intracellular stress, such as lysosomal permeabilization or endoplasmic reticulum (ER) stress (230–232). Regardless of the activating source, apoptotic signalling cascades lead to mitochondrial permeabilization and activation of the downstream effector caspases 3, 6 and 7 (233), a set of cysteine proteases whose action is to promote the ordered disassembly of the cell.

In the context of NAFLD, several experimental models have shown that hepatocyte apoptosis is profibrogenic (234,235). For instance, engulfment of apoptotic bodies by Hepatic Stellate Cells (HSCs), leads to their activation and subsequent increase in their fibrogenic activity (234). Indeed, sustained hepatocyte death is linked to the development of fibrosis in most types of liver disease, such as alcoholic liver disease (236) and viral hepatitis (237).

1.2.3.3. Oxidative stress

Oxidative stress results from the imbalance between the production of Reactive Oxygen Species (ROS) and the presence of antioxidant defences. Characteristic NAFLD features, such as heightened mitochondrial β-oxidation or increased hepatic Cyp2E1 expression can lead to oxidative stress (219,238,239). High levels of ROS induce the oxidative degradation of lipids, also known as lipid peroxidation; as well as oxidative damage to DNA (240). Both of these markers of oxidative stress are found in NAFLD/NASH patients (241–243), even though the specific relation between oxidative stress and disease progression hasn't been fully understood yet.

1.2.3.4. Endoplasmic reticulum stress

The ER is an intracellular organelle responsible for performing essential functions, such as protein folding and post-translational modifications (244). Therefore, any disturbances in normal cell physiology will cause an accumulation of unfolded proteins in the ER lumen, triggering an evolutionary-conserved stress response, known as the unfolded protein response (UPR) (244). The UPR is an adaptive mechanism that allows for the cells to survive upon changes in its physiology and is particularly important in cells with a high secretory nature, such as hepatocytes. This adaptive mechanism involves the induction of a transcriptional programme designed to increase the folding capacity of the ER and reduce the entry of proteins to it. In mammals, the UPR is sensed by three integral proteins: protein kinase RNA-like ER kinase (PERK), inositol-requiring enzyme-1 (IRE1), and activating transcription factor-6 (ATF6) (245). Hence, their downstream mediators are used as markers of ER stress. Upon activation, PERK phosphorylates eukaryotic translation initiation factor-2α (eIF2α), which leads to the expression of activating transcription factor-4 and 3 (ATF-4 and ATF-3), transcription of C/EBP-homologous protein (CHOP) and activation of NF-κB, and growth arrest and DNA damage 34 (GADD34) (246,247), with the aim to decrease overall protein translation. In parallel, IRE1 promotes the splicing of X-box-binding protein-1 (XBP1) mRNA in order to permit

the synthesis of this transcription factor (248), and the subsequent transcription of several genes involved in restoring homoeostasis and prevent cellular toxicity (249). Lastly, ATF6 collaborates with IRE1, where ATF6 induces transcription to increase XBP-1 mRNA (248).

The signalling pathways activated by ER stress have been linked to several other key NAFLD pathogenic pathways, such as lipotoxicity and inflammation. Thus, the link between ER stress and hepatic damage has been studied extensively in the recent years, especially in animal models of the disease (250,251). Yet, a study looking at UPR markers in the livers of patients with NAFLD and NASH couldn't establish a distinctive pattern that correlated with disease progression (252), which further points to NAFLD being a mechanistically heterogenous disease, where progression to NASH may be caused by different mechanisms in different people.

1.2.3.5. Cholesterol

In order to better understand the role that neutral lipids are having on NAFLD pathogenesis, recent studies have assessed the effects of free cholesterol on liver damage. Lipidomic analysis on livers and plasma of NAFLD patients showed that free cholesterol, but not cholesteryl esters, is increased in these patients (253,254). Moreover, *in vitro* and dietary animal models have established that free cholesterol sensitizes the liver to steatohepatitis (255,256). These and other studies provide the foundation that cholesterol metabolism is also involved in NAFLD pathogenesis, but the specific mechanisms linking this lipid with NAFLD pathogenesis still need to be further elucidated.

1.2.3.6. Inflammation

Stressed hepatocytes release a set of proinflammatory signals, also known as metabolic danger signals or DAMPs, that activate both Kupffer cells (KCs) and hepatic stellate cells (HSCs), triggering an inflammatory response known as "sterile inflammation" (since it is not caused by an infection); which, if prolonged, will result in an abnormal wound-healing

response leading to fibrosis (257). Interestingly, it is now recognised that DAMPs are able to activate many pattern recognition receptors, of which Toll-like receptors (TLRs) are the most well-known, and thus trigger the same downstream signalling cascades as in infectious inflammatory responses (258,259). Moreover, high levels of lipopolysaccharides and other microbial compounds that reach the liver due to gut bacterial translocation, can also contribute to the pro-inflammatory hepatic milieu (260,261).

Acute inflammation in the liver is characterized by the production of cytokines and chemokines: i.e. chemokine (C-X-C motif) ligand 1 (CXCL1), IL-1β and TNF-α (262–264); as well as platelet activation and leukocyte recruitment (265,266), including neutrophils and monocytes; and activation and expansion of resident cells, such as HSCs and dendritic cells (267). For example, liver injury leads to the production of monocyte chemoattractants, like monocyte chemoattractant protein 1 (MCP-1 or CCL2) by hepatocytes and activated KCs (268), which in turn will lead to monocyte infiltration (269), that will differentiate and contribute to the pool of hepatic macrophages. Indeed, some lines of evidence point to the capacity of infiltrating monocytes to differentiate into macrophages and replenish fully differentiated KCs (270,271). Nonetheless, whether or not monocyte-derived macrophages ultimately replenish KCs is still a controversial question.

1.2.3.7. Fibrosis

Liver fibrosis and its end-stage manifestation cirrhosis, are characterised by the accumulation of extracellular matrix (ECM), predominantly formed by type I and type III collagens, and occur as the result of a sustained wound healing response to a chronic inflammatory stimulus (272). This accumulation of scar tissue will eventually lead to architectural changes and hepatic stiffness, causing portal hypertension and hepatocyte dysfunction (273).

HSCs are the main executors of hepatic fibrogenesis, after becoming activated and gaining a myofibroblast-like phenotype in response to a wide range of signals (i.e. Transforming growth factor beta or TGF-β), and through interaction with many different cell types, such as KCs (273–276). Moreover, once activated, their fibrotic phenotype, survival and proliferative capacities get perpetuated by several positive feed-back loops (277), which amplifies their fibrotic effects. Also, activated HSCs can acquire pro-inflammatory and immune properties, where not only they secrete several cytokines and chemokines that will in turn expand the overall hepatic inflammatory milieu (278), but can also phagocytise and act as antigen presenting cells (279). Nonetheless, it must be noted that besides HSCs, ECM production in the liver can also originate from other sources, such as activated portal fibroblasts (280,281).

Surprisingly, recent clinical evidence and studies performed on animal models seem to demonstrate that if the inflammatory signal that was driving the fibrotic response is extinguished, early to moderate fibrosis can regress (282,283), even though it still remains controversial if the regressed liver is able to reach the same point as it was “pre-fibrosis”. This regression is thought to be mediated by active ECM degradation by matrix metalloproteinases (MMPs) (284,285), and the disappearance of activated myofibroblasts by apoptosis/senescence (286,287) or rapid killing by NK cells (288).

1.2.3.8. Genetic modifiers of NAFLD

Similar to other complex metabolic diseases (i.e. type 2 diabetes), NAFLD has a considerable heritable component (289). To better characterise this, genome wide association studies (GWAS) are employed to identify genetic susceptibility to a specific disease, in large populations and in an unbiased manner. In the case of NAFLD, several variants have been identified (289), but only a small number of these have been characterised in depth. A very well-validated variant, the rs738409 (Ile148Met) single nucleotide polymorphism (SNP) in the patatin-like phospholipase domain-containing protein 3 (*PNPLA3*) gene, was first identified by Romeo and colleagues, in a GWA study

on patients with and without established NAFLD from various ethnic groups (290). Later studies corroborated this variant as a strong modifier of NAFLD severity, as it highly associates with presence of steatosis and advanced fibrosis (291,292). Furthermore, a second modifier, the human transmembrane 6 superfamily member 2 (*TM6SF2*) variant encoding p.Glu167Lys, has also been established to contribute to NAFLD susceptibility by reducing VLDL secretion (293,294).

1.2.4. Treatment

Successful NAFLD treatments should aim at halting its comorbidities, but also reducing its progression to more advanced forms of the disease.

Since assessment of histological lesions are still the only reliable method to distinguish between fatty liver and NASH, there are currently only a limited number of randomised clinical trials where disease improvement or regression is considered as an endpoint (200). Moreover, competing risk from other related diseases tend to be prioritised. For example, a recent clinical trial assessing the efficacy of the potent FXR activator obeticholic acid (OCA) for the treatment of steatohepatitis was interrupted, partly due to induced lipid abnormalities in OCA-treated patients, including increased circulating total cholesterol and LDL with decreased HDL (295). For this and other reasons, such as the complex and multifactorial nature of the disease, as of 2016 there are still no approved drugs for the direct treatment of NAFLD (296). In addition, there are still no good available markers that allow for the early identification of those patients with the highest risk of progression to steatohepatitis.

Therefore, most therapeutic efforts so far have focused on tackling other components of the metabolic syndrome (297). For example, lifestyle changes, such as exercise and diet restrictions, are commonly used in clinical practice (200). Moreover, significant weight loss as a result of bariatric surgery has shown to have a big impact on histological improvement (282,283). In regard to pharmacological therapies, the use of insulin

sensitizers such as pioglitazone, a selective peroxisome proliferator-activated receptor γ (PPAR-γ) agonist, have demonstrated to have a strong association with significant reduction in steatosis, inflammation, and hepatocellular ballooning, as assessed by liver biopsy in a recent randomized, placebo-controlled, double-blind clinical trial (298).

1.3. Project Hypothesis

Changes in the phosphorylation status of LXRα at Ser196 specifically regulate its activity *in vivo* and have an impact on hepatic lipid metabolism and early signs of fibrosis in response to a high-fat high-cholesterol diet.

1.4. Aims

- Examine the impact of LXRα phosphorylation on modulation of hepatic lipid metabolism and inflammation *in vivo* on the newly generated S196A animals, using a dietary model of NAFLD.
- Determine which are the molecular mechanisms underlying the effects of LXRα phosphorylation on target gene expression, by assessing changes in DNA and cofactor binding.
- Study new stimulants that are capable of inducing LXRα phosphorylation *in vitro*, and the effects that pharmacological impairment of this modification have on the receptor's activity.

Chapter 2. Materials and methods

2.1. Generation of the S196A transgenic animal model

The S196A floxed ($S196A^{fl/fl}$) mouse line was generated by Ozgene Pty Ltd (Bentley WA, Australia). The genomic sequence for the murine LXRα (Nr1h3) gene was obtained from the Ensembl Mouse Genome Server (http://www.ensembl.org/Mus_musculus/), Ensembl gene ID: ENSMUSG00000002108. The mutant fragment, located on Exon 5, contains a serine-to-alanine mutation at Ser196 introduced by site-directed mutagenesis (Figure 2.1. A). The point-mutant exon was delivered into an intronic site inside the targeting vector, placed in opposite orientation and thus without coding capacity (Figure 2.1. B). The targeting construct was electroporated into the Bruce4 C57BL/6 ES cell line. Homologous recombinant ES cell clones were identified by Southern hybridization and injected into BALB/cJ blastocysts. Male chimeric mice were obtained and crossed to C57BL/6J females to establish heterozygous germline offsprings on a pure C57BL/6 background. The germline mice were crossed to a flipase (FLP) recombinase mouse line to remove the FLP recombinase target (FRT)-flanked selectable marker cassette (Flp'd mice) (299), which were used as wild-type (WT) controls throughout this study (Figure 2.1. B). Flp'd mice were crossed with a transgenic C57BL/6 mouse strain carrying a Cre recombinase under the PGK-1 promoter (300), resulting in the inversion and insertion of the lox-flanked mutated (loxP) vector exon 5 region in the sense orientation, and deletion of the wild-type (WT) sequence in most adult cell lineages (S196A mice) while WT controls carry the WT sequence in the sense orientation (Figure 2.1. B) (301). The germ-line expression of the Cre-recombinase causes the lox sites to be recombined permanently and the targeted allele becomes a constitutive knock-in of the mutant exon. Therefore, presence of the PGK-1 Cre is no longer necessary on following progeny.

The offspring of S196A mice had no apparent dysmorphic phenotypes and their development growth was similar to wild-type C57BL/6 mice (Table 2.1) (302,303).

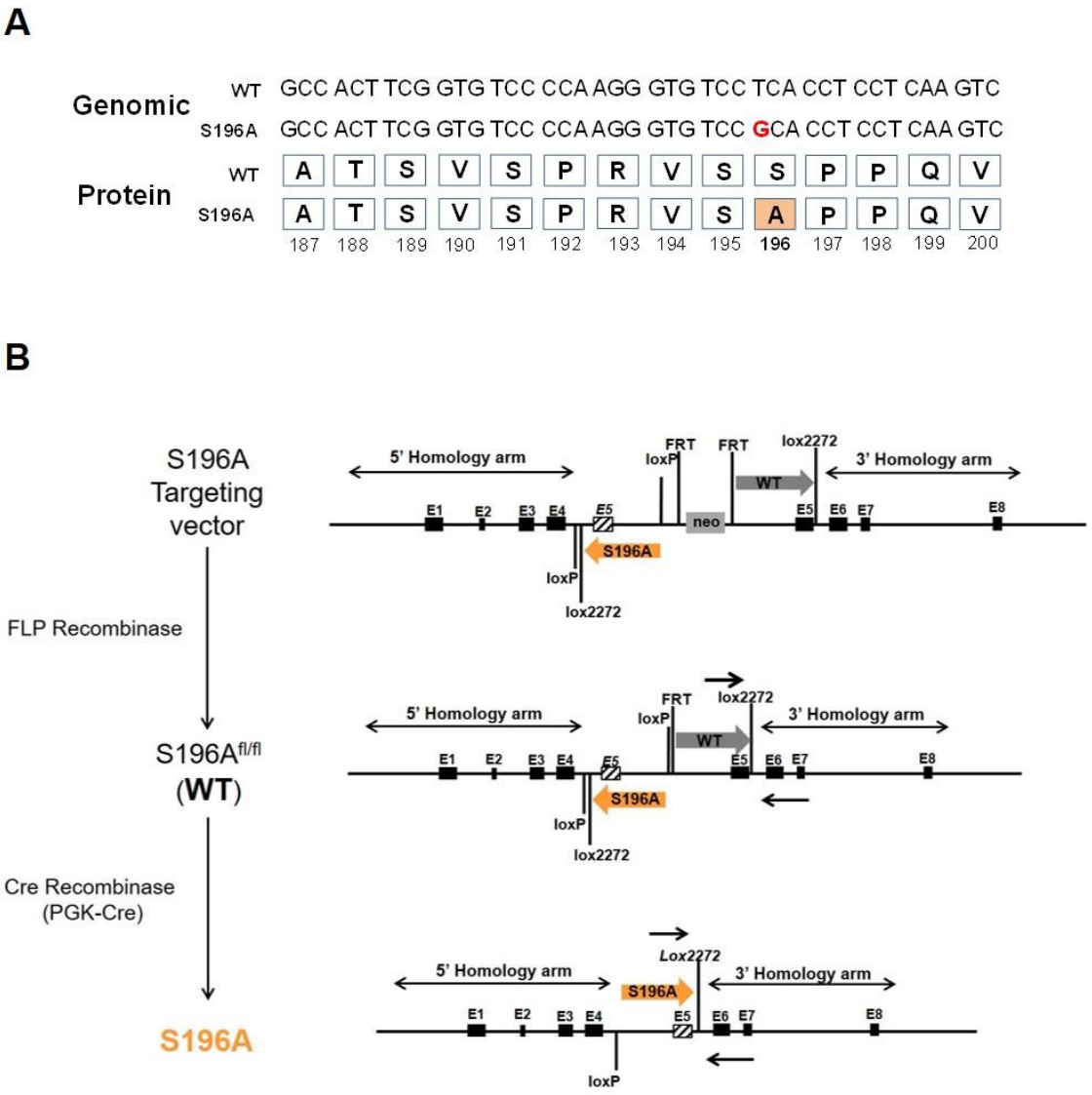

Figure 2.1. Strategy for the generation of the S196A mouse line using a Cre/loxP system.

A) Scheme showing the single-point mutation (red nucleotide) introduced in the LXRα exon 5 sequence and its translation into a serine to alanine change on the Ser196 residue.

B) Targeting construct containing the loxP and FRT sites, the predicted homologous recombinant alleles when crossed with FLP Recombinase, and the LXR knock-in locus after PGK-1 Cre-mediated recombination, thus incorporating the mutated vector in most adult cell lineages (S196A).

Weeks after weaning	0	1	2	3	4
WT (g)	18.64 ± 0.78	18.75 ± 0.91	19.17 ± 0.84	18.93 ± 1.61	22.67 ± 0.84
S196A (g)	18.36 ± 0.95	18.99 ± 1.20	19.77 ± 1.42	19.96 ± 1.37	21.83 ± 0.88
T-test	0.71	0.57	0.55	0.43	0.27

Table 2.1. WT and S196A mice developmental weight

Data represents means (n=4) ± standard deviation. Significance (p-value) was determined by Student's T-test.

2.1.2. Genetic identification of S196A mice

Recently-weaned pups were genotyped by polymerase chain reaction (PCR) analysis of genomic DNA extracted from ear-clipped samples. Genotyping of S196A mice was performed by amplifying a specific sequence downstream of the inserted S196A vector, which contains a small fragment of 34 nucleotides (Figure 2.2). This region is part of the remaining loxP flanking sequence, as a consequence of the lox-Cre insertion of the vector (S196A) leading to a product size of 656 base pairs (bp) (Figure 2.2). However, this sequence is not found if the vector hasn't been inserted (WT). Therefore, amplification product of WT sequences will be 622 bp (Figure 2.2).

DNA was extracted by incubating ear biopsies with 200 µl of 50 mM NaOH (pH = 12) at 95ºC for 10 min. Reaction was then neutralised by placing tubes on ice and adding 20 µl Tris-HCl 1M (pH = 8). Tubes were centrifuged at 13000 revolutions per minute (rpm) for 5 min 4ºC to get rid of debris and supernatant was transferred onto a clean tube. PCR amplification was performed using the Jumpstart Taq DNA Polymerase (Sigma Aldrich) and the following primers: wild-type (WT) forward 5'GGTGTCCCCAAGGGTGTCCT, reverse 5' AAGCATGACCTGCACACAAG and mutant forward 5' GGTGTCCCCAAGGGTGTCCG (Figure 2.2).

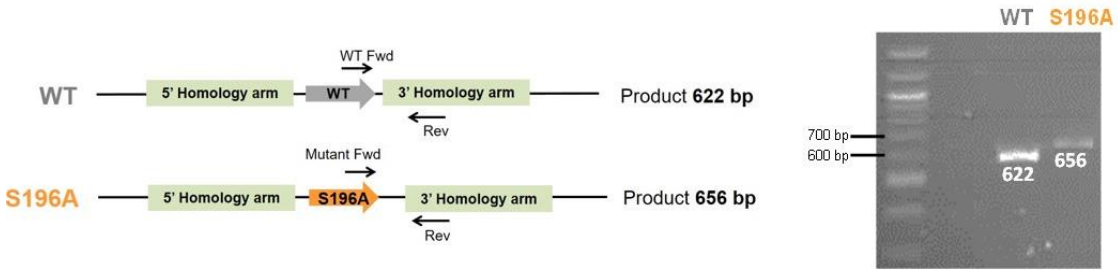

Figure 2.2. Genetic identification of S196A mice

Genotyping strategy with amplified sites and product size (Left). Gel electrophoresis of DNA amplified products using the corresponding primers (Right).

For a single reaction, the following reagents and DNA were added to a 0.5 ml microtube:

Amount	Reagent	Final Concentration
24.3 µL	Water	-
3 µL	10x PCR Buffer (with $MgCl_2$)	1x (2 mM $MgCl_2$)
0.6 µL	10 mM dNTPs	200 µM
0.3 µL	10 mM Primers	1 µM
0.5 µL	Taq DNA Polymerase	0.083 units/µL
1 µL	Template DNA	n/a
30 µL	**Total reaction volume**	

Amplification was undertaken by 35 cycles of 30 seconds of annealing at 60 °C, and 1 minute of extension at 72°C. Samples were run on a 2% high resolution agarose gel (Sigma Aldrich) in a 1X 40 mM Tris, 20 mM acetic acid, 1mM ethylenediaminetetraacetic acid (EDTA) (TAE) buffer with 1X SYBR safe DNA gel stain (Invitrogen) for 120 minutes at 80 volts (V).

2.2. Animal procedures

2.2.1. Housing and diet studies

Mice were maintained in a pathogen-free animal facility in a 12-hour light-dark cycle and were housed in the same cages whenever possible. All procedures were carried under the UK's Home Office Animals (Scientific Procedures) Act 1986.

Ten-week old WT and S196A female mice were fed *ad libitum* a High Fat-High Cholesterol (HFHC) diet (17,2% Cocoa Butter, 2,8% Soybean Oil, 1,25% Cholesterol, 0,5% Sodium Cholate; AIN-76A/Clinton Diet #4, Test Diet Limited, UK) or a chow diet (18% Protein, 6.2% Fat, 0% Cholesterol; Harlan Laboratories).

2.2.2. Plasma and tissue collection

Mice were fasted overnight prior to blood collection or terminal sacrifice. Animals were euthanized using increasing concentrations of CO_2 and death was confirmed by cervical dislocation or by cardiac bleeding.

In vivo blood sampling (corresponding to 4 weeks-readings) was collected by bleeding of the lateral saphenous vein. Saphenous vein blood collection was performed by Dr. Matthew C. Gage (University College London, UK). For terminal bleedings (chow and 6 weeks), blood was collected from euthanized mice by cardiac puncture by exposing the rib cage and slowly drawing blood from the ventricle. Blood was transferred into an EDTA-containing microtube (Microvette CB 300, Sarstedt), centrifuged (3000 x g, 6 min. at room temperature) and plasma was aliquoted and frozen at -80°C.

Tissues were dissected *post-mortem*, weighted and snap frozen by being placed in liquid nitrogen for lipid and protein analysis. For RNA analysis tissues were placed in RNAlater (Sigma Aldrich) for 24 hours at room temperature and then stored at -80°C.

2.2.3. Plasma and hepatic quantifications

2.2.3.1. Hepatic lipid extraction

For each lipid, 50 mg of frozen livers were homogenated in homogenation buffer (250 mM sucrose, 2 mM EDTA, 10 mM Tris) using ceramic beads in a Minilys Tissue Homogenizer. For triglyceride extraction, 200 µl of liver homogenates were mixed with 5 ml of isopropyl alcohol (VWR); and for total cholesterol, 150 µl of homogenates were mixed with 5 ml of a Chloroform:Methanol (1:1) solution (VWR). Tubes were left to incubate for 10 minutes at room temperature whilst shaking, and were then centrifuged (3000 x g, 10 min, room temperature). Supernatants were transferred onto a fresh tube, and for cholesterol determination were allowed to evaporate to dryness by placing the open tube at 65ºC. Dried cholesterol remnants were then resuspended with 200 µl of isopranol + 10% Triton-100X solution (Fisher Bioreagents).

Non-Esterified Free Fatty Acids (NEFAs) were extracted by incubating 200 µl of liver homogenates with a 1% Triton-100X and chloroform solution. Mixture was left in ice for 30 minutes with periodical mixing, and then spun down (13,000 x g, 10 min, 4ºC). The lower organic phase was collected and allowed to air-dry at 50ºC for approximately an hour. Dried pellet was resuspended in 200 µl of the Fatty Acid Assay Buffer (Abcam).

2.2.3.2. Total cholesterol, triglycerides and NEFAs quantification

Plasma and hepatic total cholesterol and triglyceride levels (Wako Chemicals), as well as NEFAs (Abcam), were determined by colorimetric enzymatic assay kits as per the manufacturer's recommendations, by measuring absorbance of reaction products at 595 nm in a TriStar² LB 942 Multidetection Microplate Reader (Berthold Technologies).

Hepatic lipid content was normalized to total protein concentration, which was quantified using the Coomassie (Bradford) Protein Assay (Sigma). This normalisation strategy was used due to differences in liver weight between WT and S196A mice. As the degree of fibrosis in mice upon a HFHC diet was mild, no differences were found between both groups in the protein content in liver lysates.

For this end, 2 µl of liver homogenates in homogenization buffer were added to 8 µl of water (1/5 dilution) and incubated with 200 µl of Bradford Reagent for 30 minutes at room temperature. Absorbance was measured at 595 nm in a TriStar² LB 942 Multidetection Microplate Reader.

2.2.3.3. HDL and LDL/VLDL

Plasma cholesterol concentrations in the HDL and LDL/VLDL was measured using the EnzyChrom™ AF HDL and LDL/VLDL Assay Kit (BioAssay Systems). This kit contains a precipitation buffer that once mixed with plasma, causes HDL and LDL/VLDL are to separate, and cholesterol concentrations are determined using a single Working Reagent that combines cholesterol ester hydrolysis, oxidation and colour reaction in one step. The colour intensity of the reaction product was quantified at 570nm in a TriStar² LB 942 Multidetection Microplate Reader and cholesterol levels were calculated proportional to a standard of 300 mg/dL cholesterol.

2.2.3.4. Glucose and insulin

Blood glucose measurements (Accu-Chek, Roche Diagnostics) were taken from tail blood samples after overnight fasting.

Plasma insulin concentration was measured using a rat/mouse Insulin Enzyme-Linked ImmunoSorbent Assay (ELISA) kit (Millipore), which contained a 96-well plate pre-coated with a pre-titered amount of a monoclonal mouse anti-rat insulin antibodies. Once insulin from plasma samples was captured to the plate, it was detected with binding of biotinylated polyclonal antibodies to the insulin, and subsequential binding of horseradish peroxidase to the immobilized biotinylated antibodies. After several washes, quantification of immobilized antibody-enzyme conjugates was performed by monitoring horseradish peroxidase activities in the presence of the substrate 3,3',5,5'-tetramethylbenzidine; which was measured spectrophotometrically by the increased absorbency at 450 nm, corrected from the absorbency at 590 nm on a TriStar² LB 942

Multidetection Microplate Reader (Berthold Technologies). Amount of captured insulin was derived by interpolation from a reference curve generated in the same assay with reference standards of known concentrations of rat insulin (Millipore).

2.2.3.5. Bile acids

50 mg of frozen livers were homogenized in 1 ml of 75% ethyl alcohol (VWR) using a Dounce homogeniser and homogenates were incubated at 50ºC for 2 hours. Tubes were then centrifuged for 10 min. at 6000 x g, 4ºC and supernatant was transferred onto a clean tube. 20 µl of liver supernatants or mouse plasma were mixed with 150 µl of Reagent CC3 from the Mouse Total Bile Acids kit (Crystal Chem.) in a 96-well plate and incubated at 37ºC for 5 minutes. After this, absorbance at 540 nm (A1) was measured in a TriStar² LB 942 Multidetection Microplate Reader. Then, 30 µl of Reagent CC2 from Mouse Total Bile Acids kit (Crystal Chem.) was added to each well and mixed immediately, followed by another absorbance reading at 540 nm (A2). A well containing 20 µl of 75% ethyl alcohol was used as blank, and 20 µl of a sample with a known concentration (35 µM) of bile acids was used as a calibrator. Total bile acid concentration was calculated as:

[[(sample A2-A1) - (blank A2-A1)] / [(calibrator A2-A1) - (blank A2-A1)]] * 35

Hepatic bile acids were normalized to total protein concentration, which was quantified using the Coomassie (Bradford) Protein Assay (Sigma) (see section 2.2.3.2)

2.3. RNA extraction and analysis

2.3.1. RNA extraction and cDNA synthesis

Total Ribonucleic acid (RNA) was extracted with TRIzol Reagent (Invitrogen) following manufacturer's protocol. Briefly, 50 mg of mouse liver or small intestine kept in RNAlater

were washed in 1 ml of cold Phosphate Buffer Saline (PBS) (Life Technologies) and then homogenized in 500 µl of TRIzol Reagent using ceramic beads in a Minilys Tissue Homogenizer (Bertin Corp.). Homogenates were spun down (12,000 x g for 10 minutes at 4ºC) and supernatant was transferred onto a clean 1.5 ml tube. Then, 80 µl of chloroform (Acros organics) was added to homogenates, vortex-mixed, incubated at room temperature for 2-3 minutes and then centrifuged (13,000 x g, 15 minutes at 4ºC). Following centrifugation, the entirety of the aqueous phase was transferred onto a new 1.5 ml tube and 250 µl of cold isopropyl alcohol was added to precipitate the RNA. Tubes were left to stand at room temperature for 10 minutes and then spun down at 15,800 x g, 15 minutes at 4ºC. Pellets containing precipitated RNA were washed twice with 400 µl of cold 70% molecular grade ethyl alcohol (Sigma Aldrich) and centrifuged (13,000 x g, 10 minutes at 4ºC). After the last wash, supernatants were removed completely and pellets were allowed to dry by leaving tubes uncapped at room temperature for 5 minutes. Pellets were then resuspended with 40 µl of molecular biology water (Sigma Aldrich). Sample concentration and purity was determined using a NanoDrop™ 1000 Spectrophotometer. Sample purity was assessed by 260/280 ratio and presence of contaminants by the 260/280 ratio. The minimum 260/230 ratio accepted was 1.50. 1000 µg of RNA was retrotranscripted using the qScript cDNA Synthesis Kit (Quantabio) following manufacturer's protocol.

2.3.2. Quantitative real-time PCR

Specific genes were amplified and quantified by PCR, using the PerfeCTa SYBR Green FastMix, Low ROX (Quanta) on an MX3000p system (Agilent) under the following conditions: 95ºC for 30 secs followed by 40 cycles of 55ºC for 5 secs and 60ºC for 30 secs. Amplicon specificity was assessed after every run by performing a dissociation (melt) curve: 95ºC for 1 min, 55ºC for 30 secs and 95ºC for 30 secs.

For a single reaction, the following reagents and cDNA were added to a single well in a 96-well plate:

Amount	Reagent	Final Concentration
6.2 µL	Water	-
7.5 µL	2X Reaction Buffer	1X
0.15 µL	10 µM Primers	100 nM
1 µL	250 ng of cDNA	-
15 µL	**Total reaction volume**	

All samples were run in duplicates and the relative amount of mRNAs was calculated using the comparative Ct method and normalized to the expression of *Cyclophylin* (304), which was already established in the lab not to be regulated by LXRs (data not shown). The following formula was used to quantify relative mRNA levels:

$$\Delta Ct = Ct_{gene} - Ct_{cyclophylin}$$

$$\Delta\Delta Ct = \Delta Ct_{sample} - \text{average } \Delta Ct_{control}$$

$$\text{Fold induction} = 2^{-\Delta\Delta Ct}$$

2.3.3. Primer design

Transcript sequences were obtained from the from the University of California, Santa Cruz (UCSC) Genome Browser database (https://genome.ucsc.edu) (305). Primers were obtained using the Primer3 (v. 0.4.0) online software (306), under the following parameters: amplicon size of 60-120 base pairs, primer size of 18-25 base pairs and melting temperature of 60 ºC. In order to avoid amplification of contaminating genomic DNA, primers were designed where one half hybridized to the 3′ end of one exon and the other half to the 5′ end of the adjacent exon (exon spanning). Primer efficiency was determined by running a standard curve with known cDNA concentrations, and only

those primers with an efficiency of 90-110% were used. All primer sequences used are in Table 2.2.

2.3.4. RT^2 Profiler PCR Arrays

Mouse Lipoprotein Signalling and Cholesterol Metabolism (PAMM-080Z) and Mouse Cytokines & Chemokines (PAMM-150Z) RT^2 Profiler PCR Arrays (Qiagen) were performed as per the manufacturer's instructions. Firstly, RNA integrity was assessed by qStandard (UK). All samples used had a RNA integrity number above 7.5. Then, cDNA was synthesized with the RT^2 HT first strand kit (Qiagen) using 500 ng of RNA, and quantitative PCR (qPCR) analysis was performed using RT2 SYBR Green ROX™ qPCR Mastermix (Qiagen) on the MX3000p detection system (Agilent). The relative amount of mRNAs was calculated using the comparative Ct method (see section 2.3.2) and normalized to an average of five housekeeping genes. The full list of analysed genes with these arrays can be found in Tables 3.1. and 3.2.

2.4. Protein isolation, immunoprecipitation, and immunoblotting

Single cell suspensions from livers were immunoprecipitated with antibodies that specifically recognise the human (8 µg LXRα, ab41902, Abcam) or murine (2 µg LXRα/β) (307) receptors. Antibodies were previously crosslinked to a column with Protein A/G Agarose following the manufacturer's protocol (Pierce).

Eluted protein was quantified using the BCA Protein Assay (Thermo Fisher). This assay uses the reduction of Cu^{2+} to Cu^{1+} by protein in an alkaline medium and produces a colorimetric reaction of the cuprous cation (Cu1+) by bicinchoninic acid (BCA), which was measured at 590 nm on a TriStar² LB 942 Multidetection Microplate Reader. Proteins were denaturalised by being boiled in a buffer containing 2% Sodium Dodecylsulfate (SDS) and 5% β-mercaptoethanol for 10 minutes, and separated on a

10% acrylamide gel (BioRad) for 2h 30 min at a constant voltage of 100V. Proteins were then transferred to a PVDF membrane (Millipore) by wet transfer at 100V for 1 hour. After transfer, membranes were blocked with StartingBlock™ Blocking Buffer (Thermo Fisher) for 1 hour at room temperature, and then blotted with primary antibody overnight at 4ºC. Phospho-Ser198/196 LXRα specific rabbit polyclonal antibody (163,308), mouse LXRα monoclonal antibody (Abcam) and Hsp90 polyclonal (sc-7947, Santa Cruz) were used as primary antibodies. Anti-rabbit (PO448, Dako) or anti-mouse (NA931VS, GE Healthcare) horseradish-peroxidase-tagged antibodies were used for secondary binding and chemiluminescence (ECL 2 Western Blotting Substrate, Pierce) was used to visualise proteins.

2.5. Histopathological analysis

2.5.1. Slide preparation and staining

Mouse liver was dissected and the left lobe was fixed in 10% (w/v) formalin (Sigma Aldrich) for 24-48h, processed in a TP 1050 Tissue Processor (Leica) and embedded in paraffin wax. Paraffin-embedded livers were cut into 4 μM sections. Liver sectioning was performed by the UCL IQPath Facility (University College London, UK).

Sections were stained with hematoxylin and eosin (H&E) in an automatic multiple slide stainer (Tissue-Tek DRS 2000, Sakura).

Liver histology was blindly scored by Dr. Tu Vinh Luong (University College London, UK) based on three semiquantitative items: steatosis (0–3), lobular inflammation (0–3) and hepatocellular ballooning (0–2) (201,309) (Table 2.3).

F4/80 (ab6640, Abcam) staining was performed by the UCL IQPath Facility (University College London, UK). Picrosirius Red stain was performed following manufacturer's protocol (Abcam). Briefly, liver sectons were deparaffinised and hydrated by placing them in distilled water. Then, Picro-Sirius Red Solution (Abcam) was applied on the stain

until completely covered and left to incubate for 60 min at room temperature. Slides were quickly rinsed in two changes of Acetic Acid Solution (Abcam) and dehydrated by placing them in two changes of absolute ethyl alcohol. Slides were then dried and cover-slipped using a xylene-based mounting media.

Stained sections were scanned with a NanoZoomer Digital slide scanner (Hamamatsu) and stained area quantification was performed using the ImageJ software (310) on three independent areas per section. Data is represented as the averaged positively-stained percent of area of interest.

Histological feature	Score	Criteria
Steatosis (micro and macro)	0	5%
	1	5%-33%
	2	33%-66%
	3	>66%
Lobular inflammation	0	No foci
	1	2 foci per 200x field
	2	2-4 foci per 200x field
	3	>4 foci per 200x field
Hepatocyte ballooning	0	None
	1	Few ballooned cells
	2	Prominent ballooning

Table 2.3. Grading criteria used for NAFLD scoring of mice

Grading criteria was adapted to murine pathology from the human Kleiner's Score (201).

2.5.2. Image processing for lipid droplet identification

The identification and quantification of lipid droplets were made with the help of Eli (Easy Lipids) v1.0, an in-house software developed in collaboration with Dr. Vanessa Diaz and Dr. Cesar Pichardo at the Multiscale Cardiovascular Engineering (MUSE) (University College London, UK). Scans of H&E stained liver sections were used as input. This

software uses a method based on the Hough Transform (311) for the identification of the droplets estimating the centres and radii of each of them. A final report is generated with the dimensions of the droplets (i.e. diameter and area) including a histogram describing the frequency of lipid vacuoles within specified diameter ranges (Figure 2.3). A trial of Eli v1.0 is currently available upon request on the MUSE website at UCL (www.ucl.ac.uk/muse/software).

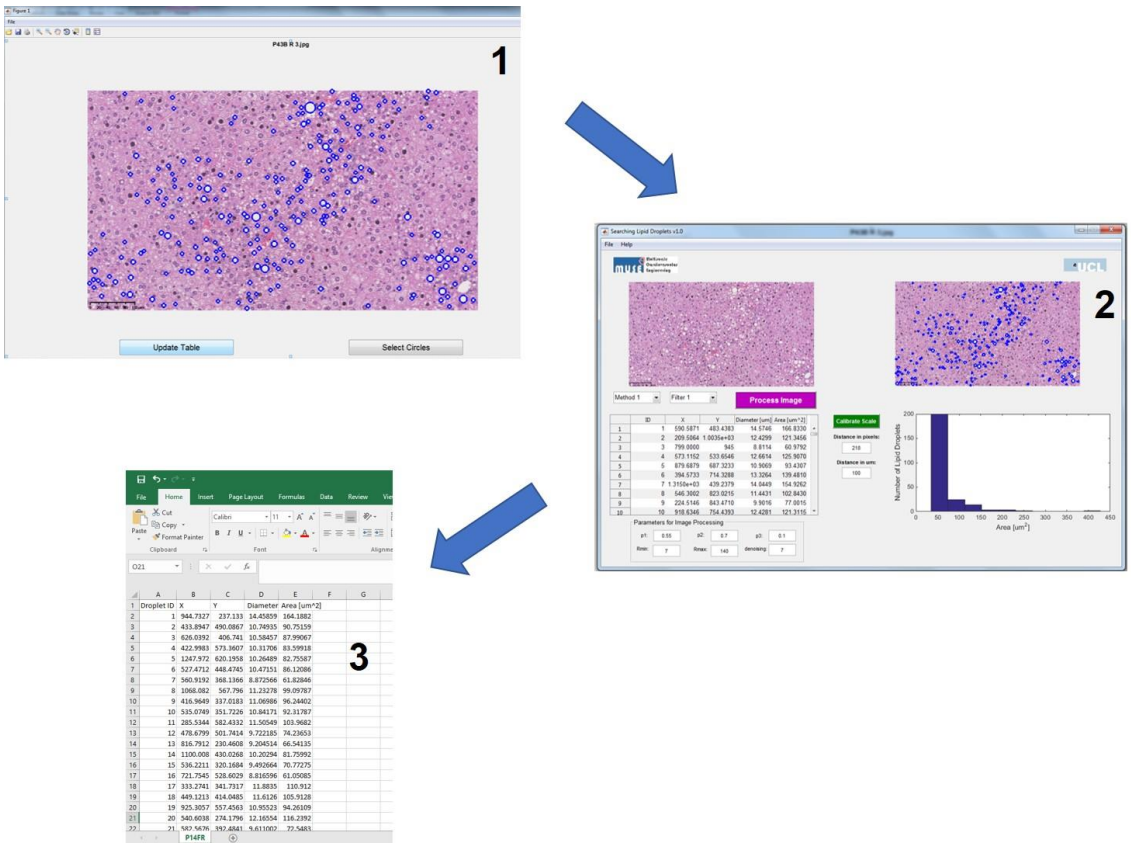

Figure 2.3. Identification of lipid droplet areas using the Eli (Easy Lipids) v1.0 software

Identification of lipid droplets on uploaded images of H&E-stained liver sections (1), then software generates a histogram (2) and a list of all the identified droplets and their area (3).

2.5.3. TUNEL staining

Apoptosis was detected *in situ* using a terminal deoxynucleotidyl transferase dUTP nick end-labeling (TUNEL) assay as per the manufacturer's instructions (R&D Systems). Paraffin-embedded liver tissue sections were incubated with a specific TdT enzyme that incorporates biotin on exposed nucleotides after DNA fragmentation. Biotin labelling was later achieved using Streptavidin-Fluorescein and sections were imaged using the Axio Imager.A1 Digital Microscope (Zeiss). Four different areas per slide were photographed at a magnification of 200X and intensity of staining was quantified by ImageJ.

2.6. Oxysterol LC-MS analysis

Oxysterol level determination was performed by Dr. Hanne Røberg-Larsen (University of Oslo, Norway). Protein was precipitated from plasma with 480 pM of the appropriate internal standards (Avanti Polar Lipids, Alabaster, AL, USA). Sample clean-up was conducted off-line, using solid phase extraction (SPE, SilactSPE C18 100 mg, Teknolab, Ski, Norway) and dryed at 30 °C, re-dissolved in 2-propanol and treated as described (312). Samples and calibration solutions were analysed using an Ultimate 3000 UHPLC connected to an Advantage QqQ (both Thermo Fisher, Waltham, MA, USA) equipped with an Automatic filtration and filter back-flush SPE add-on, as described (313).

2.7. Lipid peroxidation quantification

Thiobarbituric Acid Reactive Substances (TBARS) were measured in approximately 25 mg of frozen livers as per manufacturer's instructions (Cayman Chemicals). Briefly, lipid peroxidation was quantified by the reaction of Malondialdehyde (MDA), a product of lipid peroxidation, with thiobarbituric acid (TBA) to form a colorimetric (532 nm) product,

proportional to the MDA present, which was measured spectrophotometrically on a TriStar² LB 942 Multidetection Microplate Reader. MDA levels were calculated based by interpolation from a standard curve. Levels of MDA were normalised to total protein levels, quantified using the Bradford Assay (see section 2.2.3.2).

2.8. Chromatin Immunoprecipitations

100 mg of WT and 120 mg of S196A fatty (HFHC) livers were dissected and directly double crosslinked with 2 mM disuccinimidyl glutarate (DSG) (Thermo Scientific) for 30 minutes at room temperature, followed by 1% formaldehyde (Thermo Scientific) for 10 minutes also at room temperature. The reaction was stopped with glycine at a final concentration of 0.125 M for 5 min, room temperature. Livers were washed three times with PBS and single cell suspension was obtained by grinding liver pieces through a 70 µM cell strainer (Fisher scientific). Nuclei were isolated by incubating cell preparations for 10 minutes at 4ºC with the following lysis buffers: Buffer 1 (50 mM Hepes-KOH, pH 7.5, 140 mM NaCl, 1 mM EDTA, 10% glycerol, 0.5% NP-40 and 0.25% Triton X-100), Buffer 2 (10 mM Tris-HCl, pH 8.0, 200 mM NaCl, 1 mM EDTA and 0.5 mM EGTA), and Buffer 3 (10 mM Tris-HCl, pH 8.0, 100 mM NaCl, 1 mM EDTA, 0.5 mM EGTA, 0.1% Na-deoxycholate, and 0.5% N-Lauroylsarcosine). Pellets resuspended in 300 µl of lysis buffer 3 were sonicated for 40 cycles (30 s ON/OFF) in the UCD-300 Bioruptor (Diagenode), to generate DNA-fragment sizes of 0.2–0.5 kb. Successful sonication was confirmed by running products on a 1% agarose gel (Figure 2.1.2), in a 1X TAE buffer with 1X SYBR safe DNA gel stain (Invitrogen) for 30 minutes at 80V.

Soluble chromatin was diluted in Dilution Buffer (1% Triton X-100, 2 mM EDTA, 150 mM NaCl, 20 mM Tris.HCl pH 8.1) and immunocleared for 18 hours at 4ºC by being incubated with 2µg sheared Salmon sperm DNA (Invitrogen) and 2µg/ml Bovine Serum Albumin (Sigma Aldrich). Then, 25 µg of chromatin were immunoprecipitated with the following antibodies: 2.5 µg RXRα (sc-553, Santa Cruz), 2.5 µg Pol II (sc-9001, Santa Cruz), 5 µg

Pol II-S2P (ab5095, Abcam), 2 µg LXR (α/β) (307), 2.5 µg TBLR1 (ab24550, Abcam) and 5 µg NCoR (ABE251, Millipore). Antibody-protein-chromatin complexes were immunoprecipitated by incubating with a 50% Protein A-sepharose solution (GE Life Sciences) for 2 hours at 4ºC. Complex with beads was then washed once with the following solutions: TSE I (0,1 % SDS, 1% Triton X-100, 2 mM EDTA, 150 mM NaCl, 20 mM Tris-HCl pH 8.1), TSE II (0,1 % SDS, 1% Triton X-100, 2 mM EDTA, 500 mM NaCl, 20 mM Tris-HCl pH 8.1), Buffer III (0.25 M LiCL, 1% NP-40, 1% Deoxycholate, 1 mM EDTA, 10 mM Tris-HCl pH 8.1) and TE Buffer (10mM Tris-HCl pH 8.1, 1mM EDTA). Lastly, chromatin was eluted with three consecutive washes of Elution Buffer (1% SDS, 0.1 M $NaHCO_3$).

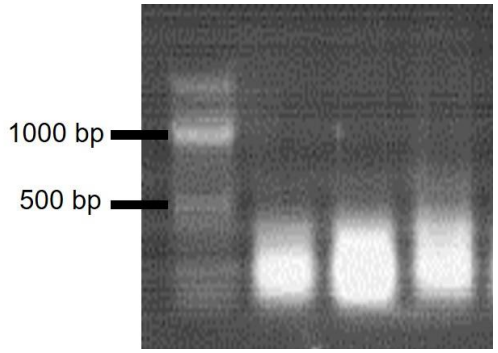

Figure 2.4. Example of mouse liver chromatin visualization after sonication
Sonicated DNA products were run on a 1% agarose gel. Sonication was considered successful when majority of DNA was lower than 500 bp.

After RNAse A (Fermentas) and proteinase K (Fermentas) treatment, the immunoprecipitated DNA was purified using the QIAquick PCR purification kit (Qiagen) and analysed by quantitative real-time PCR with corresponding primers (sequences are listed in Table 2.4). Relative occupancies were normalized to input DNA (fold difference= $2^{-Ct\text{-}sample\text{-}Ct\text{-}input}$). To control for non-specific binding, an 82 base pair fragment in a gene desert in chromosome 6 (ActiveMotif) was used. Pol II and Pol II-S2P antibody specificity was assessed against the same amount of IgG from rabbit serum (I5006, Sigma).

2.9. *In silico* screening of potential LXREs

Screening for potential DR4 sequences was performed using the available web-based software NHR Scan (http://www.cisreg.ca/cgi-bin/NHR-scan/nhr_scan.cgi) (314), which predicts potential nuclear hormone receptor binding sites on a given genomic sequence. Input sequences (gene body or sequences 30 kb upstream from transcription start site) were obtained from UCSC Genome Browser database (see section 2.3.3) and submitted under FASTA format. Plausible DR4 sequences were then chosen based on similarity to a published consensus sequence for the murine LXRE (315) (Figure 4.8)

2.10. RNA sequencing

2.10.1. RNA preparation and sequencing

Sequencing and pipeline analysis was performed by UCL Genomics (London, UK). Total RNA was extracted using TRIzol reagent (see section 2.3.1) and cDNA libraries were prepared using reagents and protocols supplied with the Stranded mRNA-Seq Kit (Kapa Biosystems). Briefly, poly-A tailed RNA was purified using paramagnetic oligo-dT beads from 200 nanograms of total RNA, with a RNA Integrity Number above 7.5 as determined by the Agilent Bioanalyzer (Agilent). The purified RNA was fragmented chemically by heating samples in the presence of Mg2+ and cDNA was synthesised using random primers supplied in the kit (Kapa Biosystems). Adapter-ligated DNA library was then amplified with 12 cycles of PCR and library fragment was estimated using the Agilent TapeStation 2200 and confirmed to be ~150bp (~280bp when including the Illumina adapters). Lastly, Library concentration was determined using the Qubit DNA HS assay (Life Technologies). Libraries were sequenced at a concentration of 1.8pM on a Illumina NextSeq 500, NCS v2.1.2 (Illumina), with a 43bp paired end protocol. Basecalling was done using the standard Illumina parameters (RTA 2.4.11).

Oligo design and qPCR validation (see section 2.3) of top upregulated and downregulated hits was performed by Lucia Martin-Gutierrez (University College London, UK). Primers used for qPCR validation can be found in Table 2.2.

All RNA-seq results are available at the Gene Expression Omnibus (GEO) data repository, under the GEO Accession numbers GSE96650 (chow livers) and GSE95359 (HFHC livers).

2.10.2. RNA-Seq computational analysis

Reads were demulitplexed using Illumina bcl2fastq v2.17 (Illumina) and then were aligned using STAR v2.5.0b to the mouse GRCm38/mm10 reference sequence. Transcript abundance was estimated using Illumina's RnaReadCounter tool and differential expression analysis performed with DESeq2.

Pathway enrichment analysis was performed with the Gene Set Enrichment Analysis (GSEA) software's pre-ranked module (316,317). A list of significant (adjusted p-value < 0.05) differentially expressed genes in S196A livers compared to WT was analysed against the Hallmark gene set database (318).

Heatmaps were created using the Multi Experiment Viewer (MeV) desktop software (319), based on differences on raw gene counts.

2.11. RAW 264.7 *in vitro* experiments

2.11.1 Cell culture

RAW 264.7 is a murine macrophage-like cell line that was established from the ascites of a tumour induced in a male mouse by injections of Abelson leukemia virus (320). This cell line is widely used to study macrophage biology as it is easy to propagate in culture, and shows optimal DNA transfection efficiency, as well as sensitivity to RNA interference.

RAW 264.7 cells were transfected as previously described (163) and grown in High Glucose Dulbecco's Modified Eagle Medium (DMEM) (Life Technologies), supplemented with 10% Fetal Bovine Serum (FBS) (Life Technologies), 2 mM glutamine (Lonza) and 20 µg/ml gentamycin (Sigma Aldrich). Cells were maintained in culture in an incubator at 37°C, 5% CO_2, and passaged every 48 hours.

2.11.2. Activation treatments

Once cells had reached 80% confluency, plates were washed once with PBS and cells were serum starved overnight by placing them in DMEM medium with low-endotoxin 1% FBS (Life technologies), and were then stimulated with the correspondent stimulants.
For mRNA experiments, cells were scrapped off the plate, counted using a Neubauer counting chamber under an optical microscope, and 5 x 10^5 cells were plated per well in a 6-well plate (Greiner Bio-One), before serum-starving them. Concentrations and incubation periods for each experiment can be found in the corresponding figure legends. Dimethyl sulfoxide (DMSO) (Sigma Aldrich) was used as a vehicle control for GW3965 (Sigma Aldrich), CX-4945 (Selleckchem) and oltipraz (Sigma Aldrich); absolute ethyl alcohol (VWR) was used as control both for desmosterol (Insight) and 24(S),25-EC (Enzo Life Sciences) and PBS was used as a control for insulin (Sigma Aldrich).

2.11.3. Immunoblotting and mRNA analysis

RAW 264.7 nuclear extracts were prepared using the NE-PER nuclear and cytoplasmic extraction reagents (Pierce) following manufacturer's protocol. Overall, addition of 300 µl of the Cytoplasmic Extraction Reagent (CER) I and 16.5 µl of CER II to a cell pellet caused cell membrane disruption and release of cytoplasmic contents. After separating the intact nuclei from the cytoplasmic extract by centrifugation (13,500 rpm, 6 min, 4°C), the proteins are extracted out of the nuclei with 50 µl of the Nuclear Extraction Reagent.

Nuclear protein was quantified using Coomassie (Bradford) Protein Assay (see section 2.2.3.2) and separated on a 10 % acrylamide gel (see section 2.4).
Densitometry analysis of membranes was performed using ImageJ and normalised to amount of Hsp90 in each sample. All the original scans can be found in Appendix 2.

RNA was extracted using Trizol reagent (see section 2.3.1). Transcript amplification and quantification by qPCR (see section 2.3.2) was performed by MSc student Daniel Wu (University College London, UK).

2.12. Human primary HSCs gene expression

Human primary HSCs were provided by Dr. Krista Rombouts (University College London, UK). 3 x 10^5 cells were plated per well in serum-free DMEM media, complemented with 2 mM glutamine (GIBCO) and antibiotic-antimyocotic 1X (GIBCO).
Unless otherwise stated, cells were used on passage 5. Cells were stimulated with 1 μM GW3965 or DMSO for 18 hours, then media was removed and RNA was extracted using the RNeasy Micro Kit (Qiagen). Briefly, cells were quickly lysed by running them through the QIAshredder spin columns (Qiagen). Then, the cell lysate was loaded onto the RNeasy MinElute spin column and spun down (10,000 rpm for 30 seconds at room temperature), so that RNA (up to 45 μg) would bind to the silica membrane. Membranes were washed once with RW1 buffer and treated with RNase-free DNase for 15 minutes at room temperature. Lastly, membranes were washed with 80% ethanol (Sigma), and RNA was eluted in RNase-free water. For qPCR see section 2.3.2.
All primer sequences used for human genes are in Table 2.6.

2.13. Human liver protein and mRNA analysis

Frozen liver biopsies obtained from males with colon carcinoma undergoing lobectomies were supplied by Dr. Krista Rombouts (University College London, United Kingdom). RNA was extracted from 5 mg of frozen liver using TRIzol Reagent following manufacturer's protocol (see section 2.3.1), and genes were quantified by qPCR (see section 2.3.2.)

For protein extraction and immunoblotting see section 2.4.

2.14. Statistical analysis

Unless stated otherwise, data is presented as mean ± Standard Error of Mean (SEM). Differences were considered significant at $p < 0.05$ by a two-tailed Student t-test. Two-tailed (unpaired) t-test was performed when comparing two independent groups of values with normal distribution and whose means were not expected to be equal.

For multiple comparisons, significance was assessed by single variance ANOVA followed by Student's T-test. When comparing the means of more than two groups, ANOVA was used as a statistical test as it is more conservative (results in less type I error) than multiple two-sample Student t-tests.

For correlation studies, R^2 value was calculated by Pearson correlation coefficient. This statistical tests was used when assessing linear covariance of two variables. R^2 has a value between +1 and −1, where 1 is total positive linear correlation, 0 is no linear correlation, and −1 is total negative linear correlation.

Statistical analysis was performed using Microsoft Excel or Graph Pad Prism.

RT-PCR	**Forward sequence** (5' to 3')	**Reverse sequence** (5' to 3')
Abca1	GGACATGCACAAGGTCCTGA	CAGAAAATCCTGGAGCTTCAAA
Abcg1	CCTTCCTCAGCATCATGCG	CCGATCCCAATGTGCGA
Abcg5	TGGATCCAACACCTCTATGCTAAA	GGCAGGTTTTCTCGATGAACTG
Abcg8	TGCCCACCTTCCACATGTC	ATGAAGCCGGCAGTAAGGTAGA
Adipophilin	GACCGTGCGGACTTGCTC	GCCATTTTTTCCTCCTGGAGA
Aim	GTTGGATCGTGTTTTTCAGA	TCCCACTAGCTGCACTTTGGT
a-Sma	CCCAGACATCAGGGAGTAATGG	TCTATCGGATACTTCAGCGTCA
Atf3	GAGGATTTTGCTAACCTGACACC	TTGACGGTAACTGACTCCAGC
Atp6v0d2	GTGCAGTGTGAGACCTTGGA	GCCAGGAAGTTGCCATAGTC
Bex1	ATGGAGTCCAAAGATCAAGGCG	CTGGCTCCCTTCTGATGGTA
Cd36	GCCAAGCTATTGCGACATGA	TCTCAATGTCCGAGACTTTTCAAC
Ces1f	TGGAGAGTCAGCAGGAGGTT	ATGAAGGCCACACCACTCTC
Chop	CTGGAAGCCTGGTATGAGGAT	CAGGGTCAAGAGTAGTGAAGGT
Col1a1	GCTCCTCTTAGGGGCCACT	CCACGTCTCACCATTGGGG
Col1a2	AAGACCTGGGGAGAGAGGAG	CTTTGAAGCCAGGAAGTCCA
Cyclophylin	GGCCGATGACGAGCCC	TGTCTTTGGAACTTTGTCTGCAA
Cyp17a1	ACCAGCCAGATCGGTTTATG	AGGGCAAATAACTGGGTGTG
Cyp2b13	ATGCTCATGTACCCCCATGT	GCCGATCACCTGATCAATCT
Cyp2b9	CTGGCCACCATGAAAGAGTT	CATTGGGCCTCCTCCTTTAT
Cyp2c69	CACAGTGGCTCATGAAGGAA	GATGAATTGGGGATCACAGG
Cxcl1	CAGTGCACCCAAACCGAAGT	GGACAATTTTCTGAACCAAGGG
Cx3cl1	ATTTGTGTACTCTGCTGCC	TCTCCAGGACAATGGCAC
Cx3cr1	TGAGTGACTGGCACTTCCTG	AAGGAGGTGGACATGGTGAG
Dgat2	CTGGCTGATAGCTGCTCTCTACTT	TGTGATCTCCTGCCACCTTTC
Elovl6	TGAACAAGCGAGCCAAGTTTG	GAGCACCGAATATACTGAAGACG
Fabp5	AGGATGGGAAGATGATCGTG	CTGGCAGCTAACTCCTGTCC
Fas	GCTGCGGAAACTTCAGGAAAT	AGAGACGTGTCACTCCTGGACTT
Fsp27	GTGTCCACTTGTGCCGTCTT	CTCGCTTGGTTGTCTTGATT
Hamp2	AGAAAGCAGGGCAGACATTG	GCAGATGGGGAAGTTGATGT
Idol	ATGCTGTGCTATGTCACGAGG	TCGATGATCCCTAGACGCCTG
Ldlr	GCATCAGCTTGGACAAGGTGT	GGGAACAGCCACCATTGTTG
L-Fabp	ATGAACTTCTCCGGCAAGTACC	CTGACACCCCCTTGATGTCC
Lpcat3	CCTTCACGGGCCTCTCAATT	CCATGAGTCGCAGGATGAGG
Lpl	ATCCATGGATGGACGGTAACG	CTGGATCCCAATACTTCGACCA
Lxra	GGTTGCTTTAGGGATAGGGTT	TTCCGCTTTTGTGGACGAAG
Mmp9	GCGTGTCTGGAGATTCGACT	ATGTCGTGTGAGTTCCAGGG
Nnmt	TGTGCAGAAAACGAGATCCTC	TGTGCAGAAAACGAGATCCTC
Ncor	ACAGAGCAAAGTCGTTATCCTTC	GAGCGGTAGTCAGGAACTGC
Ncp1l1	GAGAGCCAAAGATGCTACTATCTT	CCCGGGAAGTTGGTCATG
Osbpl3	AGACACGGAGGAGCACATCT	CGGTACATTCTGTGGTGACG
Osm	GCAGCTGTGGCTTTCTCTGG	TCGTCCCATTCCCTGAAGAC
Ppp1r3g	CTGAGACCCCGATCCCTGAT	GAGAGCGGCGATATTCCTGT
Scara3	GCTGGTGAAGACGAGGACAT	CAAAATCCGCACTGATGTGT
Scd1	CCGGAGACCCCTTAGATCGA	TAGCCTGTAAAAGATTTCTGCAAA

Table 2.2. Mouse gene primers used for qPCR

RT-PCR	**Forward sequence** (5' to 3')	**Reverse sequence** (5' to 3')
Slc22a26	ACAGAGCCCTGTATGGATGG	AGATCCACACACCAGGTTCC
Srebp1c	CAGGAGGACATC TTGCTGCTTC	TTGGGAGGCTGGTTTTGACC
Srebp2	CTGCAGCCTCAAGTGCAAAG	CAGTGTGCCATTGGCTGTCT
Stk25	ACGTT CCTCCAACCATCCG	CTTCTGTGAGCTGTGCA
Sod2	CAGACCTGCCTTACGACTATGG	CTCGGTGGCGTTGAGATTGTT
Syngr1	CTGGTTCGTGGGTTTCTGCTT	GTCCCTTCGTTCAGAGGGTTG
Tblr1	ATCGAGTCTCTGTCCCTGATAG	GCTTGTCTCTGTAGGCTTGTTG
Tgfb2	TTTGCTCCAGACAGTCCCAG	ATCTCCAGACATGCCAAGCC
Timp1	GTGGATATGCCCACAAGTCC	CTCAGAGTACGCCAGGGAAC
Thrsp	GCGGAAATACCAGGAAATGA	CGGGGTCTTCATCAGTCTTC
Tlr4	AGCCTCGAATCCTGAGCAAA	AGGCCCCAGAGTTTTGTTCT
spl Xbp1	GAGTCCGCAGCAGGTG	GTGTCAGAGTCCATGGGA
Wfdc3	CTTGGGTAGCTGCAGGAGAG	ATTCGTCTCCGGTACACAGC

Table 2.2. Mouse gene primers used for qPCR (*continued*)

	Forward primer (5' to 3')	**Reverse primer** (5' to 3')
Ces1f DR4	GGTGGTGGCCATTCAATATC	TGTCCACAAACCCTACCTGA
Ces1f TSS	CATTGACTTGGGAGCCTGTC	ACTCACCGCAAATCACACAG
Cyp2c69 DR4	CTACCCACTCCTGCTTCCTG	GGCCTAGTTGGCCATCATTA
Cyp2d69 TSS	TGTCTGGAATGCCTGATCATA	GGATCCATGGAGACCCTTCT
Srebp1c LXRE	AGGCTCTTTTCGGGGATGG	TGGGGTTACTGGCGGTCAC
Srebp1c TSS	GTGGGCCTAGTCCGAAGC	ATCTCGGCCAGTGTCTGTTC

Table 2.4. Primers used for ChIP-qPCR

	Forward primer (5' to 3')	**Reverse primer** (5' to 3')
ABCA1	TGAGCTACCCACCCTATGAACA	CCCCTGAACCCAAGGAAGTG
ABCG1	TGCAATCTTGTGCCATATTTGA	CCAGCCGACTGTTCTGATCA
ACTA2	AAAAGACAGCTACGTGGGTGA	GCCATGTTCTATCGGGTACTTC
CYCLOPHYLIN	GCATACGGGTCCTGGCATCTTGT	ATGGTGATCTTCTTGCTGGTCT
LXRA	AGAGGAGGAACAGGCTCATG	AAAGGAGCGCCGGTTACACT
LXRB	GGAGCTGGCCATCATCTCA	GTCTCTAGCAGCATGATCTCGG
SREBP1c	TCAGCGAGGCGGCTTTGGAG	CATGTCTTCGATGTCGGTCAG

Table 2.5. Human gene primers used for qPCR

Chapter 3. LXRα phosphorylation-deficiency at Ser196 attenuates diet-induced liver inflammation and fibrosis

3.1. Introduction

Fatty liver (steatosis) alone is considered relatively benign. However, it is the transition to NASH that represents a key step into further irreversible liver damage and mortality (178), although the mechanisms underlying this transition are poorly understood. Hence, most therapies for NAFLD have focused on preventing progression of fatty liver or reversing already established inflammatory or fibrotic states (200). Currently available agents such as insulin sensitizers, antioxidants, and lipid-lowering agents are not aimed at treating NAFLD directly but rather its associated conditions and thus only display limited efficacy (see section 1.2.3). Thus, understanding the factors that trigger the transition from fatty liver to NASH is crucial for the development of direct pharmacological therapies against NAFLD.

LXRs act as whole-body cholesterol sensors: they respond to oxysterols, as a consequence of increased intracellular cholesterol levels, and induce the expression of several genes involved in cholesterol metabolism (see section 1.1.3). Upon activation, LXRs prompt cholesterol catabolism and excretion, as well as decrease rates of uptake and cellular biosynthesis. Due to their important role in the regulation of cholesterol homeostasis, classic therapeutic approaches based on regulating LXR activity have focused on finding synthetic compounds that lead to reducing systemic cholesterol burden for the treatment of diseases such as atherosclerosis (65,67,321,322). However, the effects of LXR activation on fatty acid and triglyceride metabolism have presented a major obstacle in the development of LXR agonists, as pharmacological activation of LXRs stimulates hepatic *de novo* lipogenesis, being therefore a key promoter of steatosis (323,324). In contrast, LXRs have also demonstrated strong anti-inflammatory and anti-

fibrotic activities in models of acute liver disease (151,325). It would be elementary therefore, to find a strategy that would restrict LXR activity towards its therapeutic capacities without inducing the less favourable side effects.

Besides ligand binding, LXR activity can be modulated by post-translational modifications (158) (see section 1.1.4). Pineda-Torra *et al*. previously showed that the human LXRα is phosphorylated at Ser198 in macrophages under basal conditions and upon cholesterol overload *in vitro*, as well as in the plaques of ApoE-knock out (KO) mice (163). Despite previous reports showing LXRα phosphorylation in this and other residues (166,169,170), the biological consequences of changes in LXRα phosphorylation on pathophysiology, and specifically, on the progression of diet-induced chronic liver disease remain unknown. To assess the impact that changes in LXRα phosphorylation have on the receptor's activity *in vivo*, we generated a novel knock-in mice model. These animals are homozygous for a whole-body Serine196 to Alanine (S196A) mutation (for details refer to section 2.1), the homologous residue in the murine receptor to Ser198 in humans. For my studies, I have used a High Fat/High Cholesterol diet, as cholesterol metabolites are known LXR endogenous ligands (section 1.1.2.1) and cholesterol induces LXRα phosphorylation *in vitro* (163). Furthermore, diets with a high cholesterol content have been previously reported to activate LXR activity *in vivo* (143).

Thus, the primary aims of the following experiments were to:

- Investigate which is the phosphorylation status of hepatic LXRα *in vivo*
- Employ the newly-generated S196A mouse model to investigate how changes in LXRα phosphorylation change the receptor's activity on lipid homeostasis

3.2. LXRα is phosphorylated in human and mouse liver

The Ser198/196 residue is conserved between human, rat and mouse (Figure 3.1. A), suggestive of a preserved function. To assess phosphorylation levels at this residue, LXRs were immunoprecipitated in liver homogenates of wild-type C57BL/6 mice fed a chow diet, using a polyclonal antibody that recognizes both α and β subtypes of the receptor (326). Although the murine S196 phosphorylation motif is not conserved in the LXRβ subtype (Figure 3.1. B), a liver sample from LXRα KO mice (kindly provided by Dr. A. Valledor, UB, Spain), was also included to control for subtype specificity. Moreover, total LXRα was immunoprecipitated from lysates of healthy human livers (n=2), using a commercial antibody. Thus, immunoblotting with our own non-commercial antibody that specifically recognises the phospho-Ser198/196 LXRα residue (163) proved that endogenous murine (Figure 3.1. C) and human (Figure 3.1. D) LXRα is phosphorylated in the liver under basal conditions, and that this is indeed abolished in the S196A knock-in animals that carry the serine-to-alanine mutation (Figure 3.1. C).

Interestingly, although the same amount of antibody and protein lysate was used in the immunoprecipitation for both human liver samples, a considerable difference in the amount of precipitated LXRα was observed between both donors (Figure 3.1. D). To rule out a technical error, analysis by real-time qPCR was performed and confirmed that, in agreement with the protein levels, Donor A also had higher mRNA levels of both LXRα and LXRβ (Figure 3.1. E), suggestive of inter-individual variability in LXR quantities which may be independent of disease.

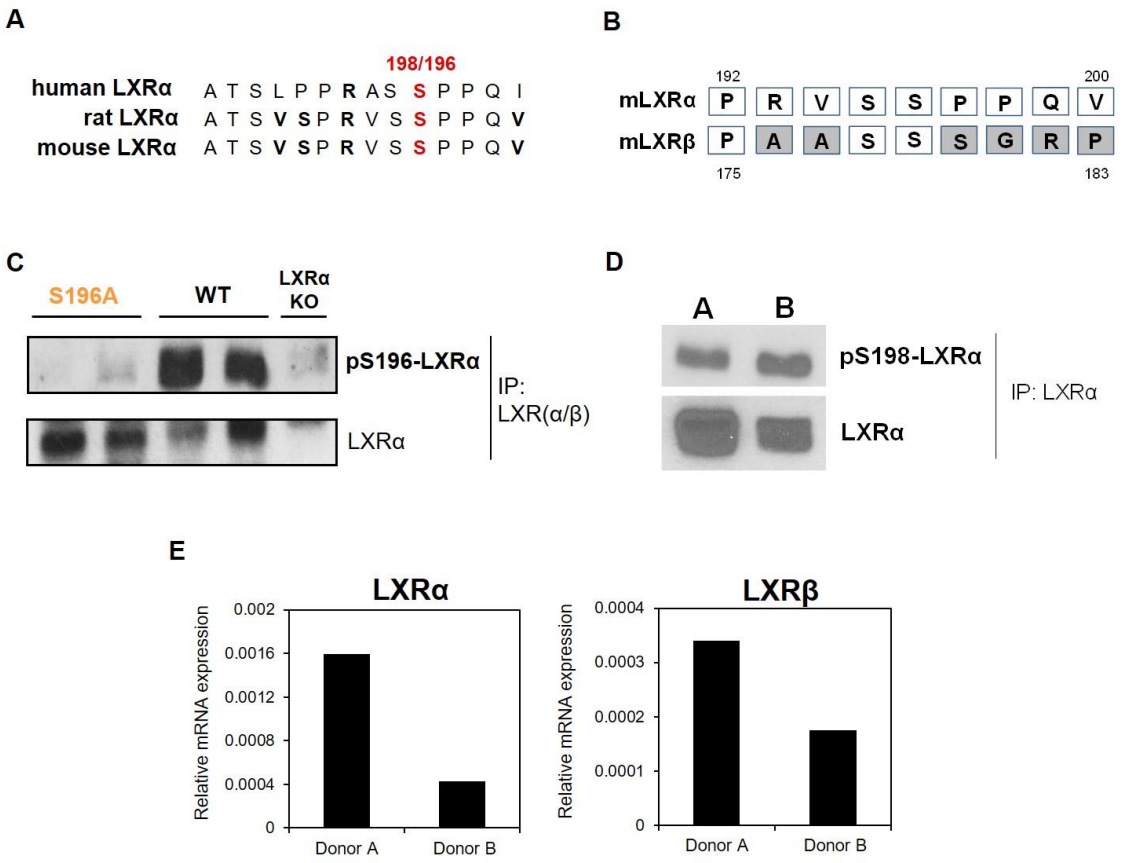

Figure 3.1. Hepatic LXRα is phosphorylated under basal conditions

A) Amino acid sequence alignment of the LXRα protein in different species containing the S198/196 phosphorylation motif.

B) Alignment of the murine LXRα and LXRβ amino acid sequence showing differences (grey boxes) in S196 phosphorylation motifs between both subtypes.

C) Murine LXRα phosphorylation at Ser196 analysed by LXRα/β immunoprecipitation of liver homogenates (WT, S196A or LXRα KO mice) and subsequent immunoblotting with a phospho-LXRα specific antibody. For each sample, immunoprecipitated total LXRα was assessed (n=2).

D) Human LXRα phosphorylation at Ser198 analysed by LXRα immunoprecipitation of liver homogenates (n=2), subsequent immunoblotting with a phospho-LXRα specific antibody. For each sample, immunoprecipitated total LXRα was assessed.

E) mRNA levels of LXRα and LXRβ quantified by real-time PCR in human livers (n = 2). Values are normalised to house-keeping gene cyclophylin.

3.3. Phosphorylation-deficient LXRα protects from plasma and hepatic dietary cholesterol accumulation

Previous studies have extensively shown the importance of LXR activity on lipid and bile acid metabolism (106,324), therefore differences in several metabolic parameters between LXRα phosphorylation-deficient and wild-type (WT) mice were investigated. Interestingly, when fed a normal chow diet, S196A mutant mice showed no difference on body weight nor most metabolic parameters when compared to wild-type controls (Table 3.1). It must be noted though, that levels of plasma triglycerides could not be determined in WT mice due to the abundant presence of hemolysis (red blood cell lysis) in those samples due to a technical error, which interfered with the assay and produced out of scale readings.

Because of the lack of any apparent metabolic phenotype on the S196A animals under basal conditions, the response of the LXRα phosphorylation-deficient animals to a High Fat/High Cholesterol diet (HFHC diet) in comparison to wild-type controls was next assessed. Many previous studies on rodents have identified sex-specific differences in lipid metabolism, where female mice tend to have a larger basal and diet-induced pool of cholesterol and higher intestinal absorption efficiencies than males (327,328). Therefore, 10-week-old S196A and WT female mice were fed the HFHC diet for 6 weeks. Comparable to chow values, plasma insulin and glucose levels were similar between genotypes (Table 3.1). Noticeably, both groups of mice had significantly lower body weight than their chow-fed counterparts (Table 3.1). This weight loss has already been reported for this type of diet (329), and it has been postulated that is due to a shift in the source of caloric intake (carbohydrate to fat) and subsequent reduction in adipose tissue mass (143). Moreover, when comparing only experimental diet-fed animals, the S196A group showed a significant decrease in their body weight (Table 3.1).

Parameter	Diet	Genotype	Mean ± SEM	*p*
Body weight (grams)	Chow	WT S196A	23.63 ± 0.6 21.70 ± 0.75	0.132
	HFHC	WT S196A	21.36 ± 0 .41[a] 19.89 ± 0.35[b]	**0.012**
% Liver weight (Liver g/Body g)	Chow	WT S196A	4.69 ± 0.25 4.41 ± 0.07	0.241
Plasma glucose (mmol/L)	Chow	WT S196A	5.35 ± 0.10 4.63 ± 0.22	0.268
	HFHC	WT S196A	4.49 ± 0.30 4.61 ± 0.24	0.762
Plasma insulin (ng/ mL)	Chow	WT S196A	0.34 ± 0.05 0.87 ± 0.24	0.103
	HFHC	WT S196A	0.60 ± 0.10 0.87 ± 0.33	0.498
Hepatic total cholesterol (µg / mg protein)	Chow	WT S196A	98.96 ± 10.48 104.43 ± 4 .05	0.688
Plasma triglycerides (mg/dL)	Chow	WT S196A	n/a 89.82 ± 8.95	n/a
Hepatic triglycerides (µg / mg protein)	Chow	WT S196A	51.95 ± 5.06 37.63 ± 4.50	0.116

Table 3.1. Biometric and metabolic parameters of WT and S196A mice fed a chow or HFHC diet

Values for mice fed either a chow diet (n=4) or HFHC diet for 6 weeks (n=6). Significance (p-value) was determined by Student's T-test.

An approximately 60% reduction in plasma total cholesterol was observed in the knock-in group after being fed the HFHC diet for 6 weeks (Figure 3.2. A). In addition, whilst WT animals showed a significant increase of plasma total cholesterol levels between 4 and 6 weeks, phosphorylation-deficient mice maintained their total cholesterol levels (Figure 3.2. A). Determination of the HDL and LDL/VLDL cholesterol in both groups of mice revealed that, besides having overall lower cholesterol levels in all fractions (Figure 3.2. B), the amount of total cholesterol found in the HDL fraction was significantly higher in the LXRα phosphorylation-deficient mice (Figure 3.2. B).

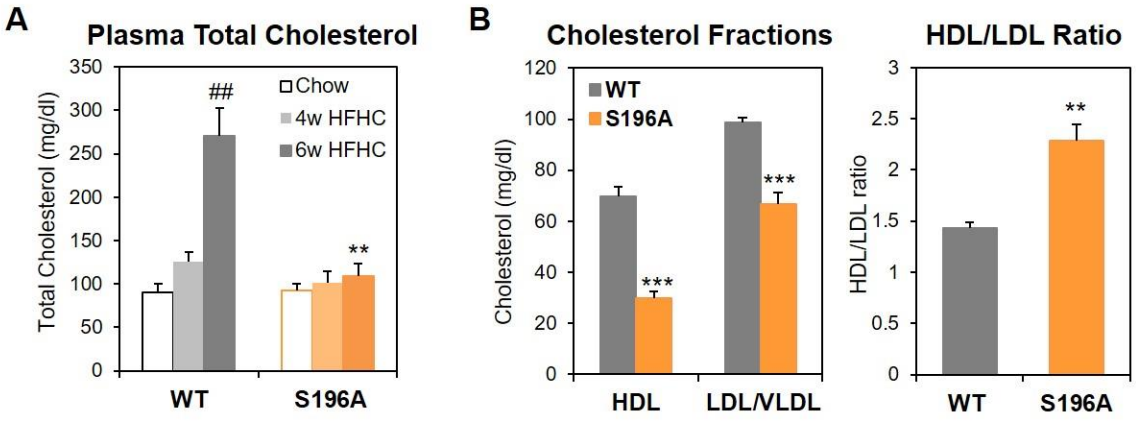

Figure 3.2. LXRα phosphorylation-deficient mice show reduced cholesterol levels in response to a HFHC diet

A) Plasma total cholesterol levels from WT and S196A mice fed a chow diet (n=4) or a HFHC diet for 4 weeks (n=6) or 6 weeks (n=5-6).

B) Plasma HDL, non-HDL (LDL and VLDL) or HDL/LDL ratio cholesterol levels from WT or S196A mice fed a HFHC diet for 6 weeks (n=5-6).

Data shown as means ± SEM. ## p-value < 0.005 4 weeks vs 6 weeks in WT group by Student's t-test. ** p < 0.005, *** p < 0.0005, relative to WT determined by Student's t-test.

Changes in organ weight were also determined, and a significant 20% decrease in liver to body weight ratio in S196A mice was detected when compared to WT controls (Figure 3.3. A). Spleen and kidney weights were also significantly lower in the mutant group, whereas the rest of the organs had similar weights (Figure 3.3. B). The change in liver to body weight could be due to a reduction on hepatic lipid accumulation, as suggested by the difference in the coloration of the livers (Figure 3.3. C) and the differences in total cholesterol levels observed in plasma (Figure 3.2. A). Determination of hepatic total cholesterol levels confirmed that control animals had almost a four-fold higher amount of total cholesterol in liver (Figure 3.2. D), suggestive of a protective effect from cholesterol accumulation in tissue and plasma by the phosphorylation-deficient LXRα. Lastly, in order to assess if the reduction in total cholesterol levels in the mutant mice could be due to its increased catabolism, plasma and hepatic bile acids were quantified in WT and S196A animals. Interestingly, instead of increased catabolism, LXRα phospho-mutant mice showed a trend towards reduced levels of plasma and hepatic bile acids (Figure 3.2. E), suggesting that a more efficient cholesterol catabolism is probably not the reason behind the differences in cholesterol levels between groups of mice.

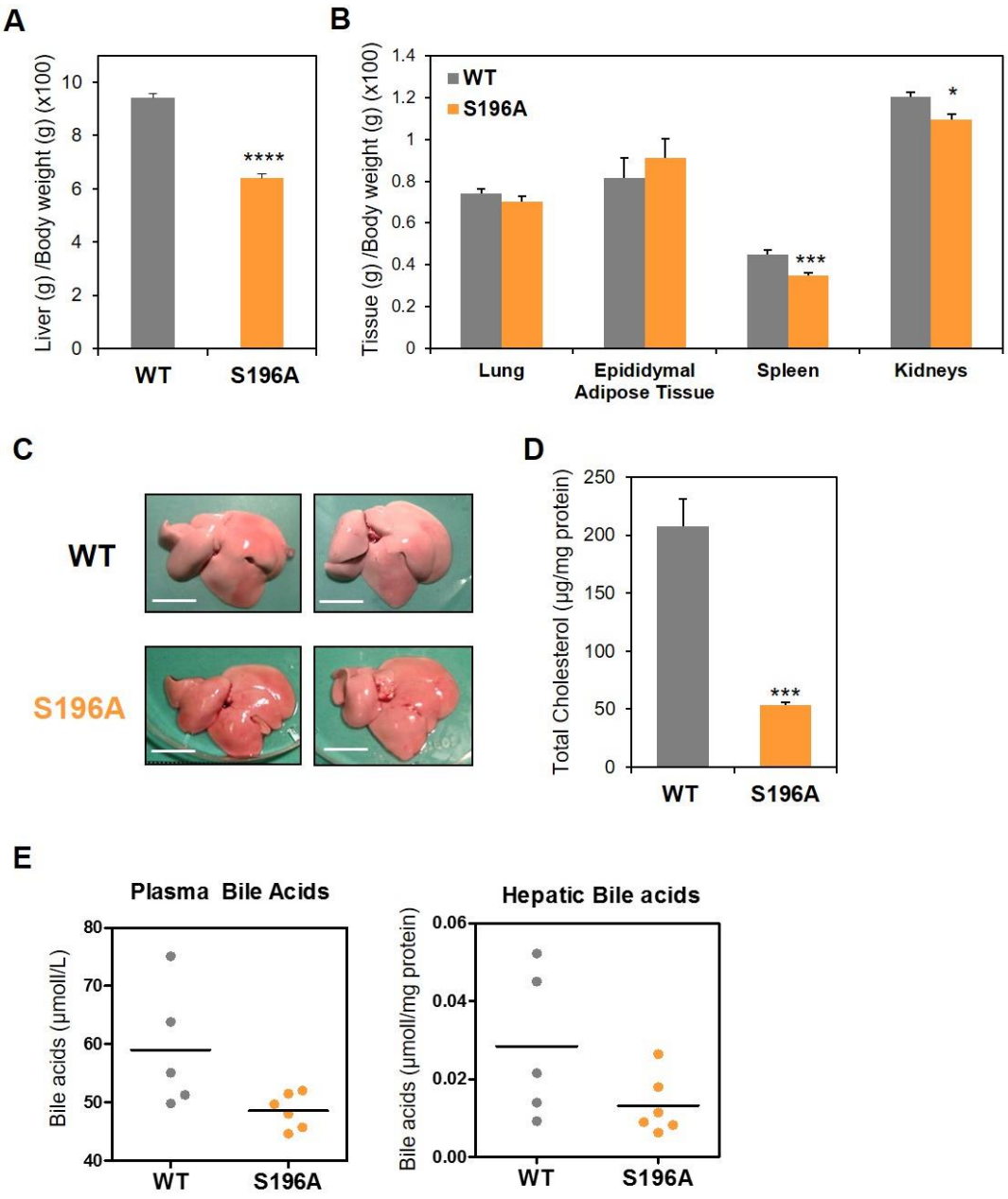

Figure 3.3. WT and S196A organ weights and hepatic total cholesterol content after being fed a HFHC diet

A-B) WT (n = 15) and S196A (n = 16) tissue mass relative to body weight on animals fed a HFHC diet.

C) Representative images of gross morphology of livers from WT and S196A mice after being fed a HFHC diet.

D) Hepatic total cholesterol levels assessed from WT and S196A mice fed a HFHC diet for (n=6).

E) Plasma and liver total bile acids on WT (n=5) and S196A (n=6) mice fed a HFHC diet. Values shown on D and E (right) are normalized to protein levels in tissue homogenates. Data represents means ± SEM.* $p < 0.05$, *** $p < 0.0005$, **** $p < 0.00005$ relative to WT determined by Student's t-test.

3.4. Impaired LXRα phosphorylation alters hepatic cholesterol homeostasis in a gene-specific manner in liver but not in small intestine

Expression of several genes involved in different cholesterol homeostasis pathways, including biosynthesis, catabolism and export were assessed by standard qPCR and through pathway-focused qPCR arrays (see section 2.3 for further details). The complete list with all the Lipoprotein Signalling and Cholesterol Metabolism RT2 Array results can be found in Table 3.2. Interestingly, analysis of pathway-focused PCR arrays showed that the expression of several genes involved in cholesterol biosynthesis (see Figure 1.2), as well as *Tm7sf2* and *Ebp*, were significantly higher in the livers of S196A mice (Figure 3.4. A). Cholesterogenic genes have been shown to be directly repressed by LXR activity (330,331), so their increased expression could be the result of an indirect feedback regulation caused by lower intrahepatic cholesterol levels, and thus not directly regulated by the non-phosphorylated LXRα. Nevertheless, investigation of the changes in expression of several genes between chow and HFHC diet fed mice in both groups revealed that, although hepatic cholesterol content remained similar in WT and S196A groups on chow (Table 3.1), expression of the cholesterogenic transcription factor *Srebp2* and its target gene *Ldlr* are reduced in chow-fed S196A livers (Figure 3.4. B). As expected, expression of these genes was strongly repressed in WT mice upon addition of dietary cholesterol (Figure 3.4. B), whereas they were largely unaffected in S196A mice. This is consistent with the unvaried levels of plasma and hepatic cholesterol between chow and HFHC groups in the mutant animals (Figure 3.2. A, 3.3. D).

Moreover, analysis of classic LXR target genes and other genes in cholesterol homeostasis, revealed that mRNA levels of the *Cyp7a1* gene, involved in cholesterol catalysis and driving the rate-limiting step in bile acid formation (44,106), didn't vary between genotypes (Figure 3.5. A). However, mRNA levels of *Cyp7b1*, a gene that takes part in the alternate/acidic pathway for primary bile acid production, and which has been shown previously to be actively repressed by LXRs (332,333), were significantly

increased in the livers of phospho-deficient mice (Figure 3.5. A).

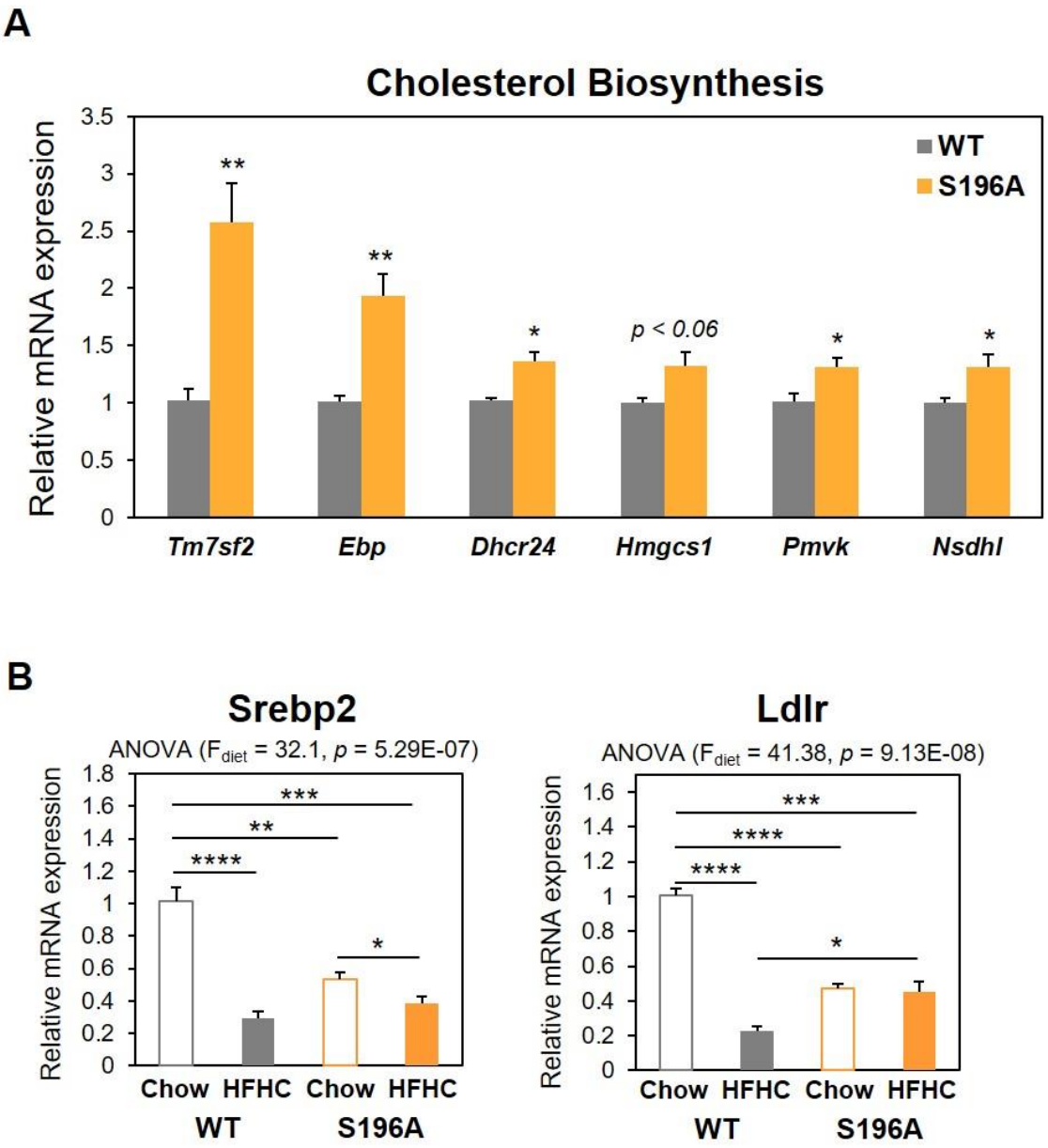

Figure 3.4. Lack of LXRα phosphorylation alters hepatic cholesterol biosynthesis

A) Hepatic gene expression from WT or S196A mice fed a HFHC diet for 6 weeks (n = 6). Results are normalized to an average of five different house-keeping genes and shown relative to WT, set as 1.

B) Hepatic gene expression of WT and S196A mice fed either a chow (n=4) or a HFHC diet (n=6). Results are normalized to cyclophilin levels and shown relative to WT Chow group. Significance was determined using single variance ANOVA followed by Student's T-test. The *F*-statistic ($df_{between}$=3, df_{within}=16) and the *P* value for the significant main effects are shown.

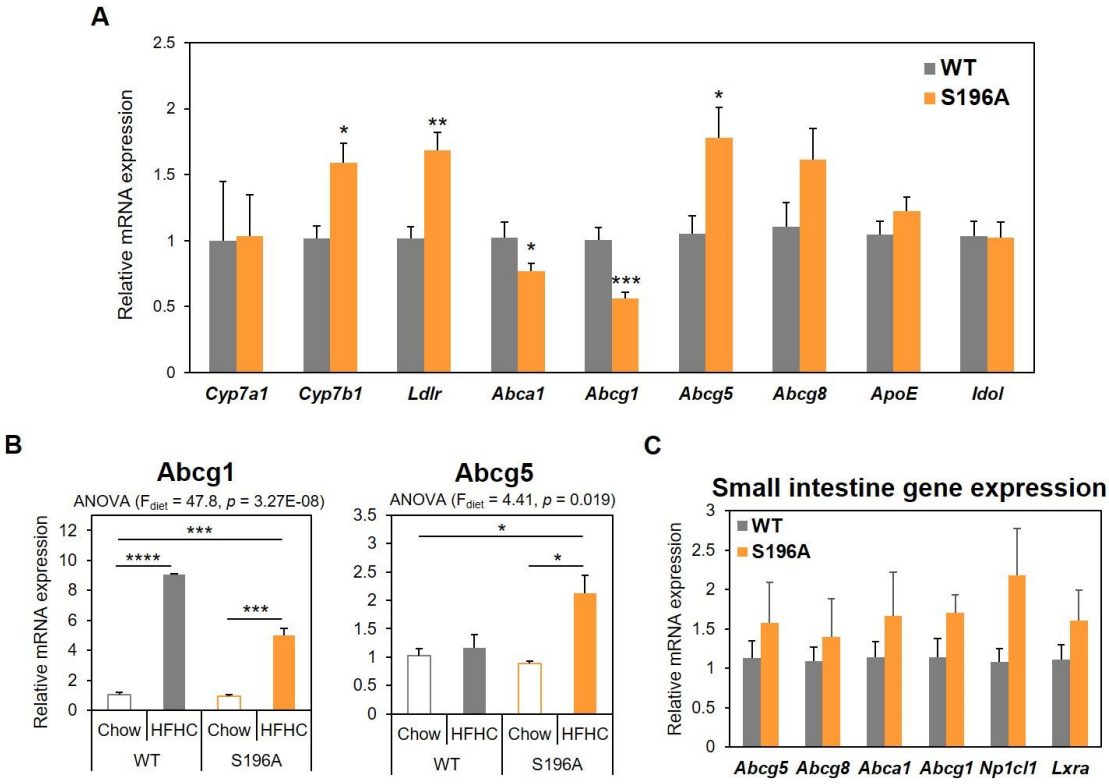

Figure 3.5. Lack of LXRα phosphorylation alters hepatic cholesterol homeostasis in a gene-specific manner in liver but not in small intestine

A) Hepatic gene expression from WT or S196A mice fed a HFHC diet for 6 weeks (n = 6). Results are normalized to the average levels of five different housekeeping genes or cyclophilin (*Abcg8* and *Idol*) and shown relative to WT set as 1.

B) Hepatic gene expression of WT and S196A mice fed either a chow (n=4) or a HFHC diet (n=6). Results are normalized to cyclophilin levels and shown relative to WT Chow group. Significance was determined using single variance ANOVA followed by Student's T-test. The *F*-statistic ($df_{between}$=3, df_{within}=16) and the *P* value for the significant main effect are shown.

C) Gene expression in small intestine of WT and S196A mice fed a HFHC diet for 6 weeks (n = 6). Results are normalized to cyclophilin levels and shown relative to WT.

Data shown as means ± SEM. * p < 0.05, ** p < 0.005, *** p < 0.0005, **** p < 0.00005 relative to WT determined by Student's t-test.

In addition, a significant decrease in the expression of the ABC-transporters *Abca1* and *Abcg1*, two classic LXR target genes, was observed in S196A genotype compared to the wild-type mice (Figure 3.5. A). *Abca1* and *Abcg1* are responsible for intracellular cholesterol efflux onto lipid-poor apolipoproteins and HDL, respectively; and are key mediators of the RCT (see section 1.2.1.3). Next, expression of other ABC transporters that are known LXR direct targets, *Abcg5* and *Abcg8* (118) which take part in the hepatobiliary secretion of cholesterol were quantified. Notably, whilst the expression of both transporters was induced in the S196A livers, only the gene encoding for Abcg5 was significantly increased ($p < 0.05$) (Figure 3.5. A). As with the cholesterogenic genes, these results led to further exploring whether WT and mutant mice respond similarly to the HFHC diet. Analysis of hepatic gene expression revealed that while *Abcg1* levels are severely induced by the diet in both groups, albeit to a different extent (9- fold for WT vs 4.9- fold for S196A), enhanced *Abcg5* expression by the diet is specific to the S196A genotype (Figure 3.5. B). Lastly, no differences in gene expression were observed for several other genes that are well established LXR target genes, such as apolipoprotein E (*ApoE*) (334) or the inducible degrader of the LDLR (*Idol*) (335) (Figure 3.5. A), thus confirming that the transcriptional regulation by the phosphorylation-deficient LXRα is gene-specific.

Intestinal absorption and excretion of cholesterol also play a very important role by which LXR modulates cholesterol homeostasis (see section 1.2.1.3). Therefore, expression of genes involved in intestinal absorption and excretion of cholesterol were assessed. No changes were observed in the expression of any of the genes tested (Figure 3.5. C), further confirming that the difference in cholesterol accumulation seen in the mutant mice is most likely due to increased hepatobiliary secretion, and not to increased transintestinal excretion.

Lastly, since some oxysterols such as 25-OHC and 27-OHC, have been reported to be significantly enhanced in patients with NAFLD (336), the levels of several circulating

oxysterols were investigated in plasma of WT and S196A mice after being fed the HFHC diet. In addition to profound differences in their cholesterol levels, LXRα phospho-mutant mice also showed significantly reduced levels for most of the plasma oxysterols analysed (Figure 3.6). Interestingly, the only oxysterol that didn't change between WT and S196A was 24(S),25-EC, which is also the only oxysterol that is not a metabolite of cholesterol (see section 1.1.2.1). Therefore, the reduction in circulating oxysterols mirrored that of circulating total cholesterol, probably due to there being less available substrate for oxysterol production.

Overall, these results show that S196A mice are protected from dietary cholesterol accumulation in liver and plasma.

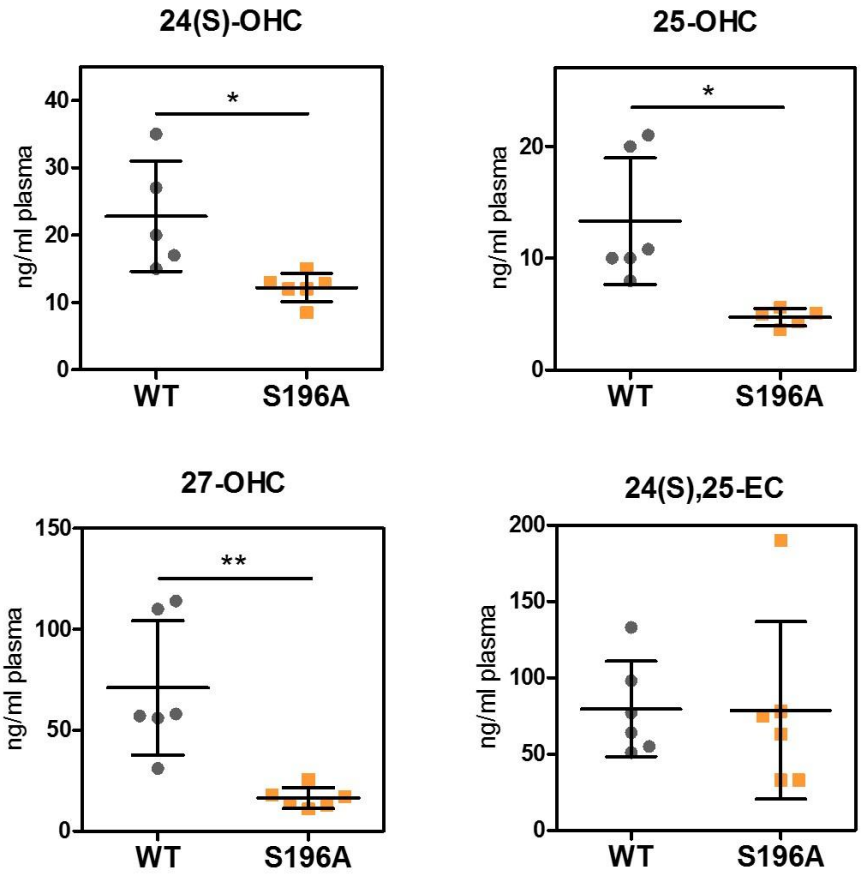

Figure 3.6. Circulating oxysterols are significantly lower in LXRα-phosphorylation mutant mice

Quantification of oxysterols in plasma of WT and S196A mice (n=6) after being fed a HFHC diet for 6 weeks. * $p < 0.05$, ** $p < 0.005$, relative to WT determined by Student's t-test.

Gene	WT	S196A	p-value
Abca1	1.02	0.77	**0.036**
Abca2	1.02	1.07	0.618
Abcg1	1.01	0.56	**0.00012**
Acaa2	1.01	1.37	**0.027**
Akr1d1	1.02	1.29	0.163
Angptl3	1.05	1.89	**0.033**
Ankra2	1.02	1.12	0.496
Apoa1	1.01	1.18	0.242
Apoa2	1.06	1.56	**0.043**
Apoa4	1.07	0.89	0.524
Apob	1.01	1.01	0.991
Apoc3	1.04	1.57	0.053
Apod	1.06	1.62	0.058
Apoe	1.05	1.22	0.351
Apof	1.01	1.24	0.068
Apol8	*n/a*	*n/a*	*n/a*
Cdh13	1.02	1.18	0.281
Cel	*n/a*	*n/a*	*n/a*
Cela3b	*n/a*	*n/a*	*n/a*
Cnbp	1.01	1.34	0.054
Colec12	1.01	1.44	**0.0006**
Crp	1.00	1.43	0.060
Cxcl16	1.01	0.75	**0.012**
Cyb5r3	1.00	0.93	0.482
Cyp11a1	*n/a*	*n/a*	*n/a*
Cyp39a1	1.02	1.49	0.127
Cyp46a1	1.07	1.79	0.130
Cyp51	1.03	1.38	0.182
Cyp7a1	2.55	2.64	0.958
Cyp7b1	1.02	1.59	**0.010**
Dhcr24	1.02	1.36	**0.019**
Dhcr7	1.01	0.99	0.876
Ebp	1.01	1.93	**0.002**
Fdft1	1.01	0.86	0.053
Fdps	1.02	1.12	0.553
Hdlbp	1.00	1.19	0.105
Hmgcr	1.01	0.94	0.517
Hmgcs1	1.00	1.32	0.051
Hmgcs2	1.04	1.33	0.132
Idi1	1.26	1.19	0.916
Il4	1.05	1.26	0.650
Insig1	1.03	2.24	**0.029**

Gene	WT	S196A	p-value
Insig2	1.04	1.55	0.064
Lcat	1.02	1.38	**0.022**
Ldlr	1.02	1.69	**0.002**
Ldlrap1	1.01	1.06	0.626
Leptin	*n/a*	*n/a*	*n/a*
Lipe	1.03	1.35	**0.031**
Lrp10	1.01	1.06	0.603
Lrp12	1.01	0.64	**0.0003**
Lrp1b	*n/a*	*n/a*	*n/a*
Lrp6	1.00	1.12	0.353
Lrpap1	1.00	1.05	0.394
Mbtps1	1.01	1.16	0.303
Mvd	1.04	0.96	0.706
Mvk	1.02	0.86	0.185
Ncp1l1	*n/a*	*n/a*	*n/a*
Shp	1.05	1.24	0.678
Fxr	1.08	1.31	0.470
Nsdhl	1.00	1.31	**0.046**
Olr1	1.26	1.37	0.864
Osbpl1a	1.00	1.06	0.633
Osbpl5	1.01	0.66	**0.0007**
Pcsk9	1.33	2.03	0.315
Pmvk	1.01	1.31	**0.018273**
Ppard	1.01	1.10	0.588
Prkaa1	1.01	0.86	0.125
Prkaa2	1.01	0.96	0.756
Prkag2	1.03	0.92	0.522
Scap	1.02	1.12	0.391
Scarf1	1.02	1.06	0.729
Snx17	1.01	1.13	0.148
Soat1	1.05	0.60	**0.016**
Soat2	1.05	1.08	0.880
Sorl1	1.04	0.68	0.060
Srebf1	1.04	2.48	0.063
Srebf2	1.03	1.25	0.211
Stab1	1.04	1.18	0.574
Stab2	1.01	1.11	0.390
Stard3	1.01	0.99	0.824
Tm7sf2	1.02	2.57	**0.002**
Trerf1	1.01	0.70	**0.023**
Vldlr	1.06	1.44	0.203

Table 3.2. Lipoprotein signalling and cholesterol metabolism RT2 Array results
Results represent means and are shown relative to WT average, p-value determined by Student's t-test (n=6). *n/a* corresponds to those genes whose expression was below the level of detection.

3.5. LXRα phospho-deficient mice have more pronounced steatosis

As LXR activity plays a key role in increased *de novo* lipogenesis (128,143,144), changes in triglyceride levels in both WT and S196A mice were assessed. Similar to cholesterol levels, no differences in hepatic triglycerides were found between groups when fed a chow diet (Table 3.1).

Remarkably, upon being fed a HFHC diet and in contrast to plasma levels (Figure 3.7. A), both hepatic Non-Esterified Fatty Acids (NEFAs) and triglyceride levels in S196A mice were about 80% and 40% higher than in WT mice, respectively (Figure 3.7. B).

Therefore, histological status in livers of WT and S196A mice was blindly assessed by an independent pathologist for markers of murine NAFLD (309). Consistent with lipid levels, histological scoring demonstrated that S196A mice have enhanced micro and macrovesicular steatosis (Figure 3.8. A,B). Further characterization of lipid droplet area by morphometric analysis of Hematoxylin & Eosin-stained liver sections revealed that mutant mice exhibit larger and more numerous lipid droplets (Figure 3.8. B,C), confirming their predominant macrovesicular steatosis, which was also accompanied by a higher expression of lipid droplet proteins (Figure 3.8. D).

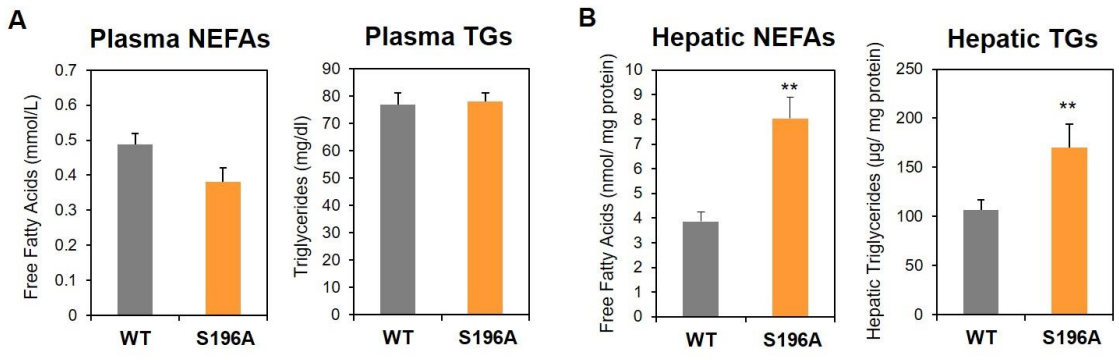

Figure 3.7. Plasma and hepatic fatty acid and triglyceride levels

A) Plasma and B) Hepatic non-esterified fatty acids (NEFAs) or triglycerides (TGs) levels from WT and S196A mice fed a HFHC diet for 6 weeks (n=6). Hepatic values shown are normalized to protein levels in tissue homogenates. Data represents means ± SEM. ** $p < 0.005$ relative to WT determined by Student's t-test.

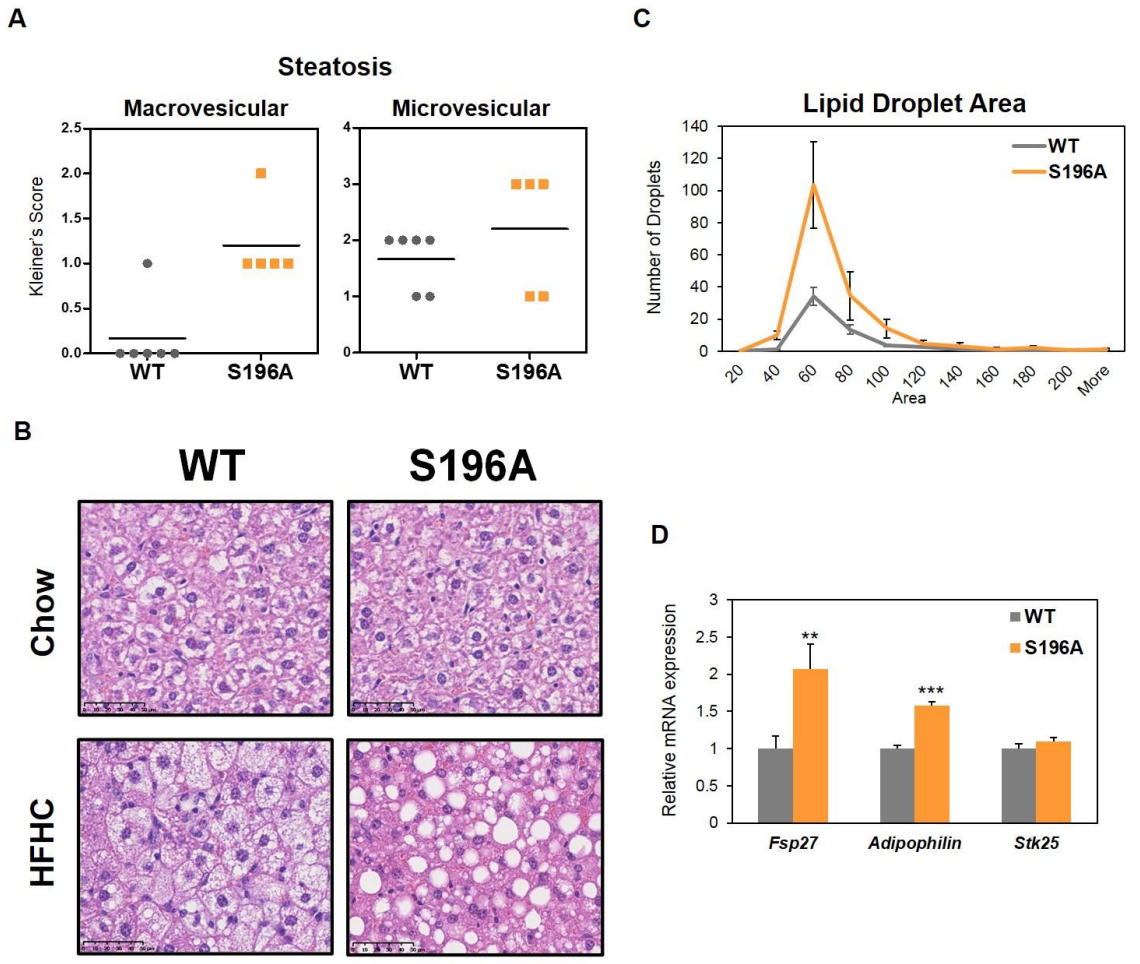

Figure 3.8. LXRα phospho-deficient mice have a more pronounced steatosis

A) Kleiner's Scores for macrovesicular and microvesicular steatosis (0-3) from liver sections of WT and S196A mice (n=5-6) after being fed a HFHC diet.

B) Representative images of Haematoxylin and Eosin (H&E) stained liver sections from WT and S196A mice before (chow) and after (HFHC) being fed a HFHC diet. Images are at 400x magnifications.

C) Distribution of lipid droplets by area in H&E-stained liver sections of WT and S196A mice (n=6) after being fed a HFHC diet.

D) Hepatic gene expression of WT or S196A mice (n = 6) after being fed a HFHC diet. Data are normalized to cyclophilin and shown relative to WT, set as 1.

Data represents means ± SEM. ** $p < 0.005$ or *** $p < 0.001$ relative to WT determined by Student's t-test.

Increased steatosis in S196A mice was associated with enhanced hepatic expression of the *Srebp-1c* lipogenic transcription factor, and other well-established LXR target genes involved in fatty acid synthesis (fatty acid synthase, *Fas*) and desaturation (stearoyl-CoA desaturase-1, *Scd-1*) (Figure 3.9). In contrast, expression of genes involved in fatty acid elongation (*Elovl6*) or uptake (*Cd36*), were not affected indicating that in this model, changes in LXRα phosphorylation alter gene expression in a gene-specific manner confirming previous findings *in vitro* (163,165), and as seen for genes involved in cholesterol metabolism (Figure 3.5. A). Interestingly, the expression of angiopoietin-like protein 3 (*Angptl3*), which has been previously shown to be induced by LXRs (337,338), was also significantly increased in the livers of S196A mice. Increased levels of this protein have been shown to raise plasma triglycerides in mice (339), which insinuates of a possible regulatory mechanism in the liver in order to get rid of the excess in fats.

Altogether, these results demonstrate that LXRα phosphorylation deficiency at S196 induces hepatic steatosis in response to a HFHC diet.

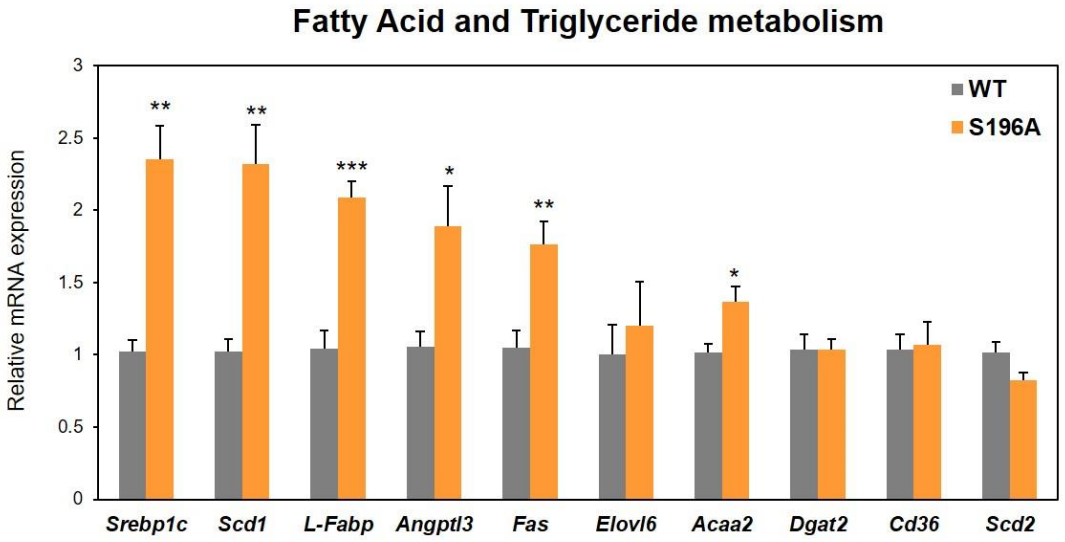

Figure 3.9. LXRα-S196A causes increased expression of genes involved in fatty acid and triglyceride synthesis

Hepatic gene expression from WT or S196A mice (n = 6) after being fed a HFHC diet. Data are normalized to the average levels of five different housekeeping genes (for *Angptl3* and *Acaa2* genes) or cyclophilin and shown relative to WT, set as 1. Data represent means ± SEM. * $p < 0.05$, ** $p < 0.005$ or *** $p < 0.001$ relative to WT determined by Student's t-test.

3.6. Impaired LXRα phosphorylation attenuates diet-induced hepatic inflammation and fibrosis

Diet-induced hepatic steatosis precedes inflammation and progression to fibrosis in experimental models (340,341). Strikingly, histological analysis of liver slides showed that not only LXRα-S196A mice scored lower for inflammation and hepatocyte ballooning (Figure 3.10. A), but they also displayed significantly less fibrosis, as quantified by levels of picrosirius red stain (Figure 3.10. B), which allows for the visualization of collagen I and III fibres. Pathway-focused analysis of mRNA expression in livers of both genotypes confirmed that attenuated inflammation and fibrosis in the S196A mice was associated with a significant decrease in the expression of several pro-inflammatory and pro-fibrotic mediators (Figure 3.10. C), such as Oncostatin M (*Osm*) (342), Chemokine (C-X-C motif) ligand 1 (*Cxcl1*) (343) and Osteopontin (*Opn* or *Spp1*) (344) as well as collagen synthesis, like Collagen type I alpha 1 chain (*Col1a1*) and Transforming growth factor, beta 2 (*Tgfb2*). The complete list with all the Cytokines & Chemokines RT2 Array results can be found in Table 3.3.

Only a subset of genes in the panel analysed was affected by changes in LXRα phosphorylation upon presence of the HFHC diet (Figure 3.10. C and Table 3.3), further corroborating the gene specific effects this modification has on LXRα activity.

Interestingly, changes in gene expression in response to the cholesterol-rich diet further evidenced the attenuated inflammatory and fibrotic response of the S196A mice (Figure 3.11). For instance, basal expression of *Spp1* and *Tgfb2* is reduced in S196A mice and is only enhanced minimally when challenged with this diet. As expected, for all of the other genes examined, differences between genotypes were only revealed upon exposure to the HFHC diet (Figure 3.11), further establishing it as an agent of hepatic injury.

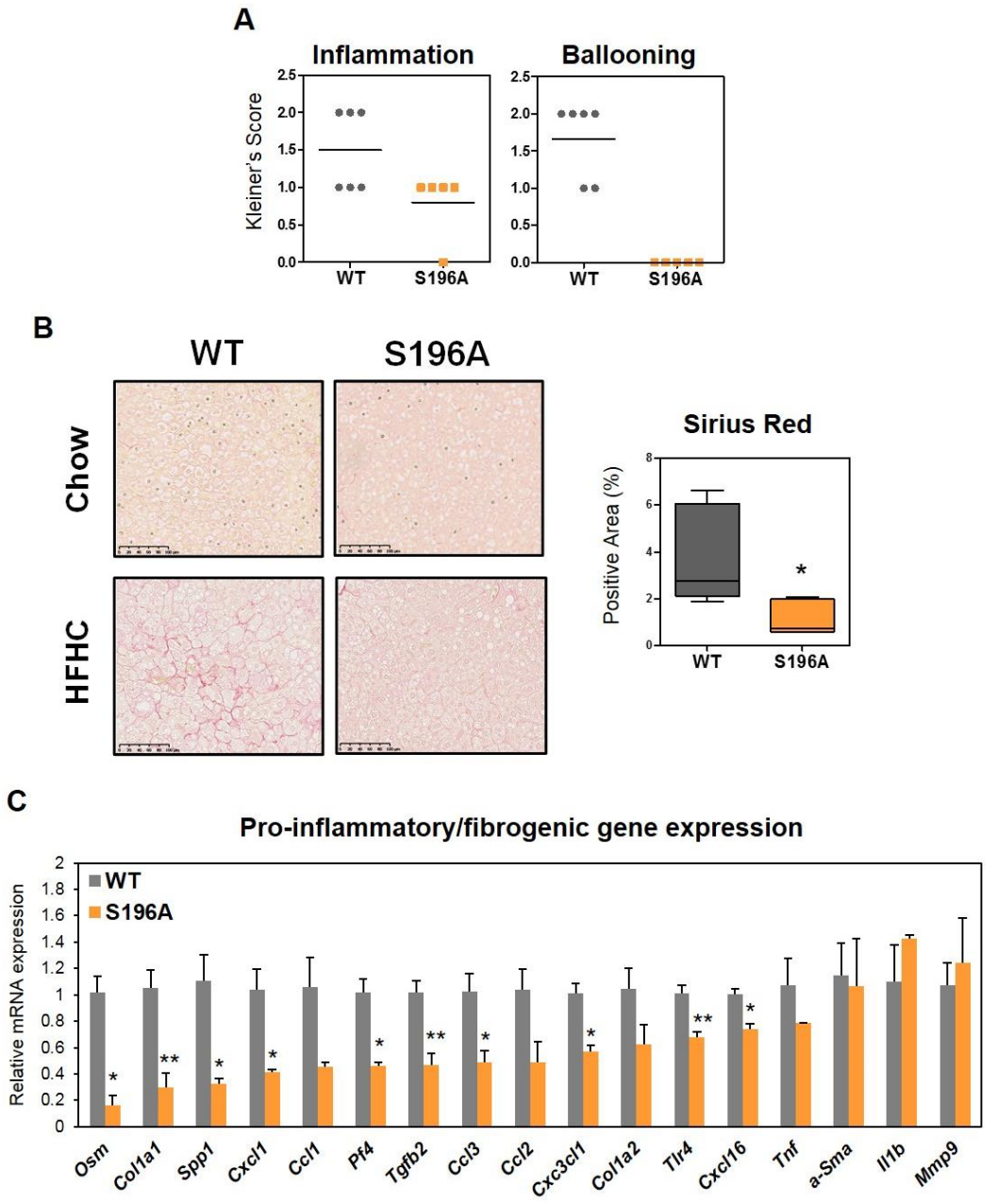

Figure 3.10. LXRα-S196A attenuates diet-induced hepatic inflammation and fibrosis

A) Kleiner's Scores for lobular inflammation (0-3) and Hepatocyte ballooning (0-2) from liver sections of WT and S196A mice (n=5-6).

B) Representative images of Picrosirius Red stained liver sections from WT and S196A mice (left). Quantification of Picrosirius red-stained areas on three independent areas per section (n = 6) (Right) by Image J. Images are at 200x magnifications.

C) Hepatic gene expression from WT or S196A mice (n = 6). Data are normalized to the average levels of five different housekeeping genes or cyclophilin (for *Col1a1*, *Col1a2*, *Tlr4*, *a-Sma* and *Mmp9* genes) and shown relative to WT.

Data represents means ± SEM. * $p < 0.05$, ** $p < 0.005$ relative to WT determined by Student's t-test.

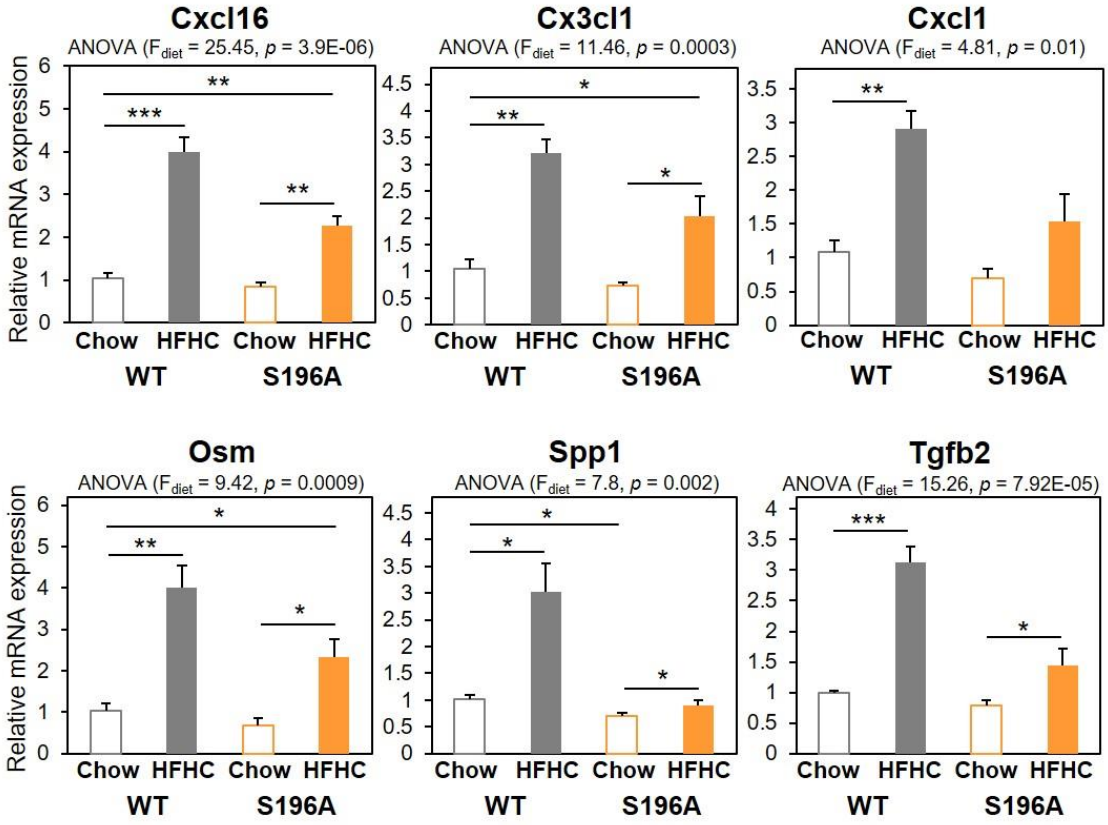

Figure 3.11. Differences in inflammatory gene expression in response to diet are gene-specific

Hepatic gene expression in WT and S196A mice fed either a chow (n=4) or a HFHC diet (n=5-6). Results are normalized to cyclophilin levels and shown relative to WT Chow group. Significance was determined using single variance ANOVA followed by Student's T-test. The *F*-statistic ($df_{between}$=3, df_{within}=15) and the *P* value for the significant main effect are shown. * $p < 0.05$, ** $p < 0.005$, *** $p < 0.0005$, relative to WT Chow as determined by Student's t-test. Data represents means ± SEM.

Gene	WT	S196A	p-value
Adipoq	1.50	1.56	0.962
Bmp2	1.00	1.41	**0.016**
Bmp4	1.04	0.95	0.677
Bmp6	1.00	1.25	**0.033**
Bmp7	1.08	1.01	0.842
Ccl1	1.06	0.45	0.089
Ccl11	1.25	1.35	0.917
Ccl12	1.59	4.36	0.074
Ccl17	1.06	2.13	0.135
Ccl19	1.01	0.86	0.456
Ccl2	1.04	0.49	0.078
Ccl20	*n/a*	*n/a*	*n/a*
Ccl22	1.21	1.71	0.395
Ccl24	1.00	1.94	0.221
Ccl3	1.02	0.49	**0.044**
Ccl4	1.05	0.65	0.204
Ccl5	1.01	1.50	**0.011**
Ccl7	1.05	0.54	0.120
Cd40 lg	1.08	0.90	0.665
Cd70	*n/a*	*n/a*	*n/a*
Cntf	1.01	1.57	**0.004**
Csf1	1.01	0.78	0.114
Csf2	1.06	1.35	0.542
Csf3	*n/a*	*n/a*	*n/a*
Ctf1	1.00	1.28	**0.009**
Cxc3cl1	1.01	0.57	0.027
Cxcl1	1.04	0.41	**0.036**
Cxcl10	1.07	1.18	0.721
Cxcl11	1.26	1.55	0.724
Cxcl12	1.00	1.11	0.435
Cxcl13	1.16	5.93	**0.002**
Cxcl16	1.00	0.74	**0.014**
Cxcl3	*n/a*	*n/a*	*n/a*
Cxcl5	1.22	0.33	0.109
Cxcl9	1.05	1.74	0.382
Fasl	1.03	1.69	**0.020**
Gpi1	1.00	0.98	0.750
Hc	1.00	1.26	**0.062**
Ifna2	0.96	0.58	0.374
Ifng	1.56	2.74	0.350
Il10	1.04	1.81	0.498
Il11	1.04	0.45	0.161

Gene	WT	S196A	p-value
Il12a	1.07	1.23	0.697
Il12b	1.13	0.44	0.146
Il13	1.05	1.12	0.862
Il15	1.00	0.81	**0.023**
Il16	1.06	0.93	0.639
Il17a	*n/a*	*n/a*	*n/a*
Il17f	1.01	1.17	0.752
Il18	1.00	1.33	**0.004**
Il1a	1.01	1.02	0.928
Il1b	1.10	1.42	0.403
Il1rn	1.01	0.61	**0.035**
Il2	*n/a*	*n/a*	*n/a*
Il21	*n/a*	*n/a*	*n/a*
Il22	*n/a*	*n/a*	*n/a*
Il23a	1.01	1.58	0.504
Il24	*n/a*	*n/a*	*n/a*
Il27	1.01	0.71	0.084
Il3	*n/a*	*n/a*	*n/a*
Il4	1.02	1.63	0.086
Il5	1.30	3.35	0.136
Il6	1.26	2.44	0.589
Il7	1.00	1.01	0.972
Il9	1.52	1.07	0.663
Lif	1.15	0.53	0.369
Lta	1.00	0.82	0.638
Ltb	1.03	0.97	0.847
Mif	1.00	1.10	0.450
Mstn	*n/a*	*n/a*	*n/a*
Nodal	1.02	1.00	0.946
Osm	1.02	0.16	**0.007**
Pf4	1.02	0.46	**0.013**
Ppbp	1.04	1.54	0.215
Spp1	1.10	0.29	**0.045**
Tgfb2	1.01	0.47	**0.005**
Thpo	1.00	0.94	0.475
Tnf	1.07	0.79	0.320
Tnfrsf11b	1.01	1.02	0.919
Tnfrsf10	1.00	1.16	0.488
Tnfrsf11	1.89	2.85	0.665
Tnfrsf13b	1.02	0.67	0.082
Vegfa	1.00	1.22	0.363
Xcl1	1.49	1.86	0.720

Table 3.3. Cytokines & Chemokines RT2 Array results
Results represent means and are shown relative to WT average, p-value determined by Student's t-test (n=6). *n/a* corresponds to those genes whose expression was below the level of detection.

To further characterize the observed differences in hepatic inflammation and fibrosis, several pathways involved in the pathogenesis of lipid-induced liver damage were investigated (see section 1.2.3). The number of apoptotic cells present was similar between genotypes as assessed by dUTP nick end labelling (TUNEL) staining of liver sections (Figure 3.12. A), and lipid peroxidation levels quantified by thiobarbituric acid reactive substances (TBARS) assay revealed no differences in oxidative stress between groups (Figure 3.12. B). No significant differences were found in the percentage of areas in the liver positive for macrophage marker F4/80, which identifies both resident Kupffer cells and infiltrating macrophages (345), as assessed by immunohistochemistry staining (Figure 3.12. C), although there was a trend towards a decreased number of F4/80+ areas in S196A livers.

Interestingly, a reduction in the expression of several factors involved in the activation of the ER stress pathway (Figure 3.12. D) such as the UPR target gene C/EBP homologous protein (*Chop*) and the Activating Transcription Factor (*Atf3*) (346) suggests that S196A mice are protected from lipotoxicity, likely through a reduction in ER stress activation. This was further supported by a significant decrease in the splicing of the transcription factor X-box-binding protein-1 (*Xbp1*) mRNA (Figure 3.12. D), which leads to the protein translocating to the nucleus and the induced expression of several factors in the UPR pathway (249).

The link between ER stress and hepatic damage has been extensively studied (see section 1.2.3.4) and it is now understood that prolonged ER stress not only increases steatosis levels but also promotes hepatic fibrosis (347). Overall, these findings demonstrate that changes in LXRα-phosphorylation at S196 attenuates lipid-induced hepatic inflammation and fibrosis partly by reducing ER stress despite the enhanced steatosis.

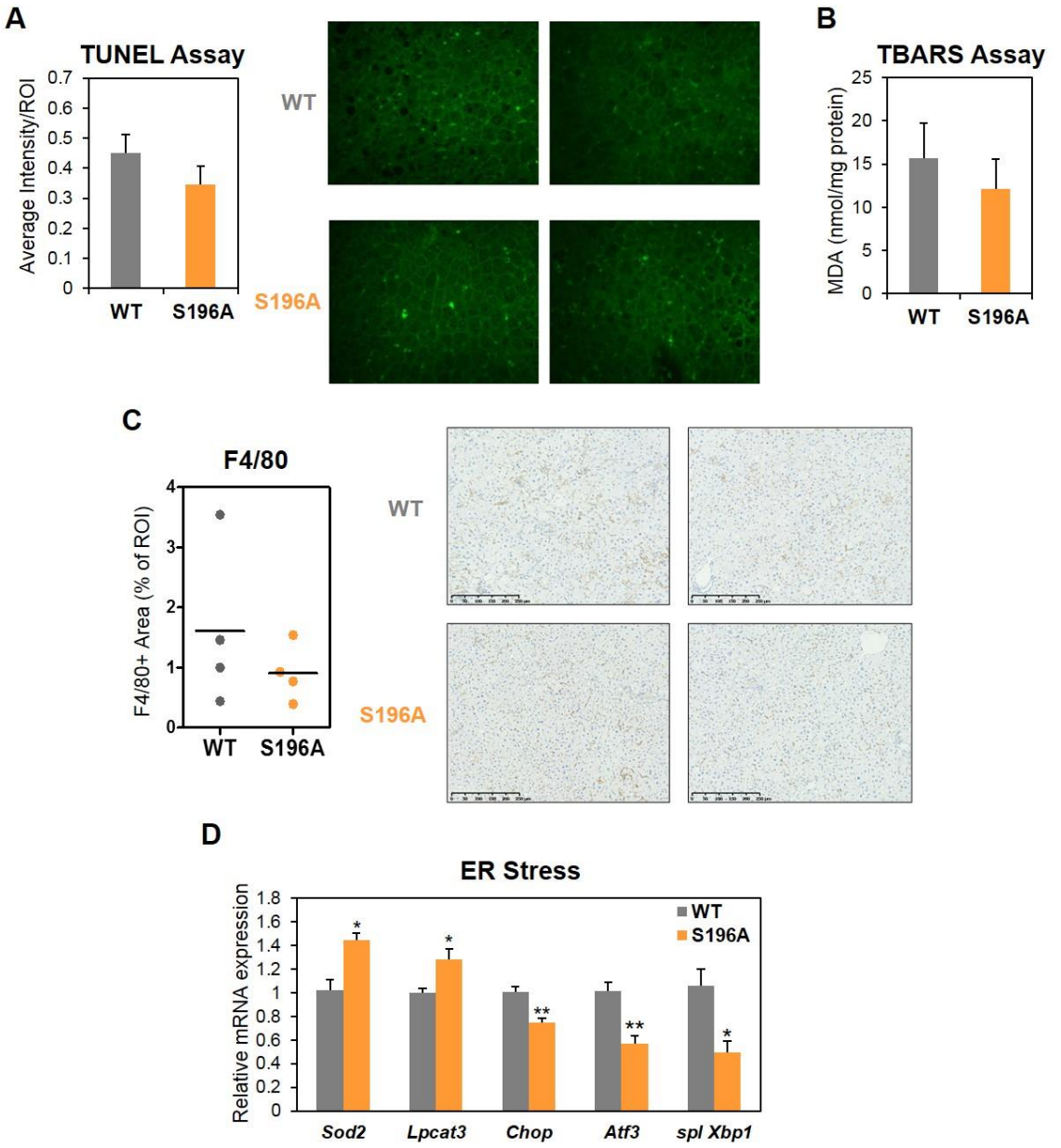

Figure 3.12. Reduction in hepatic inflammation and fibrosis is associated with reduced ER stress

A) Hepatic cell apoptosis assessed *in situ* (n = 6) by TUNEL assay (Left). Representative images of TUNEL-stained liver sections from WT and S196A mice at 200x magnification (Right).

B) Hepatic lipid peroxidation shown as MDA levels in WT and S196A livers (n = 6) normalised to protein levels in tissue homogenates.

C) Quantification of F4/80-positively stained areas in liver sections of WT and S196A mice at 200x magnification (n=4) and representative images of immunohistochemistry staining. Dots represent average of three independent areas per animal.

D) Hepatic gene expression from WT or S196A mice (n = 6). Values shown are normalized to cyclophilin and shown relative to WT.

Data are means ± SEM. * $p < 0.05$, ** $p < 0.005$ relative to WT determined by Student's t-test.

3.7. Summary

- Hepatic LXRα is phosphorylated under basal conditions in wild-type mice and human livers
- S196A mice show impaired LXRα-Ser196 phosphorylation in liver
- Phosphorylation-deficient mice show no apparent developmental differences
- S196A mice are protected from dietary cholesterol accumulation in liver and plasma, which associates with higher expression of *Abcg5*
- There are no differences in small intestine LXR target gene expression between WT and S196A groups
- LXRα phosphorylation deficiency at S196 induces steatosis in response to a HFHC diet
- Hindering LXRα-phosphorylation at S196 attenuates lipid-induced hepatic inflammation and fibrosis, partly by reducing ER stress.

3.8. Discussion

While studying the effect of LXRα phosphorylation on cholesterol homeostasis *in vivo*, no differences were observed between groups when animals were fed a chow diet (Table 3.1). This phenomenon has already been reported in previous animal models of transgenic LXR (106,107), where no apparent phenotype is detected on animals without a dietary challenge. This has been hypothesised to be caused by the fact that standard rodent chow diets contain very little if any cholesterol (see section 2.2.1. for chow diet composition), and thus the impact that LXRs may have on lipid metabolism becomes insignificant, as most of the cholesterol in these animals comes from *de novo* synthesis (see section 1.1.3.1). Indeed, even though gene expression on chow livers revealed significant differences between groups, these didn't translate into changes in plasma (Figure 3.2. A) or hepatic total cholesterol levels (Table 3.1).

Traditional understanding of NAFLD pathogenesis stated that high levels of intrahepatic NEFAs and their metabolites cause lipotoxic injury to liver cells, and this will sequentially progress into hepatic chronic inflammation and fibrosis (348). However, more recent studies have shown that the amount of saturated over unsaturated fatty acids could be key in the progression to NASH (349). Indeed, activity of SCD1, which is involved in the biosynthesis of monounsaturated fatty acids, has been found to be preventive of steatohepatitis progression (350). In our study, the S196A mice proved to have a higher expression of *Scd1* (Figure 3.9), which could account for the lower hepatic damage. Determination of the hepatic fatty acid pool composition would shed more light into whether changes in LXRα phosphorylation skew hepatic metabolism towards the production of more protective unsaturated lipid species. Therefore, future work should investigate the exact mechanism through which the phospho-mutant LXRα induces steatosis. There are several possible causes for the observed increase of hepatic fats in this study (see section 1.2.3.1 for more details), which include: increased uptake of circulating free fatty acids released from the lipolysis of adipose tissue (351); increased *de novo* lipogenesis (DNL) (215,352); diminished lipid (VLDL) secretion (353); and a reduced capacity of fatty acid beta-oxidation (354). Based on the observation that plasma NEFAs, TGs and insulin levels do not differ between genotypes (Figure 3.7. A and Table 3.1), differences in hepatic fat accumulation in S196A mice are likely to result from intrahepatic causes; most probably due to an enhanced lipogenic programme, as observed in other LXR models (61,323,355). Moreover, DNL accounts for 25% of the hepatic fat in NAFLD patients (210). However, at this point I was not able to distinguish if this is caused by a direct LXR transcriptional activity or through the increased expression of *Srebp-1c*, since the activity of this transcription factor is also tightly regulated through post-transcriptional modifications (356), and thus its increased gene expression may not necessarily translate into increased activity. In addition, *Fas* (130) and *Scd-1* (131) have been shown to be LXR direct target genes, so their increased expression may not necessarily be mediated through Srebp-1c. Thus, it would be interesting to study in the future if this phenotype can be replicated or not in S196A mice

lacking the Srebp1c transcription factor. This could be achieved by crossing the S196A mutant mice with a strain of mice in which the SREBP function can be disrupted in adulthood through conditional induction of the Cre recombinase (357). Furthermore, a preliminary study on the longer-term effect (12 weeks) of the HFHC diet on hepatic steatosis and fibrosis revealed that, despite the WT and S196A mice reaching the same degree of steatosis (Figure 3.14. A,B) at that point, protection against the onset of fibrosis remained in the phospho-mutant animals (Figure 3.15. A,B). Nonetheless, the specific mechanisms behind this protection on the S196A mice after a 12 week exposure to the HFHC diet will need to be investigated in the future.

Besides the changes in liver, the spleen and kidneys of the S196A mice also displayed significantly reduced weight (Figure 3.3. B). Probably not coincidentally, LXRα is highly present in these two organs (3). Even though most of the work exploring LXR actions has focused on their effect on immunity in the spleen (358), and the adrenergic control of sodium excretion (359) as well as the renin-angiotensin system (360) in the kidney; a recent study addressing LXR effects on tissue cholesterol metabolism, found that upon administration of the GW3965 LXR agonist to LXRα/β knock-out mice, both spleen and kidney suffered a significant increase in cholesterol ester levels (361). It would be interesting in the future to assess how changes in LXRα phosphorylation at S196 regulate lipid metabolism in other tissues besides the liver, as the phenomenon of cholesterol accumulation is linked to several pathologies, such as renal glomerular disease (362,363).

There are also other mechanisms that have been implicated in the development of NAFLD and its progression to NASH, as is the role of cholesterol. Although the effects of dietary cholesterol on NAFLD pathogenesis remain conflicting, recent studies found a correlation between cholesterol intake and a higher degree of NAFLD, especially in non-diabetic individuals with a normal body mass index (364) and non-obese animals (365). Moreover, several animal studies have demonstrated that free cholesterol (FC) can act as a hepatotoxic agent (366) and activates hepatic stellate cells, key mediators in

collagen deposition in hepatic fibrosis (367). Overall, the set of experiments in this chapter indicate that the whole-body impairment of LXRα-S196 phosphorylation confers protection from accumulation of dietary cholesterol. Based on the changes in the hepatic expression of the ABCG5/8 cholesterol transporters (Figure 3.5 A,B), I suggest a model whereby lower plasma and hepatic total cholesterol levels in LXRα phosphorylation-deficient mice are caused by a higher hepatobiliary excretion rate (Figure 3.13).

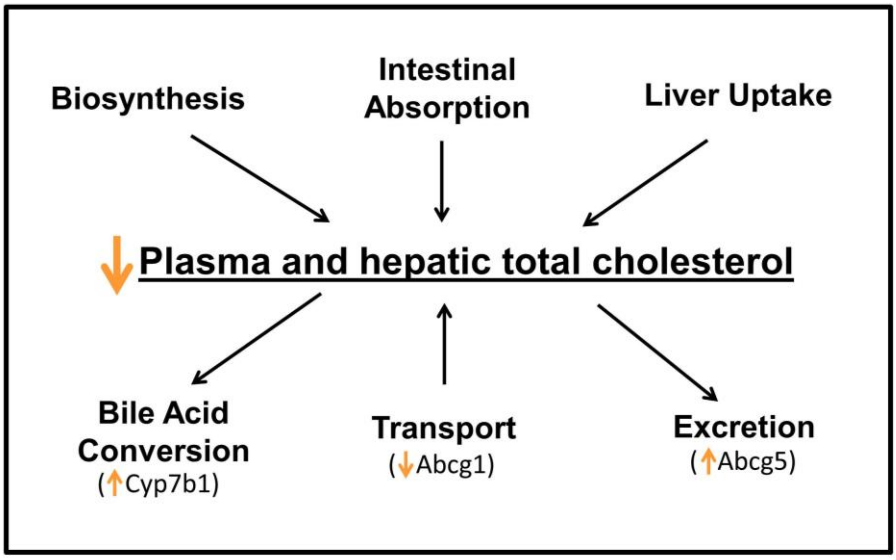

Figure 3.13. Pathways involved in the regulation of plasma and liver total cholesterol levels in S196A mice

Schematic representation of the potential pathways that may lead to decreased plasma and hepatic total cholesterol levels, and the genes seen to be differentially expressed in the S196A mice (in parenthesis).

Indeed, several previous studies have established that hepatic *Abcg5* and *Abcg8* expression alone is a strong determinant in the rate of cholesterol excretion (368,369). In addition, this effect has been shown to be modulated directly by LXR (370).This model is corroborated by the lack of difference in the expression of intestinal cholesterol transporters, and decreased plasma and hepatic bile acid levels. However, this hypothesis will need to be further confirmed by assessing the amount of neutral cholesterol and bile acids found in the faeces of both groups of mice, as well as biliary lipid composition.

In rodents, LXRs have been shown to induce catabolism of cholesterol into bile acids through the expression of *Cyp7a1* (106). Despite the beneficial effects of reducing cholesterol levels through its catabolism, hepatic accumulation of bile acids is damaging and can lead to cholestasis, a disease where bile can't flow out of the liver causing hepatotoxicity (371). In this study, no significant differences were observed in plasma and hepatic bile acid levels between genotypes, although there was a trend towards a decrease in bile acids in both compartments in the S196A mice (Figure 3.3. E). Hence, it would be interesting in the future to assess the effect that this reduction in bile acid levels has on hepatic cell toxicity, and subsequent inflammation and fibrosis.

The phospho-mutant mice proved to have a lower expression of the members of the ATP-binding cassette (ABC) transporter family, *Abca1* and *Abcg1*. These transporters are responsible for intracellular cholesterol efflux onto lipid-poor apolipoproteins and HDL, respectively; and are key mediators of the RCT process. Animals deficient for any of these two transporters show decreased levels of circulating total cholesterol and HDL (372,373). In contrast, the LXRα mutant mice exhibited a higher ratio of the HDL to LDL fractions in plasma. Besides an increase in circulating HDL, the elevated HDL/LDL ratio in the S196A mice could also be accounted for by a reduced circulating LDL fraction, caused by the increase in hepatic LDL-Receptor (*Ldlr*) expression observed in the mutant mice (Figure 3.5. A). In this study, distribution of total cholesterol on the two main lipoprotein fractions was performed by quantifying the amount of lipid found on HDL and LDL/VLDL fractions after separating them by density (see section 2.2.3.3). Although this method proves to be quick and reliable and is widely used in clinical practice to evaluate cholesterol distribution in relation to cardiovascular risk, it fails to provide information on the actual distribution of cholesterol throughout the lipoprotein classes. Therefore, future studies using more comprehensive techniques such as the quantification of plasma lipoprotein fractions by fast-performance liquid chromatography gel filtration (374) would provide a better understanding on how the plasma cholesterol in the S196A is distributed across the different lipoproteins.

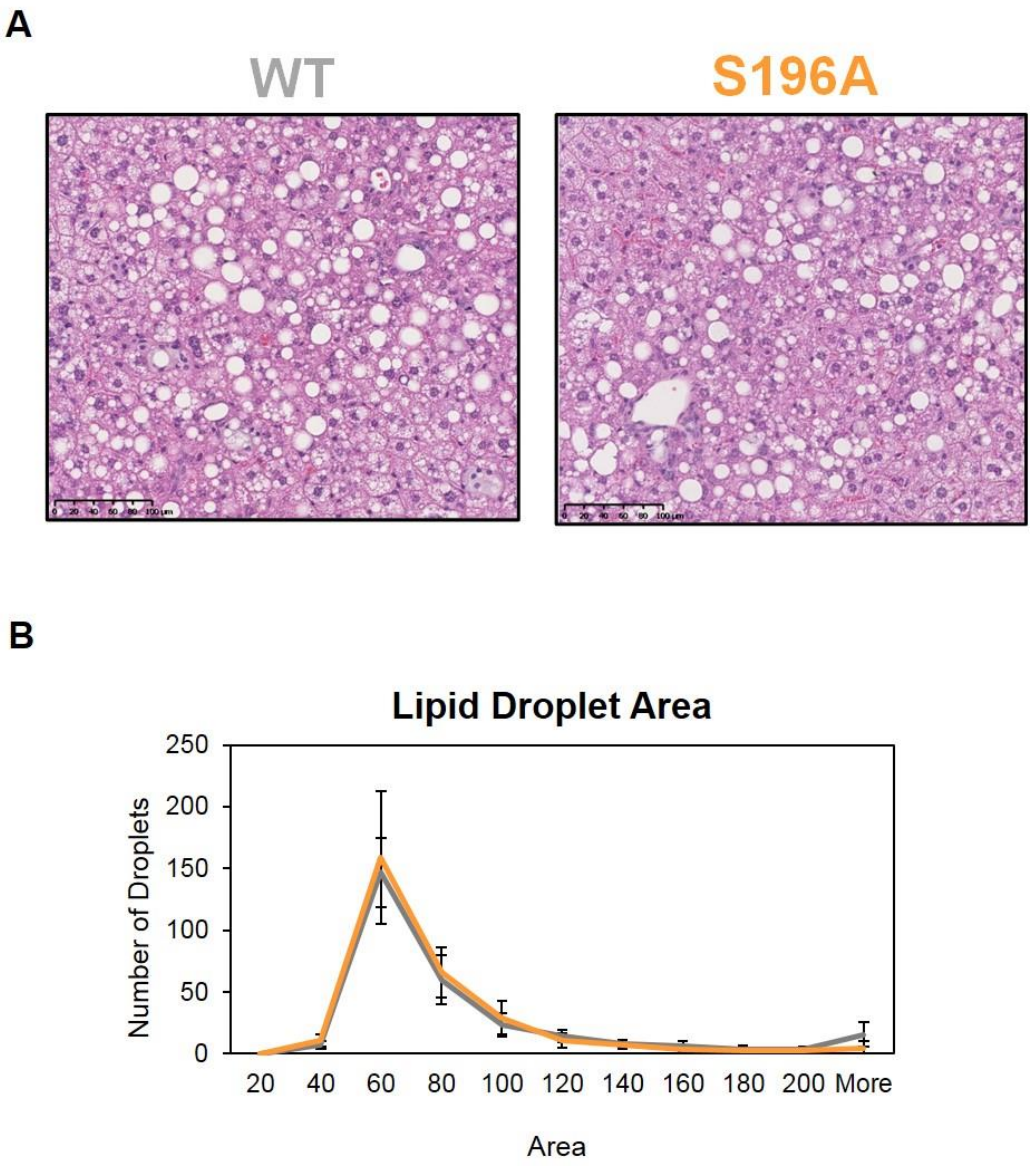

Figure 3.14. WT and S196A mice show the same level of steatosis after being fed a HFHC diet for 12 weeks

A) Representative images of H&E-stained liver sections from WT and S196A mice after being fed a HFHC diet for 12 weeks. Images are at 400x magnifications.

B) Distribution of lipid droplets by area in H&E-stained liver sections of WT and S196A mice (n=6) after being fed a HFHC diet for 12 weeks. Data represents means ± SEM.

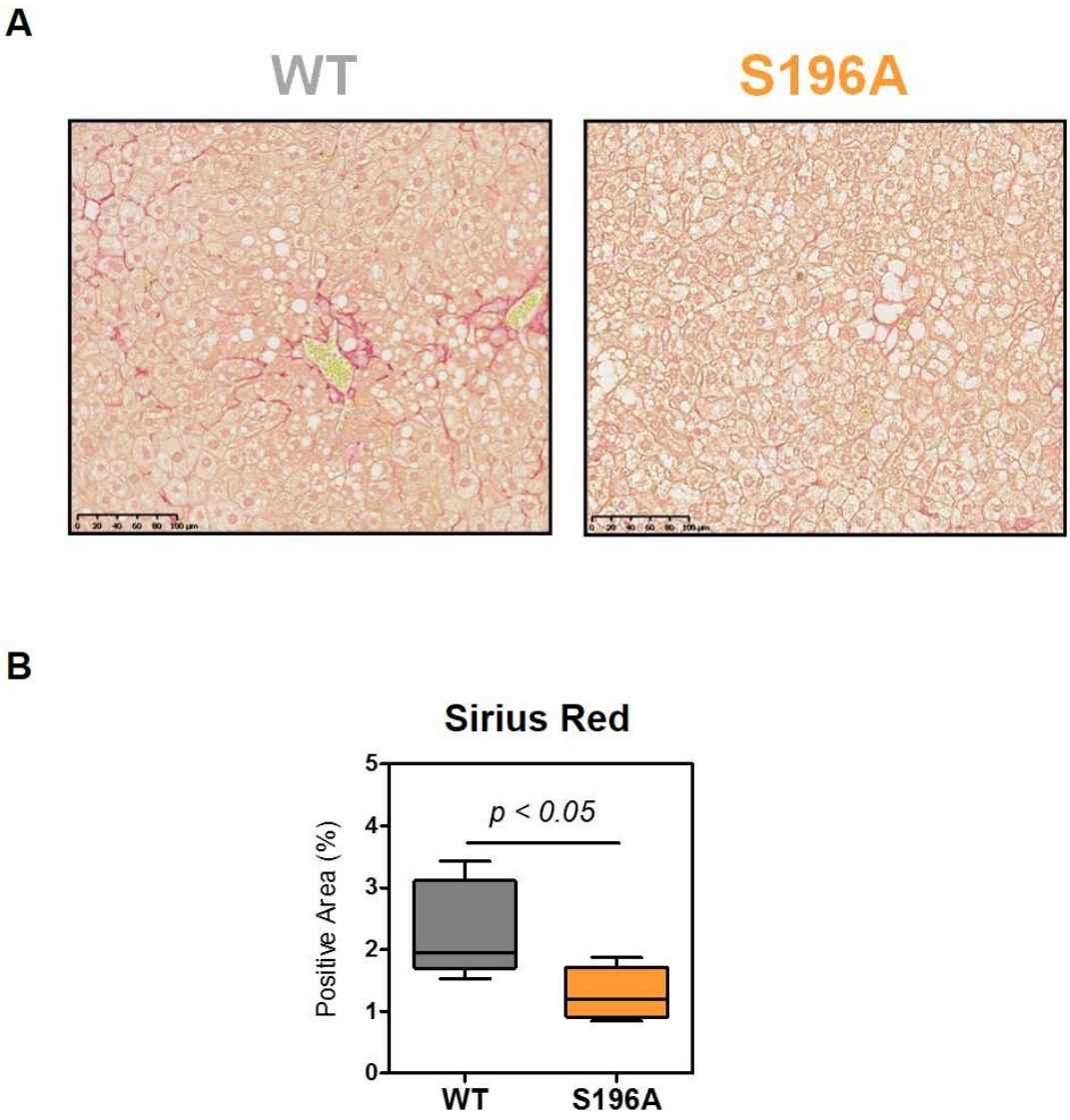

Figure 3.15. LXRα phospho-mutant mice remain protected against the onset of fibrosis after being fed a HFHC for 12 weeks

A) Representative images of Picrosirius Red-stained liver sections from WT and S196A mice. Images are at 200x magnifications

B) Quantification of Picrosirius red-stained areas on three independent areas per section (n = 6). Data represents means ± SEM. Significance determined by Student's t-test.

Chapter 4. Mechanisms underlying changes in gene regulation by LXRα phosphorylation deficiency in response to diet

4.1. Introduction

Molecular modelling studies suggest that phosphorylation of LXRα at S198 (murine S196) induces a structural change in the receptor's hinge region (163,165). This region is responsible for linking the DNA-binding and ligand-binding domains in nuclear receptors, conferring a specific structural conformation that can affect not only ligand binding, but also cellular localisation and cofactor recruitment (375). Indeed, previous *in vitro* studies looking at changes in LXRα phosphorylation uncovered how this modification affects the transcriptional activity of the receptor through several mechanisms, including binding to DNA as well as cofactor recruitment (163,165,166) (see section 1.1.4). Nonetheless, how these changes affect the receptor's functionality *in vivo* remains unknown.

Moreover, it has been demonstrated that certain genes are only sensitive to regulation by the non-phosphorylated version of LXRα (163,165); a phenomenon also attributable to other nuclear receptors and changes in their post-translational modifications (376). For example, induction of the *Ccl24* gene in RAW 264.7 cells by ligand-activated LXRα was seen to be dependent on its non-phosphorylated state at S198, either by pharmacological inhibition by the CK2 inhibitor DMAT or by RXR ligands, as well as by the genetic inhibition on the S198A mutant (163). Therefore, hepatic LXRα-S196A activity could help uncover novel target genes in the context of a HFHC-diet that haven't been previously identified as LXR targets.

To explore this and better understand the extent of disparity in diet-induced responses between WT and S196A mice (see chapter 3); as well as to identify novel pathways and genes sensitive to LXRα phosphorylation *in vivo*, genome-wide transcriptomic

differences in livers of WT and S196A mice fed a chow and HFHC diet were analysed by RNA-sequencing (RNA-seq) analysis. RNA-seq is a high-throughput technique that provides several benefits over other gene screening methods (i.e. microarrays), such as more precise measurement of levels of transcripts due to very low, if any, levels of background signal (377) .

Thus, the main focus of the work in this chapter has been to assess how changes in LXRα phosphorylation affect its transcriptional activity in response to a HFHC diet, and investigate novel target genes involved in the pathogenesis of NAFLD that may be only susceptible to the mutant form of the receptor.

With this work I show that the non-phosphorylatable LXRα-S196A receptor acts as a nutritional sensor by regulating specific pathways in response to a HFHC-diet. Moreover, the S196A mutant mice revealed novel hepatic target genes for the receptor by increasing LXR occupancy at putative binding sites, which was associated with enhanced transcriptional initiation and elongation of transcripts. These results were accompanied by an additional increased occupancy of the TBLR1 cofactor to the same LXR putative binding sites, suggesting that TBLR1 may be an important component facilitating the transcription of these genes by the LXRα phospho-mutant.

4.2. WT and S196A mice display different hepatic transcriptomes under chow and HFHC diets

When comparing RNA-seq results between chow and HFHC-fed WT and S196A samples, Principal Component Analysis (PCA) plots demonstrated that even though differences between the four groups are considerably high and they clustered together (Figure 4.1. A), samples from HFHC diet mice have a bigger intra-group variability than their chow-fed counterparts, which already suggests that the HFHC diet is having an impact on the hepatic transcriptomes of WT and S196A. RNA-seq analysis revealed that there are 667 genes whose hepatic expression is significantly different in the phospho-mutant mice fed a HFHC diet, and 539 genes were significantly different between both groups when fed a chow diet (adjusted p-value < 0.05) (Figure 4.1. B).

Notably, when comparing gene expression changes in response to diet in WT and S196A groups (chow vs HFHC for each genotype), the number of genes affected varied substantially between WT and phospho-mutant mice (Figure 4.2. A). Moreover, S196A livers appeared only to share the expression of only a certain number of these genes with the WT group (Figure 4.2. B). This supports the idea that impaired phosphorylation of LXRα at Ser196 is differentially reprogramming hepatic transcriptomes; and through it, altering these animal's susceptibility to diet-induced hepatic injury. In support of this hypothesis, most of the top upregulated genes in S196A livers under a HFHC diet were shown to be modulated by the phosphorylation-mutant LXRα only in the presence of the diet, and not under basal conditions (chow-regulated liver expression) (Figure 4.2. C). Importantly, neither of these genes have been previously reported to be subject to LXR regulation in liver, thus highlighting the relevance of LXRα phosphorylation in modulating new transcriptional responses to dietary cholesterol.

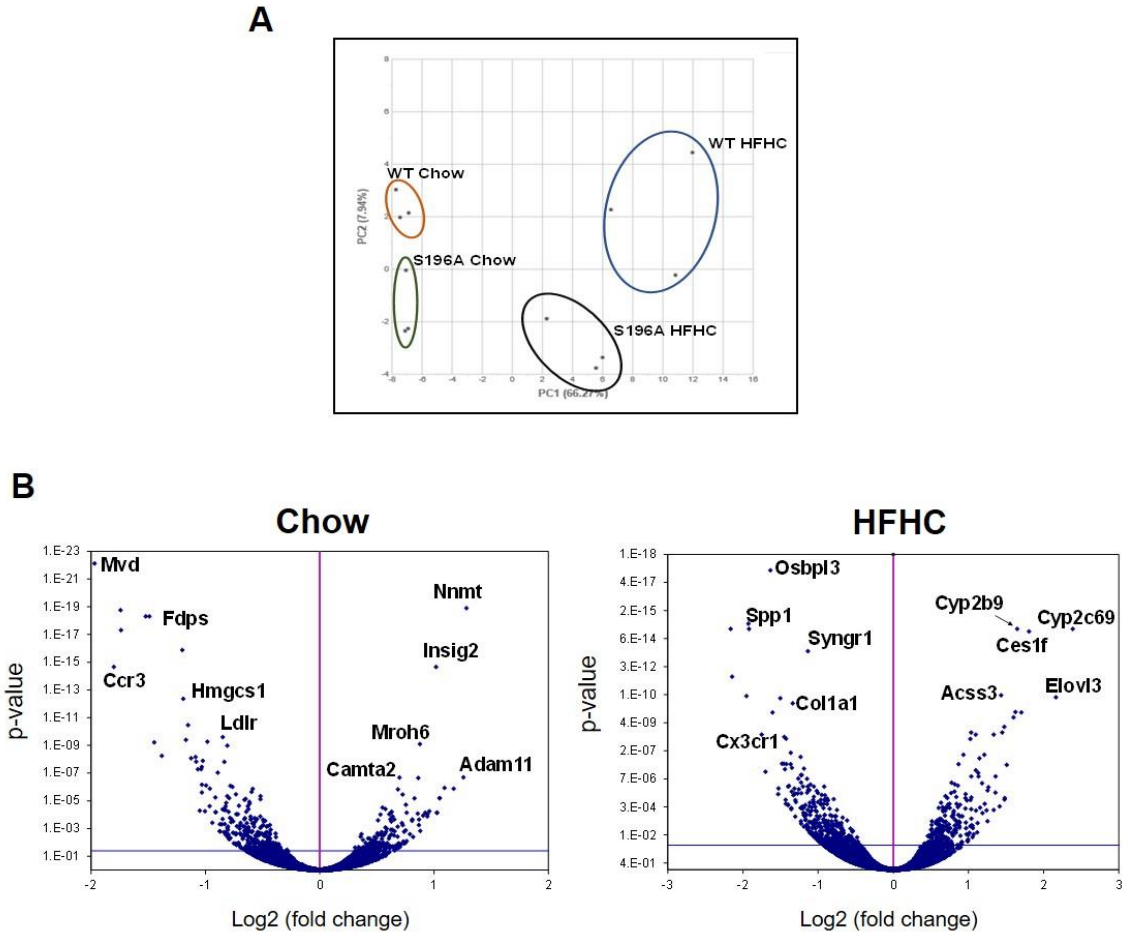

Figure 4.1. Hepatic transcriptomes on chow and HFHC diet-fed WT and S196A livers

A) Principal Component Analysis (PCA) plot showing samples analysed for RNA-seq divided in four different groups: WT Chow, WT HFHC, S196A Chow and S196A HFHC (n=3).

B) Volcano plots of $\log_2$ ratio (fold change) versus p-value of differentially expressed genes in S196A vs WT livers fed either a chow or a HFHC-diet (n=3). Blue line indicates an adjusted p-value threshold of 0.04 of the Wald Test for logistic regression. Transcript abundance was estimated using Illumina's RnaReadCounter tool and differential expression analysis was performed with DESeq2.

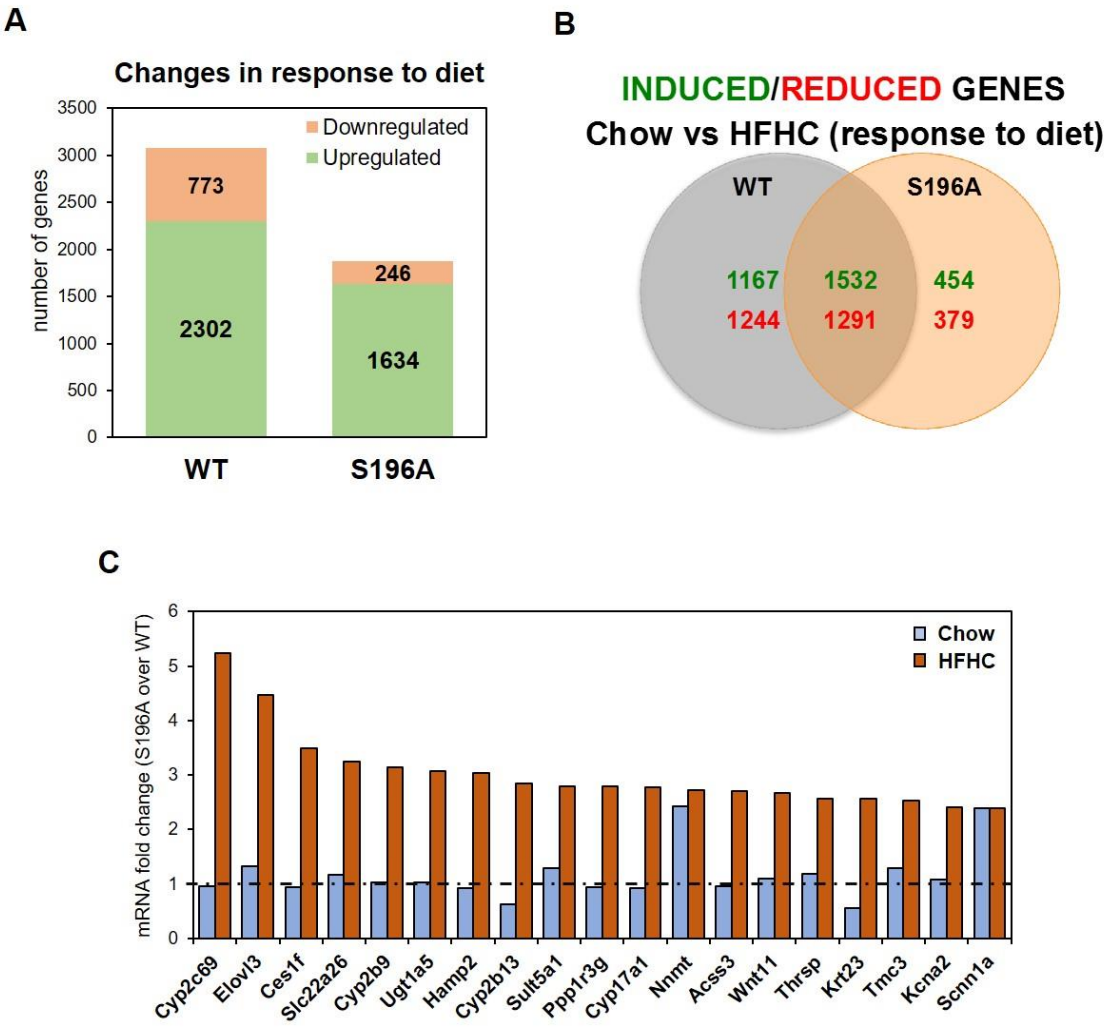

Figure 4.2. Impaired phosphorylation of LXRα at Ser196 differentially reprograms hepatic transcriptomes in response to a HFHC diet

A) Number of genes differentially expressed between Chow and HFHC-fed livers quantified by RNA-sequencing (n=3).

B) Venn's diagram of the comparison of differential gene expression between chow and HFHC livers for WT and S196A animals (n=3). Graph includes number of genes either induced (green) or repressed (red) in HFHC livers in comparison to Chow livers.

C) Graph representing fold-change of RNA-seq gene counts in livers of S196A mice relative to the values in WT livers that illustrates various examples of results obtained in enriched S196A pathways (n=3).

4.3. RNA-sequencing of HFHC livers confirms pathways involved in lipid metabolism and fibrosis are affected by changes in LXRα phosphorylation

Despite the robust sensitivity of RNA-seq, the strongest variation in gene expression on the top upregulated and downregulated hits (S196A compared to WT) was first confirmed by qPCR in a separate set of animals fed a HFHC diet (Figure 4.3). Therefore, the differences in transcript abundance reported in the RNA-seq analysis could be replicated in the livers of other WT and S196A HFHC-fed mice, which validates the robustness of the RNA-seq regardless of technical and biological sample variability.

Confirming previous data (chapter 3), pathway enrichment analysis on HFHC-fed livers showed a remarkable upregulation of genes involved in different lipid metabolism pathways (Figure 4.4 and 4.5), as well as a robust decrease in wound healing and fibrosis (epithelial-mesenchymal transition) (Figure 4.4 and 4.5) on the S196A group.

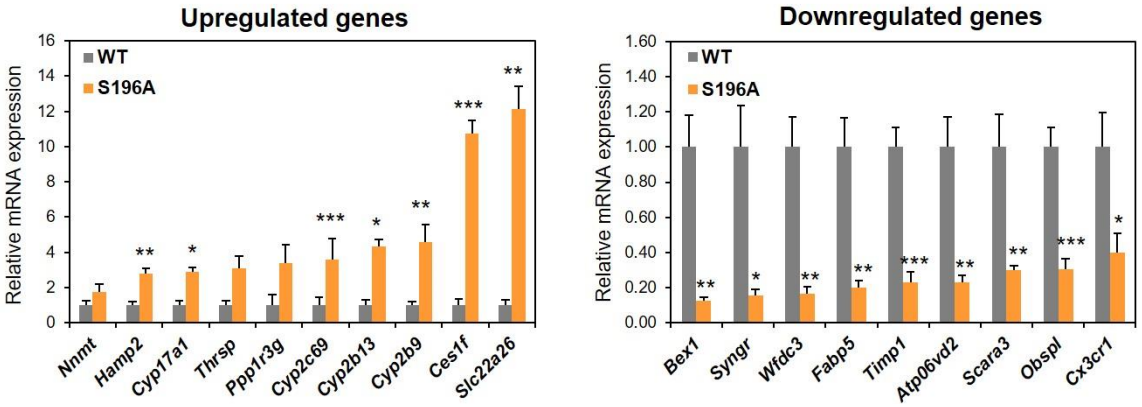

Figure 4.3. Validation of top regulated genes identified by RNA-seq comparing WT vs S196A HFHC-fed livers

qPCR validation of top upregulated and downregulated gene candidates on experimentally-independent WT and S196A livers fed a HFHC diet (n=6). Results are normalized to cyclophilin and shown relative to WT, set as 1. Data represents mean ± SEM. * $p < 0.05$ relative to WT determined by Student's t-test.

Strikingly, many of the genes that showed the most enrichment on the fatty acid metabolism pathway are involved in the oxidation of fatty acids (Figure 4.5), i.e. acyl-CoA synthetase long-chain family member 1 (*Acsl1*), which codes for the enzyme responsible for catalysing the pre-step reaction for β-oxidation; or acyl-Coenzyme A dehydrogenase, medium chain (*Acadm*), which performs the first step of medium-chain fatty acid oxidation. This further supports the idea that the high hepatic NEFA and triglyceride levels observed in the S196A mice (Figure 3.7) are probably not due to a reduction in mitochondrial β-oxidation, but rather an increased lipogenic programme (see chapter 3). Indeed, it seems plausible that the induced expression of genes involved in fatty acid oxidation in the S196A livers appears as a compensatory mechanism, with the intention to get rid of the lipid surpass in these animals.

It must be noted that due to the condensed nature of the Hallmark gene sets (318), all those genes that are related to the processes of wound healing, fibrosis and metastasis are incorporated under the “epithelial-mesenchymal transition” gene set. Amongst these, eleven collagen species; and importantly, several members of the Lysyl oxidase (LOX) and lysyl oxidase-like (LOXLs) families, responsible for collagen stabilisation through irreversible crosslinking (378–380) are strongly reduced in S196A mice (Figure 4.5). This is the first time that this class of enzymes, recently reported to promote fibrosis progression and limit its reversibility (381), have been linked to LXRα.

Tables containing all the results obtained in the pathway enrichment analysis can be found in Appendix 1.

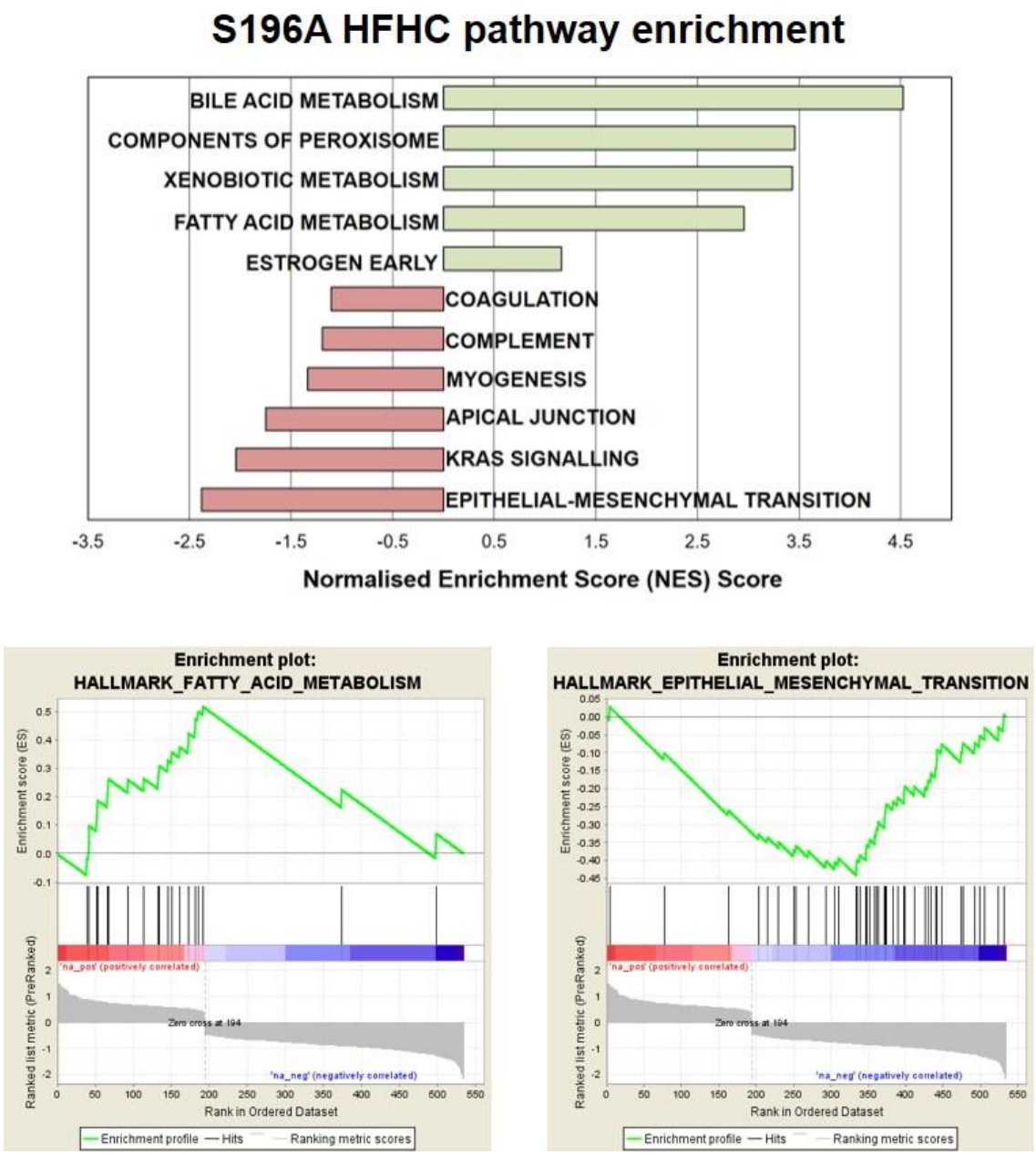

Figure 4.4. Pathway enrichment analysis of HFHC diet-fed WT and S196A livers

GSEA analysis showing positive and negative enriched pathways in S196A livers with a nominal p-value < 0.5 (100 permutations) derived from HALLMARK gene sets (Top). Enrichment profiles of Fatty Acid Metabolism and Epithelial-Mesenchymal Transition HALLMARK pathways (Bottom).

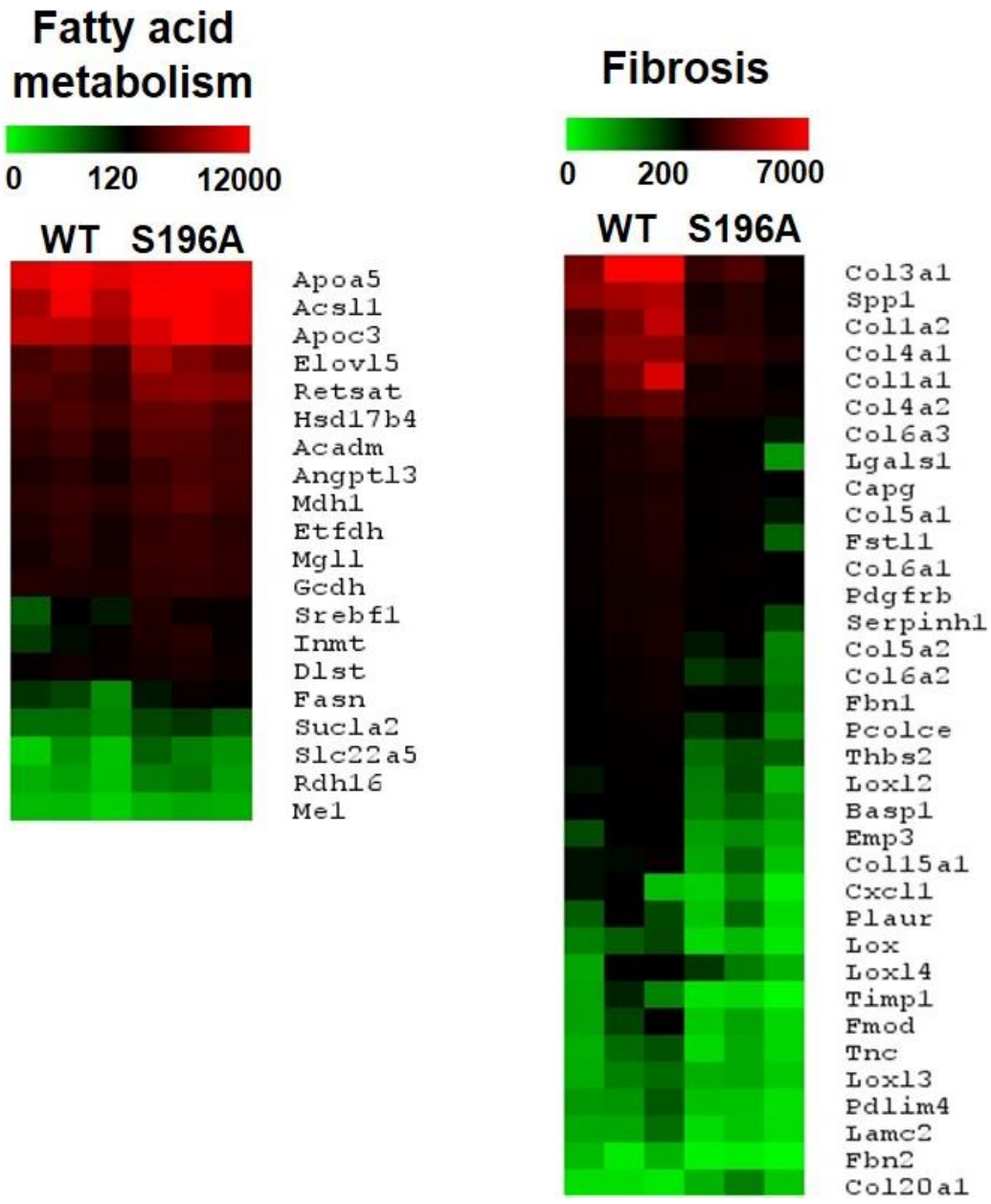

Figure 4.5. Heatmaps from HFHC-fed WT and S196A livers for fatty acid metabolism and fibrosis pathways

Heatmaps representing differences in absolute raw gene count values on WT and S196A HFHC-fed livers obtained by RNA-Seq (n=3). After sequencing reads were aligned to the mouse GRCm38/mm10 reference sequence, transcript abundance was estimated using Illumina's RnaReadCounter tool. Low (green), midpoint (black), and upper (red) limits are shown for each heatmap.

Moreover, the expression of a subset of genes that were shown to be part of a transcriptional signature that distinguishes between low-risk/mild and high-risk/severe NAFLD amongst pre-symptomatic patients (382), was remarkably different in WT and S196A mice (Figure 4.6). Interestingly, most of the genes in Figure 4.6 regarding the human NAFLD signature, such as Fibrillin 1 (*Fbn1*), Lumican (*Lum*) and numerous collagen species, are involved in extracellular matrix remodelling and tissue regeneration (383,384), further emphasizing a role for Ser196-LXRα phosphorylation in the regulation of these pathways. Overall, these differences seem to indicate that, at least at the transcriptional level, the HFHC-S196A model closely replicates the differences between early and advanced stages of human NAFLD; and suggests that changes in LXRα phosphorylation could alter pre-clinical NAFLD progression.

Interestingly, the expression of *Tm6sf2*, one of the genes whose variants have extensively been shown to contribute to the development and/or progression of human NAFLD (see section 1.2.2.5), and whose ablation in mice produces increased liver triglyceride content and decreased VLDL secretion (293), remained the same between groups (Figure 4.6);

Lastly, no differences were observed in the expression of most nuclear receptors expressed in liver (Figure 4.6). Despite this, gene expression analysis revealed that, albeit to a low extent (1.45 fold-change), *Lxra* (*N1hr3*) expression was significantly higher in the livers of S196A mice under a HFHC diet (Figure 4.6).

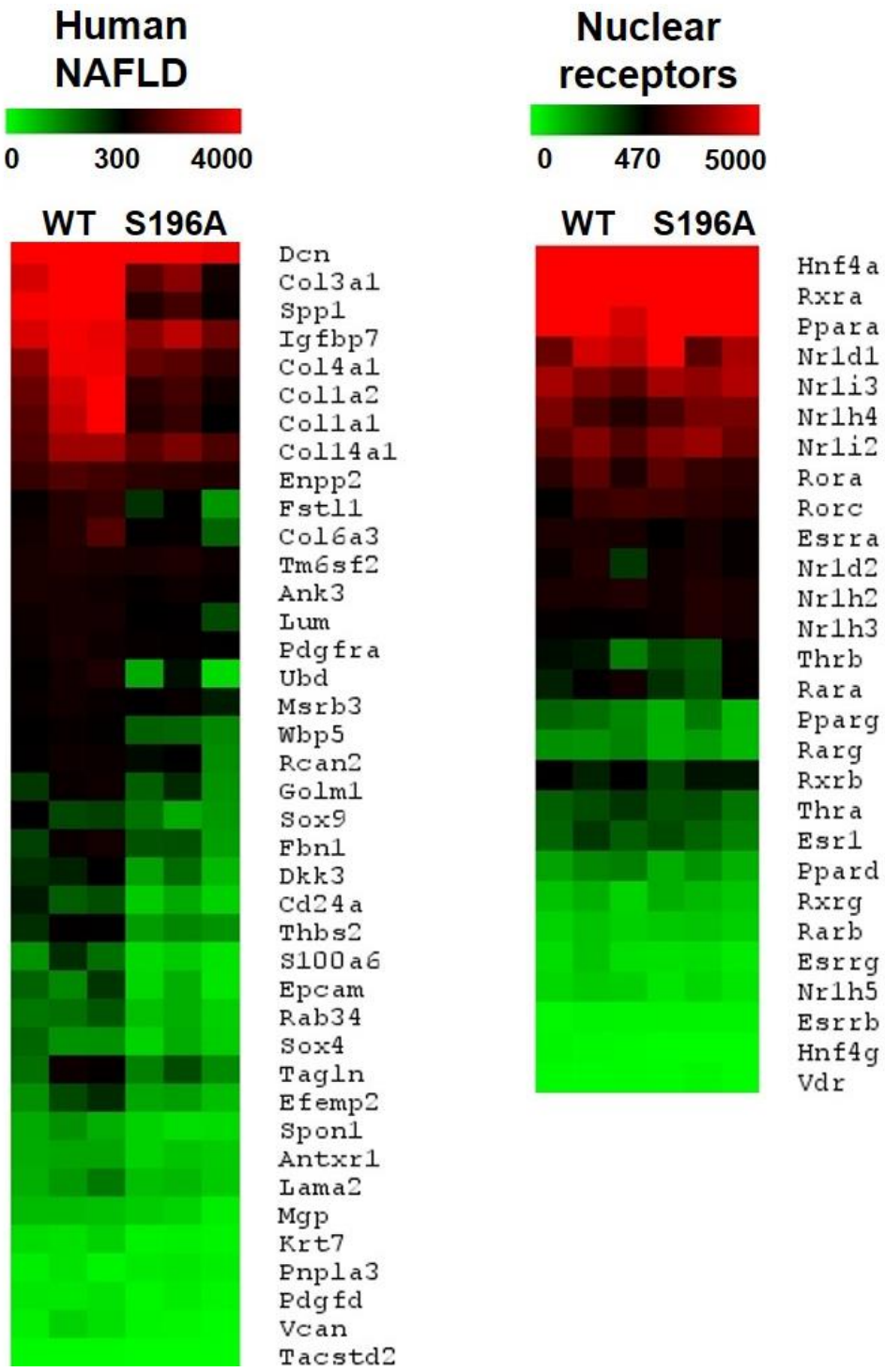

Figure 4.6. Differences in transcript abundance on HFHC-fed WT vs S196A livers for genes involved in human NAFLD and hepatic nuclear receptors

Heatmaps representing differences in absolute raw gene count values on WT and S196A HFHC-fed livers obtained by RNA-Seq (n=3). After sequencing reads were aligned to the mouse GRCm38/mm10 reference sequence, transcript abundance was estimated using Illumina's RnaReadCounter tool. Low (green), midpoint (black), and upper (red) limits are shown for each heatmap.

4.4. Impaired LXRα phosphorylation uncovers novel diet-modulated LXR target genes

One gene shown to be highly induced in HFHC-fed mutant liver, *Ces1f* (Figures 4.2. C, 4.3 and 4.7), encodes for a member of the family of carboxylesterases 1 (Ces1), a set of proteins that hydrolyse cholesterol esters and triglycerides and play an important role in hepatic lipid mobilization (385,386). RNA-seq analysis showed that in addition to *Ces1f*, other Ces1 members are differentially regulated by the LXRα phospho-mutant (*Ces1b, Ces1c, Ces1d, Ces1e*), most of which are only revealed to be sensitive to LXRα phosphorylation in a cholesterol-rich environment (Figure 4.7 A,B).

Interestingly, the form previously shown to be regulated by LXR ligands in liver (*Ces2c*) (387) barely changes in S196A livers regardless of the diet used (Figure 4.7 A,B), again pointing at unique differences in the transcriptional response exerted by changes in LXRα phosphorylation upon exposure to dietary or pharmacological environments.

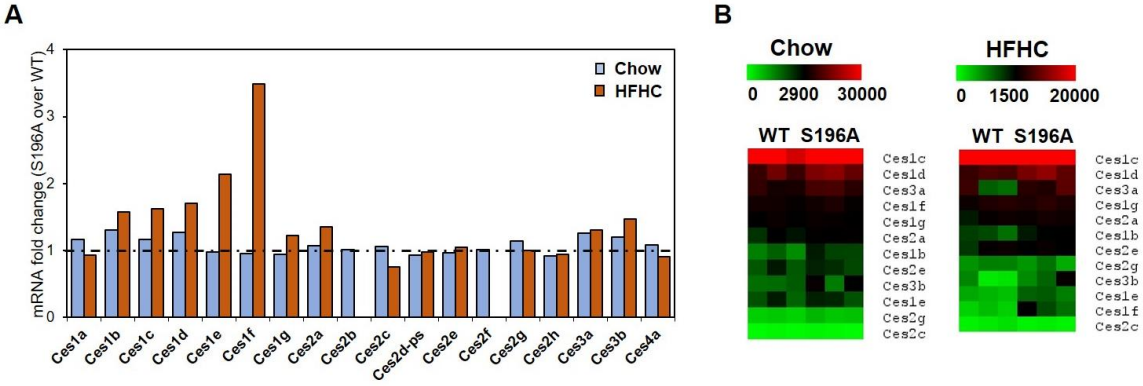

Figure 4.7. Ces1f is highly induced in S196A livers in response to a HFHC diet

A) Graph representing fold-change of RNA-seq gene counts in livers of S196A mice relative to the values in WT livers (n=3) depicting differences in expression of various members of the Ces family. After RNA extraction and sequencing, transcript abundance was estimated using Illumina's RnaReadCounter tool and differential expression analysis performed with DESeq2.

B) Heatmaps illustrating differences in absolute raw gene count of several members of the Ces family in WT and S196A livers upon chow and HFHC diets (n=3). Low (green), midpoint (black), and upper (red) limits are shown for each heatmap.

In order to test if *Ces1f* could be a target gene sensible to the non-phosphorylatable form of LXRα, the *Ces1f* gene body and promoter were scanned for potential LXREs (see section 1.1.1). *In silico* analysis uncovered a degenerated DR4 sequence resembling the published consensus LXRE in mouse liver (315) (Figure 4.8). Thereafter, binding studies by Chromatin Immunoprecipitation (ChIP) of LXR as well as its heterodimerisation partner RXRα (see section 1.1.1), were carried out in livers of HFHC-fed WT and S196A mice. Interestingly, ChIP analysis demonstrated this sequence was preferentially bound by LXR in HFHC-fed S196A livers (Figure 4.9. A). This associated with a significant increase in S196A livers of RNA Polymerase II (Pol II) and phosho-Ser2 Pol II (pSer-Pol II) occupancy to the *Ces1f* transcription start site (TSS), reflecting an enhanced transcriptional initiation and elongation of the *Ces1f* transcript, respectively (Figure 4.9 B). By comparison, binding of the LXR heterodimerisation partner RXRα to the *Ces1f* DR4 sequence was not affected (Figure 4.8. A).

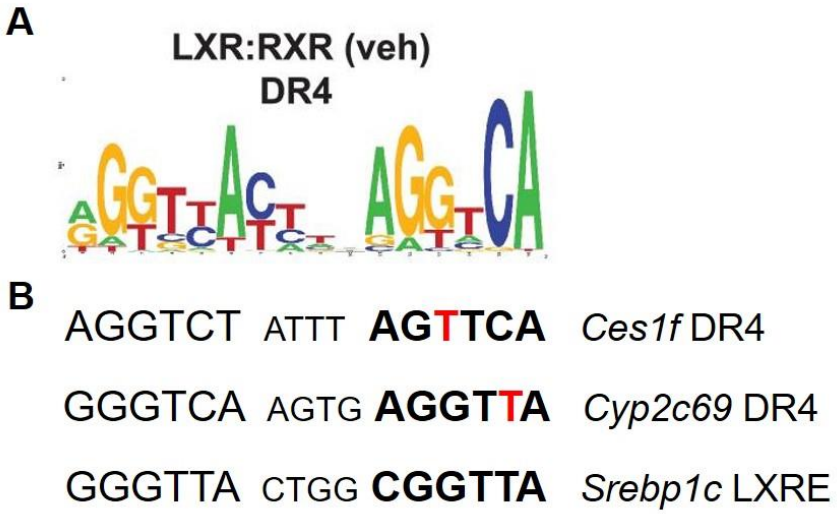

Figure 4.8. Comparison between analysed DR4 sequences and consensus LXRE
A) Web logo of consensus DR4 sequence motifs on LXR-RXR (vehicle-treated mouse livers) binding sites. Obtained from Boergesen *et al*., 2012 (315).
B) Degenerated DR4 sequences obtained *in silico* on *Ces1f* and *Cyp2c69* murine genes and established LXRE on the *Srebp1c* promoter. Nucleotides in bold correspond to the sequence where the LXR sits (5') and those in red signal the nucleotides that differ from the consensus sequence.

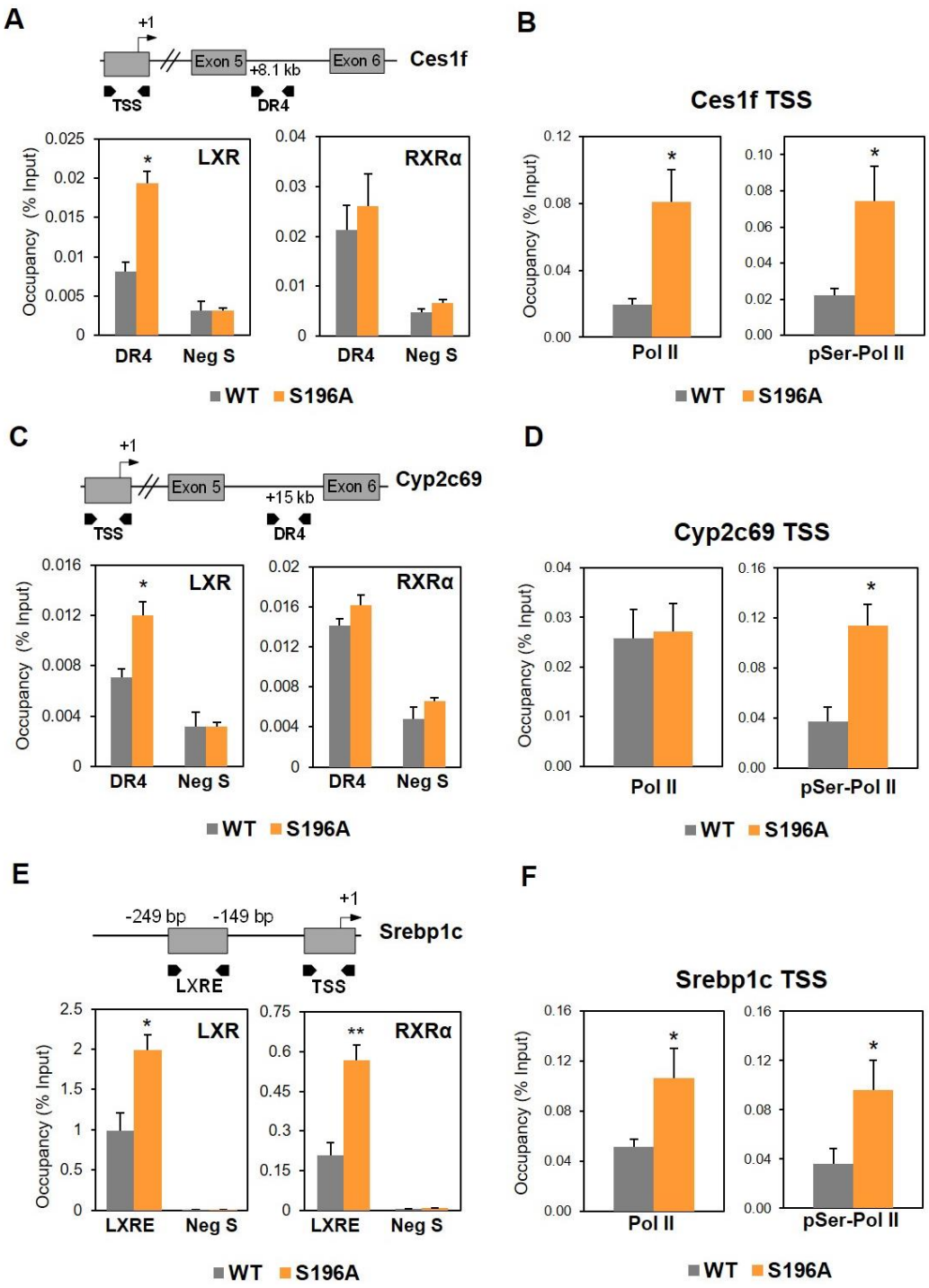

Figure 4.9. LXRα-S196A preferentially binds to degenerated DR4 sequences in novel target genes

A,C,E) LXR and RXRα occupancy at Ces1f and Cyp2c69 putative DR4 sequences and Srebp-1c LXRE in livers of WT and S196A mice fed a HFHC in comparison to a non-specific sequence (n=3-6).

B,D,F) RNA Pol II and pSer2-Pol II occupancy at Ces1f, Cyp2c69 TSS and Srebp1c TSS in livers of WT and S196A mice fed a HFHC in comparison to a non-specific sequence (n=3-6).

Results are normalized to input values and shown relative to WT. Data represents mean ± SEM. * $p < 0.05$, ** $p < 0.005$ relative to WT determined by Student's t-test.

Moreover, this binding pattern was similar, except for RNA Pol II binding, for another potential degenerated DR4 sequence identified in the *Cyp2c69* gene (Figure 4.9. C,D), whose expression is enhanced by about 5-fold in LXRα-S196A mice (Figures 4.1, 4.2. C and 4.3). In contrast, occupancy by both LXR and RXRα to the well-established LXRE in the *Srebp-1c* promoter (388), a gene that was also induced in S196A livers (Figure 3.9), was significantly increased (Figure 4.9. E), as were Pol II and pSer-Pol II to its TSS (Figure 4.9. F); although whether this pattern is also seen for other well-established LXR target genes should be confirmed. Globally, these results suggest that impaired LXRα phosphorylation at S196 allows for the transcriptional activation of a subset of genes that, at least in the case of *Ces1f* and *Cyp2c69*, contain degenerated DR4 sequences. Furthermore, the regulation of these specific set of genes seems to occur independently of changes in RXRα occupancy.

It must be noted that, due to the binding nature of RNA Polymerase II, no sequences were found that could act as a negative control for RNA Pol II and its modification pSer2-Pol II. Nonetheless, comparison of these antibodies against their Immunoglobin G (IgG) isotype control confirmed their specificity (Figure 4.10).

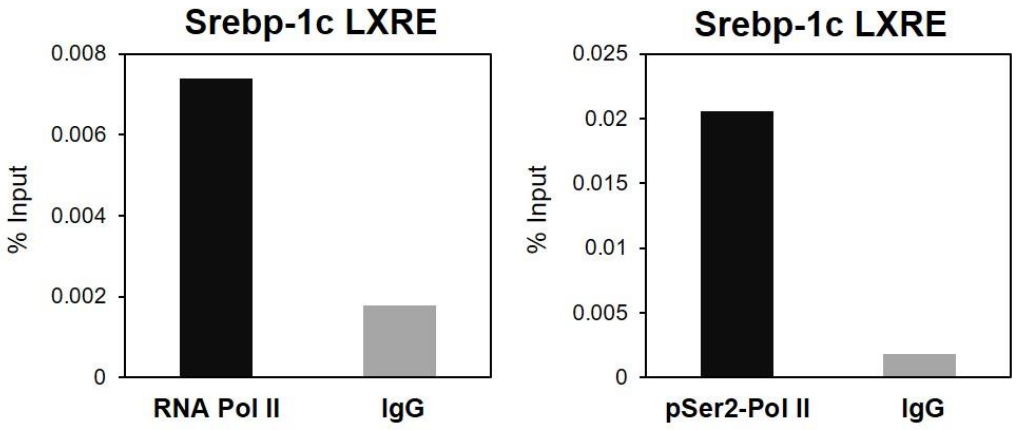

Figure 4.10. RNA Pol-II and pSer2-Pol II antibody specificity

Validation of antibodies against RNA-Pol II (Left) and pSer2-Pol II (Right) over IgG isotype control on mouse livers fed a HFHC diet. Results are normalised to input chromatin values (n=1).

Lastly, differential interaction of phospho-mutant LXRα with other cofactors was investigated as an additional possible mechanism behind changes in gene expression. Previous proteomic analysis by our collaborators in Prof. Garabedian's lab (New York University, USA) on HEK293T cells expressing vector only (Vo), FLAG-hLXRα or FLAG-hLXRα-S198A (389), revealed that the corepressor NCoR and the cofactor TBLR1 (see section 1.1.1) preferentially interact with the human LXRα-S198A *in vitro* (Figure 4.11. A), which could justify for the differences in gene expression in S196A livers. Accordingly, and consistent with increased LXRα binding (Figure 4.9. A-D), TBLR1 occupancy at Ces1f and Cyp2c69 DR4 sequences was significantly enhanced in S196A livers exposed to the HFHC diet (Figure 4.11. B,C). In contrast, no differences were detected in NCoR occupancy between genotypes (Figure 4.11. B,C). This goes against previously published evidence *in vitro*, where expression of LXRα phosphorylation-sensitive genes in response to synthetic ligands was shown to be facilitated by a reduction in NCoR recruitment (163); which reinforces the idea that the molecular mechanisms behind the activity of LXRα-S196A may differ depending on the nature of the activating stimuli. Moreover, evaluation of transcript levels in livers of WT and S196A mice confirmed that changes in LXRα phosphorylation did not alter the expression of these factors (Figure 4.11. D), suggesting that differential responses to a HFHC diet *in vivo* by the phospho-mutant animals may be mediated, in part, by changes in the binding of the TBLR1 cofactor (Figure 4.11. E).

A

VO	LXRα	S198A	Peptide
0	13	37	NCoR
0	4	22	TBLR1

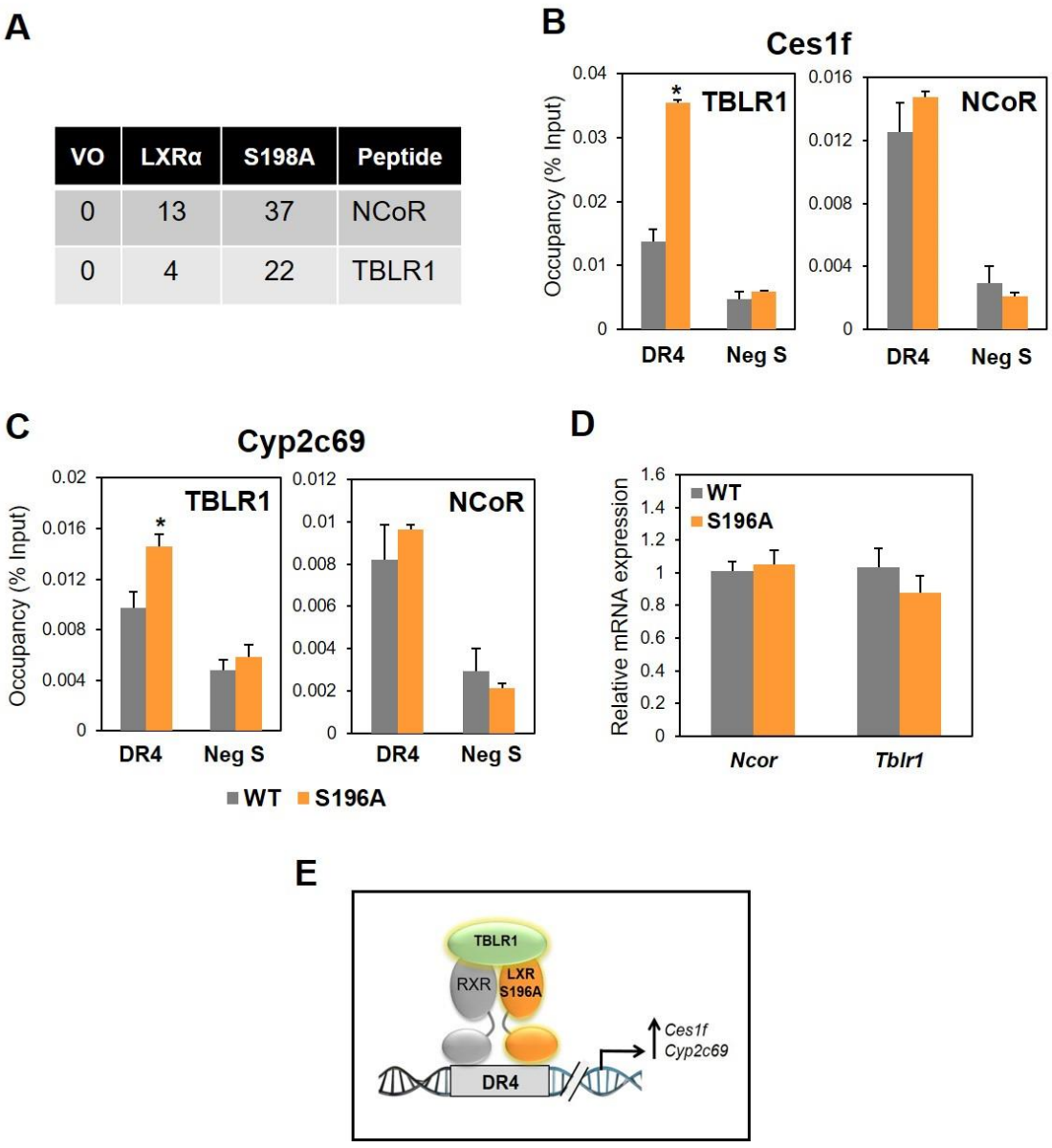

Figure 4.11. TBLR1 occupancy is increased at putative LXR binding sites in S196A livers

A) Total spectral counts obtained from immunoprecipitates of wild type LXRα (LXRα), phospho-mutant (S198A) and not expressing LXR (VO) cells identified by mass spectroscopy (n=1).

B-C) TBLR1 and NCoR occupancy at Ces1f and Cyp2c69 putative DR4 sequences in comparison to a non-specific sequence (n = 3). Results are normalized to input values and shown relative to WT, set as 1 on DR4 sequences.

D) Gene expression was measured by qPCR in livers of WT and S196A fed a HFHC diet (n = 6). Results are normalized to cyclophilin levels and shown relative to WT.

E) Diagram representing the hypothetical molecular mechanism through which the S196A-LXRα receptor binds to and induces expression of novel target genes.

Data shown as means ± SEM. * $p < 0.05$ relative to WT determined by Student's t-test.

4.5. Summary

- The LXRα-S196A receptor acts as a nutritional sensor by specifically reprogramming the hepatic transcriptome in response to a HFHC-diet.
- Impaired LXRα phosphorylation reveals unique LXRα phosphorylation/diet sensitive target genes.
- Expression of novel genes is mediated, in part, through differential binding of LXR and TBLR1 to degenerated DR4 sequences.

4.6. Discussion

The work in this chapter has uncovered novel genes sensitive to changes in LXRα phosphorylation in mouse livers, as well as the binding sequences related to the regulation of two of these genes, *Ces1f* and *Cyp2c69,* that are preferentially bound by LXRα-S196A in the context of a fat and cholesterol-rich diet. These sequences were revealed through *in silico* analysis, by high levels of homology to a previously reported LXR binding site in mouse liver (315) (Figure 4.8), given that there are currently no available high-throughput LXR binding analyses that specifically interrogate responses to experimental diets. To date, most of the available ChIP-seq studies exploring nuclear receptor cistromes – a technique used to map the global binding of a certain protein to DNA – have been traditionally performed on animals treated with specific synthetic ligands, which may not necessarily copy binding patterns observed upon activation by diets. Indeed, ChIP-seq analysis in livers of WT mouse fed a chow diet and treated with the LXR specific ligand GW3965, shows very little or no presence of LXR at the *Ces1f* and *Cyp2c69* DR4 sequences identified *in silico* (results kindly provided by Dr. E. Treuter, Karolinska Institutet, Sweden) (Figure 4.12); which further supports that both phosphorylation status of LXRα and diet environment are critical for the regulation of these genes. As previously shown, LXR agonism increases phosphorylation of the

receptor (163) (Figure 5.2.1.) and thus I speculate that in the GW-treated livers analysed by ChIP-Seq (Figure 4.12), the LXRα receptor is highly phosphorylated. This aligns with the hypothesis that the non-phosphorylatable LXRα is able to preferentially bind and consequently induce the expression of these genes.

Furthermore, despite previous studies showing that phosphorylation affects the transcriptional activity of LXRα by modulating recruitment to NCoR (163,165) no differences were detected in NCoR occupancy between genotypes at *Ces1f* and *Cyp2c69* DR4 sequences (Figure 4.11 B,C). Instead, a significant increase in TBLR1 binding could be observed. TBLR1 is as integral member of the NCoR/SMRT corepressor complexes (390), and alongside its heterodimeric partner, TBL1, was initially found to be mediating repression by unliganded Thyroid Receptor (31). However, following studies demonstrated that these factors were also essential for ligand-induced activation of gene expression, based on their ability to mediate corepressor/coactivator exchange (27,391). Hence, current evidence points to a model where TBLR1 may be recruited by both unliganded and liganded nuclear receptors and play opposite roles. The results in this chapter, based on proteomics data obtained from HEK293T cells, a human cell line of endothelial origin, shows that alongside increased LXRα-S196A occupancy, TBLR1 binds more to the DR4 sequences of the studied genes (Figure 4.11 B,C) . Therefore, direct interaction between the mutant LXRα and TBLR1 in the livers of HFHC-fed animals should be confirmed by co-immunoprecipitation and/or re-ChIP studies, a method based on sequential immunoprecipitation reactions, which allows for the identification of multiple and concurrently binding proteins on a single DNA sequence. It should be noted though, that the antibody used for the ChIP studies in this chapter can recognize both LXR subtypes (see section 2.8), since at the moment there are no available LXRα-specific antibodies that provide a good signal over background in mouse tissues. Even though levels of LXRβ in liver are almost minimal compared to the α subtype (392), and its expression was not seen to be different between the WT and S196A genotypes (*Nr1h2*, Figure 4.6); it should be taken into account that there may be a residual signal given by the LXRβ receptor.

Certain members of the Ces family are modulated by nuclear receptors such as PPARα (387). However, hepatic expression of PPARα was not substantially altered in S196A mice (Figure 4.6), and no PPARα binding was observed on the identified Ces1f and Cyp2c69 sequences based on reported genome-wide analysis of PPARα binding sites in mouse liver (315) (Figure 4.12); thus, it appears unlikely that this nuclear receptor is participating in the regulation of *Ces1f* and *Cyp2c69* expression by the mutant LXRα, at least under the experimental conditions used for my studies. However, ChIP analysis investigating PPARα occupancy on WT and S196A livers will need to be performed in order to confirm this theory.

Interestingly, previous studies investigating the effects of ligands for different nuclear receptors on various Ces family members, failed to show regulation of *Ces1f* by LXRs (387) further indicating that genetic regulation by these receptors upon synthetic ligand activation doesn't necessarily mirror that on a dietary environment. Recent reports have linked Ces1 with protection against liver inflammation and injury (393), and hepatic deficiency of Ces1 strongly increases the susceptibility to cholesterol-driven hepatic injury (394). However, the specific contribution by *Ces1f* in NAFLD progression has not been addressed to date.

In addition, the expression of the *Cyp2c69* gene was also chosen for this study as an example of phosphorylation-sensitive novel LXR target genes. This is a member of the Cyp2c cytochrome P450 subfamily, a set of enzymes that have been classically involved in Phase I drug metabolism, also known as xenobiotics (395,396). Interestingly, the presence of chronic liver diseases, and more specifically, NAFLD, has been shown to alter the levels of some members of this family (397). Although not much is known specifically about *Cyp2c69*, a recent study showed that its protein levels were actually decreased in mouse livers in response to a high fat diet (398), suggesting that, at least in mice, this enzyme is also involved in hepatic fat metabolism. Moreover, we know from gene ontology studies that it contains an arachidonic acid epoxygenase activity capacity (GO:0008392), which converts arachidonic acid into epoxyeicosatrienoic acids (EETs).

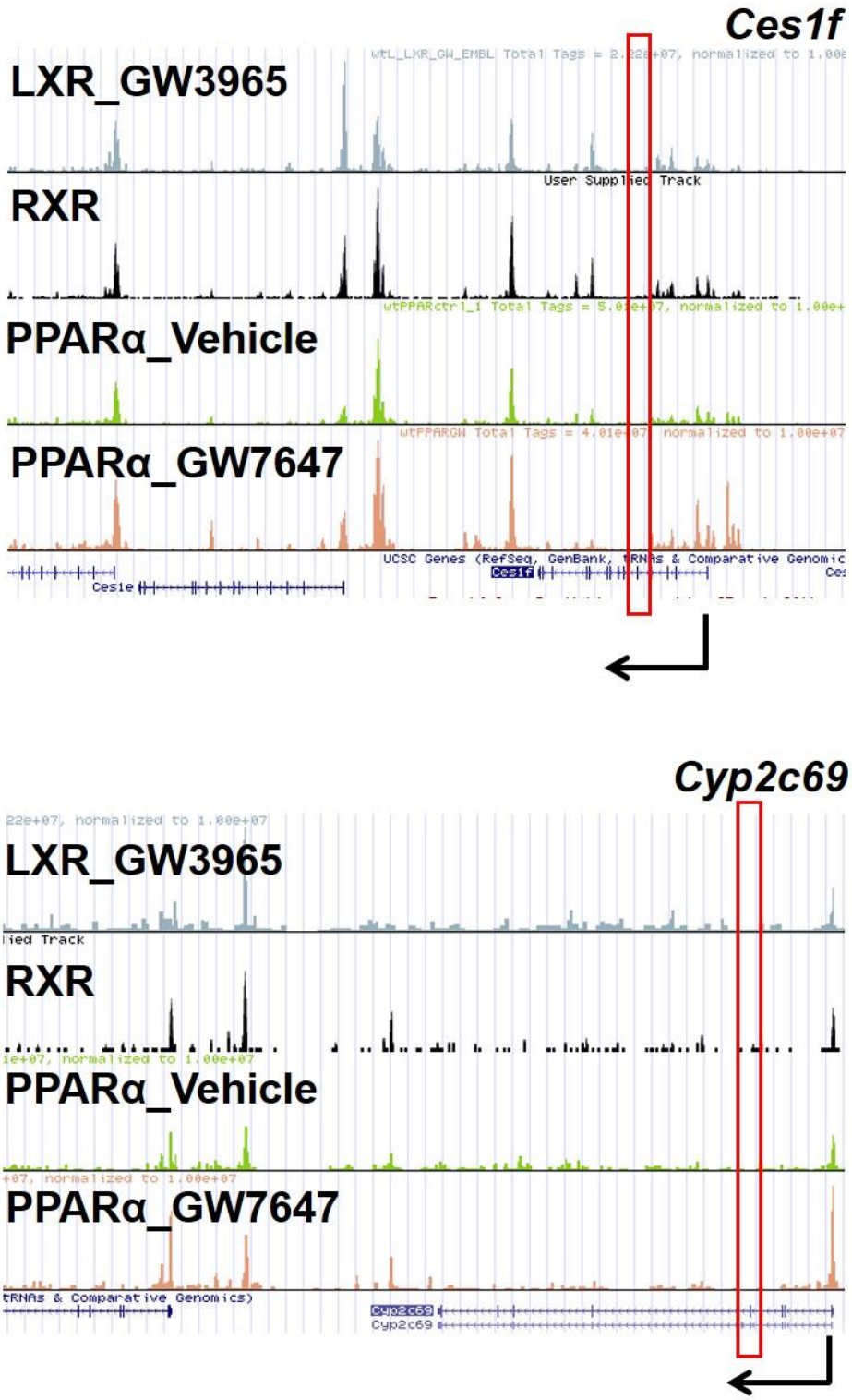

Figure 4.12. LXR and PPARα mouse liver binding upon synthetic ligand activation
Genomic region of the *Ces1f* (top) and *Cyp2c69* (bottom) genes. Indicated are ChIP-seq read alignment tracks for the LXR (gray), RXR (blue) and PPARα vehicle-treated (green) and synthetic ligand-treated (red) immunoprecipitated livers. Peaks symbolize binding enrichment for each given nuclear receptor. Red square identifies region where the identified degenerated DR4 sequences are found.
Chip-seq tracks provided by Dr. E. Treuter (Karolinska Institutet, Sweden).

Recent evidence has demonstrated that EETs have strong anti-inflammatory properties (399–401), which raises the possibility that LXRα-S196A may be protecting the liver from diet-induced inflammation and fibrosis, in part, through the induction of this enzyme, as well as other members of its family, as exampled by the enrichment in the xenobiotic metabolism pathway in these animals (Figure 4.4).

Lastly, the transcriptomic analysis by RNA-seq in this chapter revealed that those mice carrying the S196A mutation respond differently to the HFHC diet (Figure 4.2), establishing the non-phosphorylatable LXRα as a as a novel nutritional sensor that modulates specific metabolic, inflammatory and fibrotic responses that are key in diet-induced NAFLD progression. Thus, it will be interesting in the future to compare the differences between LXR ligands and exposure to a HFHC diet and how these translate to specific molecular mechanisms.

Chapter 5. *In vitro* studies on the modulation of LXRα activity and phosphorylation

5.1. PART A: LXR actions in human primary hepatic stellate cells

Most research to date on LXR function in relation to NAFLD and other liver diseases has been performed either on rodent cells or animal models of disease (see section 1.1.3.3). Thus, our knowledge on the effects of LXR actions in the pathogenesis of human NAFLD is scarce and often contradictory. This highlights the need for further studies investigating how LXRα expression and activity affects chronic liver diseases in humans.

Due to the obvious challenges of investigating ligand-induced activity in human livers *in vivo*, studies in this chapter looking at the modulation of the human receptor have been performed on primary human HSCs, key players in the development of fibrosis (402). Regarding NAFLD pathogenesis, studies in mice or in human cell lines have established the importance of LXR signalling on the modulation of HSC activation (403–405), yet the activity and expression of these receptors in human primary HSCs remains unknown. In healthy liver, HSCs are present in a quiescent state and fulfil the role of lipid storage (406,407). In response to a variety of stimuli, HSCs can undergo differentiation into activated myofibroblasts, which are responsible for the secretion of extracellular matrix and thus promote hepatic fibrogenesis (408). Activated HSCs show enhanced expression of α-Smooth Muscle Actin (αSMA or ACTA2) (249,409,410); and when cultured, these cells undergo further activation upon each culture passage, which proves an ideal tool to study pathophysiological mechanisms at different stages of HSC activation *in vitro* (411).

The objectives of the experiments below were to establish the effect of LXR activity on the activation and gene expression of human primary hepatic stellate cells.

5.1.1. LXR activity dampens human primary Hepatic Stellate Cell activation

First, *LXRA* (LXRα) and *LXRB* (LXRβ) mRNA expression was investigated in primary HSCs from one donor at different stages of activation. *LXRA* mRNA levels decreased dramatically with increased culture passage, possibly indicating an inverse association between LXRα expression and HSC activation (Figure 5.1.1). Intriguingly, this reduction was less accentuated for the *LXRB* transcript and appeared to be only transitional (Figure 5.1.1), further establishing that the alpha subtype may be the one having a more prominent role in the relation between LXRs and HSC activation.

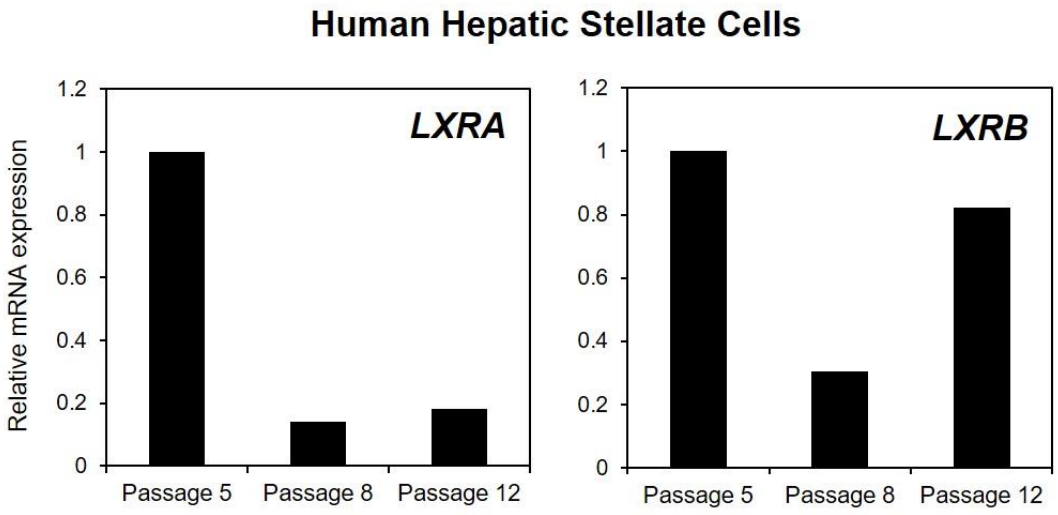

Figure 5.1.1. LXRα and LXRβ expression at different stages of Hepatic Stellate activation

Gene expression from human primary Hepatic Stellate cells from 1 donor at different passages was quantified by real time-PCR. Values are normalised to cyclophylin and shown as fold-change to Passage 5.

Next, the actions of LXR activation in primary human HSCs, stimulated with the specific synthetic LXR ligand GW3965, were analysed in cells form three different donors. LXRα expression was induced by the LXR ligand in 2 out of 3 donors, consistent with previous reports showing human LXRα autoregulation in other cell types (10) (Figure 5.1.2. A). However, LXRβ levels appeared to be only slightly affected, with an induction lesser than 1.5-fold for all the donors (Figure 5.1.2. B). In addition, induction in the levels of several known LXR target genes (Figure 5.1.2. C), which are implicated in cholesterol transport (*ABCA1*, *ABCG1*) or fatty acid synthesis (*SREBP1c*) were detected upon treatment with the LXR synthetic ligand, confirming that GW3965 can activate LXRs in primary HSCs. Indeed, this is the first time that LXR-mediated induction of these genes is shown in primary human HSCs. As expected, variability in the induction of target genes was seen between donors. Interestingly, induction of LXR levels by GW3965 (Figure 5.1.2. A,B) had no effect on the extent of target gene expression (Figure 5.1.2. C); since Donor 3 demonstrated a large induction of LXR target genes despite eliciting no changes in LXRα levels upon GW3965 treatment (Figure 5.1.2. A).

In summary, the above findings show that not only LXRs are present in primary human HSCs but also that they seem to be transcriptionally active in response to the GW3965 synthetic ligand.

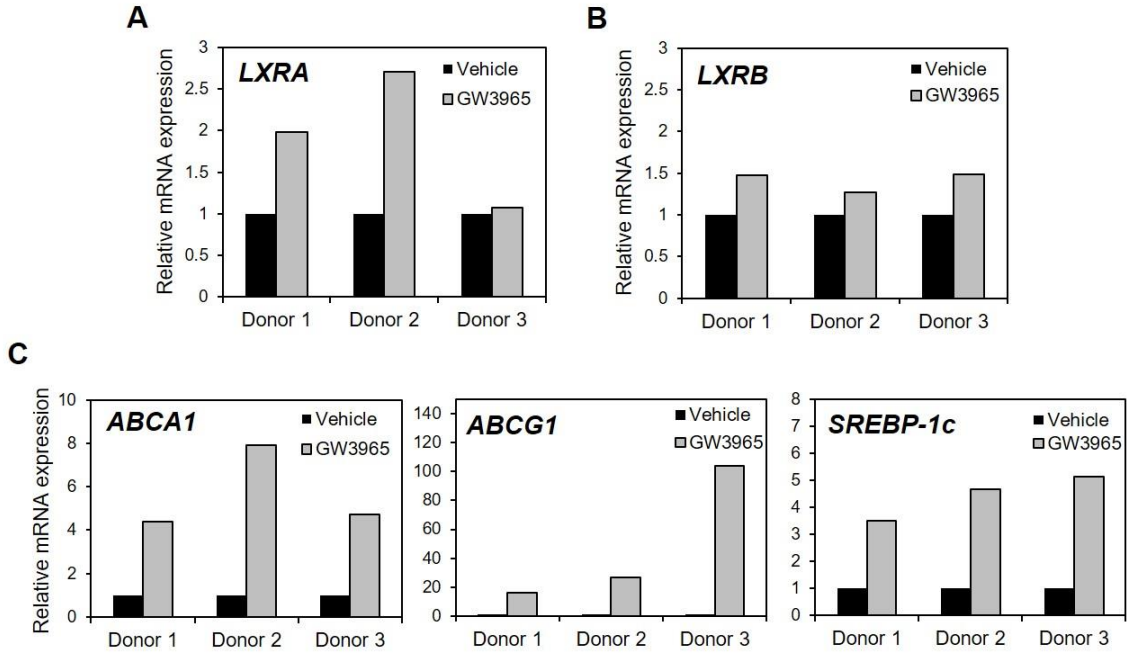

Figure 5.1.2. Induction of target genes by the LXR synthetic ligand GW3965

A-C) Primary Hepatic Stellate Cells from three different donors were stimulated with 1 μM GW3965 or vehicle (DMSO) for 18 hours. Gene expression was quantified by real time-PCR. Values are normalised to cyclophylin and shown as fold-change to vehicle control for each donor (n=1).

LXR modulation by ligands has been reported to inhibit HSC activation in mice (151). Therefore, it was next assessed whether this inhibition also occurs in primary human HSC cultures. Treatment of human HSCs with the LXR ligand GW3965 caused a substantial reduction in the expression of *ACTA2*, a marker for their activation state (249,409,410) (Figure 5.1.3. A). Remarkably, this decrease in *ACTA2* expression inversely correlated with the levels of *LXRA* but not *LXRB* (Figure 5.1.3. B), further suggesting that the alpha subtype could in fact be involved in the regulation of human HSC activation.

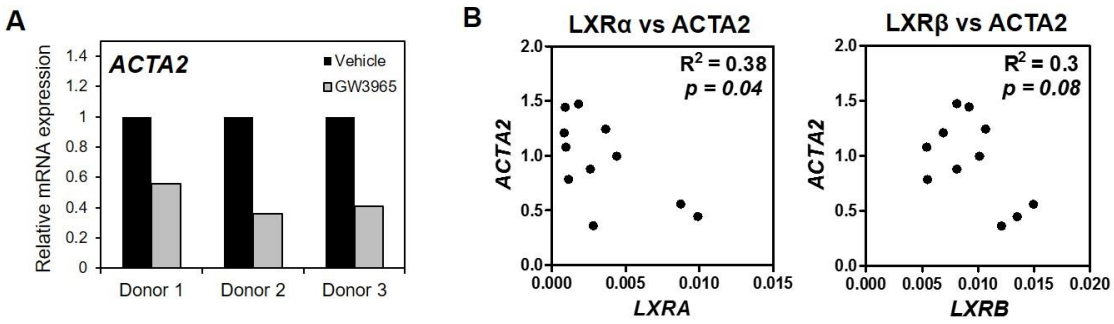

Figure 5.1.3. LXR activity decreases HSC activation

A) Primary Hepatic Stellate Cells were stimulated with 1 μM GW3965 or vehicle (DMSO) for 18 hours. Gene expression was quantified by real time-PCR. Values are normalised to cyclophylin and shown as fold-change to vehicle control for each donor (n=1).

B) Correlation of mRNA levels between *ACTA2* and *LXRA* or *LXRB*. Data represents product of Pearson's correlation coefficient (n = 3).

5.2.3. Summary and discussion

In summary, the experiments above show that:

- LXRs are activated by GW3965 in human primary HSCs and in consequence induce target gene expression
- LXR activity leads to decreased expression of the ACTA2 activation marker, which correlates with LXRα mRNA levels

Due to the difficulty in procuring human tissue and cells, the aforementioned work could only be performed in a limited number of samples. Although preliminary, these results establish the basis for pursuing future studies on the modulation of LXR activity in human primary HSCs. Besides changes in gene expression, it would be interesting to evaluate

how LXRs regulate HSC activation by looking at other functional markers, such as changes in cell morphology under light microscopy or assessment of collagen expression by histochemistry or immunoblotting (277).

Previous studies using liver biopsies from NAFLD patients indicate that LXRα levels (transcript and protein), as well as some of its regulated target genes positively correlate not only with the degree of steatosis but also with hepatic inflammation and fibrosis (412,413). These results identified LXRα as a novel factor involved in the pathogenesis of human NAFLD. Nonetheless, a more recent article looking at the expression of several nuclear receptors in patients with either fatty liver or NASH, found that LXRα is actually the only nuclear receptor whose expression is not affected during the progression of the disease (414). Also, it is still unclear whether elevated levels of LXRα represent an adaptive or a maladaptive/pathogenic response to the ongoing cellular and molecular changes. In my experiments, I didn't see a relation between LXR levels with target gene expression, although there was a trend towards decreased HSC activation. In the future, besides looking at global LXR levels, it would be interesting to assess the degree of LXRα phosphorylation, its relationship to LXR target gene expression and NAFLD progression; specifically, how LXR activity and phosphorylation correlate with the onset and development of human NAFLD. In addition, these previous studies were performed on whole liver tissue and obviate that NAFLD is a multifactorial disease with a multicellular contribution to its pathogenesis, where the specific impact of each cell type (e.g. hepatocytes or hepatic stellate cells) is disregarded. This has been mainly due to limited sample material, which also poses important technical limitations that are likely to affect the quality and reproducibility of results. The gap in the current knowledge could be addressed by studying LXR activity in different hepatic cell populations from a range of donors at various stages of NAFLD and analysing how this correlates with the onset and development of human NAFLD.

5.2. PART B: Investigating regulation of LXRα phosphorylation *in vitro*

Previous work by Dr. Pineda-Torra and colleagues demonstrated that LXRα phosphorylation occurs under basal conditions in the absence of ligand and is enhanced upon ligand activation in the RAW 264.7 macrophage-like cell line (163). Employing murine RAW 264.7 cells that overexpress either the wild-type form of the human LXRα (RAW-hLXRα) or its non-phosphorylatable S198A mutant (RAW-S198A), they showed that both synthetic (T0901317) and endogenous (24S,25-epoxycholesterol) LXR ligands, but not ligands for RXR, were able to induce the receptor's phosphorylation. This same study also showed that the inhibition of Casein Kinase 2 (CK2) by 2-dimethylamino-4,5,6,7-tetrabromo-benzimidazole (DMAT), reduced phosphorylation of LXRα at S198, indicating CK2 is one of the kinases that phosphorylates this receptor. Furthermore, other kinases have been reported to phosphorylate LXRα by other groups in different cells (169,415), which suggests that regulation of LXRα phosphorylation could be dependent on the cellular context and susceptible to a variety of stimuli. Indeed, a recent report has shown that oltipraz, a member of the dithiolethione family, attenuates LXRα phosphorylation in mouse liver cells through the inhibition of p70 ribosomal S6 kinase-1 (S6K1) (169), a major downstream effector of the mammalian target of rapamycin (mTOR) signalling pathway. However, the specific serine residue(s) phosphorylated were not identified and thus it remains to be clarified if Ser198/Ser196 is susceptible to this kinase.

Most of the work on this thesis has been performed on a model of genetic impairment of LXRα phosphorylation. However, the translational capacity of LXRα post-translational modifications will mainly depend on the extent to which these can be replicated or modulated by pharmacological compounds including kinase inhibitors.

Thus, the aims of this part of the chapter were to:

- Further identify which other stimuli induce LXRα phosphorylation *in vitro.*
- Analyse how pharmacological inhibition of LXRα phosphorylation affects the receptor's transcriptional activity *in vitro*.

5.2.1. LXRα is phosphorylated by LXR ligands and insulin

In order to explore the regulation of LXRα phosphorylation by other LXR synthetic agonists beyond T0901317, the effect of GW3965 (see section 1.1.2.2) was first evaluated. Thus, RAW-hLXRα cells were stimulated with 5 μM GW3965 and LXRα phosphorylation was assessed in their nuclear extracts. This concentration of GW3965 was chosen as it had previously been shown in my lab to induce LXRα phosphorylation in RAW-hLXRα cells (Pineda-Torra I, unpublished). Nuclear extracts of the non-phosphorylatable RAW-S198A cells were included in these phosphorylation experiments as negative controls. As previously seen with the T0901317 synthetic ligand (163), low levels of phosphorylation at S198 were observed in vehicle-treated cells, and these were enhanced after stimulation with GW3965 (Figure 5.2.1. A). Moreover, time course studies with this ligand demonstrated that LXRα phosphorylation occurred as early as one hour after stimulation, and was maintained up to 6 hours (Figure 5.2.1. A).

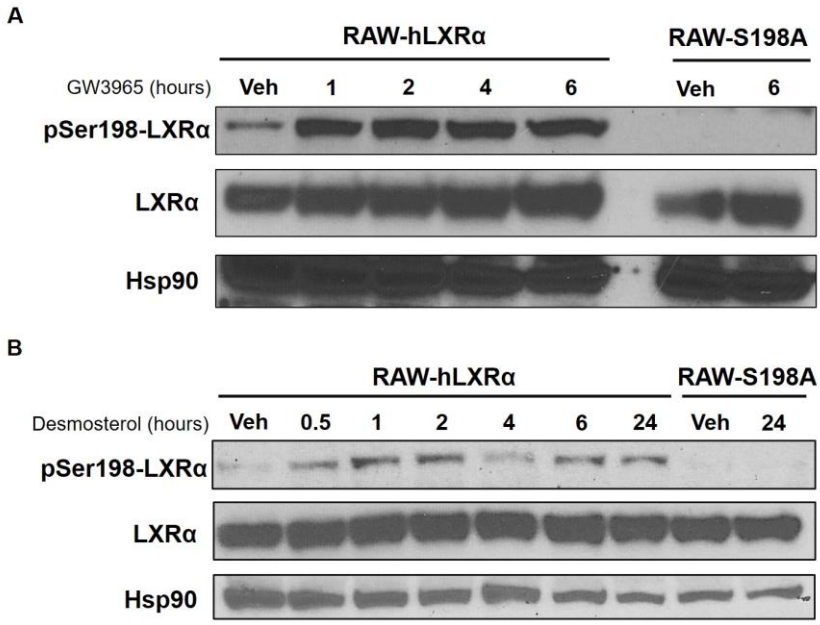

Figure 5.2.1. LXRα is phosphorylated by GW3965 and desmosterol with similar kinetics

RAW 264.7 cells stably expressing the human LXRα (RAW-hLXRα) or the S198A mutant (RAW-S198A) were incubated with or without 5 μM GW3965 (A) and 10 μM desmosterol (B) for the indicated lengths of time. Nuclear extracts were extracted and phosphoSer198-LXRα, total LXRα and Heat shock protein 90 (Hsp90) were detected by immunoblotting (n = 1).

Furthermore, in order to compare synthetic versus natural ligand effects, phosphorylation kinetics of LXRα by the cholesterol precursor desmosterol, a recently discovered endogenous agonist, was also examined (see section 1.1.2.1). Due to the lower affinity of this ligand compared to GW3965 (see Tables 1.1. and 1.2), extended time points were investigated to tease out more subtle effects. Moreover, a higher concentration (10 μM) of desmosterol was also used, as it had been shown previously to activate LXRs in murine macrophages *in vitro* (52).

Similar to GW3965 (Figure 5.2.1. A), phosphorylation of the human receptor by desmosterol was quickly induced at 30 min (0.5 hours) post-stimulation (Figure 5.2.1. B). This suggests that independently of the nature, phosphorylation of LXRα may follow a similar pattern, where this modification emerges shortly after stimulation. Nonetheless, phosphorylation by desmosterol appears to have a biphasic nature, since it decreases after 4 hours, and then goes back up at 6 hours where it remains phosphorylated until at least 24 hours post-stimulation. Nonetheless, this should be confirmed by performing additional repeats of this experiment and certify that it is not due to technical issues.

Even though not a direct LXR ligand, the effects of insulin on hepatic fat metabolism (416), and more specifically, on the expression of *Srebp-1c* (417,418), suggests a mechanism through which insulin could be regulating LXR activity without directly binding to it. Thus, the effect of insulin on LXRα phosphorylation was also investigated by treating cells at increasing concentrations of insulin for 4 hours, as LXRα had shown to be susceptible to phosphorylation at this time point, at least in response to GW3965 (Figure 5.2.1. A). Concentrations of insulin were chosen to be around 100 nM, since this amount has been shown previously to activate LXRs *in vitro* (129). In comparison to vehicle treated cells, LXRα-S198 was strongly phosphorylated upon increasing concentrations of insulin (Figure 5.2.2), establishing that LXRα phosphorylation is also responsive to insulin.

Nonetheless, a slight decrease in phosphorylation is observable at 200 nM treatment (Figure 5.2.2). As the levels of total LXRα protein and the loading control Hsp90 remain unchanged, this is most probably not due to a decrease in protein levels but most likely a technical error when stimulating these cells.

In summary, these experiments show that LXRα phosphorylation at S198 in induced by a variety of activators including a range of LXR ligands and a metabolic hormone.

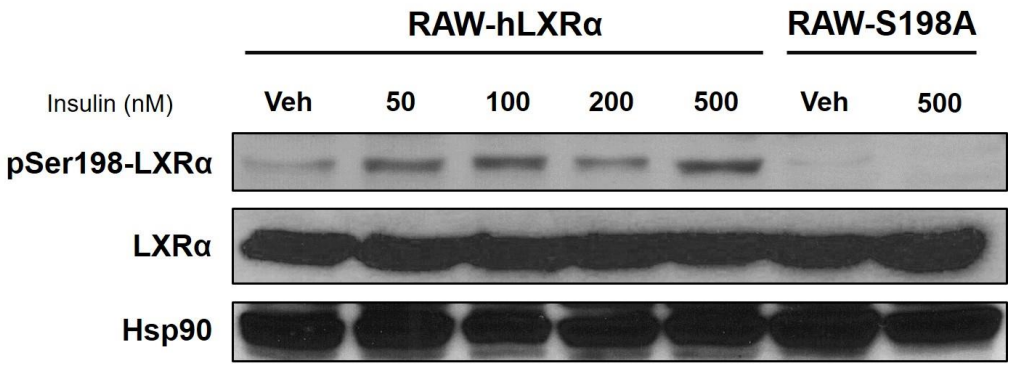

Figure 5.2.2. LXRα is phosphorylated by insulin
RAW-hLXRα and RAW-S198A cells were incubated with different concentrations of Insulin or PBS (vehicle) for 4 hours. Nuclear extracts were extracted and phosphoSer198-LXRα, total LXRα and Hsp90 were detected by immunoblotting (n = 1).

5.2.2. LXRα-S198 is phosphorylated by S6K1 and can be pharmaceutically impaired *in vitro*

Oltipraz has been previously shown to hinder LXRα phosphorylation at unspecified serine and threonine residue(s) through the inhibition of the S6K1 kinase (169). Thus, impairment of LXRα-Ser198 phosphorylation by oltipraz *in vitro* was assessed in response to both synthetic (GW3965, Figure 5.2.3. A) and endogenous (24S,25-epoxycholesterol, Figure 5.2.3. B) LXR ligands. The concentrations of oltipraz used for this experiment were chosen specifically as they had been used previously to alter LXR activity *in vitro* (169).

Firstly, and in comparison to the levels of loading control heat shock protein 90 (Hsp90), a slight decrease in S198 phosphorylation could be observed upon treatment with the highest concentration (30 μM) of oltipraz (Figure 5.2.3. A). Total LXRα levels on cells treated with GW3965 could not be blotted due to experimental problems, and thus changes in phosphorylation could not be quantified.

Then, effects of oltipraz at higher doses were tested with 24S,25-epoxycholesterol (EC), an endogenous ligand known to induce the receptor's phosphorylation (163). Upon stimulation with EC, reduced LXRα phosphorylation was observed as expected, with the highest doses (30-40 μM) of the compound (Figure 5.2.3. B). Furthermore, quantification of the ratio of phosphorylated S198 over total levels of the receptor confirmed that impairment of LXRα occurs in inverse relation to oltipraz concentrations (Figure 5.2.3. B).

Overall, these results show that LXRα-S198 residue is indeed susceptible to phosphorylation by S6K1 in RAW macrophage cells *in vitro*.

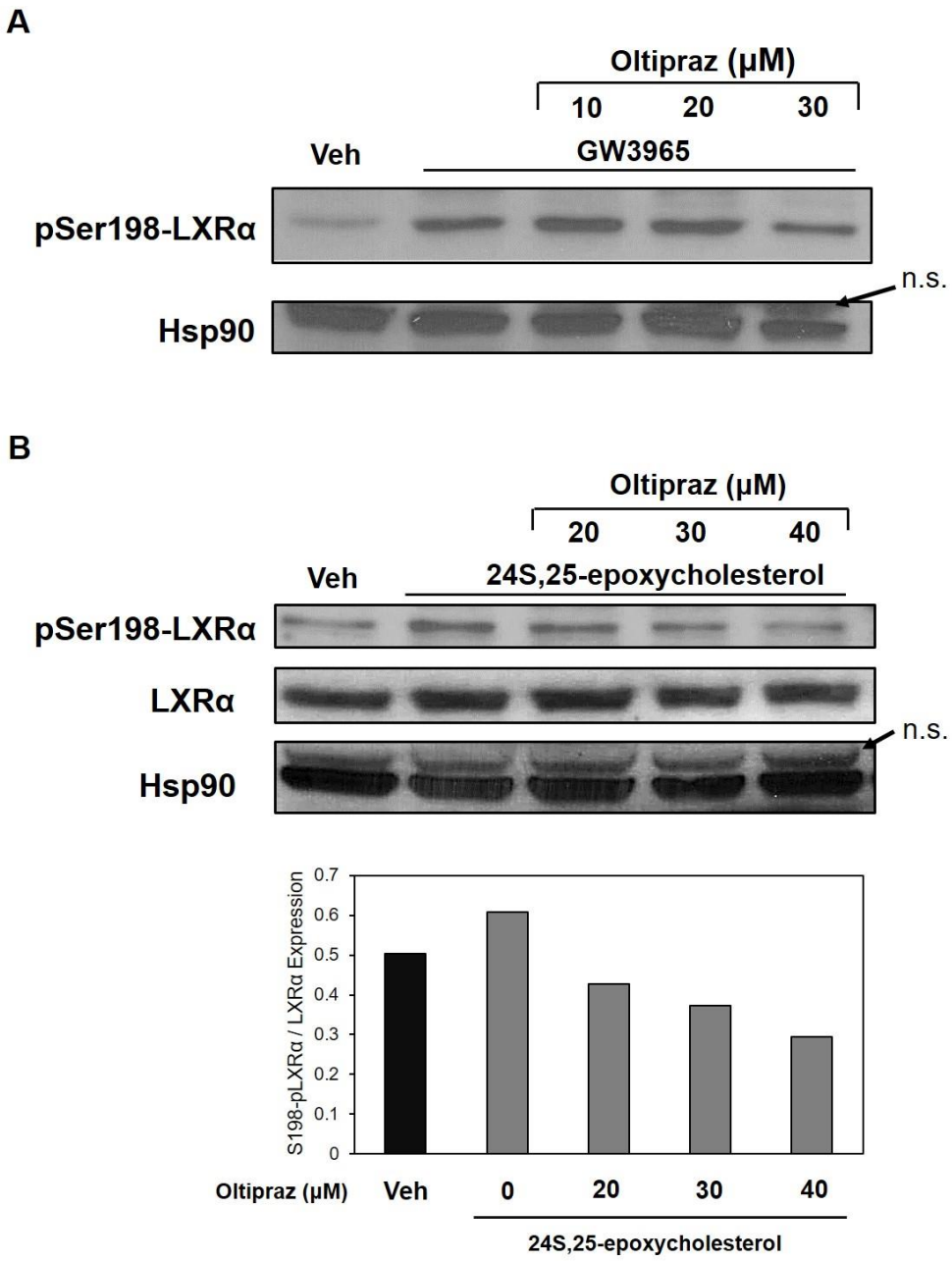

Figure 5.2.3. LXRα-S198 phosphorylation by S6K1 is impaired *in vitro* by oltipraz

A,B) RAW-hLXRα cells were pre-treated for 2 hours with different concentrations of oltipraz and incubated with 5 μM GW3965 (A) or 10 μM 24S,25-epoxycholesterol (B) for 4 hours.

Nuclear extracts were prepared and phosphoSer198-LXRα, total LXRα and Hsp90 were detected by immunoblotting (n =1).

Densitometry was performed for the immunoblot shown in B) on the levels of phosphorylated S198-LXRα over total LXRα expression, and normalised to the levels of the housekeeping Hsp90 (n=1).

5.2.3. Pharmacological inhibition of LXRα phosphorylation affects the transcriptional activity of the receptor

Previous work has established that Ser198-LXRα is a target for the CK2 kinase *in vitro* (163). Hence, efficacy of the specific CK2 inhibitor CX-4945 was tested by treating RAW-hLXRα cells with three different concentrations of the compound and then assessing its effect on GW3965-induced phosphorylation at S198. LXRα phosphorylation levels were reduced for all three concentrations tested (Figure 5.2.4. A), confirming that CK2 is indeed a *bona fide* kinase for LXRα-S198 phosphorylation *in vitro* and its effects on LXRα-S198 can be partly mitigated by CX-4945.

Next, in order to establish whether pharmacological inhibition of LXRα phosphorylation affects the transcriptional activity of the receptor, expression of several LXR target genes that had been shown before to be expressed in RAW 264.7 cells in response to LXR ligands (163), were examined on cells pre-treated with two of the CX-4945 concentrations shown to inhibit LXRα phosphorylation (Figure 5.2.4. A).

As previous studies have shown that other LXRα residues are susceptible to phosphorylation (see section 1.1.4.3), the results obtained on cells expressing the wild-type version of LXRα (hLXRα) were compared to the mutant non-phosphorylatable S198A to control for additional effects of the CX-4945 compound on other residues or on other proteins affecting LXR-mediated transcription. First, differences in the basal (vehicle-treated) expression of LXR target genes was investigated (Figure 5.2.4. B). Interestingly, treatment with CX-4945 seemed have the strongest effect on the non-phosphorylatable (S198A) rather than the wild-type (hLXRα) cells, leading to induction of *Aim* and repression of *Abca1* (Figure 5.2.4. B). This occurred in a dose-dependent manner of CX-4945 for both genes. However, this dose-dependent response was not observed for other LXR target genes, such as *Lpl* (Figure 5.2.4. B). These results suggest that, at least at the basal level, CX-4945 effect on LXR activity is not mediated through changes in S198 phosphorylation.

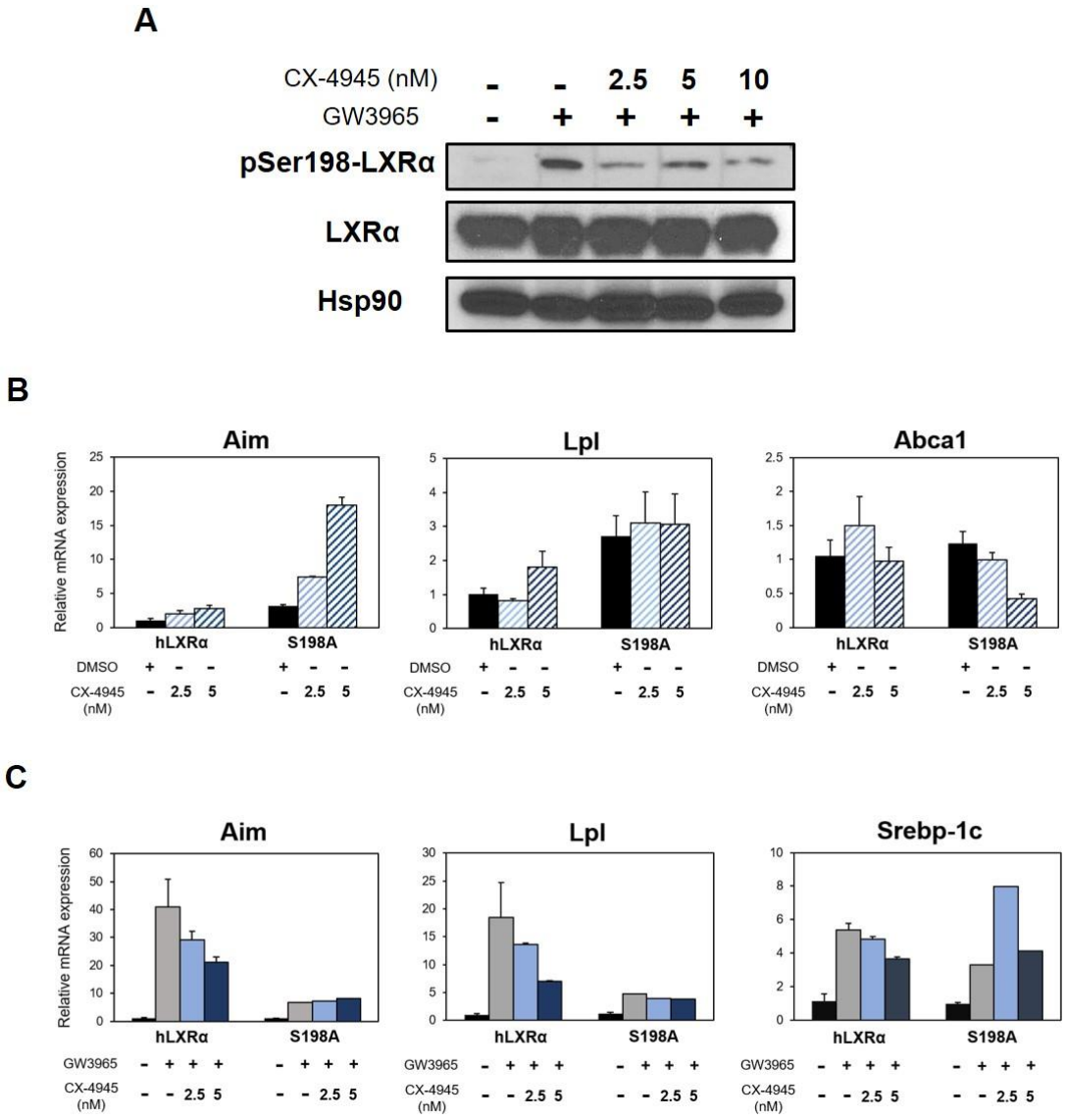

Figure 5.2.4. Pharmacological inhibition of LXRα phosphorylation affects the receptor's transcriptional activity *in vitro*

A) RAW-hLXRα were pre-treated with three different concentrations of CX-4945 for 2 hours and then stimulated with 5 μM GW3965 for 4 hours. Nuclear extracts were extracted and phospho-LXRα, total LXRα and Hsp90 were detected by immunoblotting (n =1).

B-C) mRNA expression on RAW-hLXRα or the RAW-S198A mutant. Cells were pre-treated for 2 hours with different concentrations of the CK2 inhibitor CX-4945 and then stimulated for 18 hours with DMSO as vehicle (B) or 1 μM GW3965 (C). Data represents mean ± SEM. n = 2, except GW3965-treated S198A (n=1). Values were normalised to cyclophilin and shown as fold-induction over the untreated (DMSO) samples on the hLXRα samples (B) or for both hLXRα and S198A (C).

From the available data, it appears that in contrast to what was observed at the basal level, pre-treatment with CX-4945 reduced ligand-induced gene expression on the hLXRα wild-type but not the mutant cells (Figure 5.2.4. C). Specifically, induction of *Aim* and *Lpl* expression by GW3965 was seen to be gradually reduced with increasing concentrations of the CK2 inhibitor (Figure 5.2.4. C). This effect was weaker for other genes, such as *Srebp-1c*. Surprisingly, the decrease of *Aim* and *Lpl* expression upon treatment with GW3965 can be observed, although to a different extent, on cells with either pharmacological (CX-4945 treated-hLXRα cells) or genetic (S198A cells) impairment of LXRα phosphorylation.

Collectively, these findings suggest a model where CK2 inhibition by CX-4945 affects LXR target genes differently depending on the ligand-activation and phosphorylation status of the receptor; whereby only when the receptor is strongly phosphorylated through GW3965, the pharmacological inhibition of this modification mirrors the genetic impairment (Figure 5.2.5). Moreover, this appears to occur in a gene-dependent manner. It must be noted that the results shown above are preliminary, as even though the treatment conditions were performed in duplicates, these experiments could only be performed once. Therefore, future studies should address if these results can be replicated in two or more additional independent experiments.

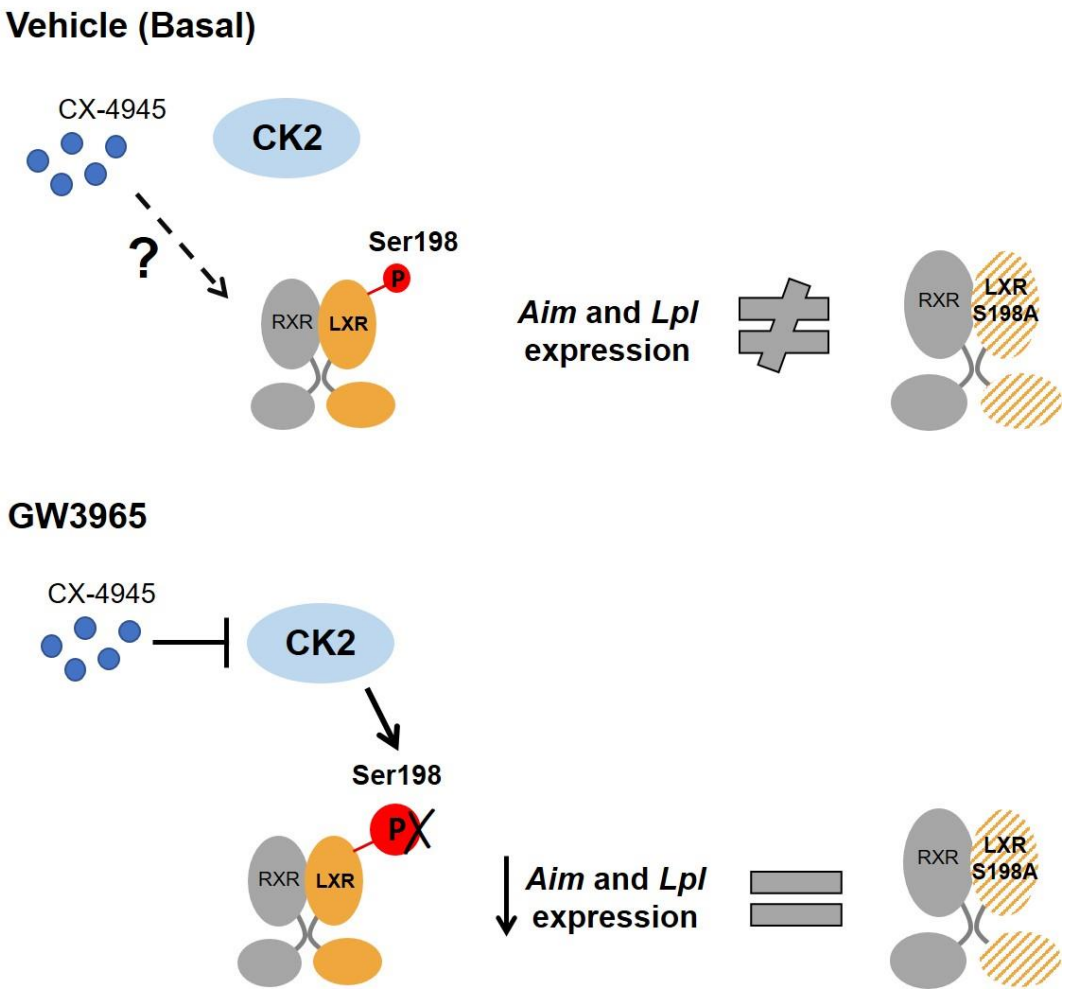

Figure 5.2.5. Diagram summarizing possible effect of CX-4945 on LXRα gene expression on basal and ligand-activated conditions *in vitro*

Results obtained so far seem to suggest that at the basal level, CX-4945 effect on LXR activity is not mediated through changes in S198 phosphorylation. Moreover, upon treatment with the LXR ligand GW3965, and consequential induction of S198 phosphorylation, CK2 inhibition by CX-4945 affects LXR target genes in a manner that mimics the effect of the genetically modified, non-phosphorylatable LXRα-S198A.

5.2.4. Discussion

Despite previous work showing that the human LXRα is susceptible to phosphorylation by synthetic and endogenous ligands (163), this was not done exhaustively for all known LXR ligand. Indeed, induction of this post-translational modification by either GW3965, desmosterol or insulin has never been demonstrated to date. The results in this chapter prove that, at least *in vitro*, human LXRα-S198 can be phosphorylated by a variety of stimuli, including known ligands and nutritional /hormonal cues.

Moreover, this work aimed to begin to study how pharmacological inhibition affects the receptor's activity *in vitro* and how it compares to genetic inhibition of LXRα phosphorylation. These studies could be relevant when evaluating the translational capacity of genetically modified animal models into identification of novel pharmacological therapies to treat diseases. The CK2 kinase is known to phosphorylate a myriad of different proteins; and very interestingly, its actions have been linked by other groups to the expression of some genes assessed in Figure 5.2.4, by mechanisms parallel to LXRs. For example, Harris *et al*. presented a study where CK2-mediated phosphorylation of the SP1 transcription factor reduced the expression of *Lpl* in response to interferon-γ *in vitro* (419). Furthermore, a study published this year looking at the mechanisms behind the lipogenic programme activation in response to insulin, demonstrated that activation of CK2 downstream from the insulin receptor led to the phosphorylation of the Mediator subunit 17 (MED17) cofactor, which caused the expression of several lipogenic genes, such as *Srebp-1c* or *Fas* (420), both known LXR target genes (see section 1.1.3.1). Remarkably, MED17, also known as TRAP80, is known to interact with LXRα and is involved in the regulation of lipogenic gene expression (421). Therefore, the regulation by CK2 of target gene expression through other proteins besides LXRs should be taken into consideration when assessing its pharmacological inhibition as a means to modulate LXR activity.

For my studies, I decided to use the more selective CK2 inhibitor CX-4945, an orally bioavailable small molecule that inhibits both CK2α and CK2α′ catalytic subunits (422), as previous reports demonstrated that DMAT, the inhibitor previously shown to abrogate LXRα phosphorylation, is also able to powerfully inhibit other kinases (423). Moreover, I have used two kinase inhibitors that are currently under clinical trial for several diseases, i.e. CX-4945 as an antitumorigenic (ClinicalTrials.gov Identifier: NCT02128282); and oltipraz for Fatty Liver disease (ClinicalTrials.gov Identifier: NCT02068339) (424). This has the benefit of having access to data about the safety and bioavailability of both compounds for human use, and through drug repurposing, raises the possibility of using them for the treatment of diseases that may be influenced by LXRα phosphorylation.

The detection of endogenous LXRα and more specifically, its phosphorylation status, remains technically challenging depending on the cell type or tissue under study. Therefore, in this thesis, work looking at the regulation of LXRα phosphorylation was performed on a particular cell line available in the lab that overexpressed the human LXRα and its non-phosphorylatable mutant. Nonetheless, protocol optimization using these cells and our non-commercially available phospho-antibodies allowed me to eventually detect endogenous phosphorylation levels in human and mouse livers (Figure 3.1. C,D); a tissue which expresses relatively large amounts of LXRα. Therefore, future studies should aim to use other cell types in order to look for cell-specific differences. A good example of these are the hepatocyte mouse cell line Hepa 1-6, as these cells express very low levels of endogenous LXRα (425), and would thus not confound with the activity of the overexpressed wild-type and mutant receptors.

Chapter 6. General discussion and future studies

This thesis aimed to investigate the regulation of LXRα phosphorylation and how this modification impacts the receptor's activity *in vivo*. To this end, a novel mouse model harbouring a whole-body mutation that disrupts LXRα phosphorylation at Ser196 was generated. Using this *in vivo* model, I have assessed the effect of this mutation on the animal's response to a HFHC diet, and have investigated the specific molecular mechanisms behind the mutant LXRα's activity. Results show that impairment of LXRα phosphorylation at Ser196 critically acts as a novel nutritional sensor that promotes a unique diet-induced transcriptome and modulates metabolic, inflammatory and fibrotic responses that known to be key in NAFLD progression (see Chapters 3 and 4, and Figure 6.1).

Moreover, by using a murine macrophage cell line stably transfected with the human wild-type version of the receptor or its non-phosphorylatable mutant (163), I have sought to examine new stimulants capable of inducing LXRα phosphorylation *in vitro*, and how this phenomenon can be pharmacologically impaired by using commercially available kinase inhibitors. Lastly, and in collaboration with Dr. Krista Rombouts (University College London, UK), I was able to acquire several human primary HSCs preparations and human liver biopsies, with which I explored how LXR activation affects the activity of these cells, key players in the pathogenesis of NAFLD. Importantly, I have also demonstrated for the first time the presence of LXRα phosphorylation at Ser198 in healthy human liver biopsies also provided by Dr Rombouts.

Post-translational modifications (PTMs) are a powerful means by which the function of nuclear receptors can be modified. Despite the documented key importance of some of these receptors in maintaining metabolic homeostasis in health and disease (158), our understanding of the functional impact that post-translational modifications have on metabolic diseases remains scarce. To date, the physiological roles of modifications such as phosphorylation, sumoylation and acetylation of LXRα have only been studied *in vitro* or non-specifically in animal models, by pharmacologically or genetically altering

the enzymes enhancing or inhibiting these modifications (158). For instance, mice deficient in *Sirt1*, which is the enzyme that promotes LXRα deacetylation and its subsequent ubiquitination and degradation, has been associated with impaired lipid metabolism and defective RCT, as well as increased hepatic and testicular cholesterol levels (156). In another study, inhibition of LXRα phosphorylation at an unspecified serine residue by oltipraz, an inhibitor for S6K1 kinase, was shown to attenuate hepatic lipogenesis and steatosis in mice fed a high-fat diet (169). Thus, this thesis is the first study to address the pathophysiological impact of LXRα phosphorylation by directly impeding this modification genetically. Moreover, the overall results of the work hereby presented have established the S196A mice as an optimal *in vivo* model for the study of this post-translational modification, as well as an important tool for future studies that further investigate regulation of LXRα phosphorylation as a potential therapeutic target.

6.1. Effects of LXRα phosphorylation on hepatic lipid metabolism

The work in chapter 3 shows that, regardless of a higher degree of steatosis consistent with an increase in *de novo* lipogenesis, S196A mice counter-intuitively exhibit less hepatic inflammation and fibrosis than WT animals. This protection from diet-induced hepatic damage was accompanied by the significant repression of numerous pro-inflammatory and pro-fibrotic mediators, as well as by lower levels of genes that code for several ER stress markers. Further analysis on the metabolic profile of these animals revealed a resistance to plasma and hepatic total cholesterol accumulation on phosphorylation-deficient mice (Figure 6.1). The increased steatosis in HFHC-fed S196A mice was associated with a higher expression of the *Srebp-1c* transcription factor, a key regulator of hepatic lipogenesis (426). This is consistent with the work of Yamamoto T *et al*., which shows that LXRα phosphorylation at several residues by Protein Kinase A represses the expression of this gene *in vitro* by enhancing recruitment of NCoR (415). However, their study failed to reconcile the link between induction of *Srebp-1c* by LXR

ligands and LXRα phosphorylation; since previous studies (163,165), as well as work shown in this thesis (Chapter 5), have demonstrated that these compounds hyper-phosphorylate the receptor. Moreover, the specific contribution of each phosphorylated residue by site-directed mutagenesis was not assessed in their study.

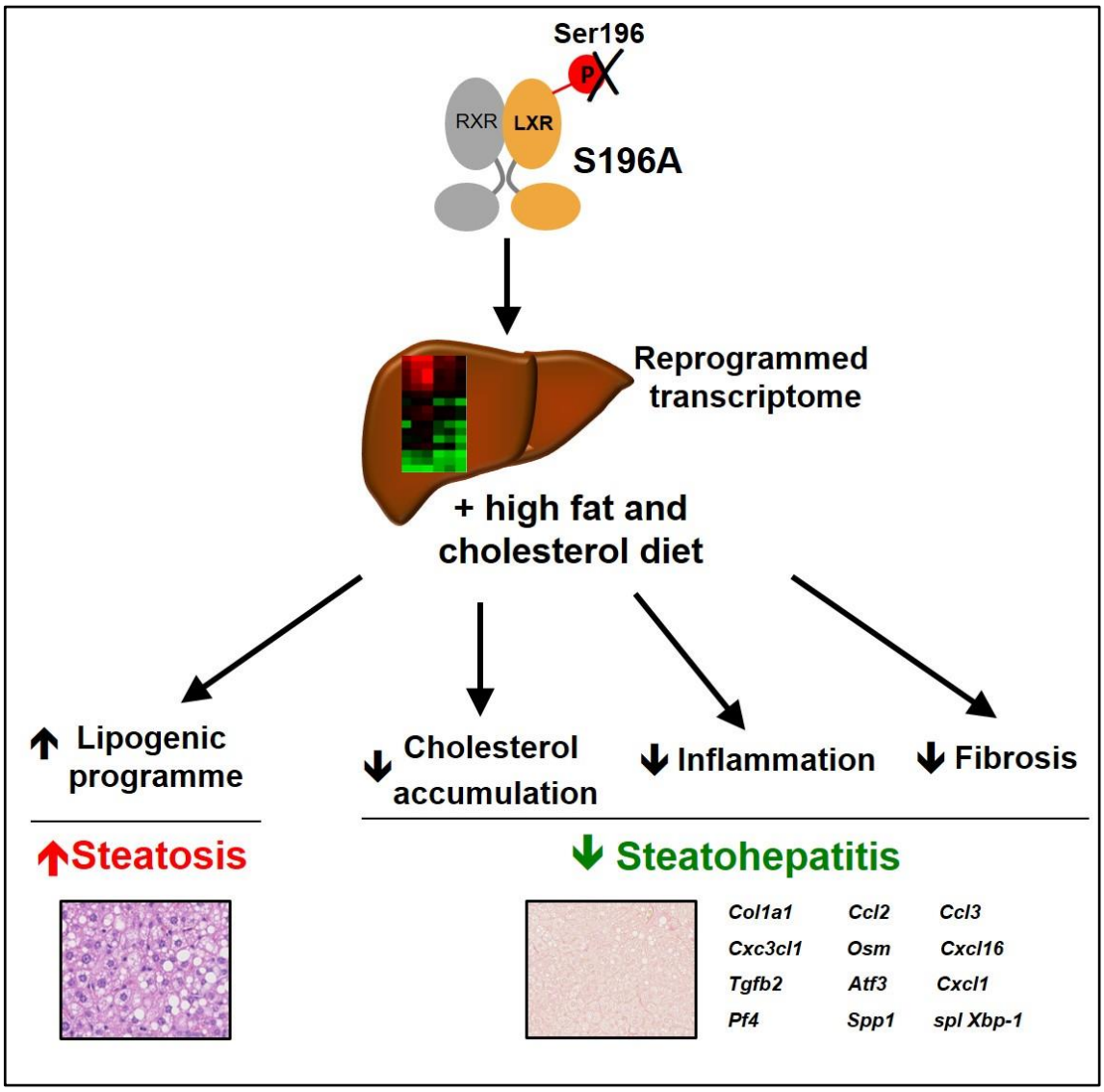

Figure 6.1. Graphical summary of LXRα-S196A effects on hepatic lipid metabolism
Impairment of phosphorylation of LXRα-S196 reprograms the hepatic transcriptome in mice, which upon being fed a HFHC diet leads to a higher degree of steatosis, as well as reduced hepatic inflammation and fibrosis (steatohepatitis).
Adapted from bioRxiv 127779.

Even though the S196A mice carry a whole-body mutation and LXRα is expressed in many other extrahepatic tissues (2,3), the animals on the HFHC diet elicited a prominent liver phenotype. I hypothesize that these relatively short-term effects may be caused by the high presence of the alpha subtype in the liver and the prominent effect that this organ has on lipid metabolism. Examining the role that deficiency in LXRα-S196 phosphorylation may be having on other tissues was beyond the scope of this thesis, and should be further explored in the future. As shown in Chapter 5, phosphorylation of the human LXRα at Ser198 is susceptible to a wide variety of stimuli, including the synthetic ligand GW3965 and insulin, which can induce the receptor's phosphorylation through different kinases. This raises the possibility that LXRα phosphorylation, and hence its impairment, could be acting in a context and tissue-specific manner depending on the stimulant and consequent activation of downstream kinase signalling.

Accordingly, it would be interesting for future studies to dissect the specific effects that the LXRα-S196A is having on the different hepatic cell types, and their specific contributions to the overall liver phenotype. This could be achieved by crossing the mice carrying the floxed S196A vector with other strains containing the Cre recombinase under cell-specific promoters, such as the lecithin-retinol acyltransferase (Lrat) for HSCs (427) or albumin (Alb) for hepatocytes (428).

It should be noted that due to the nature of the work on this thesis, which has looked at the activity of a transcription factor and its overall effects on transcriptional regulation, the experiments in Chapter 3 were primarily designed to primarily assess mRNA levels. This poses a limitation to this study, given that changes in transcript levels don't necessarily mirror by changes in protein levels. For this reason, future work should confirm if the changes observed at the mRNA expression level are translated into changes in protein expression by immunoblotting or immunohistochemistry in liver or hepatic cell protein extracts.

The diet used in my studies was initially chosen with the purpose of metabolically challenging the mice, while providing high levels of endogenous LXR ligands. Diets high

in fat and cholesterol have been used in the past as experimental models of NAFLD (329,429), as it induces hepatic damage in a less severe manner than other dietary approaches, such as the methionine and choline deficiency (MCD) diet (430,431). In addition, the diet used in this study contained high levels of sodium cholate (see section 2.2.1), which when added to cholesterol-supplemented diets has shown to induce hepatic steatosis, inflammation and fibrosis (329,432). Indeed, after only 6 weeks of being fed the HFHC diet, WT mice elicited prominent hepatocyte ballooning, a key histological feature in the human NAFLD (433,434). Nevertheless, the scientific community has lately advocated for the use of diets supplemented with high levels of sucrose or fructose, on the basis that besides promoting most hepatic characteristics of NAFLD, they also induce obesity and insulin resistance (435,436), and thus resemble more closely the dietary and phenotypical characteristics of the human disease (437,438). Future work could assess how the S196A mice respond to a diet high in fat, cholesterol and fructose, especially since LXRs also have an important role in glucose metabolism (see section 1.1.3.2).

6.2. Impairment of LXRα-S196 phosphorylation alters the hepatic transcriptome

The detailed mechanisms through which LXRα-S196A confers protection against diet-induced hepatic injury couldn't be fully elucidated in the period of time this thesis covered. Several options are possible, in reference to our current understanding on LXR actions and the pathogenesis of NAFLD (Chapter 1). Such options are: a decrease in hepatic cholesterol, a shift towards higher levels of protective fatty acid species and/or an increased transrepressive capacity of the LXRα-S196A receptor. Based on the observed reprogramming of the hepatic transcriptome in the mutant mice (Chapter 4), I speculate that the protective phenotype in S196A mice is probably due to a combination of all the above, especially in relation to such a multifactorial disease such as NAFLD. However, this hypothesis should be confirmed by assessing phenotype disappearance on animals

with a suppressed (or incremented) expression of those genes involved in the aforementioned pathways, which would only be definitive if there is only a major responsible pathway.

One unexpected aspect revealed over RNA-seq analysis of HFHC livers (Chapter 4) was that LXRα expression was slightly increased in S196A mice. Autoregulation of the mouse receptor is still not fully clarified, as it has been described to be present in certain tissues, like adipose tissue (9) but not in others, i.e. primary macrophages (10). Nonetheless, previous reports have shown that murine LXRα expression in the liver can be induced by high fatty acid levels (8), as well as a high fat and high cholesterol diet (439). Therefore, the slight induction of LXRα could be explained by the higher levels of fats present in S196A livers. Indeed, and in accordance with this hypothesis, no difference could be observed in small intestine *LXRα* levels between genotypes (Figure 3.5. C). Nonetheless, the gene-selective modulation of the LXRα-S196A, a phenomenon that had been observed previously *in vitro* (163,165), suggests that the phenotype observed in the mutant mice is most probably caused by the changes in phosphorylation rather than levels of the receptor. In fact, a previous report on a mouse model with a liver-specific increase in LXRα expression (440) showed a completely different hepatic transcriptome than the S196A mice, both under a chow and Western diet. For example, whilst the livers of chow-fed LXRα overexpressing-mice displayed no differences in the expression of *Fas*, the S196A animals suffered a significant decrease in the expression of this same gene compared to WT controls. This difference in transcriptomes further strengthens the idea that the difference in the mutant mice compared to WT is indeed caused by the genetic impairment of LXRα-S196A phosphorylation.

Regarding the mechanism of action of LXRs, the initial theory described for many nuclear receptors was that these were sitting on the promoters of their respective target genes, interacting with different cofactors depending on their activation state, and inducing or repressing gene expression accordingly (25,441). Later studies using ChIP-sequencing of LXRs and other nuclear receptors have shown that, alternatively, LXRs are bound

primarily to different transcriptional regulatory intronic and intergenic regions (315,442), distal from the TSS of genes. When investigating the regulation of the LXRα phosphorylation-sensitive genes *Ces1f* and *Cyp2c69* (Chapter 4), both DR4 sequences found *in silico* were located at intronic regions, suggesting that these may be actually acting within an enhancer region; which are short (50-1500 bp), non-protein coding sequences of DNA, whose function is to greatly increase the expression of genes in their vicinity. However, true identification of these regions as such should be confirmed in the future. One way to do so would be looking at the presence of putative enhancer elements, like the HAT p300 (443) or H3 monomethylated at K4 (H3K4me1) (444) by ChIP-seq analysis. Moreover, the results shown in Chapter 4 demonstrate that most of the genes regulated by the mutant LXRα were only modulated upon a fat and cholesterol-rich environment. Several recent studies have established that certain metabolic states induce changes in the epigenome, through chromatin modifications, both in animal models fed diets with a high fat diet and in obese and diabetic humans (445–447). These modifications, such as changes in methylation patterns, affect chromatin accessibility and are considered to act as a "metabolic imprint", causing increased disease risk. As part of an ongoing collaboration with Dr. Eckardt Treuter's group at the Karolinska Institutet (Sweden), we are now undertaking ChIP-seq studies to explore how certain histone modifications in the liver, such as H3K27ac (acetyl K27), a mark associated with "open" or active chromatin states, vary between the WT and S196A mice. This will allow us to better understand how the changes we have observed at the transcriptional level in S196A livers associate with epigenetic regulation.

The precise mechanisms that regulate the signal-dependent exchange between corepressor and coactivators are still not fully understood. This is the first study to show that changes in LXRα post-translational modifications confer the receptor with a specific transcriptional signature, by possibly affecting the cofactor exchange process. The fact that TBLR1 and its partner TBL1 are intrinsic components of the NCoR/SMRT corepressor complexes, required for both the repression and de-repression of genes (27,391), suggests a model where co-repressors found in gene promoters or other DNA

regulatory regions are in a primed state that allows for their quick release. ChIP-qPCR analysis of genes that showed to be significantly induced in S196A livers upon a HFHC diet (Chapter 4), revealed a higher occupancy of TBLR1 at those sites where LXR also binds (LXRE and degenerated DR4s). Taking also into account the *in vitro* data from our collaborators at Prof. Garabedian's lab (New York University, USA), showing that the LXRα phospho-mutant binds more to TBLR1 than the wild-type form (Figure 4.11. A), I hypothesise that the molecular mechanisms behind the changes in hepatic gene expression in S196A livers are caused, in part, through an increased presence of TBLR1-LXR complexes and its consequential increase in cofactor exchange.

Interestingly, TBLR1 activity itself has also been shown to be regulated by PTMs. Perissi and colleagues demonstrated that TBLR1-S193 is a target of ligand-induced Protein Kinase C δ-mediated phosphorylation, which happens *in situ* on the promoters of its regulated genes, and leads to the release and degradation of NCoR/SMRT (391). This further supports the idea that PTMs are used as a quick, reversible, targeted way to regulate the transcriptional machinery. Thus, it would be interesting for future studies to examine how modification of the phosphorylation status of LXRα affects TBLR1 activity, not only through their interaction, but possibly by also regulating its own PTMs.

6.3. Therapeutic opportunities for agents that modify LXRα phosphorylation

As we gradually gain more knowledge on how posttranslational modifications finely tune nuclear receptor actions, and how these mechanisms appear to be often dysregulated in pathological situations, the focus on nuclear receptor preclinical research has begun to shift towards elucidating how to manipulate these modifications as alternative therapeutic avenues. For example, several studies have now linked the phosphorylation status of the Estrogen Receptor α in breast tumours, with resistance to endocrine treatment and overall clinical outcomes (448). Importantly, this is not only restricted to

steroid receptors. Recently, based on initial observations that phosphorylation of PPARγ at Ser273 is linked to obesity and insulin resistance (449,450), a drug screening effort on 780 different Food and Drug Adminstration (FDA)-approved drugs using disruption of PPARγ phosphorylation as an endpoint (rather than PPARγ classical ligand activation) was reported (451). These efforts identified that Gleevec, a well-established anti-cancer drug, increases insulin sensitivity and overall improves the phenotype of mice fed a high-fat diet by blocking PPARγ-Ser273 phosphorylation (451). Thus, modulating nuclear receptor PTMs as a strategy to modulate their activity may soon become a plausible alternative to current therapies

In the UK, NAFLD affects about 25% of the adult population, and of those, around 30% will progress to non-alcoholic steatohepatitis (NASH) (452,453). Current treatment options such as lifestyle changes (diet change and weight loss) are inadequate for a large number of patients. Moreover, pharmacological therapies such as insulin sensitizers, antioxidants, and lipid-lowering agents are aimed at treating its associated conditions and therefore display only limited efficacy. Thus, there is a clear unmet medical need for development of novel direct pharmacological therapies targeting NAFLD. LXRα's role in promoting fatty acid and triglyceride accumulation (7) has proven a major obstacle in the development of LXR ligands as human therapeutics against metabolic and cardiovascular disorders. Concurrently, pharmacological antagonism of LXRs has been proposed in recent years to be effective against NAFLD. For instance, the liver selective LXR inverse agonist SR9238 suppresses hepatic fatty acid synthesis and lipid accumulation leading to alleviated hepatic inflammation and fibrosis in an obese rodent model (152,153). Interestingly, a recently-published study looking at LXRα preservation through inhibition of its tetratricopeptide repeat domain protein 39B (*Ttc39b*)-induced ubiquitination, showed that increased levels of hepatic LXRα reduced steatohepatitis in a dietary animal model of the disease (455). However, this protection was associated with a surprising inhibition of the hepatic lipogenic programme, which clearly links the amelioration of hepatic damage with a reduced lipotoxic presence.

Despite the high prevalence of steatosis in industrialised countries, this condition is considered to be relatively benign, where the life-expectancy of patients with early stages of NAFLD is similar to the general population (see section 1.2.1). However, a proportion of this group of patients will progress into developing fibrosis, cirrhosis or hepatocellular carcinoma (453); suffering from an increased mortality rate, mainly from cardiovascular and liver-related causes (456). Therefore, tackling the progression of NAFLD in individuals with already-established steatosis is key to reducing liver-related mortality. To my knowledge, the work presented in this thesis is the only one to have demonstrated that non-pharmacological modulation LXRα activity is able to reduce diet-induced hepatic injury despite abundant lipid accumulation. This further supports the idea that NAFLD pathogenesis is more complex than initially thought, and could be exploited to design novel LXR-based therapies to alter the progression of disease in subjects with already established steatosis. Therefore, future studies could involve the use of an inducible LXRα-S196A mouse model, where the effect of changing LXRα's phosphorylation is assessed once the early stages of NAFLD are already established. Indeed, such a model is already available in Prof. Garabedian's lab and stems from the same floxed mice used in my study (see section 2.1), but using the inducible tamoxifen-driven Cre recombinase (457).

Lastly, I have been able to show that the human LXRα is phosphorylated at Ser198 in healthy human livers (Chapter 5). At present, no Genome Wide Association studies (GWAS) on NAFLD or cardiovascular diseases have identified Single Nucleotide Polymorphisms (SNPs) related to neither LXRα-Ser196 nor its hinge region for that matter. Future studies should first address if changes in LXRα's phosphorylation status can be correlated with disease onset and progression. Thus, a better understanding of how LXRα posttranslational modifications can be modulated and the impact that they have on LXR biology could open in the future alternative therapeutic avenues for metabolic diseases.

Overall, the work described in this thesis shows that impairment of LXRα phosphorylation at Ser196 critically acts as a novel nutritional sensor *in vivo*, promoting a unique diet-induced transcriptome and modulating metabolic, inflammatory and fibrotic responses that are key in NAFLD progression. This novel work provides an important step forward towards a more exhaustive understanding of LXRα biology, and places the modulation of LXRα phosphorylation as a potential anti-inflammatory/anti-fibrotic therapeutic target.

References

1. Mangelsdorf DJ, Thummel C, Beato M, Herrlich P, Schütz G, Umesono K, Blumberg B, Kastner P, Mark M, Chambon P ER**.** The nuclear receptor superfamily: the second decade. *Cell* 1995;15(83(6)):835–9.

2. Apfel R, Benbrook D, Lernhardt E, Ortiz MA, Salbert G, Pfahl M**.** A novel orphan receptor specific for a subset of thyroid hormone-responsive elements and its interaction with the retinoid/thyroid hormone receptor subfamily. *Mol. Cell. Biol.* 1994;14(10):7025–35.

3. Willy PJ, Umesono K, Ong ES, Evans RM, Heyman RA, Mangelsdorf DJ**.** LXR, a nuclear receptor that defines a distinct retinoid response pathway. *Genes Dev.* 1995;9(9):1033–1045.

4. Song C, Kokontis JM, Hiipakka RA, Liao S**.** Ubiquitous receptor: a receptor that modulates gene activation by retinoic acid and thyroid hormone receptors. *Proc. Natl. Acad. Sci. U. S. A.* 1994;91(23):10809–13.

5. Staels B, Chinetti G, Lestavel S, Bocher V, Remaley AT, Neve B, Torra IP, Teissier E, Minnich A, Jaye M, Duverger N, Brewer HB, Fruchart J-C, Clavey V**.** PPAR-alpha and PPAR-gamma activators induce cholesterol removal from human macrophage foam cells through stimulation of the ABCA1 pathway. *Nat. Med.* 2001;7(1):53–58.

6. Chawla A, Boisvert WA, Lee C-H, Laffitte BA, Barak Y, Joseph SB, Liao D, Nagy L, Edwards PA, Curtiss LK, Evans RM, Tontonoz P**.** A PPARγ-LXR-ABCA1 Pathway in Macrophages Is Involved in Cholesterol Efflux and Atherogenesis. *Mol. Cell* 2001;7(1):161–171.

7. Juvet LK, Andresen SM, Schuster GU, Dalen KT, Tobin KAR, Hollung K, Haugen F, Jacinto S, Ulven SM, Bamberg K, Gustafsson J-Å, Nebb HI**.** On the Role of Liver X Receptors in Lipid Accumulation in Adipocytes. *Mol. Endocrinol.* 2003;17(2):172–182.

8. Tobin KA, Steineger HH, Alberti S, Spydevold O, Auwerx J, Gustafsson JA, Nebb HI**.** Cross-talk between fatty acid and cholesterol metabolism mediated by liver X receptor-alpha. *Mol. Endocrinol.* 2000;14(5):741–52.

9. Ulven SM, Dalen KT, Gustafsson J-Å, Nebb HI**.** Tissue-specific autoregulation of the LXRα gene facilitates induction of apoE in mouse adipose tissue. *J. Lipid Res.* 2004;45(11):2052–62.

10. Laffitte BA, Joseph SB, Walczak R, Pei L, Wilpitz DC, Collins JL, Tontonoz P**.** Autoregulation of the Human Liver X Receptor alpha Promoter. *Mol. Cell. Biol.* 2001;21(22):7558–7568.

11. Janowski BA, Willy PJ, Devi TR, Falck JR, Mangelsdorf DJ**.** An oxysterol signalling pathway mediated by the nuclear receptor LXR alpha. *Nature* 1996;383(6602):728–31.

12. Varga G, Su C**.** Classification and Predictive Modeling of Liver X Receptor Response Elements. *BioDrugs* 2007;21(2):117–124.

13. Willy PJ, Mangelsdorf DJ**.** Unique requirements for retinoid-dependent transcriptional activation by the orphan receptor LXR. *Genes Dev.*

1997;11(3):289–98.

14. Zhu H, Wang G, Qian J**.** Transcription factors as readers and effectors of DNA methylation. *Nat. Rev. Genet.* 2016;17(9):551–565.

15. Petty E, Pillus L**.** Balancing chromatin remodeling and histone modifications in transcription. *Trends Genet.* 2013;29(11):621–629.

16. Hörlein AJ, Näär AM, Heinzel T, Torchia J, Gloss B, Kurokawa R, Ryan A, Kamei Y, Söderström M, Glass CK, Rosenfeld MG**.** Ligand-independent repression by the thyroid hormone receptor mediated by a nuclear receptor co-repressor. *Nature* 1995;377(6548):397–404.

17. Chen JD, Evans RM**.** A transcriptional co-repressor that interacts with nuclear hormone receptors. *Nature* 1995;377(6548):454–457.

18. Hu X, Li S, Wu J, Xia C, Lala DS**.** Liver X Receptors Interact with Corepressors to Regulate Gene Expression. *Mol. Endocrinol.* 2003;17(6):1019–1026.

19. Delcuve GP, Khan DH, Davie JR, Rogers M, Lichter P, Pscherer A, Schnölzer M, Martinez E, Wong J, Rasko J, Rokhsar D, Degnan B, Mattick J, Hughes T, Strahl B, Grunstein M, Greenblatt J, Buratowski S, Krogan N, Hiebert S, Kruse U, Neubauer G, Ramsden N, Drewes G**.** Roles of histone deacetylases in epigenetic regulation: emerging paradigms from studies with inhibitors. *Clin. Epigenetics* 2012;4(1):5.

20. Heinzel T, Lavinsky RM, Mullen TM, Söderstrom M, Laherty CD, Torchia J, Yang WM, Brard G, Ngo SD, Davie JR, Seto E, Eisenman RN, Rose DW, Glass CK, Rosenfeld MG**.** A complex containing N-CoR, mSin3 and histone deacetylase mediates transcriptional repression. *Nature* 1997;387(6628):43–8.

21. Nagy L, Kao HY, Chakravarti D, Lin RJ, Hassig CA, Ayer DE, Schreiber SL, Evans RM**.** Nuclear receptor repression mediated by a complex containing SMRT, mSin3A, and histone deacetylase. *Cell* 1997;89(3):373–80.

22. Wen Y-D, Perissi V, Staszewski LM, Yang W-M, Krones A, Glass CK, Rosenfeld MG, Seto E**.** The histone deacetylase-3 complex contains nuclear receptor corepressors. *Proc Natl Acad Sci U S A.* 2000;97(13):7202–7.

23. Guenther MG, Lane WS, Fischle W, Verdin E, Lazar MA, Shiekhattar R**.** A core SMRT corepressor complex containing HDAC3 and TBL1, a WD40-repeat protein linked to deafness. *Genes Dev.* 2000;14(9):1048–1057.

24. Parker MG, Heery DM, Kalkhoven E, Hoare S**.** A signature motif in transcriptional co-activators mediates binding to nuclear receptors. *Nature* 1997;387(6634):733–736.

25. McKenna NJ, O'Malley BW**.** Combinatorial control of gene expression by nuclear receptors and coregulators. *Cell* 2002;108(4):465–74.

26. Zhang J, Guenther MG, Carthew RW, Lazar MA**.** Proteasomal regulation of nuclear receptor corepressor-mediated repression. *Genes Dev.* 1998;12(12):1775–80.

27. Perissi V, Aggarwal A, Glass CK, Rose DW, Rosenfeld MG**.** A corepressor/coactivator exchange complex required for transcriptional activation by nuclear receptors and other regulated transcription factors. *Cell* 2004;116(4):511–26.

28. Frasor J, Danes JM, Funk CC, Katzenellenbogen BS**.** Estrogen down-regulation of the corepressor N-CoR: mechanism and implications for estrogen derepression of N-CoR-regulated genes. *Proc. Natl. Acad. Sci. U. S. A.* 2005;102(37):13153–7.

29. Li J, Wang J, Wang J, Nawaz Z, Liu JM, Qin J, Wong J**.** Both corepressor proteins SMRT and N-CoR exist in large protein complexes containing HDAC3. *EMBO J.* 2000;19(16):4342–50.

30. Guenther MG, Lane WS, Fischle W, Verdin E, Lazar MA, Shiekhattar R**.** A core SMRT corepressor complex containing HDAC3 and TBL1, a WD40-repeat protein linked to deafness. *Genes Dev.* 2000;14(9):1048–57.

31. Yoon H-G, Chan DW, Huang Z-Q, Li J, Fondell JD, Qin J, Wong J**.** Purification and functional characterization of the human N-CoR complex: the roles of HDAC3, TBL1 and TBLR1. *EMBO J.* 2003;22(6):1336–46.

32. Joseph SB, Castrillo A, Laffitte BA, Mangelsdorf DJ, Tontonoz P**.** Reciprocal regulation of inflammation and lipid metabolism by liver X receptors. *Nat. Med.* 2003;9(2):213–219.

33. Ogawa S, Lozach J, Benner C, Pascual G, Tangirala RK, Westin S, Hoffmann A, Subramaniam S, David M, Rosenfeld MG, Glass CK**.** Molecular determinants of crosstalk between nuclear receptors and toll-like receptors. *Cell* 2005;122(5):707–21.

34. Ogawa D, Stone JF, Takata Y, Blaschke F, Chu VH, Towler DA, Law RE, Hsueh WA, Bruemmer D**.** Liver X Receptor Agonists Inhibit Cytokine-Induced Osteopontin Expression in Macrophages Through Interference With Activator Protein-1 Signaling Pathways. *Circ. Res.* 2005;96(7):e59–e67.

35. Ghisletti S, Huang W, Ogawa S, Pascual G, Lin M-EE, Willson TM, Rosenfeld MG, Glass CK**.** Parallel SUMOylation-Dependent Pathways Mediate Gene- and Signal-Specific Transrepression by LXRs and PPARgamma. *Mol. Cell* 2007;25(1):57–70.

36. Watanabe Y, Tanaka T, Uchiyama Y, Takeno T, Izumi A, Yamashita H, Kumakura J, Iwanari H, Shu-Ying J, Naito M, Mangelsdorf DJ, Hamakubo T, Kodama T**.** Establishment of a monoclonal antibody for human LXRalpha: Detection of LXRalpha protein expression in human macrophages. *Nucl. Recept.* 2003;1(1):1.

37. Prüfer K, Boudreaux J**.** Nuclear localization of liver X receptor α and β is differentially regulated. *J. Cell. Biochem.* 2007;100(1):69–85.

38. Mo J, Fang SJ, Chen W, Blobe GC**.** Regulation of ALK-1 signaling by the nuclear receptor LXRbeta. *J. Biol. Chem.* 2002;277(52):50788–94.

39. Hozoji M, Munehira Y, Ikeda Y, Makishima M, Matsuo M, Kioka N, Ueda K**.** Direct Interaction of Nuclear Liver X Receptor-β with ABCA1 Modulates Cholesterol Efflux. *J. Biol. Chem.* 2008;283(44):30057–30063.

40. Repa J, Kissling G, Fieselman K, Jayes F, Gerrish K, Korach K, Umetani M**.** LXRβ/estrogen receptor-α signaling in lipid rafts preserves endothelial integrity. *Science.* 2013;289(5484):1524–1529.

41. Courtaut F, Derangère V, Chevriaux A, Ladoire S, Cotte AK, Arnould L, Boidot R, Rialland M, Ghiringhelli F, Rébé C**.** Liver X receptor ligand cytotoxicity in

colon cancer cells and not in normal colon epithelial cells depends on LXRβ subcellular localization. *Oncotarget* 2015;6(29):26651–62.

42. Willy PJ, Umesono K, Ong ES, Evans RM, Heyman R a., Mangelsdorf DJ**.** LXR, a nuclear receptor that defines a distinct retinoid response pathway. *Genes Dev.* 1995;9(9):1033–1045.

43. Janowski BA, Grogan MJ, Jones SA, Wisely GB, Kliewer SA, Corey EJ, Mangelsdorf DJ**.** Structural requirements of ligands for the oxysterol liver X receptors LXRalpha and LXRbeta. *Proc. Natl. Acad. Sci. U. S. A.* 1999;96(1):266–71.

44. Lehmann JM, Kliewer SA, Moore LB, Smith-Oliver TA, Oliver BB, Su JL, Sundseth SS, Winegar DA, Blanchard DE, Spencer TA, Willson TM**.** Activation of the nuclear receptor LXR by oxysterols defines a new hormone response pathway. *J. Biol. Chem.* 1997;272(6):3137–3140.

45. Spencer TA, Li D, Russel JS, Collins JL, Bledsoe RK, Consler TG, Moore LB, Galardi CM, McKee DD, Moore JT, Watson MA, Parks DJ, Lambert MH, Willson TM**.** Pharmacophore analysis of the nuclear oxysterol receptor LXRalpha. *J. Med. Chem.* 2001;44(6):886–97.

46. Chen W, Chen G, Head DL, Mangelsdorf DJ, Russell DW**.** Enzymatic reduction of oxysterols impairs LXR signaling in cultured cells and the livers of mice. *Cell Metab.* 2007;5(1):73–9.

47. Wong J, Quinn CM, Gelissen IC, Brown AJ**.** Endogenous 24(S),25-epoxycholesterol fine-tunes acute control of cellular cholesterol homeostasis. *J. Biol. Chem.* 2008;283(2):700–7.

48. Spencer TA, Gayen AK, Phirwa S, Nelson JA, Taylor FR, Kandutsch AA, Erickson SK**.** 24(S),25-Epoxycholesterol. Evidence consistent with a role in the regulation of hepatic cholesterogenesis. *J. Biol. Chem.* 1985;260(25):13391–4.

49. Nelson JA, Steckbeck SR, Spencer TA**.** Biosynthesis of 24,25-epoxycholesterol from squalene 2,3;22,23-dioxide. *J. Biol. Chem.* 1981;256(3):1067–8.

50. Yang C, Yu L, Li W, Xu F, Cohen JC, Hobbs HH**.** Disruption of cholesterol homeostasis by plant sterols. *J. Clin. Invest.* 2004;114(6):813–822.

51. Yang C, McDonald JG, Patel A, Zhang Y, Umetani M, Xu F, Westover EJ, Covey DF, Mangelsdorf DJ, Cohen JC, Hobbs HH**.** Sterol intermediates from cholesterol biosynthetic pathway as liver X receptor ligands. *J. Biol. Chem.* 2006;281(38):27816–27826.

52. Spann NJ, Garmire LX, McDonald JG, Myers DS, Milne SB, Shibata N, Reichart D, Fox JN, Shaked I, Heudobler D, Raetz CRH, Wang EW, Kelly SL, Sullards MC, Murphy RC, Merrill AH, Brown HA, Dennis EA, Li AC, Ley K, Tsimikas S, Fahy E, Subramaniam S, Quehenberger O, Russell DW, Glass CK**.** Regulated accumulation of desmosterol integrates macrophage lipid metabolism and inflammatory responses. *Cell* 2012;151(1):138–52.

53. Mitro N, Mak PA, Vargas L, Godio C, Hampton E, Molteni V, Kreusch A, Saez E**.** The nuclear receptor LXR is a glucose sensor. *Nature* 2007;445(7124):219–223.

54. Anthonisen EH, Berven L, Holm S, Nygård M, Nebb HI, Grønning-Wang LM**.** Nuclear receptor liver X receptor is O-GlcNAc-modified in response to glucose. *J. Biol. Chem.* 2010;285(3):1607–1615.

55. Adams CM, Reitz J, De Brabander JK, Feramisco JD, Li L, Brown MS, Goldstein JL**.** Cholesterol and 25-hydroxycholesterol inhibit activation of SREBPs by different mechanisms, both involving SCAP and Insigs. *J. Biol. Chem.* 2004;279(50):52772–80.

56. Fu X, Menke JG, Chen Y, Zhou G, MacNaul KL, Wright SD, Sparrow CP, Lund EG**.** 27-hydroxycholesterol is an endogenous ligand for liver X receptor in cholesterol-loaded cells. *J. Biol. Chem.* 2001;276(42):38378–87.

57. Ou J, Tu H, Shan B, Luk A, DeBose-Boyd, R. A Bashmakov Y, Goldstein JL, Brown MS**.** Unsaturated fatty acids inhibit transcription of the sterol regulatory element-binding protein-1c (SREBP-1c) gene by antagonizing ligand-dependent activation of the LXR. *Proc. Natl. Acad. Sci. U. S. A.* 2001;98(11):6027–6032.

58. Yoshikawa T, Shimano H, Yahagi N, Ide T, Amemiya-Kudo M, Matsuzaka T, Nakakuki M, Tomita S, Okazaki H, Tamura Y, Iizuka Y, Ohashi K, Takahashi A, Sone H, Osuga J, Gotoda T, Ishibashi S, Yamada N**.** Polyunsaturated Fatty Acids Suppress Sterol Regulatory Element-binding Protein 1c Promoter Activity by Inhibition of Liver X Receptor (LXR) Binding to LXR Response Elements. *J. Biol. Chem.* 2002;277(3):1705–1711.

59. Forman BM, Ruan B, Chen J, Schroepfer GJ, Evans RM**.** The orphan nuclear receptor LXRa is positively and negatively regulated by distinct products of mevalonate metabolism. *Biochemistry* 1997;94(20):10588–10593.

60. Yeh Y-S, Goto T, Takahashi N, Egawa K, Takahashi H, Jheng H-F, Kim Y-I, Kawada T**.** Geranylgeranyl pyrophosphate performs as an endogenous regulator of adipocyte function via suppressing the LXR pathway. *Biochem. Biophys. Res. Commun.* 2016;478(3):1317–1322.

61. Schultz JR, Tu H, Luk A, Repa JJ, Medina JC, Li L, Schwendner S, Wang S, Thoolen M, Mangelsdorf DJ, Lustig KD, Shan B**.** Role of LXRs in control of lipogenesis. *Genes Dev.* 2000;14(22):2831–2838.

62. Collins JL, Binz JG, Plunket KD, Morgan DG, Beaudet EJ, Whitney KD, Kliewer SA, Willson TM, Fivush AM, Watson MA, Galardi CM, Lewis MC, Moore LB, Parks DJ, Wilson JG, Tippin TK**.** Identification of a nonsteroidal liver X receptor agonist through parallel array synthesis of tertiary amines. *J. Med. Chem.* 2002;45(10):1963–1966.

63. Houck KA, Borchert KM, Hepler CD, Thomas JS, Bramlett KS, Michael LF, Burris TP**.** T0901317 is a dual LXR/FXR agonist. *Mol. Genet. Metab.* 2004;83(1):184–187.

64. Mitro N, Vargas L, Romeo R, Koder A, Saez E**.** T0901317 is a potent PXR ligand: Implications for the biology ascribed to LXR. *FEBS Lett.* 2007;581(9):1721–1726.

65. Joseph SB, McKilligin E, Pei L, Watson MA, Collins AR, Laffitte BA, Chen M, Noh G, Goodman J, Hagger GN, Tran J, Tippin TK, Wang X, Lusis AJ, Hsueh WA, Law RE, Collins JL, Willson TM, Tontonoz P**.** Synthetic LXR ligand inhibits the development of atherosclerosis in mice. *Proc. Natl. Acad. Sci. U. S. A.* 2002;99(11):7604–9.

66. Terasaka N, Hiroshima A, Koieyama T, Ubukata N, Morikawa Y, Nakai D, Inaba T**.** T-0901317, a synthetic liver X receptor ligand, inhibits development of atherosclerosis in LDL receptor-deficient mice. *FEBS Lett.* 2003;536(1–3):6–11.

67. Yasuda T, Grillot D, Billheimer JT, Briand F, Delerive P, Huet S, Rader DJ**.** Tissue-Specific Liver X Receptor Activation Promotes Macrophage Reverse Cholesterol Transport In Vivo. *Arterioscler. Thromb. Vasc. Biol.* 2010;30(4):781–6.

68. Kratzer A, Buchebner M, Pfeifer T, Becker TM, Uray G, Miyazaki M, Miyazaki-Anzai S, Ebner B, Chandak PG, Kadam RS, Calayir E, Rathke N, Ahammer H, Radovic B, Trauner M, Hoefler G, Kompella UB, Fauler G, Levi M, Levak-Frank S, Kostner GM, Kratky D**.** Synthetic LXR agonist attenuates plaque formation in apoE-/- mice without inducing liver steatosis and hypertriglyceridemia. *J. Lipid Res.* 2008;50(2):312–326.

69. Chao EY, Caravella JA, Watson MA, Campobasso N, Ghisletti S, Billin AN, Galardi C, Wang P, Laffitte BA, Iannone MA, Goodwin BJ, Nichols JA, Parks DJ, Stewart E, Wiethe RW, Williams SP, Smallwood A, Pearce KH, Glass CK, Willson TM, Zuercher WJ, Collins JL**.** Structure-guided design of N-phenyl tertiary amines as transrepression-selective liver X receptor modulators with anti-inflammatory activity. *J. Med. Chem.* 2008;51(18):5758–65.

70. Kaneko E, Matsuda M, Yamada Y, Tachibana Y, Shimomura I, Makishima M**.** Induction of intestinal ATP-binding cassette transporters by a phytosterol-derived liver X receptor agonist. *J. Biol. Chem.* 2003;278(38):36091–8.

71. Zuercher WJ, Buckholz RG, Campobasso N, Collins JL, Galardi CM, Gampe RT, Hyatt SM, Merrihew SL, Moore JT, Oplinger JA, Reid PR, Spearing PK, Stanley TB, Stewart EL, Willson TM**.** Discovery of tertiary sulfonamides as potent liver X receptor antagonists. *J. Med. Chem.* 2010;53(8):3412–6.

72. Griffett K, Solt LA, El-Gendy BE-DM, Kamenecka TM, Burris TP**.** A Liver-Selective LXR Inverse Agonist That Suppresses Hepatic Steatosis. *ACS Chem. Biol.* 2013;8(3):559–567.

73. Song C, Hiipakka RA, Liao S**.** Auto-oxidized cholesterol sulfates are antagonistic ligands of liver X receptors: implications for the development and treatment of atherosclerosis. *Steroids* 2001;66(6):473–479.

74. Griffett K, Burris TP**.** Promiscuous activity of the LXR antagonist GSK2033 in a mouse model of fatty liver disease. *Biochem. Biophys. Res. Commun.* 2016;479(3):424–428.

75. Griffett K, Welch RD, Flaveny CA, Kolar GR, Neuschwander-Tetri BA, Burris TP**.** The LXR inverse agonist SR9238 suppresses fibrosis in a model of non-alcoholic steatohepatitis. *Mol. Metab.* 2015;4(4):353–357.

76. Brown MS, Goldstein JL**.** Suppression of 3-hydroxy-3-methylglutaryl coenzyme A reductase activity and inhibition of growth of human fibroblasts by 7-ketocholesterol. *J. Biol. Chem.* 1974;249(22):7306–14.

77. Bensinger SJ, Bradley MN, Joseph SB, Zelcer N, Janssen EM, Hausner MA, Shih R, Parks JS, Edwards PA, Jamieson BD, Tontonoz P**.** LXR Signaling Couples Sterol Metabolism to Proliferation in the Acquired Immune Response. *Cell* 2008;134(1):97–111.

78. Abifadel M, Varret M, Rabès J-P, Allard D, Ouguerram K, Devillers M, Cruaud C, Benjannet S, Wickham L, Erlich D, Derré A, Villéger L, Farnier M, Beucler I, Bruckert E, Chambaz J, Chanu B, Lecerf J-M, Luc G, Moulin P, Weissenbach J, Prat A, Krempf M, Junien C, Seidah NG, Boileau C**.** Mutations in PCSK9 cause autosomal dominant hypercholesterolemia. *Nat. Genet.* 2003;34(2):154–156.

79. Sturek JM, Castle JD, Trace AP, Page LC, Castle AM, Evans-Molina C, Parks JS, Mirmira RG, Hedrick CC**.** An intracellular role for ABCG1-mediated cholesterol transport in the regulated secretory pathway of mouse pancreatic β cells. *J. Clin. Invest.* 2010;120(7):2575–2589.

80. Dietschy JM, Turley SD**.** Control of cholesterol turnover in the mouse. *J. Biol. Chem.* 2002;277(6):3801–4.

81. Dietschy JM, Spady DK**.** Measurement of rates of cholesterol synthesis using tritiated water. *J Lipid Res.* 1984;25(13):1469–76.

82. Berg JM, Tymoczko JL, Stryer L**.** Cholesterol Is Synthesized from Acetyl Coenzyme A in Three Stages. In: *Biochemistry*. 5th ed. W H Freeman; 2002.

83. Endo A, Tsujita Y, Kuroda M, Tanzawa K**.** Inhibition of cholesterol synthesis in vitro and in vivo by ML-236A and ML-236B, competitive inhibitors of 3-hydroxy-3-methylglutaryl-coenzyme A reductase. *Eur. J. Biochem.* 1977;77(1):31–6.

84. Kandutsch A, Russell A**.** Preputial gland tumor sterols. 3. A metabolic pathway from lanosterol to cholesterol. *J. Biol. Chem.* 1960;235(Aug):2256–61.

85. Woollett LA, Wang Y, Buckley DD, Yao L, Chin S, Granholm N, Jones PJH, Setchell KDR, Tso P, Heubi JE**.** Micellar solubilisation of cholesterol is essential for absorption in humans. *Gut* 2006;55(2):197–204.

86. Altmann SW, Davis HR, Zhu L-J, Yao X, Hoos LM, Tetzloff G, Iyer SPN, Maguire M, Golovko A, Zeng M, Wang L, Murgolo N, Graziano MP**.** Niemann-Pick C1 Like 1 Protein Is Critical for Intestinal Cholesterol Absorption. *Science (80-.).* 2004;303(5661):1201–1204.

87. Ge L, Wang J, Qi W, Miao H-H, Cao J, Qu Y-X, Li B-L, Song B-L**.** The Cholesterol Absorption Inhibitor Ezetimibe Acts by Blocking the Sterol-Induced Internalization of NPC1L1. *Cell Metab.* 2008;7(6):508–519.

88. Knopp RH, Gitter H, Truitt T, Bays H, Manion C V, Lipka LJ, LeBeaut AP, Suresh R, Yang B, Veltri EP, Ezetimibe Study Group**.** Effects of ezetimibe, a new cholesterol absorption inhibitor, on plasma lipids in patients with primary hypercholesterolemia. *Eur. Heart J.* 2003;24(8):729–41.

89. Klett EL, Lee M-H, Adams DB, Chavin KD, Patel SB**.** Localization of ABCG5 and ABCG8 proteins in human liver, gall bladder and intestine. *BMC Gastroenterol.* 2004;4:21.

90. Sane AT, Sinnett D, Delvin E, Bendayan M, Marcil V, Ménard D, Beaulieu J-F, Levy E**.** Localization and role of NPC1L1 in cholesterol absorption in human intestine. *J. Lipid Res.* 2006;47(10):2112–2120.

91. Yu L, Hammer RE, Li-Hawkins J, Von Bergmann K, Lutjohann D, Cohen JC, Hobbs HH**.** Disruption of Abcg5 and Abcg8 in mice reveals their crucial role in biliary cholesterol secretion. *Proc. Natl. Acad. Sci. U. S. A.* 2002;99(25):16237–42.

92. Groen AK, Bloks VW, Bandsma RH, Ottenhoff R, Chimini G, Kuipers F**.** Hepatobiliary cholesterol transport is not impaired in Abca1-null mice lacking HDL. *J. Clin. Invest.* 2001;108(6):843–50.

93. Siperstein MD, Murray AW**.** Cholesterol metabolism in man. *J. Clin. Invest.* 1955;34(9):1449–1453.

94. Bhattacharyya AK, Connor WE, Spector AA**.** Excretion of sterols from the skin of normal and hypercholesterolemic humans. Implications for sterol balance studies. *J. Clin. Invest.* 1972;51(8):2060–70.

95. Schwartz CC, Halloran LG, Vlahcevic ZR, Gregory DH, Swell L**.** Preferential utilization of free cholesterol from high-density lipoproteins for biliary cholesterol secretion in man. *Science* 1978;200(4337):62–4.

96. Remaley AT, Schumacher UK, Stonik JA, Farsi BD, Nazih H, Brewer HB**.** Decreased Reverse Cholesterol Transport from Tangier Disease Fibroblasts : Acceptor Specificity and Effect of Brefeldin on Lipid Efflux. *Arterioscler. Thromb. Vasc. Biol.* 1997;17(9):1813–1821.

97. Bortnick AE, Rothblat GH, Stoudt G, Hoppe KL, Royer LJ, McNeish J, Francone OL**.** The correlation of ATP-binding cassette 1 mRNA levels with cholesterol efflux from various cell lines. *J. Biol. Chem.* 2000;275(37):28634–40.

98. Klucken J, Büchler C, Orsó E, Kaminski WE, Porsch-Ozcürümez M, Liebisch G, Kapinsky M, Diederich W, Drobnik W, Dean M, Allikmets R, Schmitz G**.** ABCG1 (ABC8), the human homolog of the Drosophila white gene, is a regulator of macrophage cholesterol and phospholipid transport. *Proc. Natl. Acad. Sci. U. S. A.* 2000;97(2):817–22.

99. Francis GA, Knopp RH, Oram JF**.** Defective removal of cellular cholesterol and phospholipids by apolipoprotein A-I in Tangier Disease. *J. Clin. Invest.* 1995;96(1):78–87.

100. Truong TQ, Falstrault L, Tremblay C, Brissette L**.** Low density lipoprotein-receptor plays a major role in the binding of very low density lipoproteins and their remnants on HepG2 cells. *Int. J. Biochem. Cell Biol.* 1999;31(6):695–705.

101. Acton S, Rigotti A, Landschulz KT, Xu S, Hobbs HH, Krieger M**.** Identification of scavenger receptor SR-BI as a high density lipoprotein receptor. *Science* 1996;271(5248):518–20.

102. Coleman R, Rahman K, Kan KS, Parslow RA**.** Retrograde intrabiliary injection of amphipathic materials causes phospholipid secretion into bile. Taurocholate causes phosphatidylcholine secretion, 3-[(3-cholamidopropyl)dimethylammonio]-propane-1-sulphonate (CHAPS) causes mixed phospholipid secretion. *Biochem. J.* 1989;258(1):17–22.

103. Stieger B**.** Role of the bile salt export pump, BSEP, in acquired forms of cholestasis. *Drug Metab. Rev.* 2010;42(3):437–445.

104. Wang R, Salem M, Yousef IM, Tuchweber B, Lam P, Childs SJ, Helgason CD, Ackerley C, Phillips MJ, Ling V**.** Targeted inactivation of sister of P-glycoprotein gene (spgp) in mice results in nonprogressive but persistent intrahepatic cholestasis. *Proc. Natl. Acad. Sci.* 2001;98(4):2011–2016.

105. Wang R, Chen H-L, Liu L, Sheps JA, Phillips MJ, Ling V**.** Compensatory role of P-glycoproteins in knockout mice lacking the bile salt export pump. *Hepatology* 2009;50(3):948–956.

106. Peet DJ, Turley SD, Ma W, Janowski BA, Lobaccaro JMA, Hammer RE, Mangelsdorf DJ**.** Cholesterol and bile acid metabolism are impaired in mice lacking the nuclear oxysterol receptor LXRalpha. *Cell* 1998;93(5):693–704.

107. Alberti S, Schuster G, Parini P, Feltkamp D, Diczfalusy U, Rudling M, Angelin B,

Björkhem I, Pettersson S, Gustafsson J**.** Hepatic cholesterol metabolism and resistance to dietary cholesterol in LXRβ-deficient mice. *J. Clin. Invest.* 2001;107(5):565–573.

108. Wang L, Schuster GU, Hultenby K, Zhang Q, Andersson S, Gustafsson J-A**.** Liver X receptors in the central nervous system: from lipid homeostasis to neuronal degeneration. *Proc. Natl. Acad. Sci. U. S. A.* 2002;99(21):13878–83.

109. Stanley MM, Pineda EP, Cheng SH**.** Serum Cholesterol Esters and Intestinal Cholesterol Secretion and Absorption in Obstructive Jaundice Due to Cancer. *N. Engl. J. Med.* 1959;261(8):368–373.

110. Kruit JK, Plösch T, Havinga R, Boverhof R, Groot PHE, Groen AK, Kuipers F**.** Increased fecal neutral sterol loss upon liver X receptor activation is independent of biliary sterol secretion in mice. *Gastroenterology* 2005;128(1):147–56.

111. van der Velde AE, Vrins CLJ, van den Oever K, Kunne C, Oude Elferink RPJ, Kuipers F, Groen AK**.** Direct intestinal cholesterol secretion contributes significantly to total fecal neutral sterol excretion in mice. *Gastroenterology* 2007;133(3):967–975.

112. van der Veen JN, van Dijk TH, Vrins CLJ, van Meer H, Havinga R, Bijsterveld K, Tietge UJF, Groen AK, Kuipers F**.** Activation of the liver X receptor stimulates trans-intestinal excretion of plasma cholesterol. *J. Biol. Chem.* 2009;284(29):19211–9.

113. Vrins CLJ, van der Velde AE, van den Oever K, Levels JHM, Huet S, Oude Elferink RPJ, Kuipers F, Groen AK**.** Peroxisome proliferator-activated receptor delta activation leads to increased transintestinal cholesterol efflux. *J. Lipid Res.* 2009;50(10):2046–54.

114. Naik SU, Wang X, Da Silva JS, Jaye M, Macphee CH, Reilly MP, Billheimer JT, Rothblat GH, Rader DJ**.** Pharmacological Activation of Liver X Receptors Promotes Reverse Cholesterol Transport In Vivo. *Circulation* 2005;113(1):90–97.

115. Lo Sasso G, Murzilli S, Salvatore L, D'Errico I, Petruzzelli M, Conca P, Jiang Z-Y, Calabresi L, Parini P, Moschetta A**.** Intestinal Specific LXR Activation Stimulates Reverse Cholesterol Transport and Protects from Atherosclerosis. *Cell Metab.* 2010;12(2):187–193.

116. Repa JJ, Turley SD, Lobaccaro JA, Medina J, Li L, Lustig K, Shan B, Heyman RA, Dietschy JM, Mangelsdorf DJ, Repa JJ, Turley SD, Lobaccaro JA, Medina J, Li L, Lustig K, Shan B, Heyman RA, Dietschy JM MD**.** Regulation of Absorption and ABC1-Mediated Efflux of Cholesterol by RXR Heterodimers. *Science (80-.).* 2000;289(5484):1524–1529.

117. Venkateswaran A, Repa JJ, Lobaccaro JMA, Bronson A, Mangelsdorf DJ, Edwards PA**.** Human white/murine ABC8 mRNA levels are highly induced in lipid-loaded macrophages. A transcriptional role for specific oxysterols. *J. Biol. Chem.* 2000;275(19):14700–14707.

118. Repa JJ, Berge KE, Pomajzl C, Richardson JA, Hobbs H, Mangelsdorf DJ**.** Regulation of ATP-binding cassette sterol transporters ABCG5 and ABCG8 by the liver X receptors alpha and beta. *J. Biol. Chem.* 2002;277(21):18793–18800.

119. Breevoort SR, Angdisen J, Schulman IG**.** Macrophage-Independent Regulation of Reverse Cholesterol Transport by Liver X ReceptorsSignificance. *Arterioscler.*

Thromb. Vasc. Biol. 2014;34(8):1650–60.

120. Brownsey RW, Boone AN, Elliott JE, Kulpa JE, Lee WM**.** Regulation of acetyl-CoA carboxylase. *Biochem. Soc. Trans.* 2006;34(2):223.

121. Wakil SJ**.** Fatty acid synthase, a proficient multifunctional enzyme. *Biochemistry* 1989;28(11):4523–30.

122. Matsuzaka T, Shimano H, Yahagi N, Kato T, Atsumi A, Yamamoto T, Inoue N, Ishikawa M, Okada S, Ishigaki N, Iwasaki H, Iwasaki Y, Karasawa T, Kumadaki S, Matsui T, Sekiya M, Ohashi K, Hasty AH, Nakagawa Y, Takahashi A, Suzuki H, Yatoh S, Sone H, Toyoshima H, Osuga J, Yamada N**.** Crucial role of a long-chain fatty acid elongase, Elovl6, in obesity-induced insulin resistance. *Nat. Med.* 2007;13(10):1193–1202.

123. Scorletti E, Byrne CD**.** Omega-3 Fatty Acids, Hepatic Lipid Metabolism, and Nonalcoholic Fatty Liver Disease. *Annu. Rev. Nutr.* 2013;33(1):231–248.

124. Juárez-Hernández E, Chávez-Tapia NC, Uribe M, Barbero-Becerra VJ**.** Role of bioactive fatty acids in nonalcoholic fatty liver disease. *Nutr. J.* 2016;15(1):72.

125. Ntambi JM**.** Regulation of stearoyl-CoA desaturase by polyunsaturated fatty acids and cholesterol. *J. Lipid Res.* 1999;40(9):1549–58.

126. Ntambi JM**.** Dietary regulation of stearoyl-CoA desaturase 1 gene expression in mouse liver. *J. Biol. Chem.* 1992;267(15):10925–30.

127. Yen C-LE, Stone SJ, Koliwad S, Harris C, Farese R V, Jr. Thematic review series: glycerolipids. DGAT enzymes and triacylglycerol biosynthesis. *J. Lipid Res.* 2008;49(11):2283–301.

128. Repa JJ, Liang G, Ou J, Bashmakov Y, Lobaccaro JMA, Shimomura I, Shan B, Brown MS, Goldstein JL, Mangelsdorf DJ**.** Regulation of mouse sterol regulatory element-binding protein-1c gene (SREBP-1c) by oxysterol receptors, LXRalpha and LXRbeta. *Genes Dev.* 2000;14(22):2819–2830.

129. Chen G, Liang G, Ou J, Goldstein JL, Brown MS**.** Central role for liver X receptor in insulin-mediated activation of Srebp-1c transcription and stimulation of fatty acid synthesis in liver. *Proc. Natl. Acad. Sci. U. S. A.* 2004;101(31):11245–50.

130. Joseph SB, Laffitte BA, Patel PH, Watson MA, Matsukuma KE, Walczak R, Collins JL, Osborne TF, Tontonoz P**.** Direct and indirect mechanisms for regulation of fatty acid synthase gene expression by liver X receptors. *J. Biol. Chem.* 2002;277(13):11019–25.

131. Chu K, Miyazaki M, Man WC, Ntambi JM**.** Stearoyl-Coenzyme A Desaturase 1 Deficiency Protects against Hypertriglyceridemia and Increases Plasma High-Density Lipoprotein Cholesterol Induced by Liver X Receptor Activation. *Mol. Cell. Biol.* 2006;26(18):6786–6798.

132. Hagenfeldt L, Wahren J, Pernow B, Räf L**.** Uptake of individual free fatty acids by skeletal muscle and liver in man. *J. Clin. Invest.* 1972;51(9):2324–2330.

133. Lambert MS, Avella MA, Berhane Y, Shervill E, Botham KM**.** The fatty acid composition of chylomicron remnants influences their binding and internalization by isolated hepatocytes. *Eur. J. Biochem.* 2001;268(14):3983–92.

134. Hamilton JA, Johnson RA, Corkey B, Kamp F**.** Fatty Acid Transport: The

Diffusion Mechanism in Model and Biological Membranes. *J. Mol. Neurosci.* 2001;16(2–3):99–108.

135. Doege H, Baillie RA, Ortegon AM, Tsang B, Wu Q, Punreddy S, Hirsch D, Watson N, Gimeno RE, Stahl A, Foufelle F, Liu ZX, Dong J, Cline G, Stahl A, Lodish HF, Shulman GI**.** Targeted deletion of FATP5 reveals multiple functions in liver metabolism: alterations in hepatic lipid homeostasis. *Gastroenterology* 2006;130(4):1245–58.

136. Koonen DPY, Jacobs RL, Febbraio M, Young ME, Soltys C-LM, Ong H, Vance DE, Dyck JRB**.** Increased Hepatic CD36 Expression Contributes to Dyslipidemia Associated With Diet-Induced Obesity. *Diabetes* 2007;56(12):2863–71.

137. Zhou J, Febbraio M, Wada T, Zhai Y, Kuruba R, He J, Lee JH, Khadem S, Ren S, Li S, Silverstein RL, Xie W**.** Hepatic Fatty Acid Transporter Cd36 Is a Common Target of LXR, PXR, and PPARγ in Promoting Steatosis. *Gastroenterology* 2008;134(2):556–567.

138. Storch J, Thumser AE**.** Tissue-specific functions in the fatty acid-binding protein family. *J. Biol. Chem.* 2010;285(43):32679–83.

139. Newberry EP, Xie Y, Kennedy S, Han X, Buhman KK, Luo J, Gross RW, Davidson NO**.** Decreased Hepatic Triglyceride Accumulation and Altered Fatty Acid Uptake in Mice with Deletion of the Liver Fatty Acid-binding Protein Gene. *J. Biol. Chem.* 2003;278(51):51664–51672.

140. Newberry EP, Xie Y, Kennedy SM, Luo J, Davidson NO**.** Protection against Western diet-induced obesity and hepatic steatosis in liver fatty acid-binding protein knockout mice. *Hepatology* 2006;44(5):1191–1205.

141. Cao G, Liang Y, Broderick CL, Oldham BA, Beyer TP, Schmidt RJ, Zhang Y, Stayrook KR, Suen C, Otto KA, Miller AR, Dai J, Foxworthy P, Gao H, Ryan TP, Jiang X-C, Burris TP, Eacho PI, Etgen GJ**.** Antidiabetic Action of a Liver X Receptor Agonist Mediated By Inhibition of Hepatic Gluconeogenesis. *J. Biol. Chem.* 2003;278(2):1131–1136.

142. Laffitte BA, Chao LC, Li J, Walczak R, Hummasti S, Joseph SB, Castrillo A, Wilpitz DC, Mangelsdorf DJ, Collins JL, Saez E, Tontonoz P**.** Activation of liver X receptor improves glucose tolerance through coordinate regulation of glucose metabolism in liver and adipose tissue. *Proc. Natl. Acad. Sci. U. S. A.* 2003;100(9):5419–24.

143. Kalaany NY, Gauthier KC, Zavacki AM, Mammen PPA, Kitazume T, Peterson JA, Horton JD, Garry DJ, Bianco AC, Mangelsdorf DJ**.** LXRs regulate the balance between fat storage and oxidation. *Cell Metab.* 2005;1(4):231–244.

144. Beaven SW, Matveyenko A, Wroblewski K, Chao L, Wilpitz D, Hsu TW, Lentz J, Drew B, Hevener AL, Tontonoz P**.** Reciprocal Regulation of Hepatic and Adipose Lipogenesis by Liver X Receptors in Obesity and Insulin Resistance. *Cell Metab.* 2013;18(1):106–117.

145. Tangirala RK, Bischoff ED, Joseph SB, Wagner BL, Walczak R, Laffitte BA, Daige CL, Thomas D, Heyman RA, Mangelsdorf DJ, Wang X, Lusis AJ, Tontonoz P, Schulman IG**.** Identification of macrophage liver X receptors as inhibitors of atherosclerosis. *Proc. Natl. Acad. Sci. U. S. A.* 2002;99(18):11896–901.

146. Korf H, Vander Beken S, Romano M, Steffensen KR, Stijlemans B, Gustafsson

J-A, Grooten J, Huygen K**.** Liver X receptors contribute to the protective immune response against Mycobacterium tuberculosis in mice. *J. Clin. Invest.* 2009;119(6):1626–37.

147. Castrillo A, Joseph SB, Vaidya SA, Haberland M, Fogelman AM, Cheng G, Tontonoz P**.** Crosstalk between LXR and toll-like receptor signaling mediates bacterial and viral antagonism of cholesterol metabolism. *Mol. Cell* 2003;12(4):805–16.

148. Beyer C, Huang J, Beer J, Zhang Y, Palumbo-Zerr K, Zerr P, Distler A, Dees C, Maier C, Munoz L, Krönke G, Uderhardt S, Distler O, Jones S, Rose-John S, Oravecz T, Schett G, Distler JHW**.** Activation of liver X receptors inhibits experimental fibrosis by interfering with interleukin-6 release from macrophages. *Ann. Rheum. Dis.* 2014;74(6):1317–24.

149. Kurowska-Stolarska M, Hasoo MK, Welsh DJ, Stewart L, McIntyre D, Morton BE, Johnstone S, Miller AM, Asquith DL, Millar NL, Millar AB, Feghali-Bostwick CA, Hirani N, Crick PJ, Wang Y, Griffiths WJ, McInnes IB, McSharry C**.** The role of microRNA-155/liver X receptor pathway in experimental and idiopathic pulmonary fibrosis. *J. Allergy Clin. Immunol.* 2017;139(6):1946–1956.

150. Wouters K, van Bilsen M, van Gorp PJ, Bieghs V, Lütjohann D, Kerksiek A, Staels B, Hofker MH, Shiri-Sverdlov R**.** Intrahepatic cholesterol influences progression, inhibition and reversal of non-alcoholic steatohepatitis in hyperlipidemic mice. *FEBS Lett.* 2010;584(5):1001–5.

151. Beaven SW, Wroblewski K, Wang J, Hong C, Bensinger S, Tsukamoto H, Tontonoz P**.** Liver X Receptor Signaling Is a Determinant of Stellate Cell Activation and Susceptibility to Fibrotic Liver Disease. *Gastroenterology* 2011;140(3):1052–1062.

152. Griffett K, Solt L, El-Gendy B-D, Kamenecka T, Burris T**.** A liver-selective LXR inverse agonist that suppresses hepatic steatosis. *ACS Chem. Biol.* 2013;8(3):559–67.

153. Griffett K, Welch RD, Flaveny CA, Kolar GR, Neuschwander-Tetri BA, Burris TP**.** The LXR inverse agonist SR9238 suppresses fibrosis in a model of non-alcoholic steatohepatitis. *Mol. Metab.* 2015;4(4):353–357.

154. Verdone L, Caserta M, Di Mauro E**.** Role of histone acetylation in the control of gene expression. *Biochem Cell Biol* 2005;83(3):344–353.

155. Glozak MA, Sengupta N, Zhang X, Seto E**.** Acetylation and deacetylation of non-histone proteins. *Gene* 2005;363(1–2):15–23.

156. Li X, Zhang S, Blander G, Tse JG, Krieger M, Guarente L**.** SIRT1 Deacetylates and Positively Regulates the Nuclear Receptor LXR. *Mol. Cell* 2007;28(1):91–106.

157. Defour A, Dessalle K, Castro Perez A, Poyot T, Castells J, Gallot YS, Durand C, Euthine V, Gu Y, Béchet D, Peinnequin A, Lefai E, Freyssenet D**.** Sirtuin 1 Regulates SREBP-1c Expression in a LXR-Dependent Manner in Skeletal Muscle. *PLoS One* 2012;7(9):e43490.

158. Becares N, Gage MC, Pineda-Torra I**.** Posttranslational Modifications of Lipid-Activated Nuclear Receptors: Focus on Metabolism. *Endocrinology* 2016;158(2):213–225.

159. Hart GW, Housley MP, Slawson C**.** Cycling of O-linked beta-N-acetylglucosamine on nucleocytoplasmic proteins. *Nature* 2007;446(7139):1017–1022.

160. Love DC, Hanover JA**.** The hexosamine signaling pathway: deciphering the "O-GlcNAc code." *Sci STKE.* 2005;2005(312):re13.

161. Yang X, Ongusaha PP, Miles PD, Havstad JC, Zhang F, So WV, Kudlow JE, Michell RH, Olefsky JM, Field SJ, Evans RM**.** Phosphoinositide signalling links O-GlcNAc transferase to insulin resistance. *Nature* 2008;451(7181):964–969.

162. Manning G, Whyte DB, Martinez R, Hunter T SS**.** The protein kinase complement of the human genome. *Science (80-.).* 2002;298(5600):1912–34.

163. Torra IP, Ismaili N, Feig JE, Xu C-F, Cavasotto C, Pancratov R, Rogatsky I, Neubert TA, Fisher EA, Garabedian MJ**.** Phosphorylation of liver X receptor alpha selectively regulates target gene expression in macrophages. *Mol. Cell. Biol.* 2008;28(8):2626–2636.

164. Chen M, Bradley MN, Beaven SW, Tontonoz P**.** Phosphorylation of the liver X receptors. *FEBS Lett.* 2006;580(20):4835–4841.

165. Wu C, Hussein M, Shrestha E, Leone S, Aiyegbo MS, Lambert WM, Pourcet B, Cardozo T, Gustaffson J-A, Fisher EA, Pineda-Torra I, Garabedian MJ**.** Modulation of macrophage gene expression via LXRα serine 198 phosphorylation. *Mol. Cell. Biol.* 2015;35(11):2024–2034.

166. Yamamoto T, Shimano H, Inoue N, Nakagawa Y, Matsuzaka T, Takahashi A, Yahagi N, Sone H, Suzuki H, Toyoshima H YN**.** Protein Kinase A Suppresses Sterol Regulatory Element-binding Protein-1C Expression via Phosphorylation of Liver X Receptor in the Liver. *J Biol Chem.* 2007;282(16):11687–95.

167. Benson AB**.** Oltipraz: a laboratory and clinical review. *J. Cell. Biochem. Suppl.* 1993;17F:278–91.

168. Brooks SC, Brooks JS, Lee WH, Lee MG, Kim SG**.** Therapeutic potential of dithiolethiones for hepatic diseases. *Pharmacol. Ther.* 2009;124(1):31–43.

169. Hwahng SH, Ki SH, Bae EJ, Kim HE, Kim SG**.** Role of adenosine monophosphate-activated protein kinase-p70 ribosomal S6 kinase-1 pathway in repression of liver X receptor-alpha-dependent lipogenic gene induction and hepatic steatosis by a novel class of dithiolethiones. *Hepatology* 2009;49(6):1913–1925.

170. Cho K, Chung JY, Cho SK, Shin H-W, Jang I-J, Park J-W, Yu K-S, Cho J-Y**.** Antihyperglycemic mechanism of metformin occurs via the AMPK/LXRα/POMC pathway. *Sci. Rep.* 2015;5:8145.

171. Flotho A, Melchior F**.** Sumoylation: a regulatory protein modification in health and disease. *Annu. Rev. Biochem.* 2013;82:357–85.

172. Hay RT**.** SUMO: A history of modification. *Mol. Cell* 2005;18(1):1–12.

173. Ghisletti S, Huang W, Ogawa S, Pascual G, Lin ME, Willson TM, Rosenfeld MG, Glass CK**.** Parallel SUMOylation-Dependent Pathways Mediate Gene- and Signal-Specific Transrepression by LXRs and PPARgamma. *Mol. Cell* 2007;25(1):57–70.

174. Pascual G, Fong AL, Ogawa S, Gamliel A, Li AC, Perissi V, Rose DW, Willson TM, Rosenfeld MG, Glass CK**.** A SUMOylation-dependent pathway mediates transrepression of inflammatory response genes by PPAR-gamma. *Nature* 2005;437(7059):759–763.

175. Huang W, Ghisletti S, Saijo K, Gandhi M, Aouadi M, Tesz GJ, Zhang DX, Yao J, Czech MP, Goode BL, Rosenfeld MG, Glass CK**.** Coronin 2A mediates actin-dependent de-repression of inflammatory response genes. *Nature* 2011;470(7334):414–418.

176. Pascual-García M, Rué L, León T, Julve J, Carbó JM, Matalonga J, Auer H, Celada A, Escolà-Gil JC, Steffensen KR, Pérez-Navarro E, Valledor AF**.** Reciprocal negative cross-talk between liver X receptors (LXRs) and STAT1: effects on IFN-γ-induced inflammatory responses and LXR-dependent gene expression. *J. Immunol.* 2013;190(12):6520–32.

177. Ito A, Hong C, Rong X, Zhu X, Tarling EJ, Hedde PN, Gratton E, Parks J, Tontonoz P**.** LXRs link metabolism to inflammation through Abca1-dependent regulation of membrane composition and TLR signaling. *Elife* 2015;4:e08009.

178. Matteoni CA, Younossi ZM, Gramlich T, Boparai N, Liu YC, McCullough AJ**.** Nonalcoholic fatty liver disease: a spectrum of clinical and pathological severity. *Gastroenterology* 1999;116(6):1413–9.

179. Bellentani S, Scaglioni F, Marino M, Bedogni G**.** Epidemiology of Non-Alcoholic Fatty Liver Disease. *Dig. Dis.* 2010;28(1):155–161.

180. Neuschwander-Tetri BA CS**.** Nonalcoholic steatohepatitis: summary of an AASLD Single Topic Conference. *Hepatology* 2003;37(5):1202–19.

181. Perlemuter G, Sabile A, Letteron P, Vona G, Topilco A, Chrétien Y, Koike K, Pessayre D, Chapman J, Barba G, Bréchot C**.** Hepatitis C virus core protein inhibits microsomal triglyceride transfer protein activity and very low density lipoprotein secretion: a model of viral-related steatosis. *FASEB J.* 2002;16(2):185–194.

182. Koike K, Moriya K**.** Metabolic aspects of hepatitis C viral infection: steatohepatitis resembling but distinct from NASH. *J. Gastroenterol.* 2005;40(4):329–336.

183. Bruno S, Maisonneuve P, Castellana P, Rotmensz N, Rossi S, Maggioni M, Persico M, Colombo A, Monasterolo F, Casadei-Giunchi D, Desiderio F, Stroffolini T, Sacchini V, Decensi A, Veronesi U**.** Incidence and risk factors for non-alcoholic steatohepatitis: prospective study of 5408 women enrolled in Italian tamoxifen chemoprevention trial. *BMJ* 2005;330(7497):932.

184. Söderberg C, Stål P, Askling J, Glaumann H, Lindberg G, Marmur J, Hultcrantz R**.** Decreased survival of subjects with elevated liver function tests during a 28-year follow-up. *Hepatology* 2010;51(2):595–602.

185. Ekstedt M, Hagström H, Nasr P, Fredrikson M, Stål P, Kechagias S, Hultcrantz R**.** Fibrosis stage is the strongest predictor for disease-specific mortality in NAFLD after up to 33 years of follow-up. *Hepatology* 2015;61(5):1547–54.

186. Wanless IR, Lentz JS**.** Fatty liver hepatitis (steatohepatitis) and obesity: an autopsy study with analysis of risk factors. *Hepatology* 1990;12(5):1106–10.

187. Chang Y, Jung H-S, Cho J, Zhang Y, Yun KE, Lazo M, Pastor-Barriuso R, Ahn

J, Kim C-W, Rampal S, Cainzos-Achirica M, Zhao D, Chung EC, Shin H, Guallar E, Ryu S**.** Metabolically Healthy Obesity and the Development of Nonalcoholic Fatty Liver Disease. *Am. J. Gastroenterol.* 2016;111(8):1133–1140.

188. Gaggini M, Morelli M, Buzzigoli E, DeFronzo R, Bugianesi E, Gastaldelli A**.** Non-Alcoholic Fatty Liver Disease (NAFLD) and Its Connection with Insulin Resistance, Dyslipidemia, Atherosclerosis and Coronary Heart Disease. *Nutrients* 2013;5(5):1544–1560.

189. Bugianesi E, McCullough AJ, Marchesini G**.** Insulin resistance: A metabolic pathway to chronic liver disease. *Hepatology* 2005;42(5):987–1000.

190. Leite NC, Salles GF, Araujo ALE, Villela-Nogueira CA, Cardoso CRL**.** Prevalence and associated factors of non-alcoholic fatty liver disease in patients with type-2 diabetes mellitus. *Liver Int.* 2009;29(1):113–119.

191. Vernon G, Baranova A, Younossi ZM**.** Systematic review: the epidemiology and natural history of non-alcoholic fatty liver disease and non-alcoholic steatohepatitis in adults. *Aliment. Pharmacol. Ther.* 2011;34(3):274–85.

192. Marchesini G, Bugianesi E, Forlani G, Cerrelli F, Lenzi M, Manini R, Natale S, Vanni E, Villanova N, Melchionda N, Rizzetto M**.** Nonalcoholic fatty liver, steatohepatitis, and the metabolic syndrome. *Hepatology* 2003;37(4):917–923.

193. Younossi ZM, Koenig AB, Abdelatif D, Fazel Y, Henry L, Wymer M**.** Global epidemiology of nonalcoholic fatty liver disease-Meta-analytic assessment of prevalence, incidence, and outcomes. *Hepatology* 2016;64(1):73–84.

194. Sanyal AJ**.** AGA technical review on nonalcoholic fatty liver disease. *Gastroenterology* 2002;123(5):1705–1725.

195. Adams LA, Lymp JF, Sauver JS, Sanderson SO, Lindor KD, Feldstein A, Angulo P**.** The Natural History of Nonalcoholic Fatty Liver Disease: A Population-Based Cohort Study. *Gastroenterology* 2005;129(1):113–21.

196. Byrne CD, Targher G**.** NAFLD: A multisystem disease. *J. Hepatol.* 2015;62(S1):S47–S64.

197. Charlton MR, Burns JM, Pedersen RA, Watt KD, Heimbach JK DR**.** Frequency and outcomes of liver transplantation for nonalcoholic steatohepatitis in the United States. *Gastroenterology* 2011;141(4):1249–53.

198. Ong JP, Pitts A, Younossi ZM**.** Increased overall mortality and liver-related mortality in non-alcoholic fatty liver disease. *J. Hepatol.* 2008;49(4):608–612.

199. Ekstedt M, Franzén LE, Mathiesen UL, Thorelius L, Holmqvist M, Bodemar G, Kechagias S**.** Long-term follow-up of patients with NAFLD and elevated liver enzymes. *Hepatology* 2006;44(4):865–73.

200. EASL, EASD, EASO**.** EASL–EASD–EASO Clinical Practice Guidelines for the management of non-alcoholic fatty liver disease. *J. Hepatol.* 2016;59(6):1388–1402.

201. Kleiner DE, Brunt EM, Van Natta M, Behling C, Contos MJ, Cummings OW, Ferrell LD, Liu YC, Torbenson MS, Unalp-Arida A, Yeh M, McCullough AJ, Sanyal AJ**.** Design and validation of a histological scoring system for nonalcoholic fatty liver disease. *Hepatology* 2005;41(6):1313–1321.

202. Brunt EM, Janney CG, Bisceglie AM, Neuschwander-Tetri BA, Bacon BR**.** Nonalcoholic steatohepatitis: a proposal for grading and staging the histological lesions. *Am. J. Gastroenterol.* 1999;94(9):2467–2474.

203. Lee SS, Park SH**.** Radiologic evaluation of nonalcoholic fatty liver disease. *World J. Gastroenterol.* 2014;20(23):7392.

204. Hui JM, Hodge A, Farrell GC, Kench JG, Kriketos A, George J**.** Beyond insulin resistance in NASH: TNF-alpha or adiponectin? *Hepatology* 2004;40(1):46–54.

205. Jarrar MH, Baranova A, Collantes R, Ranard B, Stepanova M, Bennett C, Fang Y, Elariny H, Goodman Z, Chandhoke V, Younossi ZM**.** Adipokines and cytokines in non-alcoholic fatty liver disease. *Aliment. Pharmacol. Ther.* 2008;27(5):412–21.

206. Day CP, James OFW, Macdonald G, Cowley L, Walker N, Ward P, Jazwinska E, Powell L, Fromenty B, Pessayre D**.** Steatohepatitis: A tale of two “hits”? *Gastroenterology* 1998;114(4):842–845.

207. Madan K, Bhardwaj P, Thareja S, Gupta SD, Saraya A**.** Oxidant stress and antioxidant status among patients with nonalcoholic fatty liver disease (NAFLD). *J. Clin. Gastroenterol.* 2006;40(10):930–5.

208. Wolfs MGM, Gruben N, Rensen SS, Verdam FJ, Greve JW, Driessen A, Wijmenga C, Buurman WA, Franke L, Scheja L, Koonen DPY, Shiri-Sverdlov R, van Haeften TW, Hofker MH, Fu J**.** Determining the association between adipokine expression in multiple tissues and phenotypic features of non-alcoholic fatty liver disease in obesity. *Nutr. Diabetes* 2015;5(2):e146.

209. Tilg H, Moschen AR**.** Evolution of inflammation in nonalcoholic fatty liver disease: The multiple parallel hits hypothesis. *Hepatology* 2010;52(5):1836–1846.

210. Donnelly KL, Smith CI, Schwarzenberg SJ, Jessurun J, Boldt MD, Parks EJ**.** Sources of fatty acids stored in liver and secreted via lipoproteins in patients with nonalcoholic fatty liver disease. *J. Clin. Invest.* 2005;115(5):1343–51.

211. Toshimitsu K, Matsuura B, Ohkubo I, Niiya T, Furukawa S, Hiasa Y, Kawamura M, Ebihara K, Onji M**.** Dietary habits and nutrient intake in non-alcoholic steatohepatitis. *Nutrition* 2007;23(1):46–52.

212. Oddy WH, Herbison CE, Jacoby P, Ambrosini GL, O’Sullivan TA, Ayonrinde OT, Olynyk JK, Black LJ, Beilin LJ, Mori TA, Hands BP, Adams LA**.** The Western Dietary Pattern Is Prospectively Associated With Nonalcoholic Fatty Liver Disease in Adolescence. *Am. J. Gastroenterol.* 2013;108(5):778–785.

213. Nielsen TS, Jessen N, Jørgensen JOL, Møller N, Lund S**.** Dissecting adipose tissue lipolysis: molecular regulation and implications for metabolic disease. *J. Mol. Endocrinol.* 2014;52(3):R199-222.

214. Kotronen A, Juurinen L, Tiikkainen M, Vehkavaara S, Yki-Järvinen H**.** Increased liver fat, impaired insulin clearance, and hepatic and adipose tissue insulin resistance in type 2 diabetes. *Gastroenterology* 2008;135(1):122–30.

215. Lambert JE, Ramos-Roman MA, Browning JD, Parks EJ**.** Increased de novo lipogenesis is a distinct characteristic of individuals with nonalcoholic fatty liver disease. *Gastroenterology* 2014;146(3):726–35.

216. Seppälä-Lindroos A, Vehkavaara S, Häkkinen A-M, Goto T, Westerbacka J, Sovijärvi A, Halavaara J, Yki-Järvinen H**.** Fat Accumulation in the Liver Is Associated with Defects in Insulin Suppression of Glucose Production and Serum Free Fatty Acids Independent of Obesity in Normal Men. *J. Clin. Endocrinol. Metab.* 2002;87(7):3023–3028.

217. Berg JM, Tymoczko JL, Stryer L**.** Fatty Acid Metabolism. In: W H Freeman; 2002. Available at: https://www.ncbi.nlm.nih.gov/books/NBK21173/. Accessed May 22, 2017.

218. Caldwell SH, Swerdlow RH, Khan EM, Iezzoni JC, Hespenheide EE, Parks JK, Parker WD**.** Mitochondrial abnormalities in non-alcoholic steatohepatitis. *J. Hepatol.* 1999;31(3):430–4.

219. Sanyal AJ, Campbell-Sargent C, Mirshahi F, Rizzo WB, Contos MJ, Sterling RK, Luketic VA, Shiffman ML, Clore JN**.** Nonalcoholic steatohepatitis: association of insulin resistance and mitochondrial abnormalities. *Gastroenterology* 2001;120(5):1183–92.

220. Ibdah JA, Perlegas P, Zhao Y, Angdisen J, Borgerink H, Shadoan MK, Wagner JD, Matern D, Rinaldo P, Cline JM**.** Mice heterozygous for a defect in mitochondrial trifunctional protein develop hepatic steatosis and insulin resistance. *Gastroenterology* 2005;128(5):1381–90.

221. Adiels M, Taskinen M-R, Packard C, Caslake MJ, Soro-Paavonen A, Westerbacka J, Vehkavaara S, Häkkinen A, Olofsson S-O, Yki-Järvinen H, Borén J**.** Overproduction of large VLDL particles is driven by increased liver fat content in man. *Diabetologia* 2006;49(4):755–765.

222. Cuchel M, Bloedon LT, Szapary PO, Kolansky DM, Wolfe ML, Sarkis A, Millar JS, Ikewaki K, Siegelman ES, Gregg RE, Rader DJ**.** Inhibition of Microsomal Triglyceride Transfer Protein in Familial Hypercholesterolemia. *N. Engl. J. Med.* 2007;356(2):148–156.

223. Dongiovanni P, Petta S, Maglio C, Fracanzani AL, Pipitone R, Mozzi E, Motta BM, Kaminska D, Rametta R, Grimaudo S, Pelusi S, Montalcini T, Alisi A, Maggioni M, Kärjä V, Borén J, Käkelä P, Di Marco V, Xing C, Nobili V, Dallapiccola B, Craxi A, Pihlajamäki J, Fargion S, Sjöström L, Carlsson LM, Romeo S, Valenti L**.** Transmembrane 6 superfamily member 2 gene variant disentangles nonalcoholic steatohepatitis from cardiovascular disease. *Hepatology* 2015;61(2):506–514.

224. Yamaguchi K, Yang L, McCall S, Huang J, Yu XX, Pandey SK, Bhanot S, Monia BP, Li Y-X, Diehl AM**.** Inhibiting triglyceride synthesis improves hepatic steatosis but exacerbates liver damage and fibrosis in obese mice with nonalcoholic steatohepatitis. *Hepatology* 2007;45(6):1366–74.

225. Gluchowski NL, Becuwe M, Walther TC, Farese R V. Lipid droplets and liver disease: from basic biology to clinical implications. *Nat. Rev. Gastroenterol. Hepatol.* 2017;14(6):343–355.

226. Straub BK, Stoeffel P, Heid H, Zimbelmann R, Schirmacher P**.** Differential pattern of lipid droplet-associated proteins and de novo perilipin expression in hepatocyte steatogenesis. *Hepatology* 2008;47(6):1936–1946.

227. Feldstein AE, Canbay A, Angulo P, Taniai M, Burgart LJ, Lindor KD, Gores GJ**.** Hepatocyte apoptosis and fas expression are prominent features of human nonalcoholic steatohepatitis. *Gastroenterology* 2003;125(2):437–43.

228. Ribeiro PS, Cortez-Pinto H, Sola S, Castro RE, Ramalho RM, Baptista A, Moura MC, Camilo ME, Rodrigues CMP**.** Hepatocyte Apoptosis, Expression of Death Receptors, and Activation of NF-kappaB in the Liver of Nonalcoholic and Alcoholic Steatohepatitis Patients. *Am. J. Gastroenterol.* 2004;99(9):1708–1717.

229. Canbay A, Higuchi H, Bronk SF, Taniai M, Sebo TJ, Gores GJ**.** Fas enhances fibrogenesis in the bile duct ligated mouse: a link between apoptosis and fibrosis. *Gastroenterology* 2002;123(4):1323–30.

230. Malhi H, Barreyro FJ, Isomoto H, Bronk SF, Gores GJ**.** Free fatty acids sensitise hepatocytes to TRAIL mediated cytotoxicity. *Gut* 2007;56(8):1124–1131.

231. Nakagawa T, Zhu H, Morishima N, Li E, Xu J, Yankner BA, Yuan J**.** Caspase-12 mediates endoplasmic-reticulum-specific apoptosis and cytotoxicity by amyloid-β. *Nature* 2000;403(6765):98–103.

232. Feldstein AE, Werneburg NW, Canbay A, Guicciardi ME, Bronk SF, Rydzewski R, Burgart LJ, Gores GJ**.** Free fatty acids promote hepatic lipotoxicity by stimulating TNF-α expression via a lysosomal pathway. *Hepatology* 2004;40(1):185–194.

233. Salvesen GS, Dixit VM**.** Caspase activation: the induced-proximity model. *Proc. Natl. Acad. Sci. U. S. A.* 1999;96(20):10964–7.

234. Canbay A, Taimr P, Torok N, Higuchi H, Friedman S, Gores GJ**.** Apoptotic body engulfment by a human stellate cell line is profibrogenic. *Lab. Invest.* 2003;83(5):655–63.

235. Watanabe A, Hashmi A, Gomes DA, Town T, Badou A, Flavell RA, Mehal WZ**.** Apoptotic hepatocyte DNA inhibits hepatic stellate cell chemotaxis via toll-like receptor 9. *Hepatology* 2007;46(5):1509–1518.

236. Natori S, Rust C, Stadheim LM, Srinivasan A, Burgart LJ, Gores GJ**.** Hepatocyte apoptosis is a pathologic feature of human alcoholic hepatitis. *J. Hepatol.* 2001;34(2):248–253.

237. Hiramatsu N, Hayashi N, Katayama K, Mochizuki K, Kawanishi Y, Kasahara A, Fusamoto H, Kamada T**.** Immunohistochemical detection of Fas antigen in liver tissue of patients with chronic hepatitis C. *Hepatology* 1994;19(6):1354–9.

238. Weltman MD, Farrell GC, Hall P, Ingelman-Sundberg M, Liddle C**.** Hepatic cytochrome P450 2E1 is increased in patients with nonalcoholic steatohepatitis. *Hepatology* 1998;27(1):128–133.

239. Satapati S, Kucejova B, Duarte JAG, Fletcher JA, Reynolds L, Sunny NE, He T, Nair LA, Livingston K, Fu X, Merritt ME, Sherry AD, Malloy CR, Shelton JM, Lambert J, Parks EJ, Corbin I, Magnuson MA, Browning JD, Burgess SC, Burgess SC**.** Mitochondrial metabolism mediates oxidative stress and inflammation in fatty liver. *J. Clin. Invest.* 2015;125(12):4447–4462.

240. Girotti AW**.** Mechanisms of lipid peroxidation. *J. Free Radic. Biol. Med.* 1985;1(2):87–95.

241. Chalasani N, Deeg MA, Crabb DW**.** Systemic Levels of Lipid Peroxidation and Its Metabolic and Dietary Correlates in Patients with Nonalcoholic Steatohepatitis. *Am. J. Gastroenterol.* 2004;99(8):1497–1502.

242. Seki S, Kitada T, Sakaguchi H**.** Clinicopathological significance of oxidative

cellular damage in non-alcoholic fatty liver diseases. *Hepatol. Res.* 2005;33(2):132–134.

243. Madan K, Bhardwaj P, Thareja S, Gupta SD, Saraya A**.** Oxidant Stress and Antioxidant Status Among Patients With Nonalcoholic Fatty Liver Disease (NAFLD). *J. Clin. Gastroenterol.* 2006;40(10):930–935.

244. Walter P, Ron D**.** The Unfolded Protein Response: From Stress Pathway to Homeostatic Regulation. *Science (80-.).* 2011;334(6059):1081–1086.

245. Hetz C**.** The unfolded protein response: controlling cell fate decisions under ER stress and beyond. *Nat. Rev. Mol. Cell Biol.* 2012;13(2):89–102.

246. Harding HP, Novoa I, Zhang Y, Zeng H, Wek R, Schapira M, Ron D**.** Regulated translation initiation controls stress-induced gene expression in mammalian cells. *Mol. Cell* 2000;6(5):1099–108.

247. Jiang H-Y, Wek SA, McGrath BC, Lu D, Hai T, Harding HP, Wang X, Ron D, Cavener DR, Wek RC**.** Activating transcription factor 3 is integral to the eukaryotic initiation factor 2 kinase stress response. *Mol. Cell. Biol.* 2004;24(3):1365–77.

248. Yoshida H, Matsui T, Yamamoto A, Okada T, Mori K**.** XBP1 mRNA is induced by ATF6 and spliced by IRE1 in response to ER stress to produce a highly active transcription factor. *Cell* 2001;107(7):881–91.

249. Heindryckx F, Binet F, Ponticos M, Rombouts K, Lau J, Kreuger J, Gerwins P**.** Endoplasmic reticulum stress enhances fibrosis through IRE1α-mediated degradation of miR-150 and XBP-1 splicing. *EMBO Mol. Med.* 2016;8(7):729–44.

250. Wang D, Wei Y, Pagliassotti MJ**.** Saturated Fatty Acids Promote Endoplasmic Reticulum Stress and Liver Injury in Rats with Hepatic Steatosis. *Endocrinology* 2006;147(2):943–951.

251. Yang L, Jhaveri R, Huang J, Qi Y, Diehl AM**.** Endoplasmic reticulum stress, hepatocyte CD1d and NKT cell abnormalities in murine fatty livers. *Lab. Investig.* 2007;87(9):927–937.

252. Puri P, Mirshahi F, Cheung O, Natarajan R, Maher JW, Kellum JM, Sanyal AJ**.** Activation and Dysregulation of the Unfolded Protein Response in Nonalcoholic Fatty Liver Disease. *Gastroenterology* 2008;134(2):568–576.

253. Puri P, Baillie RA, Wiest MM, Mirshahi F, Choudhury J, Cheung O, Sargeant C, Contos MJ, Sanyal AJ**.** A lipidomic analysis of nonalcoholic fatty liver disease. *Hepatology* 2007;46(4):1081–1090.

254. Puri P, Wiest MM, Cheung O, Mirshahi F, Sargeant C, Min H-K, Contos MJ, Sterling RK, Fuchs M, Zhou H, Watkins SM, Sanyal AJ**.** The plasma lipidomic signature of nonalcoholic steatohepatitis. *Hepatology* 2009;50(6):1827–1838.

255. Marí M, Caballero F, Colell A, Morales A, Caballeria J, Fernandez A, Enrich C, Fernandez-Checa JC, García-Ruiz C**.** Mitochondrial free cholesterol loading sensitizes to TNF- and Fas-mediated steatohepatitis. *Cell Metab.* 2006;4(3):185–198.

256. Van Rooyen DM, Larter CZ, Haigh WG, Yeh MM, Ioannou G, Kuver R, Lee SP, Teoh NC, Farrell GC**.** Hepatic Free Cholesterol Accumulates in Obese, Diabetic

Mice and Causes Nonalcoholic Steatohepatitis. *Gastroenterology* 2011;141(4):1393–1403.e5.

257. Kubes P, Mehal WZ**.** Sterile Inflammation in the Liver. *Gastroenterology* 2012;143(5):1158–1172.

258. Ohashi K, Burkart V, Flohé S, Kolb H**.** Cutting Edge: Heat Shock Protein 60 Is a Putative Endogenous Ligand of the Toll-Like Receptor-4 Complex. *J. Immunol.* 2000;164(2):558–61.

259. Imaeda AB, Watanabe A, Sohail MA, Mahmood S, Mohamadnejad M, Sutterwala FS, Flavell RA, Mehal WZ**.** Acetaminophen-induced hepatotoxicity in mice is dependent on Tlr9 and the Nalp3 inflammasome. *J. Clin. Invest.* 2009;119(2):305–14.

260. Gäbele E, Dostert K, Hofmann C, Wiest R, Schölmerich J, Hellerbrand C, Obermeier F**.** DSS induced colitis increases portal LPS levels and enhances hepatic inflammation and fibrogenesis in experimental NASH. *J. Hepatol.* 2011;55(6):1391–1399.

261. Clemente JC, Ursell LK, Parfrey LW, Knight R**.** The Impact of the Gut Microbiota on Human Health: An Integrative View. *Cell* 2012;148(6):1258–1270.

262. Wobser H, Dorn C, Weiss TS, Amann T, Bollheimer C, Büttner R, Schölmerich J, Hellerbrand C**.** Lipid accumulation in hepatocytes induces fibrogenic activation of hepatic stellate cells. *Cell Res.* 2009;19(8):996–1005.

263. Bertola A, Bonnafous S, Anty R, Patouraux S, Saint-Paul M-C, Iannelli A, Gugenheim J, Barr J, Mato JM, Le Marchand-Brustel Y, Tran A, Gual P**.** Hepatic expression patterns of inflammatory and immune response genes associated with obesity and NASH in morbidly obese patients. *PLoS One* 2010;5(10):e13577.

264. de Fraia Pinto L, Compri CM, Fornari JV, Bartchewsky W, Cintra DE, Trevisan M, de Oliveira Carvalho P, Ribeiro ML, Velloso LA, Saad MJ, Pedrazzoli J, Gambero A**.** The immunosuppressant drug, thalidomide, improves hepatic alterations induced by a high-fat diet in mice. *Liver Int.* 2010;30(4):603–610.

265. Shetty S, Lalor PF, Adams DH**.** Lymphocyte recruitment to the liver: Molecular insights into the pathogenesis of liver injury and hepatitis. *Toxicology* 2008;254(3):136–146.

266. Chauhan A, Adams DH, Watson SP, Lalor PF**.** Platelets: No longer bystanders in liver disease. *Hepatology* 2016;64(5):1774–1784.

267. Sutti S, Locatelli I, Bruzzì S, Jindal A, Vacchiano M, Bozzola C, Albano E**.** CX3CR1-expressing inflammatory dendritic cells contribute to the progression of steatohepatitis. *Clin. Sci.* 2015;129(9):797–808.

268. Haukeland JW, Damås JK, Konopski Z, Løberg EM, Haaland T, Goverud I, Torjesen PA, Birkeland K, Bjøro K, Aukrust P**.** Systemic inflammation in nonalcoholic fatty liver disease is characterized by elevated levels of CCL2. *J. Hepatol.* 2006;44(6):1167–1174.

269. Karlmark KR, Weiskirchen R, Zimmermann HW, Gassler N, Ginhoux F, Weber C, Merad M, Luedde T, Trautwein C, Tacke F**.** Hepatic recruitment of the inflammatory Gr1+ monocyte subset upon liver injury promotes hepatic fibrosis. *Hepatology* 2009;50(1):261–274.

270. Scott CL, Zheng F, De Baetselier P, Martens L, Saeys Y, De Prijck S, Lippens S, Abels C, Schoonooghe S, Raes G, Devoogdt N, Lambrecht BN, Beschin A, Guilliams M**.** Bone marrow-derived monocytes give rise to self-renewing and fully differentiated Kupffer cells. *Nat. Commun.* 2016;7:10321.

271. Beattie L, Sawtell A, Mann J, Frame TCM, Teal B, de Labastida Rivera F, Brown N, Walwyn-Brown K, Moore JWJ, MacDonald S, Lim E-K, Dalton JE, Engwerda CR, MacDonald KP, Kaye PM**.** Bone marrow-derived and resident liver macrophages display unique transcriptomic signatures but similar biological functions. *J. Hepatol.* 2016;65(4):758–768.

272. Friedman SL**.** Liver fibrosis – from bench to bedside. *J. Hepatol.* 2003;38(SUPPL 1):38–53.

273. Hernandez-Gea V, Friedman SL**.** Pathogenesis of Liver Fibrosis. *Annu. Rev. Pathol. Mech. Dis.* 2011;6(1):425–456.

274. Pradere J-P, Kluwe J, De Minicis S, Jiao J-J, Gwak G-Y, Dapito DH, Jang M-K, Guenther ND, Mederacke I, Friedman R, Dragomir A-C, Aloman C, Schwabe RF**.** Hepatic macrophages but not dendritic cells contribute to liver fibrosis by promoting the survival of activated hepatic stellate cells in mice. *Hepatology* 2013;58(4):1461–1473.

275. Seki E, De Minicis S, Österreicher CH, Kluwe J, Osawa Y, Brenner DA, Schwabe RF**.** TLR4 enhances TGF-β signaling and hepatic fibrosis. *Nat. Med.* 2007;13(11):1324–1332.

276. Gressner AM, Lotfi S, Gressner G, Haltner E, Kropf J**.** Synergism between hepatocytes and Kupffer cells in the activation of fat storing cells (perisinusoidal lipocytes). *J. Hepatol.* 1993;19(1):117–32.

277. Lee YA, Wallace MC, Friedman SL**.** Pathobiology of liver fibrosis: a translational success story. *Gut* 2015;64(5):830–41.

278. Harvey SAK, Dangi A, Tandon A, Gandhi CR**.** The Transcriptomic Response of Rat Hepatic Stellate Cells to Endotoxin: Implications for Hepatic Inflammation and Immune Regulation. Ryffel B, ed. *PLoS One* 2013;8(12):e82159.

279. Viñas O, Bataller R, Sancho-Bru P, Ginès P, Berenguer C, Enrich C, Nicolás JM, Ercilla G, Gallart T, Vives J, Arroyo V, Rodés J**.** Human hepatic stellate cells show features of antigen-presenting cells and stimulate lymphocyte proliferation. *Hepatology* 2003;38(4):919–929.

280. Tang L, Tanaka Y, Marumo F, Sato C**.** Phenotypic change in portal fibroblasts in biliary fibrosis. *Liver* 1994;14(2):76–82.

281. Cassiman D, Libbrecht L, Desmet V, Denef C, Roskams T**.** Hepatic stellate cell/myofibroblast subpopulations in fibrotic human and rat livers. *J. Hepatol.* 2002;36(2):200–9.

282. Kral JG, Thung SN, Biron S, Hould F-S, Lebel S, Marceau S, Simard S, Marceau P**.** Effects of surgical treatment of the metabolic syndrome on liver fibrosis and cirrhosis. *Surgery* 2004;135(1):48–58.

283. Dixon JB, Bhathal PS, Hughes NR, O'Brien PE**.** Nonalcoholic fatty liver disease: Improvement in liver histological analysis with weight loss. *Hepatology* 2004;39(6):1647–1654.

284. Zhou X, Hovell CJ, Pawley S, Hutchings MI, Arthur MJP, Iredale JP, Benyon RC**.** Expression of matrix metalloproteinase-2 and -14 persists during early resolution of experimental liver fibrosis and might contribute to fibrolysis. *Liver Int.* 2004;24(5):492–501.

285. Fallowfield JA, Mizuno M, Kendall TJ, Constandinou CM, Benyon RC, Duffield JS, Iredale JP**.** Scar-associated macrophages are a major source of hepatic matrix metalloproteinase-13 and facilitate the resolution of murine hepatic fibrosis. *J. Immunol.* 2007;178(8):5288–95.

286. Novo E, Marra F, Zamara E, Valfrè di Bonzo L, Monitillo L, Cannito S, Petrai I, Mazzocca A, Bonacchi A, De Franco RSM, Colombatto S, Autelli R, Pinzani M, Parola M**.** Overexpression of Bcl-2 by activated human hepatic stellate cells: resistance to apoptosis as a mechanism of progressive hepatic fibrogenesis in humans. *Gut* 2006;55(8):1174–82.

287. Krizhanovsky V, Yon M, Dickins RA, Hearn S, Simon J, Miething C, Yee H, Zender L, Lowe SW**.** Senescence of Activated Stellate Cells Limits Liver Fibrosis. *Cell* 2008;134(4):657–667.

288. Radaeva S, Sun R, Jaruga B, Nguyen VT, Tian Z, Gao B**.** Natural Killer Cells Ameliorate Liver Fibrosis by Killing Activated Stellate Cells in NKG2D-Dependent and Tumor Necrosis Factor–Related Apoptosis-Inducing Ligand–Dependent Manners. *Gastroenterology* 2006;130(2):435–452.

289. Anstee QM, Day CP**.** The genetics of NAFLD. *Nat. Rev. Gastroenterol. Hepatol.* 2013;10(11):645–655.

290. Romeo S, Kozlitina J, Xing C, Pertsemlidis A, Cox D, Pennacchio LA, Boerwinkle E, Cohen JC, Hobbs HH**.** Genetic variation in PNPLA3 confers susceptibility to nonalcoholic fatty liver disease. *Nat. Genet.* 2008;40(12):1461–1465.

291. Rotman Y, Koh C, Zmuda JM, Kleiner DE, Liang TJ, NASH CRN**.** The association of genetic variability in patatin-like phospholipase domain-containing protein 3 (PNPLA3) with histological severity of nonalcoholic fatty liver disease. *Hepatology* 2010;52(3):894–903.

292. Speliotes EK, Yerges-Armstrong LM, Wu J, Hernaez R, Kim LJ, Palmer CD, Gudnason V, Eiriksdottir G, Garcia ME, Launer LJ, Nalls MA, Clark JM, Mitchell BD, Shuldiner AR, Butler JL, Tomas M, Hoffmann U, Hwang S-J, Massaro JM, O'Donnell CJ, Sahani D V., Salomaa V, Schadt EE, Schwartz SM, Siscovick DS, Voight BF, Carr JJ, Feitosa MF, Harris TB, Fox CS, Smith A V., Kao WHL, Hirschhorn JN, Borecki IB, Kao WHL, Hirschhorn JN, Borecki IB, GOLD Consortium**.** Genome-Wide Association Analysis Identifies Variants Associated with Nonalcoholic Fatty Liver Disease That Have Distinct Effects on Metabolic Traits. McCarthy MI, ed. *PLoS Genet.* 2011;7(3):e1001324.

293. Kozlitina J, Smagris E, Stender S, Nordestgaard BG, Zhou HH, Tybjærg-Hansen A, Vogt TF, Hobbs HH, Cohen JC**.** Exome-wide association study identifies a TM6SF2 variant that confers susceptibility to nonalcoholic fatty liver disease. *Nat. Genet.* 2014;46(4):352–356.

294. Ehrhardt N, Doche ME, Chen S, Mao HZ, Walsh MT, Bedoya C, Guindi M, Xiong W, Ignatius Irudayam J, Iqbal J, Fuchs S, French SW, Mahmood Hussain M, Arditi M, Arumugaswami V, Péterfy M**.** Hepatic Tm6sf2 overexpression affects cellular ApoB-trafficking, plasma lipid levels, hepatic steatosis and atherosclerosis. *Hum. Mol. Genet.* 2017. doi:10.1093/hmg/ddx159.

295. Neuschwander-Tetri BA, Loomba R, Sanyal AJ, Lavine JE, Van Natta ML, Abdelmalek MF, Chalasani N, Dasarathy S, Diehl AM, Hameed B, Kowdley K V, McCullough A, Terrault N, Clark JM, Tonascia J, Brunt EM, Kleiner DE, Doo E, NASH Clinical Research Network**.** Farnesoid X nuclear receptor ligand obeticholic acid for non-cirrhotic, non-alcoholic steatohepatitis (FLINT): a multicentre, randomised, placebo-controlled trial. *Lancet (London, England)* 2015;385(9972):956–65.

296. Lombardi R, Onali S, Thorburn D, Davidson BR, Gurusamy KS, Tsochatzis E**.** Pharmacological interventions for non-alcohol related fatty liver disease (NAFLD). *Cochrane Database Syst. Rev.* 2017;(3):CD011640.

297. Ratziu V, Goodman Z, Sanyal A**.** Current efforts and trends in the treatment of NASH. *J. Hepatol.* 2015;62(1):S65–S75.

298. Sanyal AJ, Chalasani N, Kowdley K V., McCullough A, Diehl AM, Bass NM, Neuschwander-Tetri BA, Lavine JE, Tonascia J, Unalp A, Van Natta M, Clark J, Brunt EM, Kleiner DE, Hoofnagle JH, Robuck PR**.** Pioglitazone, Vitamin E, or Placebo for Nonalcoholic Steatohepatitis. *N. Engl. J. Med.* 2010;362(18):1675–1685.

299. Takeuchi T, Nomura T, Tsujita M, Suzuki M, Fuse T, Mori H, Mishina M**.** Flp recombinase transgenic mice of C57BL/6 strain for conditional gene targeting. *Biochem. Biophys. Res. Commun.* 2002;293(3):953–957.

300. Koentgen F, Suess G, Naf D**.** Engineering the Mouse Genome to Model Human Disease for Drug Discovery. In: *Methods in molecular biology (Clifton, N.J.)*.Vol 602.; 2010:55–77.

301. Schnütgen F, Doerflinger N, Calléja C, Wendling O, Chambon P, Ghyselinck NB**.** A directional strategy for monitoring Cre-mediated recombination at the cellular level in the mouse. *Nat. Biotechnol.* 2003;21(5):562–565.

302. Gargiulo S, Gramanzini M, Megna R, Greco A, Albanese S, Manfredi C, Brunetti A**.** Evaluation of growth patterns and body composition in C57Bl/6J mice using dual energy X-ray absorptiometry. *Biomed Res. Int.* 2014;2014:253067.

303. The Jackson Laboratory**.** Body Weight Information for C57BL/6J (000664). Available at: https://www.jax.org/jax-mice-and-services/strain-data-sheet-pages/body-weight-chart-000664. Accessed February 20, 2017.

304. Pourcet B, Gage MC, León TE, Waddington KE, Pello OM, Steffensen KR, Castrillo A, Valledor AF, Pineda-Torra I**.** The nuclear receptor LXR modulates interleukin-18 levels in macrophages through multiple mechanisms. *Sci. Rep.* 2016;6:25481.

305. Tyner C, Barber GP, Casper J, Clawson H, Diekhans M, Eisenhart C, Fischer CM, Gibson D, Gonzalez JN, Guruvadoo L, Haeussler M, Heitner S, Hinrichs AS, Karolchik D, Lee BT, Lee CM, Nejad P, Raney BJ, Rosenbloom KR, Speir ML, Villarreal C, Vivian J, Zweig AS, Haussler D, Kuhn RM, Kent WJ**.** The UCSC Genome Browser database: 2017 update. *Nucleic Acids Res.* 2017;45(D1):D626–D634.

306. Untergasser A, Cutcutache I, Koressaar T, Ye J, Faircloth BC, Remm M, Rozen SG**.** Primer3—new capabilities and interfaces. *Nucleic Acids Res.* 2012;40(15):e115–e115.

307. Pehkonen P, Welter-Stahl L, Diwo J, Ryynänen J, Wienecke-Baldacchino A,

Heikkinen S, Treuter E, Steffensen KR, Carlberg C**.** Genome-wide landscape of liver X receptor chromatin binding and gene regulation in human macrophages. *BMC Genomics* 2012;13(1):50.

308. Torra IP, Staverosky JA, Ha S, Logan SK, Garabedian MJ**.** Development of Phosphorylation Site-Specific Antibodies to Nuclear Receptors. In: *Methods in molecular biology (Clifton, N.J.)*.Vol 505.; 2009:221–235.

309. Liang W, Menke AL, Driessen A, Koek GH, Lindeman JH, Stoop R, Havekes LM, Kleemann. R, Van Den Hoek AM**.** Establishment of a general NAFLD scoring system for rodent models and comparison to human liver pathology. *PLoS One* 2014;9(12):1–17.

310. Schindelin J, Arganda-Carreras I, Frise E, Kaynig V, Longair M, Pietzsch T, Preibisch S, Rueden C, Saalfeld S, Schmid B, Tinevez J-Y, White DJ, Hartenstein V, Eliceiri K, Tomancak P, Cardona A**.** Fiji: an open-source platform for biological-image analysis. *Nat. Methods* 2012;9(7):676–82.

311. Duda RO, Hart PE**.** Use of the Hough transformation to detect lines and curves in pictures. *Commun. ACM* 1972;15(1):11–15.

312. Roberg-Larsen H, Lund K, Vehus T, Solberg N, Vesterdal C, Misaghian D, Olsen PA, Krauss S, Wilson SR, Lundanes E**.** Highly automated nano-LC/MS-based approach for thousand cell-scale quantification of side chain-hydroxylated oxysterols. *J. Lipid Res.* 2014;55(7):1531–6.

313. Roberg-Larsen H, Lund K, Seterdal KE, Solheim S, Vehus T, Solberg N, Krauss S, Lundanes E, Wilson SR**.** Mass spectrometric detection of 27-hydroxycholesterol in breast cancer exosomes. *J. Steroid Biochem. Mol. Biol.* 2016. doi:10.1016/j.jsbmb.2016.02.006.

314. Sandelin A, Wasserman WW**.** Prediction of Nuclear Hormone Receptor Response Elements. *Mol. Endocrinol.* 2005;19(3):595–606.

315. Boergesen M, Pedersen TA, Gross B, van Heeringen SJ, Hagenbeek D, Bindesboll C, Caron S, Lalloyer F, Steffensen KR, Nebb HI, Gustafsson J-A, Stunnenberg HG, Staels B, Mandrup S**.** Genome-Wide Profiling of Liver X Receptor, Retinoid X Receptor, and Peroxisome Proliferator-Activated Receptor in Mouse Liver Reveals Extensive Sharing of Binding Sites. *Mol. Cell. Biol.* 2012;32(4):852–867.

316. Mootha VK, Lindgren CM, Eriksson K-F, Subramanian A, Sihag S, Lehar J, Puigserver P, Carlsson E, Ridderstråle M, Laurila E, Houstis N, Daly MJ, Patterson N, Mesirov JP, Golub TR, Tamayo P, Spiegelman B, Lander ES, Hirschhorn JN, Altshuler D, Groop LC**.** PGC-1α-responsive genes involved in oxidative phosphorylation are coordinately downregulated in human diabetes. *Nat. Genet.* 2003;34(3):267–273.

317. Subramanian A, Tamayo P, Mootha VK, Mukherjee S, Ebert BL, Gillette MA, Paulovich A, Pomeroy SL, Golub TR, Lander ES, Mesirov JP**.** Gene set enrichment analysis: a knowledge-based approach for interpreting genome-wide expression profiles. *Proc. Natl. Acad. Sci. U. S. A.* 2005;102(43):15545–50.

318. Liberzon A, Birger C, Thorvaldsdóttir H, Ghandi M, Mesirov JP, Tamayo P**.** The Molecular Signatures Database Hallmark Gene Set Collection. *Cell Syst.* 2015;1(6):417–425.

319. Saeed AI, Sharov V, White J, Li J, Liang W, Bhagabati N, Braisted J, Klapa M,

Currier T, Thiagarajan M, Sturn A, Snuffin M, Rezantsev A, Popov D, Ryltsov A, Kostukovich E, Borisovsky I, Liu Z, Vinsavich A, Trush V, Quackenbush J**.** TM4: a free, open-source system for microarray data management and analysis. *Biotechniques* 2003;34(2):374–8.

320. Raschke WC, Baird S, Ralph P, Nakoinz I**.** Functional macrophage cell lines transformed by Abelson leukemia virus. *Cell* 1978;15(1):261–7.

321. Bradley MN, Hong C, Chen M, Joseph SB, Wilpitz DC, Wang X, Lusis AJ, Collins A, Hseuh WA, Collins JL, Tangirala RK, Tontonoz P**.** Ligand activation of LXR beta reverses atherosclerosis and cellular cholesterol overload in mice lacking LXR alpha and apoE. *J. Clin. Invest.* 2007;117(8):2337–46.

322. Katz A, Udata C, Ott E, Hickey L, Burczynski ME, Burghart P, Vesterqvist O, Meng X**.** Safety, Pharmacokinetics, and Pharmacodynamics of Single Doses of LXR-623, a Novel Liver X-Receptor Agonist, in Healthy Participants. *J. Clin. Pharmacol.* 2009;49(6):643–649.

323. Grefhorst A, Elzinga BM, Voshol PJ, Plösch T, Kok T, Bloks VW, Van Der Sluijs FH, Havekes LM, Romijn JA, Verkade HJ, Kuipers F**.** Stimulation of lipogenesis by pharmacological activation of the liver X receptor leads to production of large, triglyceride-rich very low density lipoprotein particles. *J. Biol. Chem.* 2002;277(37):34182–34190.

324. Zhang Y, Breevoort SR, Angdisen J, Fu M, Schmidt DR, Holmstrom SR, Kliewer SA, Mangelsdorf DJ, Schulman IG**.** Liver LXRα expression is crucial for whole body cholesterol homeostasis and reverse cholesterol transport in mice. *J. Clin. Invest.* 2012;122(5):1688–1699.

325. Hamilton JP, Koganti L, Muchenditsi A, Pendyala VS, Huso D, Hankin J, Murphy RC, Huster D, Merle U, Mangels C, Yang N, Potter JJ, Mezey E, Lutsenko S**.** Activation of liver X receptor/retinoid X receptor pathway ameliorates liver disease in Atp7B(-/-) (Wilson disease) mice. *Hepatology* 2016;63(6):1828–41.

326. Jakobsson T, Venteclef N, Toresson G, Damdimopoulos AE, Ehrlund A, Lou X, Sanyal S, Steffensen KR, Gustafsson J-Å, Treuter E**.** GPS2 Is Required for Cholesterol Efflux by Triggering Histone Demethylation, LXR Recruitment, and Coregulator Assembly at the ABCG1 Locus. *Mol. Cell* 2009;34(4):510–518.

327. Duan L-P, Wang HH, Ohashi A, Wang DQ-H**.** Role of intestinal sterol transporters Abcg5, Abcg8, and Npc1l1 in cholesterol absorption in mice: gender and age effects. *Am. J. Physiol. Gastrointest. Liver Physiol.* 2006;290(2):G269-76.

328. Lorbek G, Perše M, Horvat S, Björkhem I, Rozman D**.** Sex differences in the hepatic cholesterol sensing mechanisms in mice. *Molecules* 2013;18(9):11067–85.

329. Matsuzawa N, Takamura T, Kurita S, Misu H, Ota T, Ando H, Yokoyama M, Honda M, Zen Y, Nakanuma Y, Miyamoto K, Kaneko S**.** Lipid-induced oxidative stress causes steatohepatitis in mice fed an atherogenic diet. *Hepatology* 2007;46(5):1392–1403.

330. Sallam T, Jones MC, Gilliland T, Zhang L, Wu X, Eskin A, Sandhu J, Casero D, Vallim TQ de A, Hong C, Katz M, Lee R, Whitelegge J, Tontonoz P**.** Feedback modulation of cholesterol metabolism by the lipid-responsive non-coding RNA LeXis. *Nature* 2016;534(7605):124–128.

331. Wang Y, Rogers PM, Su C, Varga G, Stayrook KR, Burris TP**.** Regulation of cholesterologenesis by the oxysterol receptor, LXRalpha. *J. Biol. Chem.* 2008;283(39):26332–26339.

332. Wada T, Kang HS, Angers M, Gong H, Bhatia S, Khadem S, Ren S, Ellis E, Strom SC, Jetten AM, Xie W**.** Identification of Oxysterol 7 -Hydroxylase (Cyp7b1) as a Novel Retinoid-Related Orphan Receptor (ROR) (NR1F1) Target Gene and a Functional Cross-Talk between ROR and Liver X Receptor (NR1H3). *Mol. Pharmacol.* 2007;73(3):891–899.

333. Uppal H, Saini SPS, Moschetta A, Mu Y, Zhou J, Gong H, Zhai Y, Ren S, Michalopoulos GK, Mangelsdorf DJ, Xie W**.** Activation of LXRs prevents bile acid toxicity and cholestasis in female mice. *Hepatology* 2007;45(2):422–432.

334. Laffitte BA, Repa JJ, Joseph SB, Wilpitz DC, Kast HR, Mangelsdorf DJ, Tontonoz P**.** LXRs control lipid-inducible expression of the apolipoprotein E gene in macrophages and adipocytes. *Proc. Natl. Acad. Sci. U. S. A.* 2001;98(2):507–512.

335. Zelcer N, Hong C, Boyadjian R, Tontonoz P**.** LXR regulates cholesterol uptake through Idol-dependent ubiquitination of the LDL receptor. *Science* 2009;325(5936):100–4.

336. Ikegami T, Hyogo H, Honda A, Miyazaki T, Tokushige K, Hashimoto E, Inui K, Matsuzaki Y, Tazuma S**.** Increased serum liver X receptor ligand oxysterols in patients with non-alcoholic fatty liver disease. *J. Gastroenterol.* 2012;47(11):1257–66.

337. Kaplan R, Zhang T, Hernandez M, Gan FX, Wright SD, Waters MG, Cai T-Q**.** Regulation of the angiopoietin-like protein 3 gene by LXR. *J. Lipid Res.* 2003;44(1):136–43.

338. Inaba T, Matsuda M, Shimamura M, Takei N, Terasaka N, Ando Y, Yasumo H, Koishi R, Makishima M, Shimomura I**.** Angiopoietin-like protein 3 mediates hypertriglyceridemia induced by the liver X receptor. *J. Biol. Chem.* 2003;278(24):21344–51.

339. Koishi R, Ando Y, Ono M, Shimamura M, Yasumo H, Fujiwara T, Horikoshi H, Furukawa H**.** Angptl3 regulates lipid metabolism in mice. *Nat. Genet.* 2002;30(2):151–157.

340. Deng Q, She H, Cheng JH, French SW, Koop DR, Xiong S, Tsukamoto H**.** Steatohepatitis induced by intragastric overfeeding in mice. *Hepatology* 2005;42(4):905–914.

341. Matsuzawa N, Takamura T, Kurita S, Misu H, Ota T, Ando H, Yokoyama M, Honda M, Zen Y, Nakanuma Y, Miyamoto K, Kaneko S**.** Lipid-induced oxidative stress causes steatohepatitis in mice fed an atherogenic diet. *Hepatology* 2007;46(5):1392–1403.

342. Znoyko I, Sohara N, Spicer SS, Trojanowska M, Reuben A**.** Expression of oncostatin M and its receptors in normal and cirrhotic human liver. *J. Hepatol.* 2005;43(5):893–900.

343. Semba T, Nishimura M, Nishimura S, Ohara O, Ishige T, Ohno S, Nonaka K, Sogawa K, Satoh M, Sawai S, Matsushita K, Imazeki F, Yokosuka O, Nomura F**.** The FLS (Fatty liver Shionogi) mouse reveals local expressions of lipocalin-2, CXCL1 and CXCL9 in the liver with non-alcoholic steatohepatitis. *BMC*

Gastroenterol. 2013;13(1):120.

344. Syn W-K, Choi SS, Liaskou E, Karaca GF, Agboola KM, Oo YH, Mi Z, Pereira TA, Zdanowicz M, Malladi P, Chen Y, Moylan C, Jung Y, Bhattacharya SD, Teaberry V, Omenetti A, Abdelmalek MF, Guy CD, Adams DH, Kuo PC, Michelotti GA, Whitington PF, Diehl AM**.** Osteopontin is induced by hedgehog pathway activation and promotes fibrosis progression in nonalcoholic steatohepatitis. *Hepatology* 2011;53(1):106–15.

345. Heymann F, Tacke F**.** Immunology in the liver — from homeostasis to disease. *Nat. Rev. Gastroenterol. Hepatol.* 2016;13(2):88–110.

346. Lebeaupin C, Proics E, de Bieville CHD, Rousseau D, Bonnafous S, Patouraux S, Adam G, Lavallard VJ, Rovere C, Le Thuc O, Saint-Paul MC, Anty R, Schneck AS, Iannelli A, Gugenheim J, Tran A, Gual P, Bailly-Maitre B**.** ER stress induces NLRP3 inflammasome activation and hepatocyte death. *Cell Death Dis.* 2015;6(9):e1879.

347. Dara L, Ji C, Kaplowitz N**.** The contribution of endoplasmic reticulum stress to liver diseases. *Hepatology* 2011;53(5):1752–63.

348. Sanyal AJ**.** Mechanisms of Disease: pathogenesis of nonalcoholic fatty liver disease. *Nat. Clin. Pract. Gastroenterol. Hepatol.* 2005;2(1):46–53.

349. Alkhouri N, Dixon LJ, Feldstein AE**.** Lipotoxicity in nonalcoholic fatty liver disease: not all lipids are created equal. *Expert Rev. Gastroenterol. Hepatol.* 2009;3(4):445–451.

350. Li ZZ, Berk M, McIntyre TM, Feldstein AE**.** Hepatic lipid partitioning and liver damage in nonalcoholic fatty liver disease: role of stearoyl-CoA desaturase. *J. Biol. Chem.* 2009;284(9):5637–44.

351. Musso G, Gambino R, Durazzo M, Biroli G, Carello M, Fagà E, Pacini G, De Michieli F, Rabbione L, Premoli A, Cassader M, Pagano G**.** Adipokines in NASH: Postprandial lipid metabolism as a link between adiponectin and liver disease. *Hepatology* 2005;42(5):1175–1183.

352. Shimomura I, Hammer RE, Richardson JA, Ikemoto S, Bashmakov Y, Goldstein JL, Brown MS**.** Insulin resistance and diabetes mellitus in transgenic mice expressing nuclear SREBP-1c in adipose tissue: model for congenital generalized lipodystrophy. *Genes Dev.* 1998;12(20):3182–94.

353. Lettéron P, Sutton A, Mansouri A, Fromenty B, Pessayre D**.** Inhibition of microsomal triglyceride transfer protein: Another mechanism for drug-induced steatosis in mice. *Hepatology* 2003;38(1):133–140.

354. Zhang D, Liu Z-X, Choi CS, Tian L, Kibbey R, Dong J, Cline GW, Wood PA, Shulman GI**.** Mitochondrial dysfunction due to long-chain Acyl-CoA dehydrogenase deficiency causes hepatic steatosis and hepatic insulin resistance. *Proc. Natl. Acad. Sci.* 2007;104(43):17075–17080.

355. Fungwe T V, Fox JE, Cagen LM, Wilcox HG, Heimberg M**.** Stimulation of fatty acid biosynthesis by dietary cholesterol and of cholesterol synthesis by dietary fatty acid. *J Lipid Res.* 1994;35(2):311–8.

356. Wang X, Sato R, Brown MS, Hua X, Goldsteln JL**.** SREBP-1 , a Membrane-Bound Transcription Factor Released by Sterol-Regulated Proteolysis. *Cell* 1994;77(1):53–62.

357. Matsuda M, Korn BS, Hammer RE, Moon YA, Komuro R, Horton JD, Goldstein JL, Brown MS, Shimomura I**.** SREBP cleavage-activating protein (SCAP) is required for increased lipid synthesis in liver induced by cholesterol deprivation and insulin elevation. *Genes Dev.* 2001;15(10):1206–1216.

358. A-Gonzalez N, Guillen JA, Gallardo G, Diaz M, de la Rosa J V, Hernandez IH, Casanova-Acebes M, Lopez F, Tabraue C, Beceiro S, Hong C, Lara PC, Andujar M, Arai S, Miyazaki T, Li S, Corbi AL, Tontonoz P, Hidalgo A, Castrillo A**.** The nuclear receptor LXRα controls the functional specialization of splenic macrophages. *Nat. Immunol.* 2013;14(8):831–839.

359. Promporn R, Chatsudthipong V, Muanprasat C, Soodvilai S**.** Activation of liver X receptors reduces CFTR-mediated Cl(-) transport in kidney collecting duct cells. *Am J Physiol Ren. Physiol.* 2013;305(4):F583-91.

360. Morello F, de Boer RA, Steffensen KR, Gnecchi M, Chisholm JW, Boomsma F, Anderson LM, Lawn RM, Gustafsson J-A, Lopez-Ilasaca M, Pratt RE, Dzau VJ**.** Liver X receptors alpha and beta regulate renin expression in vivo. *J. Clin. Invest.* 2005;115(7):1913–22.

361. Bentinger M, Tekle M, Dallner G, Brismar K, Gustafsson J-Å, Steffensen KR, Catrina S-B**.** Influence of liver-X-receptor on tissue cholesterol, coenzyme Q and dolichol content. *Mol. Membr. Biol.* 2012;29(7):299–308.

362. Wu J, Zhang Y, Wang N, Davis L, Yang G, Wang X, Zhu Y, Breyer MD, Guan Y**.** Liver X receptor-alpha mediates cholesterol efflux in glomerular mesangial cells. *AJP Ren. Physiol.* 2004;287(5):F886–F895.

363. Jiang T, Liebman SE, Scott Lucia M, Li J, Levi M**.** Role of altered renal lipid metabolism and the sterol regulatory element binding proteins in the pathogenesis of age-related renal disease. *Kidney Int.* 2005;68(6):2608–2620.

364. Musso G, Gambino R, De Michieli F, Cassader M, Rizzetto M, Durazzo M, Fagà E, Silli B, Pagano G**.** Dietary habits and their relations to insulin resistance and postprandial lipemia in nonalcoholic steatohepatitis. *Hepatology* 2003;37(4):909–916.

365. Kainuma M, Fujimoto M, Sekiya N, Tsuneyama K, Cheng C, Takano Y, Terasawa K, Shimada Y**.** Cholesterol-fed rabbit as a unique model of nonalcoholic, nonobese, non-insulin-resistant fatty liver disease with characteristic fibrosis. *J. Gastroenterol.* 2006;41(10):971–980.

366. Marí M, Caballero F, Colell A, Morales A, Caballeria J, Fernandez A, Enrich C, Fernandez-Checa JC, García-Ruiz C**.** Mitochondrial free cholesterol loading sensitizes to TNF-and Fas-mediated steatohepatitis. *Cell Metab.* 2006;4(3):185–98.

367. Tomita K, Teratani T, Suzuki T, Shimizu M, Sato H, Narimatsu K, Okada Y, Kurihara C, Irie R, Yokoyama H, Shimamura K, Usui S, Ebinuma H, Saito H, Watanabe C, Komoto S, Kawaguchi A, Nagao S, Sugiyama K, Hokari R, Kanai T, Miura S, Hibi T**.** Free cholesterol accumulation in hepatic stellate cells: Mechanism of liver fibrosis aggravation in nonalcoholic steatohepatitis in mice. *Hepatology* 2014;59(1):154–169.

368. Yu L, Li-Hawkins J, Hammer RE, Berge KE, Horton JD, Cohen JC, Hobbs HH**.** Overexpression of ABCG5 and ABCG8 promotes biliary cholesterol secretion and reduces fractional absorption of dietary cholesterol. *J. Clin. Invest.* 2002;110(5):671–80.

369. Wu JE, Basso F, Shamburek RD, Amar MJA, Vaisman B, Szakacs G, Joyce C, Tansey T, Freeman L, Paigen BJ, Thomas F, Brewer HB, Santamarina-Fojo S**.** Hepatic ABCG5 and ABCG8 overexpression increases hepatobiliary sterol transport but does not alter aortic atherosclerosis in transgenic mice. *J. Biol. Chem.* 2004;279(22):22913–22925.

370. Plosch T, Kok T, Bloks VW, Smit MJ, Havinga R, Chimini G, Groen AK, Kuipers F**.** Increased Hepatobiliary and Fecal Cholesterol Excretion upon Activation of the Liver X Receptor Is Independent of ABCA1. *J. Biol. Chem.* 2002;277(37):33870–33877.

371. Trauner M, Fuchs CD, Halilbasic E, Paumgartner G**.** New therapeutic concepts in bile acid transport and signaling for management of cholestasis. *Hepatology* 2017;65(4):1393–1404.

372. McNeish J, Aiello RJ, Guyot D, Turi T, Gabel C, Aldinger C, Hoppe KL, Roach ML, Royer LJ, de Wet J, Broccardo C, Chimini G, Francone OL**.** High density lipoprotein deficiency and foam cell accumulation in mice with targeted disruption of ATP-binding cassette transporter-1. *Proc. Natl. Acad. Sci. U. S. A.* 2000;97(8):4245–50.

373. Wiersma H, Nijstad N, de Boer JF, Out R, Hogewerf W, Van Berkel TJ, Kuipers F, Tietge UJF**.** Lack of Abcg1 results in decreased plasma HDL cholesterol levels and increased biliary cholesterol secretion in mice fed a high cholesterol diet. *Atherosclerosis* 2009;206(1):141–147.

374. Hafiane A, Genest J**.** High density lipoproteins: Measurement techniques and potential biomarkers of cardiovascular risk. *BBA Clin.* 2015;3:175–188.

375. Pawlak M, Lefebvre P, Staels B**.** General molecular biology and architecture of nuclear receptors. *Curr. Top. Med. Chem.* 2012;12(6):486–504.

376. Stein S, Lemos V, Xu P, Demagny H, Wang X, Ryu D, Jimenez V, Bosch F, Lüscher TF, Oosterveer MH, Schoonjans K**.** Impaired SUMOylation of nuclear receptor LRH-1 promotes nonalcoholic fatty liver disease. *J. Clin. Invest.* 2017;127(2):583–592.

377. Marioni JC, Mason CE, Mane SM, Stephens M, Gilad Y**.** RNA-seq: an assessment of technical reproducibility and comparison with gene expression arrays. *Genome Res.* 2008;18(9):1509–17.

378. Barry-Hamilton V, Spangler R, Marshall D, McCauley S, Rodriguez HM, Oyasu M, Mikels A, Vaysberg M, Ghermazien H, Wai C, Garcia CA, Velayo AC, Jorgensen B, Biermann D, Tsai D, Green J, Zaffryar-Eilot S, Holzer A, Ogg S, Thai D, Neufeld G, Van Vlasselaer P, Smith V**.** Allosteric inhibition of lysyl oxidase-like-2 impedes the development of a pathologic microenvironment. *Nat. Med.* 2010;16(9):1009–17.

379. Liu SB, Ikenaga N, Peng Z-W, Sverdlov DY, Greenstein A, Smith V, Schuppan D, Popov Y**.** Lysyl oxidase activity contributes to collagen stabilization during liver fibrosis progression and limits spontaneous fibrosis reversal in mice. *FASEB J.* 2016;30(4):1599–609.

380. Ikenaga N, Peng Z-W, Vaid KA, Liu SB, Yoshida S, Sverdlov DY, Mikels-Vigdal A, Smith V, Schuppan D, Popov Y V**.** Selective targeting of lysyl oxidase-like 2 (LOXL2) suppresses hepatic fibrosis progression and accelerates its reversal. *Gut* 2017:gutjnl-2016-312473.

381. Liu SB, Ikenaga N, Peng Z-W, Sverdlov DY, Greenstein A, Smith V, Schuppan D, Popov Y**.** Lysyl oxidase activity contributes to collagen stabilization during liver fibrosis progression and limits spontaneous fibrosis reversal in mice. *FASEB J.* 2016;30(4):1599–609.

382. Moylan CA, Pang H, Dellinger A, Suzuki A, Garrett ME, Guy CD, Murphy SK, Ashley-Koch AE, Choi SS, Michelotti GA, Hampton DD, Chen Y, Tillmann HL, Hauser MA, Abdelmalek MF, Diehl AM**.** Hepatic gene expression profiles differentiate presymptomatic patients with mild versus severe nonalcoholic fatty liver disease. *Hepatology* 2014;59(2):471–82.

383. Lorena D, Darby IA, Reinhardt DP, Sapin V, Rosenbaum J, Desmoulière A**.** Fibrillin-1 expression in normal and fibrotic rat liver and in cultured hepatic fibroblastic cells: modulation by mechanical stress and role in cell adhesion. *Lab. Investig.* 2004;84(2):203–212.

384. Charlton M, Viker K, Krishnan A, Sanderson S, Veldt B, Kaalsbeek AJ, Kendrick M, Thompson G, Que F, Swain J, Sarr M**.** Differential expression of lumican and fatty acid binding protein-1: new insights into the histologic spectrum of nonalcoholic fatty liver disease. *Hepatology* 2009;49(4):1375–84.

385. Zhao B, Natarajan R, Ghosh S**.** Human liver cholesteryl ester hydrolase: cloning, molecular characterization, and role in cellular cholesterol homeostasis. *Physiol. Genomics* 2005;23(3):304–310.

386. Quiroga AD, Li L, Trötzmüller M, Nelson R, Proctor SD, Köfeler H, Lehner R**.** Deficiency of carboxylesterase 1/esterase-x results in obesity, hepatic steatosis, and hyperlipidemia. *Hepatology* 2012;56(6):2188–2198.

387. Jones RD, Taylor AM, Tong EY, Repa JJ**.** Carboxylesterases are uniquely expressed among tissues and regulated by nuclear hormone receptors in the mouse. *Drug Metab. Dispos.* 2013;41(1):40–9.

388. Yoshikawa T, Shimano H, Amemiya-Kudo M, Yahagi N, Hasty AH, Matsuzaka T, Okazaki H, Tamura Y, Iizuka Y, Ohashi K, Osuga J, Harada K, Gotoda T, Kimura S, Ishibashi S, Yamada N**.** Identification of liver X receptor-retinoid X receptor as an activator of the sterol regulatory element-binding protein 1c gene promoter. *Mol. Cell. Biol.* 2001;21(9):2991–3000.

389. Shrestha E, Hussein MA, Savas JN, Ouimet M, Barrett TJ, Leone S, Yates JR, Moore KJ, Fisher EA, Garabedian MJ**.** Poly(ADP-ribose) Polymerase 1 Represses Liver X Receptor-mediated ABCA1 Expression and Cholesterol Efflux in Macrophages. *J. Biol. Chem.* 2016;291(21):11172–11184.

390. Zhang J, Kalkum M, Chait BT, Roeder RG**.** The N-CoR-HDAC3 nuclear receptor corepressor complex inhibits the JNK pathway through the integral subunit GPS2. *Mol. Cell* 2002;9(3):611–623.

391. Perissi V, Scafoglio C, Zhang J, Ohgi KA, Rose DW, Glass CK, Rosenfeld MG**.** TBL1 and TBLR1 Phosphorylation on Regulated Gene Promoters Overcomes Dual CtBP and NCoR/SMRT Transcriptional Repression Checkpoints. *Mol. Cell* 2008;29(6):755–766.

392. Repa JJ, Mangelsdorf DJ**.** The role of orphan nuclear receptors in the regulation of cholesterol homeostasis. *Annu. Rev. Cell Dev. Biol.* 2000.

393. Xu J, Xu Y, Li Y, Jadhav K, You M, Yin L, Zhang Y, Starr SP, Raines D, Gao B, Bataller R, Shen Z, Wang HJ, Gao B, Zakhari S, Nagy LE, Lee JY, Sohn KH,

Rhee SH, Hwang D, Lakshminarayanan V, Beno DW, Costa RH, Hritz I, Shen Z, Liang X, Rogers CQ, Rideout D, You M, Canto C, Canto C, Auwerx J, Quiroga AD, Xu J, Ghosh S, Clair RW, Rudel LL, Xu J, Zhao B, Song J, Clair RW, Ghosh S, Hayhurst GP, Lee YH, Lambert G, Ward JM, Gonzalez FJ, Yin L, Ma H, Ge X, Edwards PA, Zhang Y, Bertola A, Mathews S, Ki SH, Wang H, Gao B, Labonne BEF, Bulua AC, Nakahira K, Naik E, Dixit VM, Shokolenko I, Venediktova N, Bochkareva A, Wilson GL, Alexeyev MF, Merali Z, Ross S, Pare G, You M, Fischer M, Cho WK, Crabb D, Babeu JP, Boudreau F, Xu Y, McClain CJ, Su LC, Kang X, Quiroga AD, Lian JH, Lehner R, Clugston RD, Fleming CD, Diczfalusy MA, Bjorkhem I, Einarsson C, Hillebrant CG, Alexson SE, Li Y, Ge XM, Mastrodonato M, Edwards M, Houseman L, Phillips IR, Shephard EA, Guan X, Rubin E, Anni H, Mishin V, Gray JP, Heck DE, Laskin DL, Laskin JD**.** Carboxylesterase 1 Is Regulated by Hepatocyte Nuclear Factor 4α and Protects Against Alcohol- and MCD diet-induced Liver Injury. *Sci. Rep.* 2016;6:24277.

394. Li J, Wang Y, Matye DJ, Chavan H, Krishnamurthy P, Li F, Li T**.** Sortilin 1 Modulates Hepatic Cholesterol Lipotoxicity in Mice via Functional Interaction with Liver Carboxylesterase 1. *J. Biol. Chem.* 2017;292(1):146–160.

395. Sun H, Scott DO**.** Impact of genetic polymorphisms of cytochrome P450 2 C (CYP2C) enzymes on the drug metabolism and design of antidiabetics. *Chem. Biol. Interact.* 2011;194(2–3):159–167.

396. Zanger UM, Schwab M**.** Cytochrome P450 enzymes in drug metabolism: Regulation of gene expression, enzyme activities, and impact of genetic variation. *Pharmacol. Ther.* 2013;138(1):103–141.

397. Fisher CD, Lickteig AJ, Augustine LM, Ranger-Moore J, Jackson JP, Ferguson SS, Cherrington NJ**.** Hepatic cytochrome P450 enzyme alterations in humans with progressive stages of nonalcoholic fatty liver disease. *Drug Metab. Dispos.* 2009;37(10):2087–94.

398. Benard O, Lim J, Apontes P, Jing X, Angeletti RH, Chi Y**.** Impact of high-fat diet on the proteome of mouse liver. *J. Nutr. Biochem.* 2016;31:10–19.

399. Node K, Huo Y, Ruan X, Yang B, Spiecker M, Ley K, Zeldin DC, Liao JK**.** Anti-inflammatory Properties of Cytochrome P450 Epoxygenase-Derived Eicosanoids. *Science (80-.).* 1999;285(5431). Available at: http://science.sciencemag.org/content/285/5431/1276?ijkey=ae8a69dc8715d7022497eee76fc68bf50aef63d9&keytype2=tf_ipsecsha. Accessed April 22, 2017.

400. Schuck RN, Zha W, Edin ML, Gruzdev A, Vendrov KC, Miller TM, Xu Z, Lih FB, DeGraff LM, Tomer KB, Jones HM, Makowski L, Huang L, Poloyac SM, Zeldin DC, Lee CR**.** The cytochrome P450 epoxygenase pathway regulates the hepatic inflammatory response in fatty liver disease. *PLoS One* 2014;9(10):e110162.

401. Chen G, Xu R, Zhang S, Wang Y, Wang P, Edin ML, Zeldin DC, Wang DW**.** CYP2J2 overexpression attenuates nonalcoholic fatty liver disease induced by high-fat diet in mice. *Am. J. Physiol. Endocrinol. Metab.* 2015;308(2):E97–E110.

402. Friedman SL**.** Hepatic Stellate Cells: Protean, Multifunctional, and Enigmatic Cells of the Liver. *Physiol Rev.* 2010;88(1):125–172.

403. Beaven SW, Wroblewski K, Wang J, Hong C, Bensinger S, Tsukamoto H, Tontonoz P**.** Liver X Receptor Signaling Is a Determinant of Stellate Cell Activation and Susceptibility to Fibrotic Liver Disease. *Gastroenterology* 2011;140(3):1052–1062.

404. O'Mahony F, Wroblewski K, O'Byrne SM, Jiang H, Clerkin K, Benhammou J, Blaner WS, Beaven SW**.** Liver X receptors balance lipid stores in hepatic stellate cells through Rab18, a retinoid responsive lipid droplet protein. *Hepatology* 2015;62(2):615–26.

405. Xing Y, Zhao T, Gao X, Wu Y, DeMatteo RP**.** Liver X receptor α is essential for the capillarization of liver sinusoidal endothelial cells in liver injury. *Sci. Rep.* 2016;6(1):21309.

406. Wake K**.** "Sternzellen" in the liver: Perisinusoidal cells with special reference to storage of vitamin A. *Am. J. Anat.* 1971;132(4):429–461.

407. Blaner WS, O'Byrne SM, Wongsiriroj N, Kluwe J, D'Ambrosio DM, Jiang H, Schwabe RF, Hillman EMC, Piantedosi R, Libien J**.** Hepatic stellate cell lipid droplets: A specialized lipid droplet for retinoid storage. *Biochim. Biophys. Acta - Mol. Cell Biol. Lipids* 2009;1791(6):467–473.

408. Friedman SL, Roll FJ, Boyles J, Bissell DM**.** Hepatic lipocytes: the principal collagen-producing cells of normal rat liver. *Proc. Natl. Acad. Sci. U. S. A.* 1985;82(24):8681–5.

409. Desmoulière A**.** Factors influencing myofibroblast differentiation during wound healing and fibrosis. *Cell Biol. Int.* 1995;19(5):471–6.

410. Holt AP, Haughton EL, Lalor PF, Filer A, Buckley CD, Adams DH**.** Liver Myofibroblasts Regulate Infiltration and Positioning of Lymphocytes in Human Liver. *Gastroenterology* 2009;136(2):705–714.

411. Friedman SL, Rockey DC, McGuire RF, Maher JJ, Boyles JK, Yamasaki G**.** Isolated hepatic lipocytes and Kupffer cells from normal human liver: morphological and functional characteristics in primary culture. *Hepatology* 1992;15(2):234–243.

412. Ahn SB, Jang K, Jun DW, Lee BH, Shin KJ**.** Expression of liver X receptor correlates with intrahepatic inflammation and fibrosis in patients with nonalcoholic fatty liver disease. *Dig Dis Sci* 2014;59(12):2975–2982.

413. Lima-Cabello E, García-Mediavilla MV, Miquilena-Colina ME, Vargas-Castrillón J, Lozano-Rodríguez T, Fernández-Bermejo M, Olcoz JL, González-Gallego J, García-Monzón C, Sánchez-Campos S**.** Enhanced expression of pro-inflammatory mediators and liver X-receptor-regulated lipogenic genes in non-alcoholic fatty liver disease and hepatitis C. *Clin. Sci. (Lond).* 2011;120(6):239–250.

414. Aguilar-olivos NE, Carrillo-córdova D, Oria-hernández J, Sánchez-valle V, Ponciano-rodríguez G, Ramírez-jaramillo M**.** The nuclear receptor FXR , but not LXR , up-regulates bile acid transporter expression in non-alcoholic fatty liver disease. *Ann. Hepatol. Off. J. Mex. Assoc. Hepatol.* 2015;14(4):487–493.

415. Yamamoto T, Shimano H, Inoue N, Nakagawa Y, Matsuzaka T, Takahashi A, Yahagi N, Sone H, Suzuki H, Toyoshima H, Yamada N**.** Protein kinase A suppresses sterol regulatory element-binding protein-1C expression via phosphorylation of liver X receptor in the liver. *J. Biol. Chem.* 2007;282(16):11687–11695.

416. Leavens KF, Birnbaum MJ**.** Insulin signaling to hepatic lipid metabolism in health and disease. *Crit. Rev. Biochem. Mol. Biol.* 2011;46(3):200–215.

417. Shimomura I, Bashmakov Y, Ikemoto S, Horton JD, Brown MS, Goldstein JL**.** Insulin selectively increases SREBP-1c mRNA in the livers of rats with streptozotocin-induced diabetes. *Proc. Natl. Acad. Sci. U. S. A.* 1999;96(24):13656–61.

418. Cagen LM, Deng X, Wilcox HG, Park EA, Raghow R, Elam MB**.** Insulin activates the rat sterol-regulatory-element-binding protein 1c (SREBP-1c) promoter through the combinatorial actions of SREBP, LXR, Sp-1 and NF-Y cis-acting elements. *Biochem. J.* 2005;385(Pt 1):207–16.

419. Harris SM, Harvey EJ, Hughes TR, Ramji DP**.** The interferon-γ-mediated inhibition of lipoprotein lipase gene transcription in macrophages involves casein kinase 2- and phosphoinositide-3-kinase-mediated regulation of transcription factors Sp1 and Sp3. *Cell. Signal.* 2008;20(12):2296–2301.

420. Viscarra JA, Wang Y, Hong I-H, Sul HS**.** Transcriptional activation of lipogenesis by insulin requires phosphorylation of MED17 by CK2. *Sci. Signal.* 2017;10(467):eaai8596.

421. Kim GH, Oh G-S, Yoon J, Lee GG, Lee K-U, Kim S-W**.** Hepatic TRAP80 selectively regulates lipogenic activity of liver X receptor. *J. Clin. Invest.* 2015;125(1):183–193.

422. Siddiqui-Jain A, Drygin D, Streiner N, Chua P, Pierre F, O'Brien SE, Bliesath J, Omori M, Huser N, Ho C, Proffitt C, Schwaebe MK, Ryckman DM, Rice WG, Anderes K**.** CX-4945, an orally bioavailable selective inhibitor of protein kinase CK2, inhibits prosurvival and angiogenic signaling and exhibits antitumor efficacy. *Cancer Res.* 2010;70(24):10288–98.

423. Pagano MA, Bain J, Kazimierczuk Z, Sarno S, Ruzzene M, Di Maira G, Elliott M, Orzeszko A, Cozza G, Meggio F, Pinna LA**.** The selectivity of inhibitors of protein kinase CK2: an update. *Biochem. J.* 2008;415(3):353–365.

424. Kim W, Kim BG, Lee JS, Lee CK, Yeon JE, Chang MS, Kim JH, Kim H, Yi S, Lee J, Cho J-Y, Kim SG, Lee J-H, Kim YJ**.** Randomised clinical trial: the efficacy and safety of oltipraz, a liver X receptor alpha-inhibitory dithiolethione in patients with non-alcoholic fatty liver disease. *Aliment. Pharmacol. Ther.* 2017;45(8):1073–1083.

425. Quinet EM, Savio DA, Halpern AR, Chen L, Schuster GU, Gustafsson J-A, Basso MD, Nambi P**.** Liver X Receptor (LXR)-beta Regulation in LXR -Deficient Mice: Implications for Therapeutic Targeting. *Mol. Pharmacol.* 2006;70(4):1340–1349.

426. Liang G, Yang J, Horton JD, Hammer RE, Goldstein JL, Brown MS**.** Diminished Hepatic Response to Fasting/Refeeding and Liver X Receptor Agonists in Mice with Selective Deficiency of Sterol Regulatory Element-binding Protein-1c. *J. Biol. Chem.* 2002;277(11):9520–9528.

427. Mederacke I, Hsu CC, Troeger JS, Huebener P, Mu X, Dapito DH, Pradere J-P, Schwabe RF**.** Fate tracing reveals hepatic stellate cells as dominant contributors to liver fibrosis independent of its aetiology. *Nat. Commun.* 2013;4:2823.

428. Postic C, Shiota M, Niswender KD, Jetton TL, Chen Y, Moates JM, Shelton KD, Lindner J, Cherrington AD, Magnuson MA**.** Dual roles for glucokinase in glucose homeostasis as determined by liver and pancreatic beta cell-specific gene knock-outs using Cre recombinase. *J. Biol. Chem.* 1999;274(1):305–15.

429. Li Z, Soloski MJ, Diehl AM**.** Dietary factors alter hepatic innate immune system in mice with nonalcoholic fatty liver disease. *Hepatology* 2005;42(4):880–885.

430. Weltman MD, Farrell GC, Liddle C**.** Increased hepatocyte CYP2E1 expression in a rat nutritional model of hepatic steatosis with inflammation. *Gastroenterology* 1996;111(6):1645–53.

431. Ip E, Farrell G, Hall P, Robertson G, Leclercq I**.** Administration of the potent PPARalpha agonist, Wy-14,643, reverses nutritional fibrosis and steatohepatitis in mice. *Hepatology* 2004;39(5):1286–1296.

432. Jeong W-I, Jeong D-H, Do S-H, Kim Y-K, Park H-Y, Kwon O-D, Kim T-H, Jeong K-S**.** Mild hepatic fibrosis in cholesterol and sodium cholate diet-fed rats. *J. Vet. Med. Sci.* 2005;67(3):235–42.

433. Caldwell S, Ikura Y, Dias D, Isomoto K, Yabu A, Moskaluk C, Pramoonjago P, Simmons W, Scruggs H, Rosenbaum N, Wilkinson T, Toms P, Argo CK, Al-Osaimi AMS, Redick JA**.** Hepatocellular ballooning in NASH. *J. Hepatol.* 2010;53(4):719–23.

434. Lackner C**.** Hepatocellular ballooning in nonalcoholic steatohepatitis: the pathologist's perspective. *Expert Rev. Gastroenterol. Hepatol.* 2011;5(2):223–31.

435. Kohli R, Kirby M, Xanthakos SA, Softic S, Feldstein AE, Saxena V, Tang PH, Miles L, Miles M V, Balistreri WF, Woods SC, Seeley RJ**.** High-fructose, medium chain trans fat diet induces liver fibrosis and elevates plasma coenzyme Q9 in a novel murine model of obesity and nonalcoholic steatohepatitis. *Hepatology* 2010;52(3):934–44.

436. Asgharpour A, Cazanave SC, Pacana T, Seneshaw M, Vincent R, Banini BA, Kumar DP, Daita K, Min H-K, Mirshahi F, Bedossa P, Sun X, Hoshida Y, Koduru S V, Contaifer D, Warncke UO, Wijesinghe DS, Sanyal AJ**.** A diet-induced animal model of non-alcoholic fatty liver disease and hepatocellular cancer. *J. Hepatol.* 2016;65(3):579–88.

437. Ouyang X, Cirillo P, Sautin Y, McCall S, Bruchette JL, Diehl AM, Johnson RJ, Abdelmalek MF**.** Fructose consumption as a risk factor for non-alcoholic fatty liver disease. *J. Hepatol.* 2008;48(6):993–999.

438. Abdelmalek MF, Suzuki A, Guy C, Unalp-Arida A, Colvin R, Johnson RJ, Diehl AM, Nonalcoholic Steatohepatitis Clinical Research Network**.** Increased fructose consumption is associated with fibrosis severity in patients with nonalcoholic fatty liver disease. *Hepatology* 2010;51(6):1961–1971.

439. Zou Y, Du H, Yin M, Zhang L, Mao L, Xiao N, Ren G, Zhang C, Pan J**.** Effects of high dietary fat and cholesterol on expression of PPARα, LXRα, and their responsive genes in the liver of apoE and LDLR double deficient mice. *Mol. Cell. Biochem.* 2009;323(1–2):195–205.

440. Lehrke M, Lebherz C, Millington SC, Guan H-P, Millar J, Rader DJ, Wilson JM, Lazar MA**.** Diet-dependent cardiovascular lipid metabolism controlled by hepatic LXRα. *Cell Metab.* 2005;1(5):297–308.

441. Wagner BL, Valledor AF, Shao G, Daige CL, Bischoff ED, Petrowski M, Jepsen K, Baek SH, Heyman RA, Rosenfeld MG, Schulman IG, Glass CK**.** Promoter-specific roles for liver X receptor/corepressor complexes in the regulation of ABCA1 and SREBP1 gene expression. *Mol. Cell. Biol.* 2003;23(16):5780–9.

442. Heinz S, Benner C, Spann N, Bertolino E, Lin YC, Laslo P, Cheng JX, Murre C, Singh H, Glass CK**.** Simple combinations of lineage-determining transcription factors prime cis-regulatory elements required for macrophage and B cell identities. *Mol. Cell* 2010;38(4):576–89.

443. Visel A, Blow MJ, Li Z, Zhang T, Akiyama JA, Holt A, Plajzer-Frick I, Shoukry M, Wright C, Chen F, Afzal V, Ren B, Rubin EM, Pennacchio LA**.** ChIP-seq accurately predicts tissue-specific activity of enhancers. *Nature* 2009;457(7231):854–858.

444. Heintzman ND, Stuart RK, Hon G, Fu Y, Ching CW, Hawkins RD, Barrera LO, Van Calcar S, Qu C, Ching KA, Wang W, Weng Z, Green RD, Crawford GE, Ren B**.** Distinct and predictive chromatin signatures of transcriptional promoters and enhancers in the human genome. *Nat. Genet.* 2007;39(3):311–318.

445. Leung A, Parks BW, Du J, Trac C, Setten R, Chen Y, Brown K, Lusis AJ, Natarajan R, Schones DE**.** Open chromatin profiling in mice livers reveals unique chromatin variations induced by high fat diet. *J. Biol. Chem.* 2014;289(34):23557–67.

446. Yuan W, Xia Y, Bell CG, Yet I, Ferreira T, Ward KJ, Gao F, Loomis AK, Hyde CL, Wu H, Lu H, Liu Y, Small KS, Viñuela A, Morris AP, Berdasco M, Esteller M, Brosnan MJ, Deloukas P, McCarthy MI, John SL, Bell JT, Wang J, Spector TD**.** An integrated epigenomic analysis for type 2 diabetes susceptibility loci in monozygotic twins. *Nat. Commun.* 2014;5:5719.

447. Leung A, Trac C, Du J, Natarajan R, Schones DE**.** Persistent Chromatin Modifications Induced by High Fat Diet. *J. Biol. Chem.* 2016;291(20):10446–55.

448. Anbalagan M, Rowan BG**.** Estrogen receptor alpha phosphorylation and its functional impact in human breast cancer. *Mol. Cell. Endocrinol.* 2015;418:264–272.

449. Choi JH, Banks AS, Estall JL, Kajimura S, Boström P, Laznik D, Ruas JL, Chalmers MJ, Kamenecka TM, Blüher M, Griffin PR, Spiegelman BM**.** Anti-diabetic drugs inhibit obesity-linked phosphorylation of PPARc by Cdk5. *Nature* 2010;466(7305):451–456.

450. Choi JH, Banks AS, Kamenecka TM, Busby SA, Chalmers MJ, Kumar N, Kuruvilla DS, Shin Y, He Y, Bruning JB, Marciano DP, Cameron MD, Laznik D, Jurczak MJ, Schürer SC, Vidovi D, Shulman GI, Spiegelman BM, Griffin PR**.** Antidiabetic actions of a non-agonist PPARc ligand blocking Cdk5-mediated phosphorylation. *Nature* 2011;477(7365):477–481.

451. Choi S, Kim E, Jung J, Marciano DP, Jo A, Young J**.** PPARγ antagonist Gleevec improves insulin sensitivity and promotes the browning of white adipose tissue. *Diabetes* 2016;65(4):829–839.

452. Armstrong MJ, Houlihan DD, Bentham L, Shaw JC, Cramb R, Olliff S, Gill PS, Neuberger JM, Lilford RJ, Newsome PN**.** Presence and severity of non-alcoholic fatty liver disease in a large prospective primary care cohort. *J. Hepatol.* 2012;56(1):234–240.

453. Younossi ZM, Koenig AB, Abdelatif D, Fazel Y, Henry L, Wymer M**.** Global epidemiology of nonalcoholic fatty liver disease-Meta-analytic assessment of prevalence, incidence, and outcomes. *Hepatology* 2016;64(1):73–84.

454. Cha J-Y, Repa JJ**.** The liver X receptor (LXR) and hepatic lipogenesis. The

carbohydrate-response element-binding protein is a target gene of LXR. *J. Biol. Chem.* 2007;282(1):743–51.

455. Hsieh J, Koseki M, Molusky MM, Yakushiji E, Ichi I, Westerterp M, Iqbal J, Chan RB, Abramowicz S, Tascau L, Takiguchi S, Yamashita S, Welch CL, Di Paolo G, Hussain MM, Lefkowitch JH, Rader DJ, Tall AR**.** TTC39B deficiency stabilizes LXR reducing both atherosclerosis and steatohepatitis. *Nature* 2016;535(7611):303–7.

456. Ekstedt M, Franzén LE, Mathiesen UL, Thorelius L, Holmqvist M, Bodemar G, Kechagias S**.** Long-term follow-up of patients with NAFLD and elevated liver enzymes. *Hepatology* 2006;44(4):865–873.

457. Feil R, Brocard J, Mascrez B, LeMeur M, Metzger D, Chambon P**.** Ligand-activated site-specific recombination in mice. *Proc. Natl. Acad. Sci. U. S. A.* 1996;93(20):10887–90.

Appendix 1

RNA-seq pathway enrichment analysis

Gene Symbol	Gene title	Ranking score	Function
SLC27A5	solute carrier family 27 (fatty acid transporter), member 5	0.889	Bile acid synthesis
RETSAT	retinol saturase (all-trans-retinol 13,14-reductase)	0.858	Retinol saturation
SLC27A2	solute carrier family 27 (fatty acid transporter), member 2	0.858	Fatty acid degradation
PECR	peroxisomal trans-2-enoyl-CoA reductase	0.831	Fatty acid unsaturation
CYP7B1	cytochrome P450, family 7, subfamily B, polypeptide 1	0.694	Bile acid synthesis
ACSL1	acyl-CoA synthetase long-chain family member 1	0.684	Fatty acid degradation
PEX6	peroxisomal biogenesis factor 6	0.671	Peroxisome biosynthesis
CROT	carnitine O-octanoyltransferase	0.666	Fatty acid degradation
GNMT	glycine N-methyltransferase	0.652	Detoxification
PEX11A	peroxisomal biogenesis factor 11A	0.649	Peroxisome biosynthesis
PIPOX	pipecolic acid oxidase	0.603	Amino acid metabolism
EPHX2	epoxide hydrolase 2, cytoplasmic	0.595	Arachidonic acid metabolism
HACL1	2-hydroxyacyl-CoA lyase 1	0.585	Fatty acid degradation
ABCD3	ATP-binding cassette, sub-family D (ALD), member 3	0.576	Peroxisome biosynthesis
ABCA6	ATP-binding cassette, sub-family A (ABC1), member 6	0.518	Bile acid transport
HSD17B4	hydroxysteroid (17-beta) dehydrogenase 4	0.480	Fatty acid degradation
TTR	transthyretin (prealbumin, amyloidosis type I)	0.480	Retinol transport

Bile acid metabolism

Gene Symbol	Gene title	Ranking score	Function
RETSAT	retinol saturase (all-trans-retinol 13,14-reductase)	0.858	Retinol saturation
SLC27A2	solute carrier family 27 (fatty acid transporter), member 2	0.858	Fatty acid degradation
ACOX1	acyl-Coenzyme A oxidase 1, palmitoyl	0.805	Fatty acid degradation
ELOVL5	ELOVL family member 5, elongation of long chain fatty acids	0.740	Fatty acid elongation
ACSL1	acyl-CoA synthetase long-chain family member 1	0.684	Fatty acid degradation
PEX6	peroxisomal biogenesis factor 6	0.672	Peroxisome biosynthesis
PEX11A	peroxisomal biogenesis factor 11A	0.649	Peroxisome biosynthesis
ALB	albumin	0.611	Transport
EPHX2	epoxide hydrolase 2, cytoplasmic	0.595	Arachidonic acid metabolism
ABCD3	ATP-binding cassette, sub-family D (ALD), member 3	0.576	Peroxisome biosynthesis
EHHADH	enoyl-Coenzyme A, hydratase/3-hydroxyacyl Coenzyme A dehydrogenase	0.576	Fatty acid degradation
ABCB4	ATP-binding cassette, sub-family B (MDR/TAP), member 4	0.531	Phospholipid transport
HSD17B4	hydroxysteroid (17-beta) dehydrogenase 4	0.480	Fatty acid degradation
TTR	transthyretin (prealbumin, amyloidosis type I)	0.459	Retinol transport

Components of peroxisome

Gene Symbol	Gene title	Ranking score	Function
CYP17A1	cytochrome P450, family 17, subfamily A, polypeptide 1	1.476	Steroid biosynthesis
RETSAT	retinol saturase (all-trans-retinol 13,14-reductase)	0.858	Retinol saturation
ACOX1	acyl-Coenzyme A oxidase 1, palmitoyl	0.805	Fatty acid degradation
ANGPTL3	angiopoietin-like 3	0.774	Cell adhesion
LEAP2	liver expressed antimicrobial peptide 2	0.758	Antimicrobial
HSD11B1	hydroxysteroid (11-beta) dehydrogenase 1	0.751	Cortisol inactivation
ELOVL5	ELOVL family member 5, elongation of long chain fatty acids	0.740	Fatty acid elongation
CROT	carnitine O-octanoyltransferase	0.666	Fatty acid degradation
MCCC2	methylcrotonoyl-Coenzyme A carboxylase 2 (beta)	0.664	Amino acid metabolism
GNMT	glycine N-methyltransferase	0.653	Detoxification
NDRG2	NDRG family member 2	0.629	Cell proliferation
FBP1	fructose-1,6-bisphosphatase 1	0.622	Glucose metabolism
AHCY	S-adenosylhomocysteine hydrolase	0.609	Amino acid metabolism
HACL1	2-hydroxyacyl-CoA lyase 1	0.586	Fatty acid degradation
ASL	argininosuccinate lyase	0.584	Amino acid metabolism
ABHD6	abhydrolase domain containing 6	0.551	Cannabinoid system
ENPEP	glutamyl aminopeptidase (aminopeptidase A)	0.516	Amino acid metabolism
ETFDH	electron-transferring-flavoprotein dehydrogenase	0.462	Mitochondrial respiration

Xenobiotic metabolism

Gene Symbol	Gene title	Ranking score	Function
SLC22A5	solute carrier family 22 (organic cation transporter), member 5	0.878	Carnitine transport
FASN	fatty acid synthase	0.865	Fatty acid synthesis
RETSAT	retinol saturase (all-trans-retinol 13,14-reductase)	0.858	Retinol saturation
INMT	indolethylamine N-methyltransferase	0.807	Xenobiotic degradation
ACOX1	acyl-Coenzyme A oxidase 1, palmitoyl	0.805	Fatty acid degradation
RDH16	retinol dehydrogenase 16 (all-trans)	0.747	Retinol synthesis
ELOVL5	ELOVL family member 5, elongation of long chain fatty acids	0.740	Fatty acid elongation
ACSL1	acyl-CoA synthetase long-chain family member 1	0.684	Fatty acid degradation
MGLL	monoglyceride lipase	0.637	Triglyceride hydrolysis
ACADM	acyl-Coenzyme A dehydrogenase, C-4 to C-12 straight chain	0.606	Fatty acid degradation
AADAT	aminoadipate aminotransferase	0.603	Amino acid metabolism
EHHADH	enoyl-Coenzyme A, hydratase/3-hydroxyacyl Coenzyme A dehydrogenase	0.576	Fatty acid degradation
SUCLA2	succinate-CoA ligase, ADP-forming, beta subunit	0.563	Fatty acid synthesis
ME1	malic enzyme 1, NADP(+)-dependent, cytosolic	0.533	Fatty acid synthesis
MDH1	malate dehydrogenase 1, NAD (soluble)	0.514	Glycogen metabolism
HMGCS2	3-hydroxy-3-methylglutaryl-Coenzyme A synthase 2 (mitochondrial)	0.513	Fatty acid degradation
HSD17B4	hydroxysteroid (17-beta) dehydrogenase 4	0.480	Fatty acid degradation
ETFDH	electron-transferring-flavoprotein dehydrogenase	0.462	Mitochondrial respiration

Fatty acid metabolism

Gene Symbol	Gene title	Ranking score	Function
SCNN1A	sodium channel, nonvoltage-gated 1 alpha	1.254	Transport
CBFA2T3	core-binding factor, runt domain, alpha subunit 2; translocated to, 3	0.912	Transcriptional cofactor
SLC22A5	solute carrier family 22 (organic cation transporter), member 5	0.878	Carnitine transport
FASN	fatty acid synthase	0.865	Fatty acid synthesis
SLC27A2	solute carrier family 27 (fatty acid transporter), member 2	0.858	Fatty acid degradation
CYP26B1	cytochrome P450, family 26, subfamily B, polypeptide 1	0.851	Xenobiotic metabolism
ELOVL5	ELOVL family member 5, elongation of long chain fatty acids	0.740	Fatty acid elongation
KCNK5	potassium channel, subfamily K, member 5	0.725	Transport
PEX11A	peroxisomal biogenesis factor 11A	0.649	Peroxisome biosynthesis
GFRA1	GDNF family receptor alpha 1	0.628	Cell surface receptor
ABAT	4-aminobutyrate aminotransferase	0.574	Transaminase

Estrogen early

Gene Symbol	Gene title	Ranking score	Function
MMP14	matrix metallopeptidase 14 (membrane-inserted)	-0.509	Extracellular matrix degradation
CD9	CD9 molecule	-0.609	Cell adhesion
PLEK	pleckstrin	-0.677	Platelet biology
MMP2	matrix metallopeptidase 2	-0.777	Extracellular matrix degradation
FBN1	fibrillin 1	-0.882	Extracellular matrix protein
MMP7	matrix metallopeptidase 7 (matrilysin, uterine)	-0.895	Extracellular matrix degradation
PLAU	plasminogen activator, urokinase	-0.950	Extracellular matrix degradation
SPARC	secreted protein, acidic, cysteine-rich (osteonectin)	-1.036	Extracellular matrix protein
PLAT	plasminogen activator, tissue	-1.140	Clotting
ANXA1	annexin A1	-1.228	Membrane binding
CTSK	cathepsin K (pycnodysostosis)	-1.422	Extracellular matrix degradation
TIMP1	TIMP metallopeptidase inhibitor 1	-1.529	Extracellular matrix composition

Coagulation

Gene Symbol	Gene title	Ranking score	Function
MMP14	matrix metallopeptidase 14 (membrane-inserted)	-0.509	Extracellular matrix degradation
ATOX1	ATX1 antioxidant protein 1 homolog (yeast)	-0.553	Metal trafficking
PLEK	pleckstrin	-0.677	Platelet biology
GNG2	guanine nucleotide binding protein (G protein), gamma 2	-0.678	Membrane signalling
FCER1G	Fc fragment of IgE, high affinity I, receptor for; gamma polypeptide	-0.698	Immune response mediator
CTSD	cathepsin D (lysosomal aspartyl peptidase)	-0.720	Protein degradation
PLAUR	plasminogen activator, urokinase receptor	-0.869	Extracellular matrix degradation
TIMP2	TIMP metallopeptidase inhibitor 2	-0.879	Extracellular matrix composition
CXCL1	chemokine (C-X-C motif) ligand 1 (melanoma growth stimulating activity, alpha)	-0.905	Immune response mediator
CTSS	cathepsin S	-1.003	Protein degradation
MMP12	matrix metallopeptidase 12 (macrophage elastase)	-1.022	Extracellular matrix degradation
COL4A2	collagen, type IV, alpha 2	-1.068	Extracellular matrix protein
ITGAM	integrin, alpha M (complement component 3 receptor 3 subunit)	-1.107	Chemotaxis
PLAT	plasminogen activator, tissue	-1.140	Clotting
LGALS3	lectin, galactoside-binding, soluble, 3 (galectin 3)	-1.365	Adhesion
TIMP1	TIMP metallopeptidase inhibitor 1	-1.529	Extracellular matrix composition

Complement

Gene Symbol	Gene title	Ranking score	Function
KIFC3	kinesin family member C3	-0.597	Mitosis
LARGE	like-glycosyltransferase	-0.645	Glycoprotein synthesis
SLC6A8	solute carrier family 6 (neurotransmitter transporter), member 8	-0.665	Creatinine transport
CKB	creatine kinase, brain	-0.720	Creatinine metabolism
AEBP1	AE binding protein 1	-0.726	Transcriptional repressor
LSP1	lymphocyte-specific protein 1	-0.742	Cell motility
PDLIM7	PDZ and LIM domain 7	-0.758	Mitosis
CRYAB	crystallin, alpha B	-0.815	Chaperone
NQO1	NAD(P)H dehydrogenase, quinone 1	-0.910	ROS detoxification
ITGB4	integrin, beta 4	-0.924	Adhesion
COL1A1	collagen, type I, alpha 1	-0.939	Extracellular matrix protein
COL3A1	collagen, type III, alpha 1 (Ehlers-Danlos syndrome type IV, autosomal dominant)	-0.943	Extracellular matrix protein
GPX3	glutathione peroxidase 3 (plasma)	-0.953	ROS detoxification
AK1	adenylate kinase 1	-0.963	Energy metabolism
SPARC	secreted protein, acidic, cysteine-rich (osteonectin)	-1.036	Extracellular matrix protein
COL6A2	collagen, type VI, alpha 2	-1.048	Extracellular matrix protein
COL4A2	collagen, type IV, alpha 2	-1.068	Extracellular matrix protein
COL15A1	collagen, type XV, alpha 1	-1.168	Extracellular matrix protein
COL6A3	collagen, type VI, alpha 3	-1.169	Extracellular matrix protein

Myogenesis

Gene Symbol	Gene title	Ranking score	Function
CNN2	calponin 2	-0.661	Cytoskeleton
SIRPA	signal-regulatory protein alpha	-0.697	Signal transduction
ARHGEF6	Rac/Cdc42 guanine nucleotide exchange factor (GEF) 6	-0.714	Rho GTPase
MMP2	matrix metallopeptidase 2	-0.777	Extracellular matrix degradation
CDH1	cadherin 1, type 1, E-cadherin (epithelial)	-0.848	Adhesion
WNK4	WNK lysine deficient protein kinase 4	-0.874	Potassium homeostasis
FBN1	fibrillin 1	-0.882	Extracellular matrix protein
LAMC2	laminin, gamma 2	-0.886	Extracellular matrix protein
ADAMTS5	ADAM metallopeptidase with thromboscdhpondin type 1 motif, 5 (aggrecanase-2)	-0.890	Extracellular matrix degradation
CD276	CD276 molecule	-0.899	Immune response mediator
ITGA3	integrin, alpha 3 (antigen CD49C, alpha 3 subunit of VLA-3 receptor)	-0.912	Adhesion
ITGB4	integrin, beta 4	-0.924	Adhesion
CLDN4	claudin 4	-0.964	Tight junction protein
CDH3	cadherin 3, type 1, P-cadherin (placental)	-0.979	Adhesion
CLDN7	claudin 7	-0.999	Tight junction protein
ATP1A3	ATPase, Na+/K+ transporting, alpha 3 polypeptide	-1.330	Ion transport

Apical junction

Gene Symbol	Gene title	Ranking score	Function
TMEM176A	transmembrane protein 176A	-0.633	Immune response mediator
LAPTM5	lysosomal associated multispanning membrane protein 5	-0.684	Lysosome biology
FCER1G	Fc fragment of IgE, high affinity I, receptor for; gamma polypeptide	-0.698	Immune response mediator
TMEM176B	transmembrane protein 176B	-0.724	Immune response mediator
C3AR1	complement component 3a receptor 1	-0.839	Complement system
GPRC5B	G protein-coupled receptor, family C, group 5, member B	-0.861	G protein signal transduction
PLAUR	plasminogen activator, urokinase receptor	-0.869	Extracellular matrix degradation
SPON1	spondin 1, extracellular matrix protein	-0.875	Adhesion
SLPI	secretory leukocyte peptidase inhibitor	-0.936	Epithelial tissue protection
PLAU	plasminogen activator, urokinase	-0.950	Extracellular matrix degradation
CTSS	cathepsin S	-1.003	Protein degradation
F13A1	coagulation factor XIII, A1 polypeptide	-1.005	Coagulation
CPE	carboxypeptidase E	-1.077	Hormone synthesis
ACE	angiotensin I converting enzyme (peptidyl-dipeptidase A) 1	-1.084	Renin-angiotensin system
PLAT	plasminogen activator, tissue	-1.140	Clotting
IL7R	interleukin 7 receptor	-1.191	Immune response mediator
EMP1	epithelial membrane protein 1	-1.349	Unknown
HKDC1	hexokinase domain containing 1	-1.433	Glucose metabolism
GPNMB	glycoprotein (transmembrane) nmb	-1.442	Matrix maturation
LAT2	linker for activation of T cells family, member 2	-1.482	Immune response mediator
ADAM8	ADAM metallopeptidase domain 8	-1.606	Extracellular matrix remodelling
SPP1	secreted phosphoprotein 1 (osteopontin, bone sialoprotein I, early T-lymphocyte activation 1)	-1.927	Immune response mediator

Kras signalling

Gene Symbol	Gene title	Ranking score	Function
PCOLCE	procollagen C-endopeptidase enhancer	-0.832	Collagen metabolism
TNC	tenascin C (hexabrachion)	-0.833	Adhesion
PDLIM4	PDZ and LIM domain 4	-0.845	Mitosis
PDGFRB	platelet-derived growth factor receptor, beta polypeptide	-0.865	Mitogen
PLAUR	plasminogen activator, urokinase receptor	-0.869	Extracellular matrix degradation
COL4A1	collagen, type IV, alpha 1	-0.875	Extracellular matrix protein
FBN1	fibrillin 1	-0.882	Extracellular matrix protein
SERPINH1	serpin peptidase inhibitor, clade H (heat shock protein 47), member 1	-0.883	Collagen metabolism
LAMC2	laminin, gamma 2	-0.886	Extracellular matrix protein
CAPG	capping protein (actin filament), gelsolin-like	-0.901	Actin regulation
CXCL1	chemokine (C-X-C motif) ligand 1	-0.905	Immune response mediator
LGALS1	lectin, galactoside-binding, soluble, 1 (galectin 1)	-0.907	Adhesion
THBS2	thrombospondin 2	-0.926	Cell-matrix interaction
COL1A1	collagen, type I, alpha 1	-0.939	Extracellular matrix protein
COL3A1	collagen, type III, alpha 1	-0.943	Extracellular matrix protein
COL5A1	collagen, type V, alpha 1	-0.978	Extracellular matrix protein

Epithelial-mesenchymal transition

Gene Symbol	Gene title	Ranking score	Function
EMP3	epithelial membrane protein 3	-1.019	Unknown
FMOD	fibromodulin	-1.023	Collagen metabolism
SPARC	secreted protein, acidic, cysteine-rich (osteonectin)	-1.036	Extracellular matrix protein
LOXL2	lysyl oxidase-like 2	-1.045	Extracellular matrix protein
COL6A2	collagen, type VI, alpha 2	-1.048	Extracellular matrix protein
COL4A2	collagen, type IV, alpha 2	-1.068	Extracellular matrix protein
FSTL1	follistatin-like 1	-1.166	Inflammation
COL6A3	collagen, type VI, alpha 3	-1.169	Extracellular matrix protein
COL5A2	collagen, type V, alpha 2	-1.229	Extracellular matrix protein
LOX	lysyl oxidase	-1.303	Extracellular matrix composition
COL1A2	collagen, type I, alpha 2	-1.353	Extracellular matrix protein
TIMP1	TIMP metallopeptidase inhibitor 1	-1.529	Extracellular matrix composition
SPP1	secreted phosphoprotein 1 (osteopontin, bone sialoprotein I, early T-lymphocyte activation 1)	-1.927	Immune response mediator

Epithelial-mesenchymal transition (*continued*)

Appendix 2

Western blot scans

pS198-LXRα **LXRα**

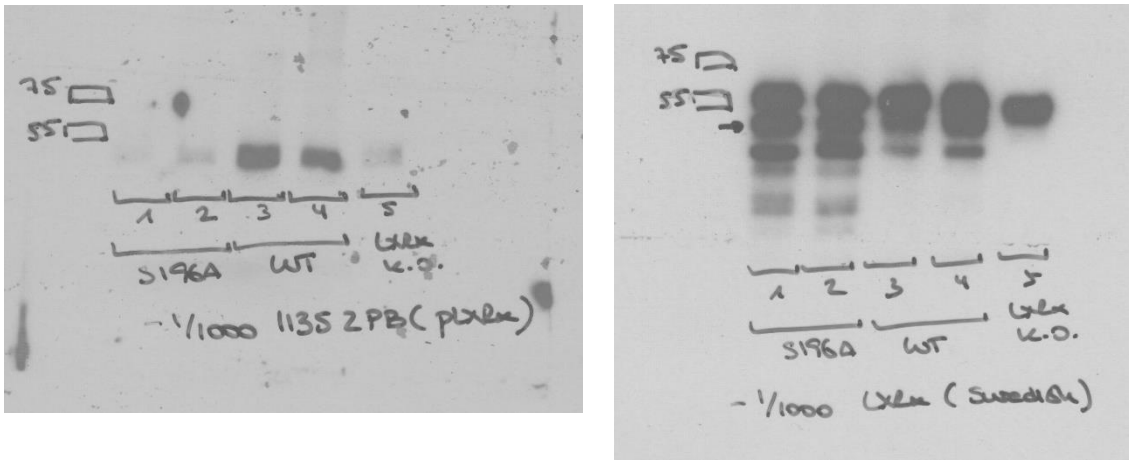

Scans Figure 3.1. C

pS198-LXRα **LXRα**

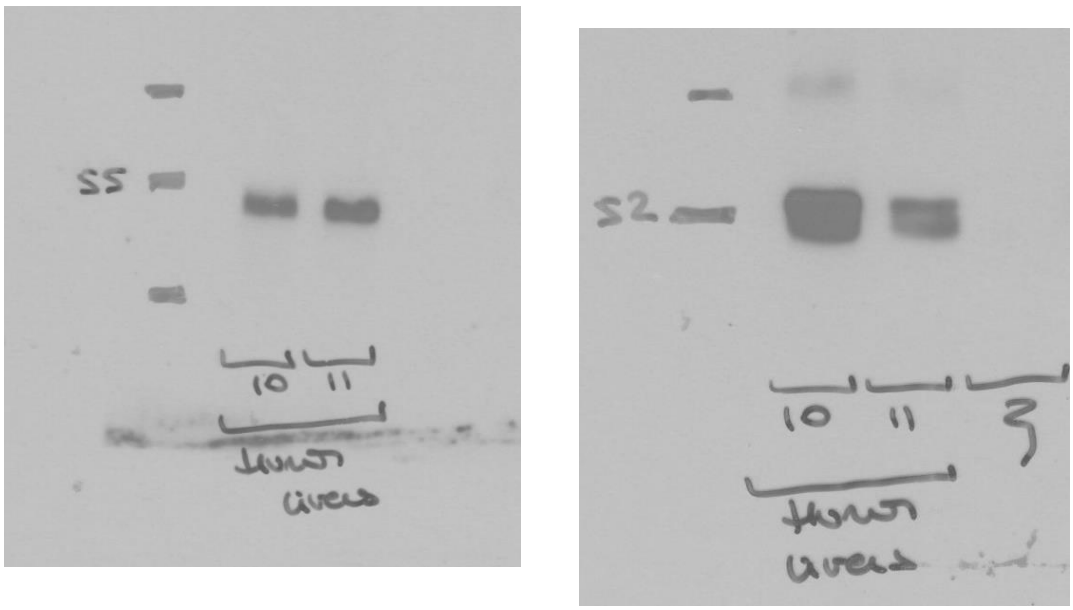

Scans Figure 3.1. D

pS198-LXRα, Hsp90

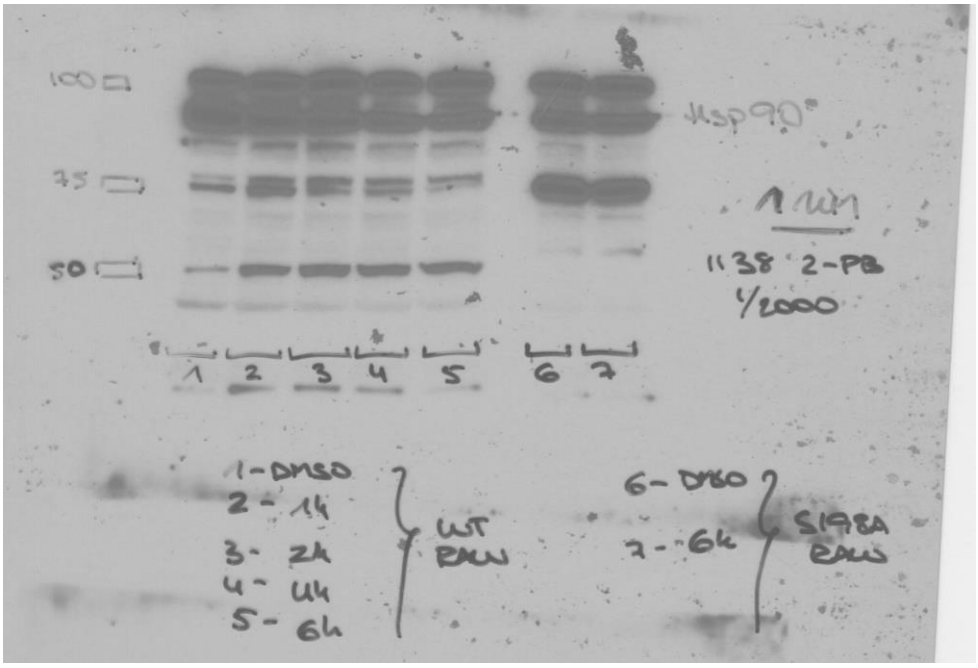

LXRα

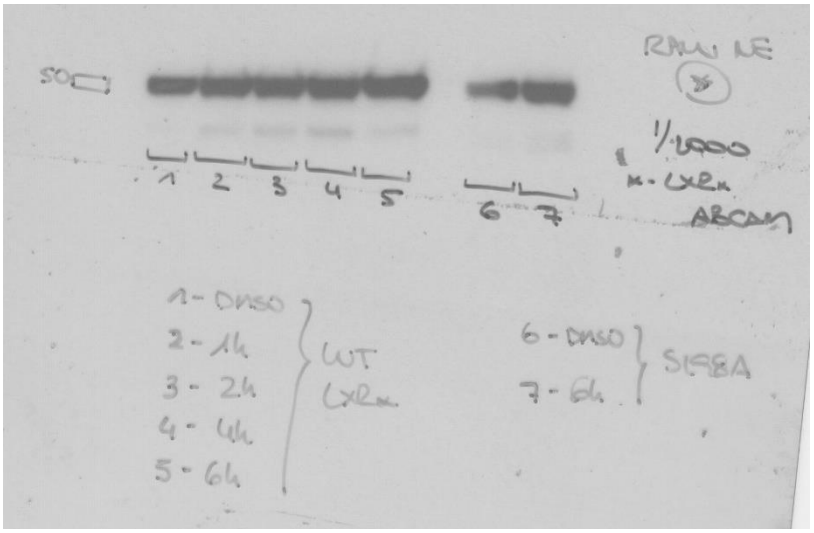

Scans Figure 5.2.1. A

pS198-LXRα, Hsp90

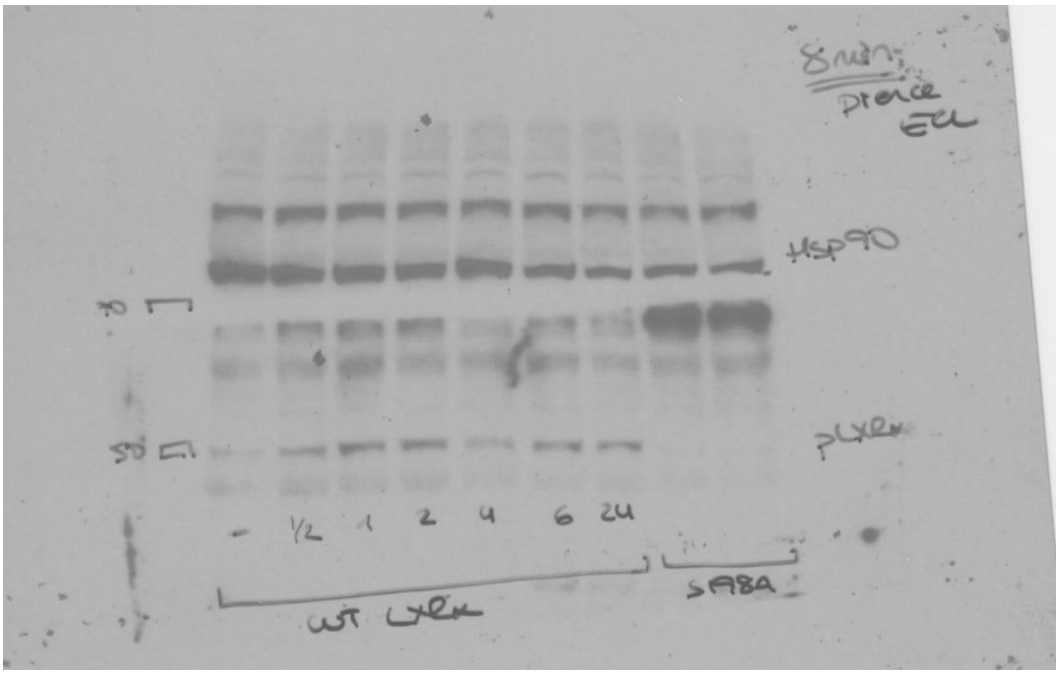

LXRα

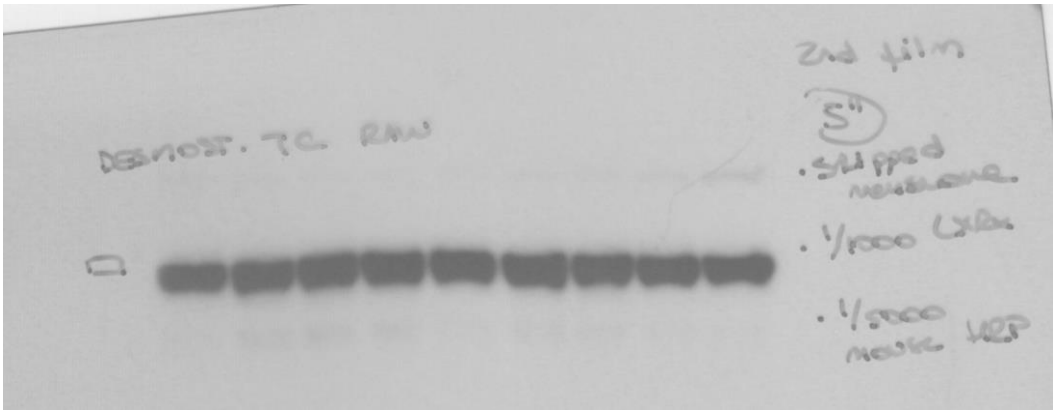

Scans Figure 5.2.1. B

pS198-LXRα, Hsp90

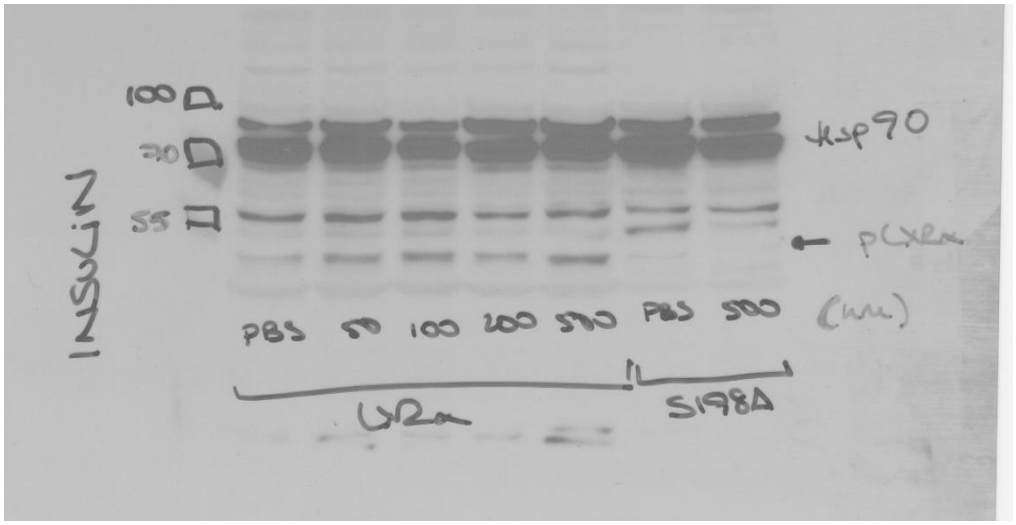

LXRα

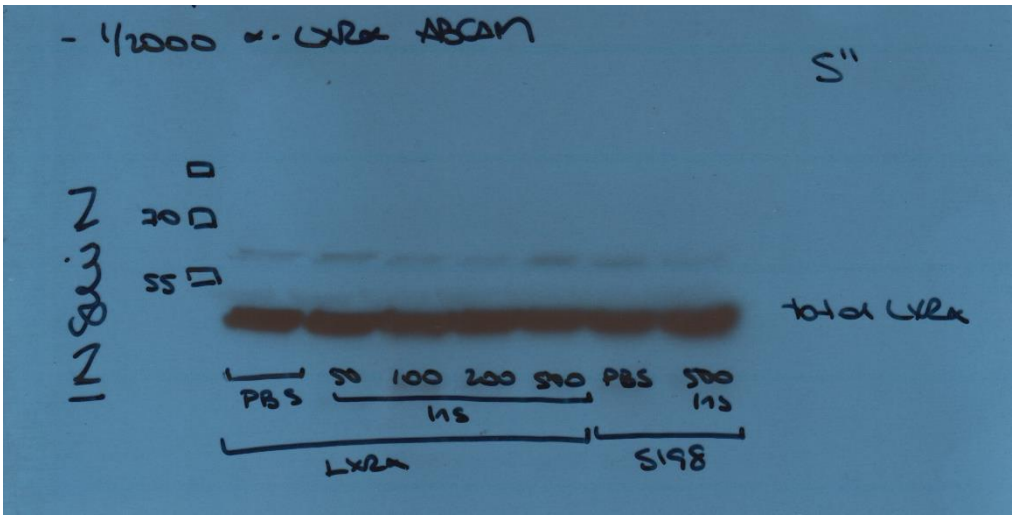

Scans Figure 5.2.2

pS198-LXRα, Hsp90

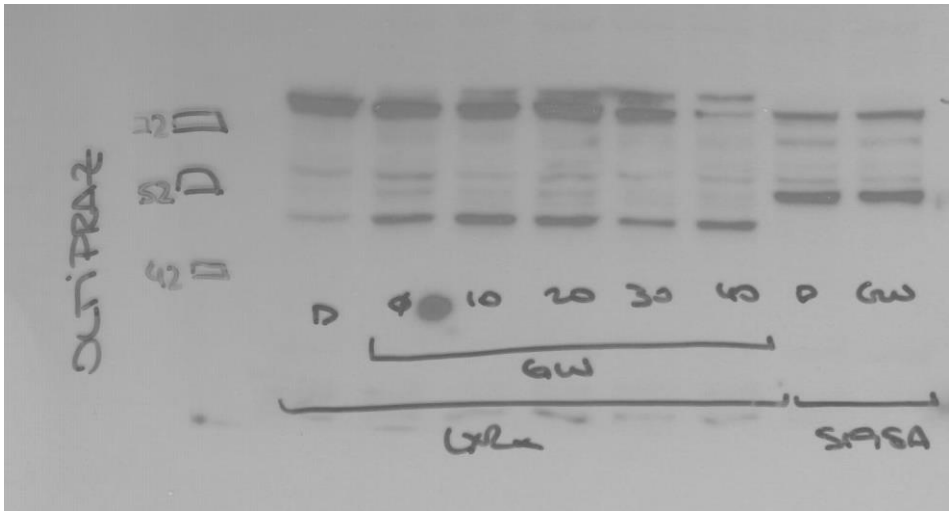

Scan Figure 5.2.3. A

pS198-LXRα, Hsp90

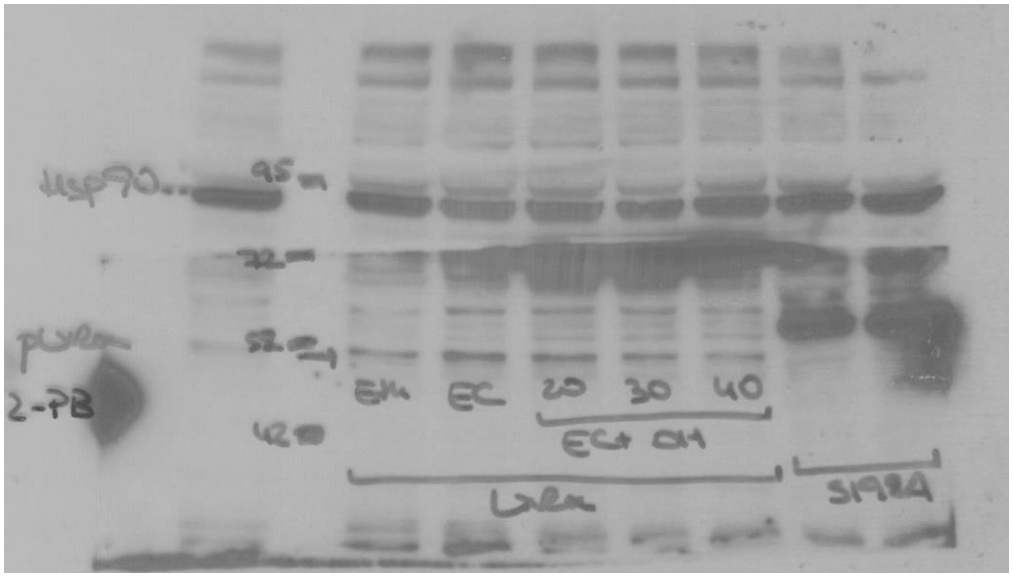

LXRα

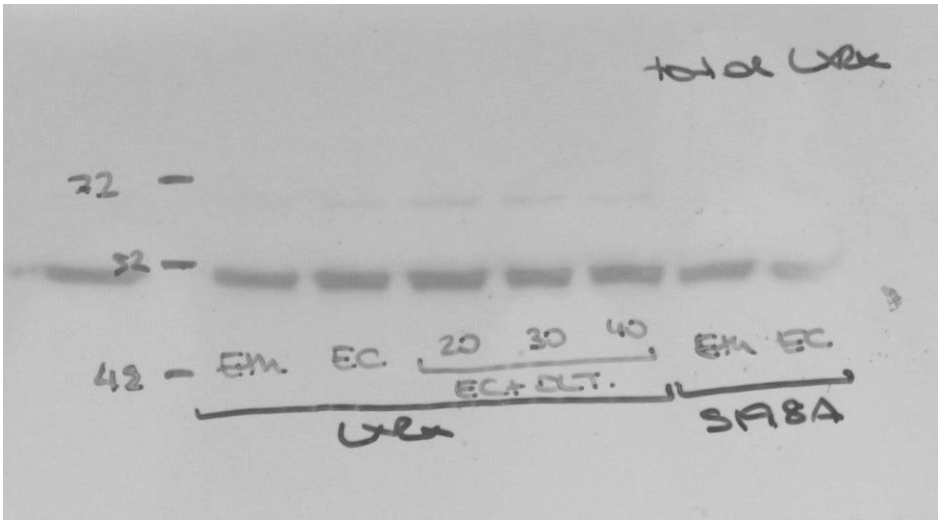

Scans Figure 5.2.3. B

pS198-LXRα, Hsp90

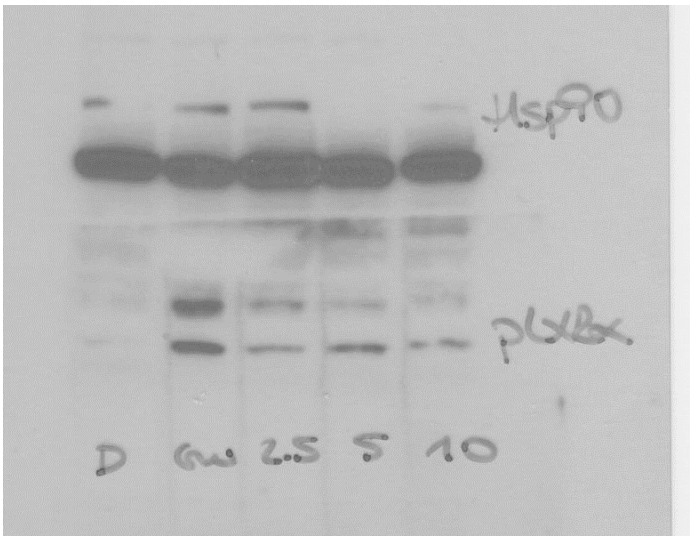

LXRα

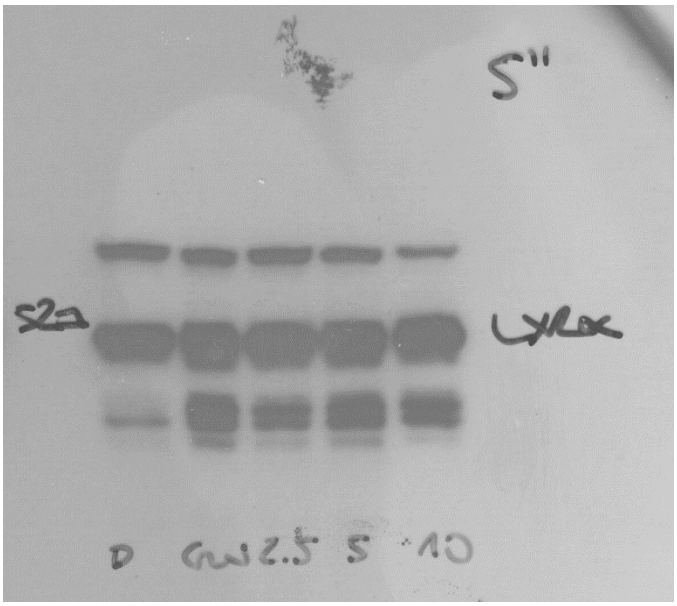

Scans Figure 5.2.4